

STRUCTURES AND CRYSTAL CHEMISTRY
OF
WOLLASTONITE AND PECTOLITE

by

CHARLES THOMPSON PREWITT

S. B., Massachusetts Institute of Technology
(1955)

S. M., Massachusetts Institute of Technology
(1960)

SUBMITTED IN PARTIAL FULFILLMENT
OF THE REQUIREMENTS FOR THE
DEGREE OF DOCTOR OF
PHILOSOPHY

at the

MASSACHUSETTS INSTITUTE OF TECHNOLOGY

September, 1962

Signature of Author
Department of Geology and Geophysics, August 20, 1962

Certified by
Thesis Supervisor

Accepted by
Chairman, Departmental Committee
on Graduate Students

✓

Structures and crystal chemistry of
wollastonite and pectolite

by
Charles T. Prewitt

Submitted to the Department of Geology and Geophysics on
August 20, 1962, in partial fulfillment of the requirement for the
degree of Doctor of Philosophy.

ABSTRACT

Wollastonite, CaSiO_3 , and pectolite, $\text{Ca}_2\text{NaHSi}_3\text{O}_9$, have similar triclinic cells; because of this and their analogous chemical compositions, they have been regarded as belonging to the same mineral family. An examination of the results of least-squares refinement of three-dimensional x-ray diffraction data reveals that although the structures contain similar metasilicate chains, they are not as closely isotypic as had been supposed. The principle differences are in the coordinations of calcium and sodium and in the way these atoms share oxygens with the silicon atoms. The final R-factors for wollastonite and pectolite are, respectively, 0.089 and 0.075.

The structures of both wollastonite and pectolite contain pseudomonoclinic subcells which are joined together on (100) to give an overall symmetry different from that of the subcell. The geometries of these subcells and the possibility of their being joined in different ways are important in explaining the types of twinning which occur in wollastonite and pectolite. Twinning which produces an overall crystal symmetry different from some subcell, known as space group twinning, probably occurs in many types of silicate minerals.

Programs written for the IBM 7090 digital computer, including full-matrix crystallographic least-squares refinement and diffractometer settings programs, are included as part of a system designed for automated crystal structure solution and refinement. Such a system is not available at present but should be ready within two years.

Thesis Supervisor: Martin J. Buerger
Title: Institute Professor

Preface

This thesis is divided into three parts, A, B, and C. Part A consists of four chapters, each of which is intended for publication. Part B contains an account of work which was done during the thesis period and which is not intended for publication in its present form. There is, however, a possibility that some of this material will be used as a base for future publication. Part C contains four appendices, the first three of which are descriptions and listings of computer programs written during the period of thesis research. It is hoped that these programs will be of use to others doing crystal structure work, and that they will eventually be incorporated into a complete system for crystal structure investigations. The fourth appendix contains observed and calculated structure factor data on wollastonite and pectolite.

Acknowledgements

The author gratefully acknowledges the advice and support of Professor M. J. Buerger in this work on wollastonite and pectolite.

Crystals of wollastonite, pectolite, and larsenite were kindly provided by Professor Clifford Frondel of Harvard University. Mr. Alden Carpenter of Harvard loaned several specimens of parawollastonite. Pectolite and wollastonite were obtained from Dr. George Switzer and Mr. Roy S. Clarke of the U. S. National Museum. The author would like to especially thank Professor A. Pabst of the University of California for sending oscillation photographs and specimens of Crestmore parawollastonite and for his comments on parawollastonite. Dr. Waldemar Schaller of the U. S. Geological Survey gave valuable advice on the pectolite-schizolite-serandite series.

Many useful and informative discussions with Mr. Donald Peacor have contributed greatly to the successful completion of this work, particularly in connection with his investigations of bustamite and rhodonite. Mrs. Hilda Cid-Dresdner, Mr. Bernhardt Wuensch, and Mr. Wayne Dollase are thanked for their interest and help throughout the period of investigation. Many conversations with Dr. Charles Burnham about computing were especially useful. Miss Gay Lorraine and Mrs. Shirley Veale contributed greatly

through their typing of the entire thesis. Particular thanks are due Miss Lorraine for proofreading and for her advice on the format of the final draft.

My wife, Gretchen, helped greatly through her moral support and through the preparation of many of the illustrations.

Finally, the support of the National Science Foundation through part-time Research Assistantships, and the M. I. T. Computation Center through the use of the IBM 709 and 7090 computers is gratefully acknowledged.

Table of Contents

Title page	i
Abstract	ii
Preface	iii
Acknowledgements	iv
Table of Contents	v
List of Tables	x
List of Figures	xi
Part A	
Chapter I. Crystal structures of wollastonite and pectolite	1
Attempts to solve the wollastonite structure from Patterson projections	2
New diffractometer data	3
The three-dimensional Patterson function and its solution	3
Refinement of the wollastonite structure	5
Attempt to fit pectolite into a wollastonite pattern	7
Preliminary refinement of the pectolite structure	8
Comparison of the pectolite and wollastonite structures	9
Chapter II. Comparison of the crystal structures of wollastonite and pectolite	14
Abstract	14
Introduction	15
Confirmation of the structure	16
Comparison of structures	18
Pseudomonoclinic symmetry	27
Distribution of Ca and Na	35
Interatomic distances and interbond angles	40
Twinning	48
Conclusions	56
Acknowledgements	57

Chapter III. Drilling coordinates for crystal structure models	58
Abstract	58
Introduction	59
Coordinate systems	59
Calculation of ρ and ϕ	63
Discussion	66
Acknowledgements	67
References	68
Chapter IV. Refinement of pectolite	69
Introduction	69
Selection of material	69
Unit cell data	71
Space group	73
Intensity collection	73
Refinement	75
Evaluation of the structure	78
Conclusions	87
References	88
Part B	
Chapter V. Review of the crystallographic investigation of metasilicates	91
Status of structural work	93
Future possibilities for ino-metasilicate investigations	95
References	97
Chapter VI. Twinning in silicate crystallography	99
Structure and space group twinning	99
Implications of space group twinning	101
Energy relations in parawollastonite and bustamite	111
Space group twinning in other silicates	112
References	115

Chapter VII. Crystal structures related to wollastonite and pectolite	116
Status of structural information	116
Pseudowollastonite	118
Hydrated calcium silicates	120
References	122
Chapter VIII. Crystal structure of larsenite, PbZnSiO_4	124
Experimental work	124
Occurrence	124
Unit cell and space group	125
Intensity collection	125
Solution of the structure	126
Refinement	131
Discussion of results	133
Oxygen packing	133
Substructures and heavy atoms	134
Direct methods	135
References	136
Chapter IX. Automatic crystal structure analysis	137
Present capabilities	137
Future capabilities	138
Expected results of automated crystal structure analysis	140
Part C Appendices	142
Appendix I. SFLSQ3, a structure factor and least- squares refinement program for the IBM 7090 digital computer	143
Introduction	143
Common storage	145
Sense indicators	145
Tape usage	145
Punched output	150

Description of the main program and its subroutines	151
MAIN	151
READ1	154
READ2	154
READ3	155
SET	155
LOOKUP	155
WEIGHT	155
SPGRP	156
REJECT	166
STAT	167
PRSF	167
STMAT	169
PRST	169
CHLNK3	169
TEST	172
CARD	173
DIST	173
Running the program	173
Data deck	173
Submitting a run	180
References	181
Program listing	183
Appendix II. Program for computation of drilling coordinates for crystal structure models	209
Directions for running the program DRILL	210
Data cards for DRILL	210
Description of data deck	211
Description of output	212
Program listing	213

Appendix III. Computation of diffractometer settings	215
Program description	215
DFSET	215
INDEX1	216
INDEX2	216
OUTPUT	217
MIFLIP	217
TERM	217
Speed of computation	217
Running the program	218
Data deck	218
References	222
Program listing	223
Appendix IV. Observed and calculated structure factors for wollastonite and pectolite	235
Wollastonite structure factors	235
Pectolite structure factors	264
Biographical note	290

List of Tables

Chapter I	
1. Refined coordinates of atoms in wollastonite and pectolite, all referred to pectolite origin	10
Chapter II	
1. Unit cells of wollastonite, NaAsO_3 , and pectolite	17
2. Atom coordinates for wollastonite and pectolite	23
3. Atom coordinates of wollastonite and pectolite referred to a pseudomonoclinic cell $\underline{P}2_1/\underline{m}$ (origin at $\bar{1}$)	33
4. Interatomic distances and interbond angles in wollastonite and pectolite	41
5. Coordination of oxygens in wollastonite and pectolite	45
Chapter IV	
1. Compositions of two pectolites and the hypothetical composition computed from $\text{Ca}_2\text{NaHSi}_3\text{O}_9$	72
2. Results of least-squares refinement of pectolite cell constants	74
3. Refined coordinates for pectolite	79
4. Interatomic distances in pectolite	82
5. Oxygen coordination in pectolite	86
Chapter V	
1. List of crystallographically interesting metasilicates	92
Chapter VII	
1. Classification of compounds with formula ABX_3	117
Chapter VIII	
1. Comparison of larsenite and forsterite cells	127
2. The forsterite structure. The larsenite structure.	128
3. Atom coordinates for larsenite	132
Appendix I	
1. Symbols assigned to COMMON storage	146
2. Tape assignments for SFLSQ3 at M. I. T. Computation Center	149
3. Derivatives of $\underline{F}_c(hkl)$ or $\underline{F}_c^2(hkl)$ with respect to varied parameters	152
4. Quantities evaluated by general space group subroutine	158
5. Expressions evaluated in CHLNK3	171

List of Figures

(The page numbers given are those of the figure legends.)

Chapter II	
1. Projection of the wollastonite structure along \underline{b}	19
2. Projection of the pectolite structure along \underline{b}	21
3. Projections of the pectolite and wollastonite structures along \underline{b}	25
4. Projection of the wollastonite structure along \underline{c}	28
5. Projection of pectolite along \underline{c} corresponding to that of wollastonite of Figure 4	30
6. Structure of wollastonite projected onto (101) of four adjacent pseudomonoclinic cells	36
7. Structure of pectolite projected onto (101) of the four pseudomonoclinic cells	38
8. Three ways in which the pseudomonoclinic unit can be stacked on (100) to produce different overall diffraction effects	49
9. Reciprocal lattices corresponding to the geometries shown in Figures 8a, 8b, and 8c	52
Chapter III	
1. Coordination group of atoms \underline{N}_1 , \underline{N}_2 , \underline{N}_3 and central atom \underline{N}_0 , and its relation to the spherical coordinate system	61
2. Vectors used in the calculation of angle $\underline{\phi}_3$	64
Chapter IV	
1. Pectolite structure projected onto (101)	80
Chapter VI	
1. Schematic representations of the ways in which pseudomonoclinic subcells can be joined to give a different overall symmetry	102
2. Pseudomonoclinic CaSiO_3 subcells joined on (100) to give wollastonite (top) and parawollastonite (bottom)	104
3. Schematic representations of the wollastonite (top) and bustamite (bottom) structures	107
4. Result of joining CaSiO_3 subcells as described in Figure 3 to give the wollastonite structure (top) and the bustamite structure (bottom)	109
Chapter VIII	
1. $\text{Pb}_1 + \text{Pb}_2 \text{M}_8(xy\frac{1}{4})$ map of larsentte	129

•
Part A

Chapter I.

The Crystal Structures of Wollastonite and Pectolite.

Wollastonite, CaSiO_3 , and pectolite, $\text{Ca}_2\text{NaHSi}_3\text{O}_9$, belong to the same mineral family. They have the same symmetry, $\underline{\text{P}\bar{1}}$, and similar cells:

	Wollastonite	Pectolite
a	7.94 Å	7.99 Å
b	7.32 Å	7.04 Å
c	7.07 Å	7.02 Å
α	$90^\circ 02'$	$90^\circ 31'$
β	$95^\circ 22'$	$95^\circ 11'$
γ	$103^\circ 26'$	$102^\circ 28'$
Z	6CaSiO_3	$2\text{Ca}_2\text{NaHSi}_3\text{O}_9$

The structure of pectolite was solved by Buerger^{1,2}, and the structure of wollastonite was solved shortly thereafter by Mamedov and Belov³. Curiously enough, although the two structures have

¹ Buerger, M.J. The arrangement of atoms in the wollastonite group of metasilicates. Proc. Nat. Acad. Sci., 42, (1956) 113-116.

² Buerger, M.J. The determination of the crystal structure of pectolite, $\text{Ca}_2\text{NaHSi}_3\text{O}_9$. Zeit. Krist., 108, (1956) 248-261.

³ Mamedov, K.S., and N.V. Belov. Crystal structure of wollastonite. Doklady Akad. Nauk. SSSR, 107 (1956) 463-466.

rather similar arrangements, they are not the same, and they are described by different sets of coordinates for corresponding atoms.

For two crystals of the same family to have different coordinates suggests that one of the structures might be incorrect. Since pectolite was solved in this laboratory, we were prejudiced in favor of the correctness of that structure. Accordingly we attempted to fit the wollastonite structure to the pectolite pattern with curious consequences which are noted below.

Attempts to Solve the Wollastonite Structure from Patterson Projections.

The structure of pectolite had been solved from the Patterson projections $\underline{P(xy)}$, $\underline{P(yz)}$, and $\underline{P(xz)}$. These were based upon intensities determined from precession photographs. The intensities were rather crude since a coarse crystal had been used, and the intensities had not been corrected for absorption. In spite of these poor data, the structure was readily solved by constructing minimum functions based upon these three Patterson projections.

The same strategy, when applied to wollastonite, was not successful. Patterson peaks corresponding to the Ca_{1+2} inversion peaks in pectolite were used for image points, and they gave pectolite-like projections. But the structures corresponding

to these projections had excessive distances from Si_3 to some of the oxygen atoms of its tetrahedron, and their structure factors had high values of \underline{R} . This failure was attributed to poor data, so that, in due course, a new set of intensities was measured with the aid of a single-crystal diffractometer.

New Diffractometer Data

The copper hemisphere for wollastonite contains 1,769 reflections. The intensities of all of these which were within recording range of our instrument (namely 1,503) were measured with the aid of a special diffractometer¹ using a Geiger tube as detector. Due care was exercised not to exceed the linearity limit of the detector. The resulting data were corrected for Lorentz and polarization factors, and then an approximate absorption correction was applied².

The Three-Dimensional Patterson Function and Its Solution.

The resulting $\underline{F(hkl)}$'s were used to compute a three-dimensional Patterson function. This was studied in sections

¹ Buerger, M. J., and N. Niizeki. The correction for absorption for rod-shaped single crystals. *Amer. Mineral.* 43 (1958) 726-731.

² Liebau, Friedrich. *Über die Struktur des Schizoliths.* *Neues Jb. Mineral.*, (1958) 227-229.

parallel to (010) made at intervals of $\underline{b}/30$.

Although this Patterson function did not have a clear-cut indication of the obvious image point to be used to start the minimum-function routine, as pectolite had, a peak was present in a location corresponding to that of a Ca_{1+2} inversion peak in pectolite. This was used in forming an $\underline{M}_2(\underline{xyz})$ function. This preliminary function yielded an approximation to the substructure¹ which closely resembled that of pectolite. This revealed the location of Ca_3 (corresponding to Na of pectolite) and this atom location permitted construction of another $\underline{M}_2(\underline{xyz})$ function. With these two $\underline{M}_2(\underline{xyz})$ functions, a stronger $\underline{M}_4(\underline{xyz})$ function was formed. This still resembled pectolite, except that appropriate locations for O_7 and O_8 could not be found, and an ambiguity existed in placing Si_1 , Si_2 and O_9 . None of the structures based upon this solution of the Patterson function had a small value of \underline{R} , and none could be refined below $\underline{R} = 26\%$.

Since a pectolite-like model of wollastonite had evidently failed, the model proposed by Mamadov and Belov² was tested.

¹ Buerger, M.J. The determination of the crystal structure of pectolite, $\text{Ca}_2\text{NaHSi}_3\text{O}_9$. op. cit.

² Mamedov, K.S., and N.V. Belov, op. cit.

Using our new values of $\underline{F}(\underline{hkl})$ and Mamedov and Belov's coordinates, the initial value of \underline{R} was 31%, and this proved to be refinable, as noted later.

It seemed desirable to re-examine the Patterson function in the light of these new coordinates. Accordingly, they were used as a basis for finding the Ca_{1+2} inversion vector, and this was used to decompose the Patterson function. As in the earlier trial, this permitted forming an $\underline{M}_2(\underline{xyz})$ function, then an $\underline{M}_4(\underline{xyz})$ function based upon all the calcium atoms. The resulting peaks of the final minimum function located all the atoms of the model on which the original inversion peak was based, and with correct weights. It was therefore evident that this solution of the Patterson corresponds to the actual structure of wollastonite. But it is also true that, as discussed in the first part of this section, if a pectolite-like image point is used as a start, a pectolite-like structure is predicted. This curious situation made it advisable to check the correctness of the pectolite structure. (The confirmation and preliminary refinement of the pectolite structure are reported in a subsequent section of this paper.)

Refinement of the Wollastonite Structure

Mamedov and Belov based their solution of the wollastonite structure on finding sign relations among 204 $\underline{h0l}$ reflections. This

provided signs for 30% of the reflections and permitted computing a crude electron-density map. With the aid of the peaks of this map, and on the basis of experience with cuspidine and xonotlite, the Patterson projection was interpreted. This gave a model for which $\underline{R} = 24\%$ for 224 reflections. Further refinement of this important structure is obviously called for.

We started with our extensive Geiger-counter data for 1,503 $\underline{F}(\underline{hkl})$'s and Mamedov and Belov's original coordinates (except that they were transformed to the pectolite origin by adding $\frac{1}{2} 0 \frac{1}{2}$). We employed Busing and Levy's least-squares refinement program¹ for the IBM 704 computer, using an appropriate weighting scheme. After the initial cycle to find an approximate scale factor, the value of \underline{R} started at 31%.

After four cycles of refinement using reasonable fixed isotropic temperature factors, the value of \underline{R} was reduced to 11.4%. The isotropic temperature factors (as well as coordinates) were allowed to vary in three succeeding cycles, and this reduced \underline{R} to 9.3%. An additional cycles in which the anisotropic temperature factors were refined reduced \underline{R} to 8.9%. The final coordinates of the atoms, their standard deviations, and their isotropic temperature factors are listed in Table 1.

¹ Busing, W.R., and H.A. Levy. A crystallographic least-squares program for the IBM 704. (Oak Ridge National Laboratories, Oak Ridge, Tennessee, 1959).

Attempt to Fit Pectolite into a Wollastonite Pattern.

Wollastonite and pectolite have long been regarded as members of the same family. Yet the structure proposed by Mamedov and Belov for wollastonite and that proposed by Buerger for pectolite (and later by Liebau¹ for schizolite) are different. Since we confirmed the correctness of the wollastonite structure, there arose a suspicion that the structure proposed for pectolite was incorrect, and that it perhaps had the wollastonite structure.

From the earlier investigation² there were available the following sets of reduced intensity data: $\underline{F}^2(\underline{hk}0)$, $\underline{F}^2(\underline{h}0\underline{l})$, and $\underline{F}^2(0\underline{k}\underline{l})$. In addition, the Patterson projections based upon these sets of \underline{F}^2 's were available, namely $\underline{P}(\underline{xy})$, $\underline{P}(\underline{xz})$ and $\underline{P}(\underline{yz})$.

One of the fundamental differences between the wollastonite structure and Buerger's pectolite structure is the location of Ca_1 and Ca_2 . These atoms were used in the original pectolite investigation for the initial \underline{M}_2 minimum functions which were used to solve the structure. The locations were found by making use of the conjugate-peak relation.

Knowing the general location of Ca_1 and Ca_2 in wollastonite,

¹ Liebau, Friedrich. *Über die Struktur des Schizoliths*. Neues Jb. Mineral., (1958) 227-229.

² Buerger, M. J. The determination of the crystal structure of pectolite, $\text{Ca}_2\text{NaHSi}_3\text{O}_9$; *op. cit.*

a peak was found in the Patterson projection $\underline{P}(\underline{xz})$ of pectolite whose location would correspond to an inversion peak for Ca_1 and Ca_2 if these atoms had the locations they have in wollastonite. A minimum function $\underline{M}_2(\underline{xz})$ was found using this peak as an image point, and interestingly enough, a wollastonite-like pattern of peaks was revealed. The other two projections of the structure, namely $\underline{M}_2(\underline{xy})$ and $\underline{M}_2(\underline{yz})$, were formed from the Patterson projections $\underline{P}(\underline{xy})$ and $\underline{P}(\underline{yz})$. Each had a wollastonite-like pattern.

These projections provided the approximate values of the three coordinates \underline{xyz} for each atom. But this structure turned out to have a discrepancy $\underline{R}(\underline{hkl}) = 62\%$ based upon the reflections $\underline{F}(\underline{hk0})$, $\underline{F}(\underline{h0l})$, and $\underline{F}(\underline{0kl})$. An attempt was made to refine these three sets together by least-squares as described later, but $\underline{R}(\underline{hkl})$ could not be reduced below 52%. In spite of the possibility of forming minimum functions having a wollastonite-like pattern of atoms, such a structure cannot be refined and must be incorrect.

Preliminary Refinement of the Pectolite Structure.

Since pectolite evidently does not have a wollastonite-like pattern of atoms, it appeared that the solution of the pectolite structure given by Buerger¹ was probably correct. The original

¹ Buerger, M. J. The determination of the crystal structure of pectolite, $\text{Ca}_2\text{NaHSi}_3\text{O}_9$; op. cit.

structure determination included a modest refinement by difference maps which left the discrepancies at

$$\underline{R}(\underline{hk0}) = 16\%; \quad \underline{R}(\underline{0kl}) = 21\%; \quad \underline{R}(\underline{h0l}) = 25\%.$$

To improve this state of the structure, the original sets of $\underline{F}(\underline{hk0})$, $\underline{F}(\underline{0kl})$, and $\underline{F}(\underline{h0l})$ were treated together as a single three-dimensional least-squares refinement with a different scale factor applied to each set, using the Busing and Levy program for the IBM 704 computer¹. In two cycles the refinement converged to a set of coordinates for which the over-all $\underline{R}(\underline{hkl})$ was 17%. Considering the crude nature of the original intensity measurements, this can be regarded as a successful refinement, and it confirms the correctness of the original pectolite structure determination. The new values of the coordinates are given in Table 1.

Comparison of the Pectolite and Wollastonite Structures

As a result of this investigation it is evident that wollastonite and pectolite, though belonging to the same mineral family, have distinct but related structures. The relations between the two structures will be discussed in a forthcoming paper.

¹ Busing, W. R., and H. A. Levy, op. cit.

Table I

Refined Coordinates of Atoms in Wollastonite (upper values) and Pectolite (lower values), All Referred to Pectolite Origin¹.

		<u>x</u>	$\sigma(\underline{x})$	<u>y</u>	$\sigma(\underline{y})$	<u>z</u>	$\sigma(\underline{z})$	<u>B</u>
Ca ₁	(Ca _{II} ¹)	0.1985	0.0001	0.4228	0.0001	0.7608	0.0001	0.41
		0.143		0.404		0.854		
Ca ₂	(Ca _{II})	0.2027	0.0001	0.9293	0.0001	0.7640	0.0001	0.45
		0.157		0.916		0.861		
Ca ₃	(Ca _I)	0.4966	0.0001	0.2495	0.0001	0.4720	0.0001	0.37
Na		0.448		0.735		0.656		
Si _I	(Si _I ¹)	0.1852	0.0002	0.3870	0.0002	0.2687	0.0002	0.24
		0.221		0.402		0.337		

¹ Belov's designations for atoms of wollastonite in parentheses. Because of the poorer intensity data for pectolite, standard deviations of coordinates and individual temperature factors are omitted.

(Table I continued)

		\underline{x}	$\sigma(\underline{x})$	\underline{y}	$\sigma(\underline{y})$	\underline{z}	$\sigma(\underline{z})$	\underline{B}
Si ₂	(Si _I)	0.1849	0.0002	0.9545	0.0002	0.2692	0.0002	0.24
		0.210		0.945		0.344		
Si ₃	(Si _{II})	0.3970	0.0002	0.7235	0.0002	0.0560	0.0002	0.22
		0.451		0.735		0.148		
O ₁	(O _I ¹)	0.4291	0.0005	0.2314	0.0006	0.8019	0.0005	0.48
		0.348		0.212		0.875		
O ₂	(O _I)	0.4008	0.0005	0.7259	0.0006	0.8302	0.0005	0.37
		0.322		0.702		0.943		
O ₃	(O _{II} ¹)	0.3037	0.0005	0.4635	0.0006	0.4641	0.0006	0.60
		0.185		0.496		0.538		
O ₄	(O _{II})	0.3017	0.0005	0.9374	0.0006	0.4655	0.0006	0.64
		0.171		0.839		0.541		

(Table I continued)

		\underline{x}	$\sigma(\underline{x})$	\underline{y}	$\sigma(\underline{y})$	\underline{z}	$\sigma(\underline{z})$	\underline{B}
O ₅	(O _{III} ¹)	0.0154	0.0005	0.6254	0.0006	0.7343	0.0006	0.63
		0.070		0.393		0.171		
O ₆	(O _{III})	0.0175	0.0005	0.1319	0.0006	0.7353	0.0006	0.71
		0.053		0.896		0.179		
O ₇	(O _{IV} ¹)	0.2732	0.0004	0.5118	0.0005	0.0919	0.0005	0.37
		0.396		0.533		0.275		
O ₈	(O _{IV})	0.2713	0.0005	0.8717	0.0005	0.0940	0.0005	0.51
		0.402		0.906		0.275		
O ₉	(O _V)	0.2188	0.0005	0.1784	0.0005	0.2228	0.0005	0.68
		0.260		0.182		0.381		

This work was supported by a grant from the National Science Foundation. Part of the computation work was carried out at the M. I. T. Computation Center.

Chapter II.

Comparison of the Crystal Structures of Wollastonite and Pectolite.

Abstract

Wollastonite, CaSiO_3 , and pectolite, $\text{CaNaHSi}_3\text{O}_9$, have similar triclinic cells; because of this and their analogous chemical compositions they have long been regarded as belonging to the same mineral family. An examination of the results of least-squares refinement reveals that although the structures contain similar metasilicate chains, they are not as closely isotypic as had been supposed. The principal differences are in the location of the large cations between layers of oxygen atoms parallel to (101) and in the relative orientations of the metasilicate chains.

The structures of both wollastonite and pectolite contain pseudomonoclinic subcells which are joined together on (100) to give an overall symmetry different from that of the subcell. The geometries of these subcells and the possibility of their being joined in different ways are important in explaining the types of twinning which occur in wollastonite and pectolite.

Introduction

Pectolite and wollastonite belong to the same mineral family and have distinct but related crystal structures. Buerger and Prewitt (1962)¹ have shown that the crystal structures proposed by Buerger (1956)² for pectolite and by Mamedov and Belov (1956)³ for wollastonite are correct. The present paper describes in detail the similarities and differences between the two structures and attempts to explain some of the puzzling features of these minerals which have been observed in the past.

¹ Buerger, M.J., and C.T. Prewitt (1962). The crystal structures of wollastonite and pectolite. Chapter I, this thesis.

² Buerger, M.J. (1956). The determination of the crystal structure of pectolite, $\text{Ca}_2\text{NaHSi}_3\text{O}_9$. Z. Krist., 108, 248-261.

³ Mamedov, K.S., and N.V. Belov (1956). Crystal structure of wollastonite. Doklady Akad. Nauk SSSR, 107, 463-466.

Confirmation of the Structures

Unit cell information for pectolite, wollastonite, and NaAsO_3 is given in Table 1. The similarity of the triclinic cells (space group $\underline{P\bar{1}}$) and the analogous chemical compositions indicate that these substances might have the same structure. A comparison of the results given by Mamedov and Belov (1956)¹ for wollastonite and Liebau (1956)² for NaAsO_3 shows that these two structures are identical. If either of these is compared to the pectolite structure given by Buerger (1956)³ certain discrepancies are noted. For example, while in both structures the silicate chains have repeat units of three tetrahedra, they do not have the same orientation in the two structures, and the large cations all lie in a sheet parallel to (101), but do not have the same distribution in the sheet.

In order to determine whether these differences were real,

¹ Mamedov, K. S., and N. V. Belov, op. cit.

² Liebau, Friedrich (1956). "Über die kristallstruktur des natriumpolyarsenats, $(\text{NaAsO}_3)_x$ ". Acta Cryst., 9, 811-817.

³ Buerger, M. J., op. cit.

Table 1. Unit Cells of Wollastonite, NaAsO_3 , and Pectolite.

	Wollastonite		Pectolite
	$\text{Ca}_3\text{Si}_3\text{O}_9$	$\text{Na}_3\text{As}_3\text{O}_9$	$\text{Ca}_2\text{NaHSi}_3\text{O}_9$
<u>a</u>	7.94 Å	8.07 Å	7.99 Å
<u>b</u>	7.32 Å	7.44 Å	7.04 Å
<u>c</u>	7.07 Å	7.32 Å	7.02 Å
α	$90^\circ 82'$	90°	$90^\circ 31'$
β	$95^\circ 22'$	$91^\circ 30'$	$95^\circ 11'$
γ	$103^\circ 26'$	104°	$102^\circ 28'$

Buerger and Prewitt (1962)¹ collected three-dimensional x-ray intensities for wollastonite and refined the structure by least-squares. In addition, they refined pectolite using relatively crude intensity data originally obtained by Buerger (1956)². The final R factors for wollastonite and pectolite, respectively, were 8.9% and 17%. When the structures and x-ray data were interchanged, the wollastonite data could not be refined below 26% and the pectolite data not below 52%. Therefore, the structures as proposed must be correct but different.

Comparison of Structures

Figures 1 and 2 are projections of the wollastonite and pectolite structures along b, respectively. Coordinates for the figures in this paper were given originally by Buerger and Prewitt (1962)¹ and are reproduced in Table 2 with a few changes so that all coordinates refer to atoms in or near the same silicate chain. Unless otherwise noted, the origin for the figures is that of the coordinates of Table 2.

¹ Buerger, M. J., and C. T. Prewitt, op. cit.

² Buerger, M. J., op. cit.

Figure 1.

Projection of the wollastonite structure along b.

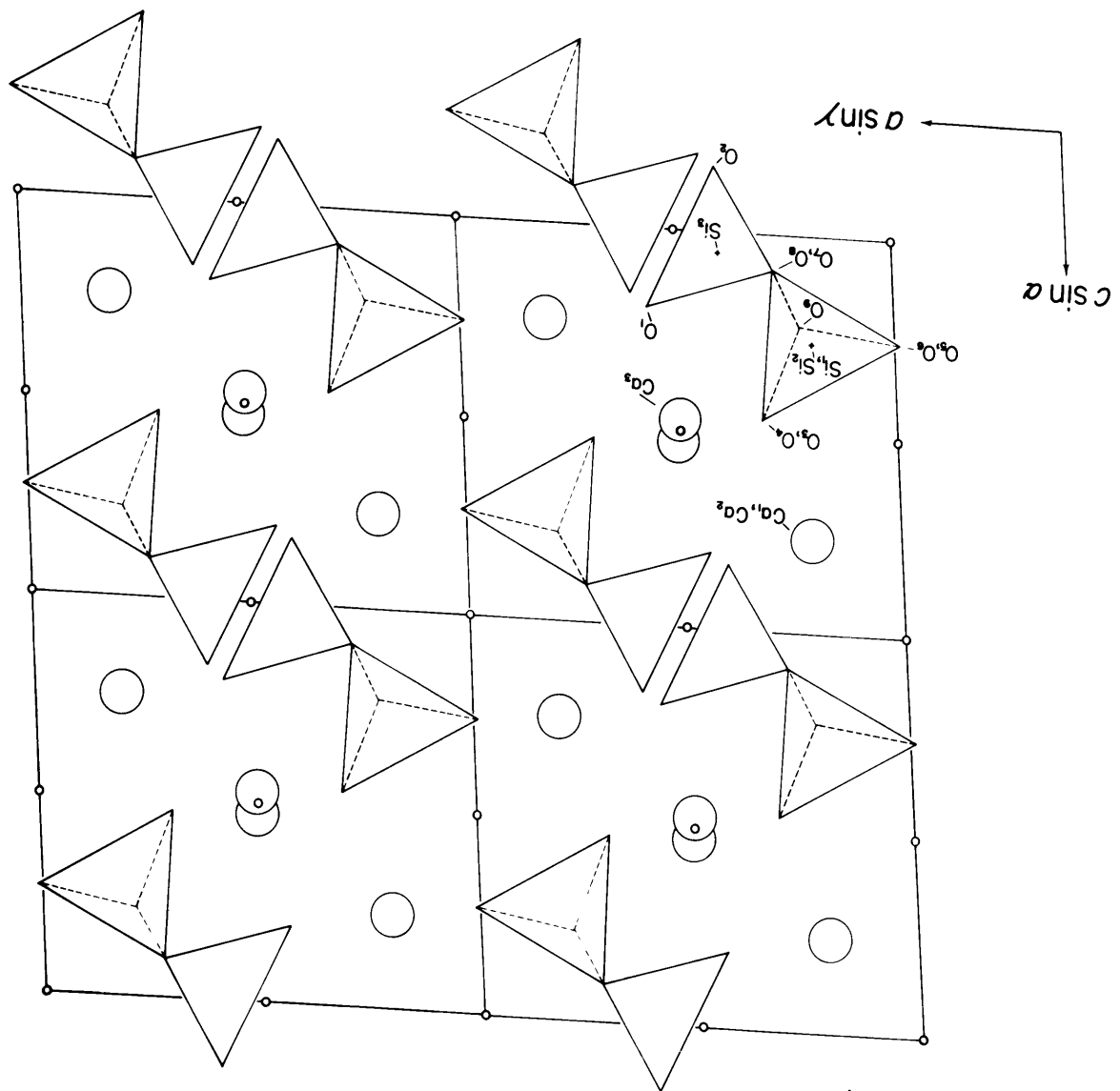


Figure 2.

Projection of the pectolite structure along \underline{b} . Although the Si_1 and Si_2 tetrahedra should not be exactly superimposed, they are presented this way to simplify the drawing.

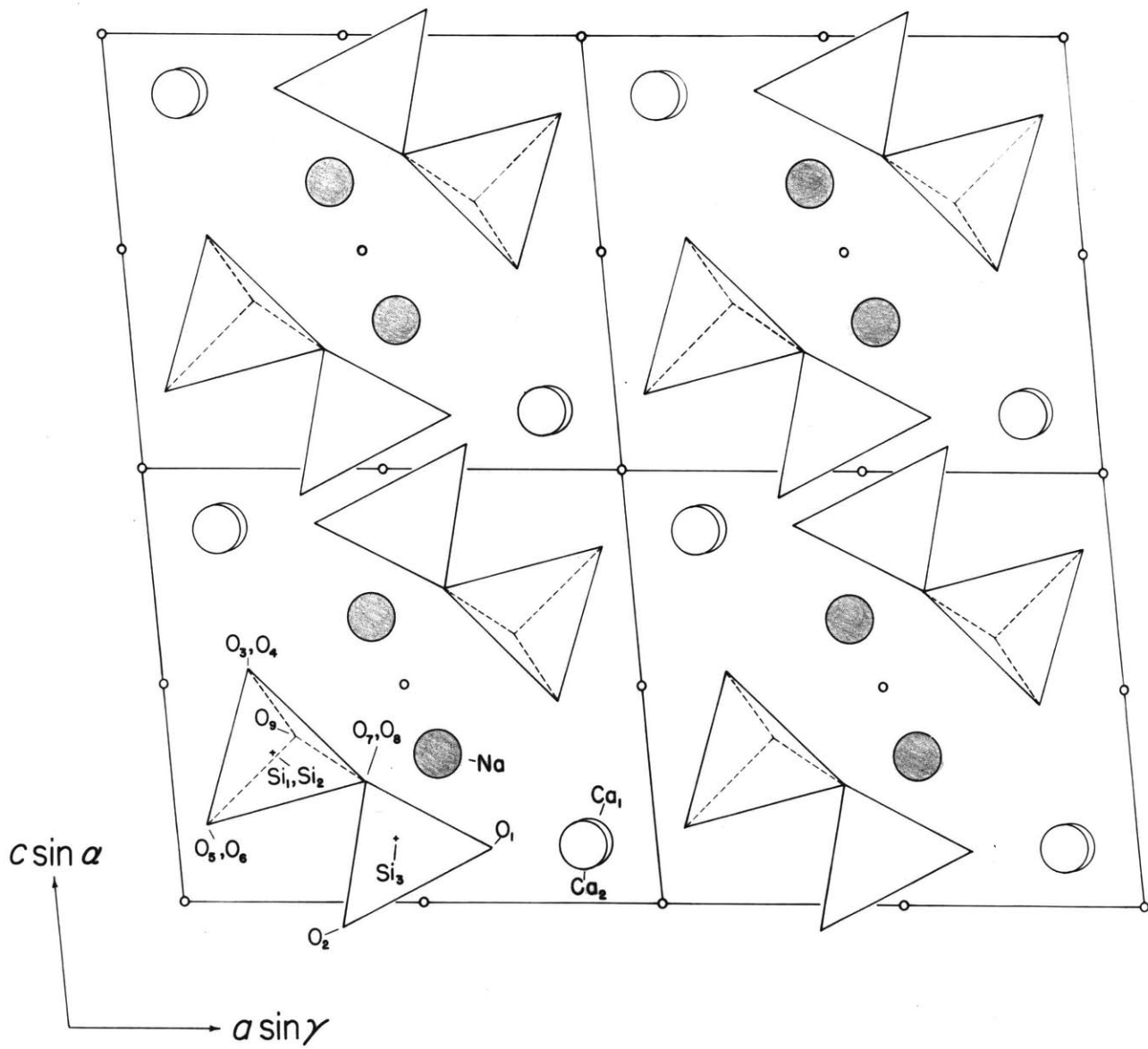


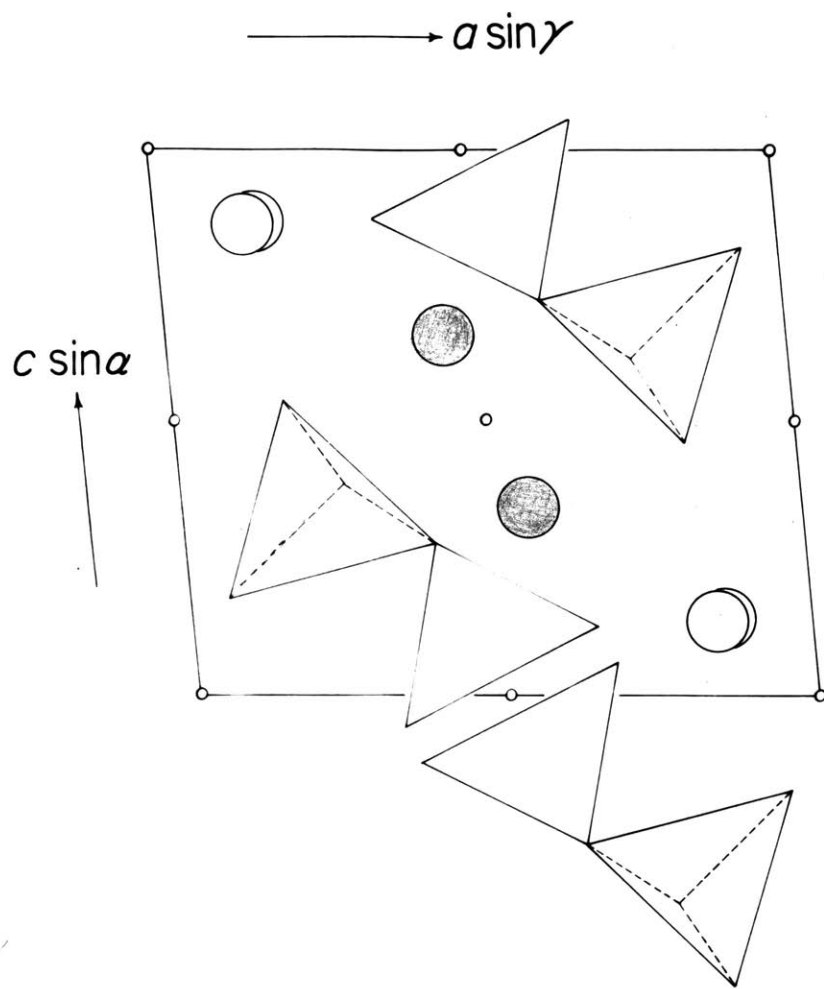
Table 2. Atom Coordinates for Wollastonite and Pectolite.

Wollastonite				Pectolite			
Atom	<u>x</u>	<u>y</u>	<u>z</u>	Atom	<u>x</u>	<u>y</u>	<u>z</u>
Ca ₁	.1985	.4228	.7608	Ca ₁	.857	.596	.146
Ca ₂	.2027	.9293	.7640	Ca ₂	.843	.074	.139
Ca ₃	.5034	.7505	.5280	Na	.552	.265	.344
Si ₁	.1852	.3870	.2687	Si ₁	.221	.402	.337
Si ₂	.1849	.9545	.2692	Si ₂	.210	.954	.344
Si ₃	.3970	.7235	.0560	Si ₃	.451	.735	.148
O ₁	.5709	.7686	.1981	O ₁	.652	.788	.125
O ₂	.4008	.7259	-.1698	O ₂	.322	.702	-.057
O ₃	.3037	.4635	.4641	O ₃	.185	.496	.538
O ₄	.3017	.9374	.4655	O ₄	.171	.839	.541
O ₅	-.0154	.3746	.2657	O ₅	.070	.393	.171
O ₆	-.0175	.8681	.2647	O ₆	.053	.896	.179
O ₇	.2732	.5118	.0919	O ₇	.396	.533	.275
O ₈	.2713	.8717	.0940	O ₈	.402	.906	.275
O ₉	.2188	.1784	.2228	O ₉	.260	.182	.381

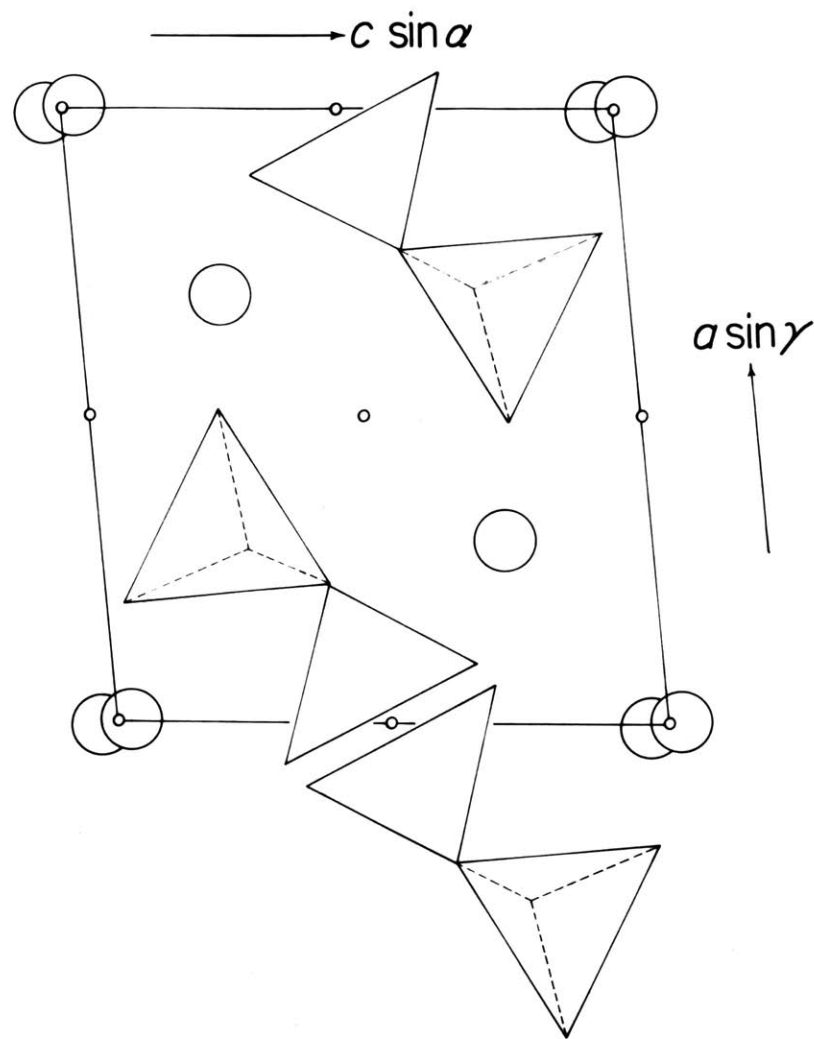
Figures 1 and 2 reveal that the structures are topologically different. For example, the bonds between the superposed Si_1 and Si_2 tetrahedra and the Si_3 tetrahedron are reversed. The large cations, however, occupy approximately the same positions in the two structures. One immediately wonders whether the misfit is merely a result of identical structures being oriented in different ways. The authors spent some time in considering this possibility and found that the structures can be oriented so that the silicate chains are nearly superposed. This is accomplished by interchanging the a and c axes and shifting the origin of one of the structures. Figure 3 shows projections of wollastonite and pectolite along b in which the silicate chains are oriented to correspond with one another. The y coordinates of the atoms in the respective chains are about as close to each other as are the x and z coordinates. The locations of the large cations, however, are not similar. In fact, the large cations occupy completely different interstices between oxygens when the structures are oriented in this way. The structures must then be different even though the packing of oxygens is roughly similar. The authors originally thought that this kind of comparison might be more useful than the conventional one, but further investigation as reported below showed that the conventional orientations should be retained.

Figure 3.

Projections of the pectolite and wollastonite structures along \underline{b} . The origin and orientation of wollastonite has been changed from that of Fig. 1 so that the silicate chains in wollastonite have the same orientation as in pectolite.



PECTOLITE



WOLLASTONITE

Pseudomonoclinic Symmetry

A number of investigators have commented on the unusual features which are observed in x-ray diffraction photographs of wollastonite and pectolite. Among these features are a mirror symmetry between relative even-numbered reciprocal lattice levels normal to \underline{b} , and the presence of a substructure along \underline{b} with a period of $\underline{b}/2$ as indicated by the average spot intensity in even-numbered reciprocal lattice levels normal to \underline{b} being greater than in the odd-numbered levels. Ito (1950)¹ discussed these effects and proposed that triclinic wollastonite could be constructed by starting with a hypothetical monoclinic cell and shifting successive cells along (100) in increments of $\pm \frac{1}{4} \underline{b}$. To this pseudomonoclinic cell he attributed a symmetry of $\underline{P}2/\underline{m}$ or $\underline{P}2_1/\underline{m}$. Figures 4 and 5 show that both wollastonite and pectolite can indeed be so regarded, and that the space group of this unit, which is infinite in the \underline{b} and \underline{c} directions and one unit cell thick along \underline{a} , is $\underline{P}2_1/\underline{m}$. Liebau (1956)² also noticed that NaAsO_3 can be so regarded.

This shift between successive pseudomonoclinic units not only determines the triclinic symmetry in pectolite and wollastonite, but is also the key to twinning in these minerals and probably will be found to be significant in other triclinic metasilicates as well.

¹ Ito, T. (1950). X-ray studies on polymorphism. Maruzen, Tokyo, 93-110.

² Liebau, Friedrich, op. cit.

Figure 4.

Projection of the wollastonite structure along \underline{c} .
The mirror planes and screw axes are elements
of the pseudomonoclinic unit.

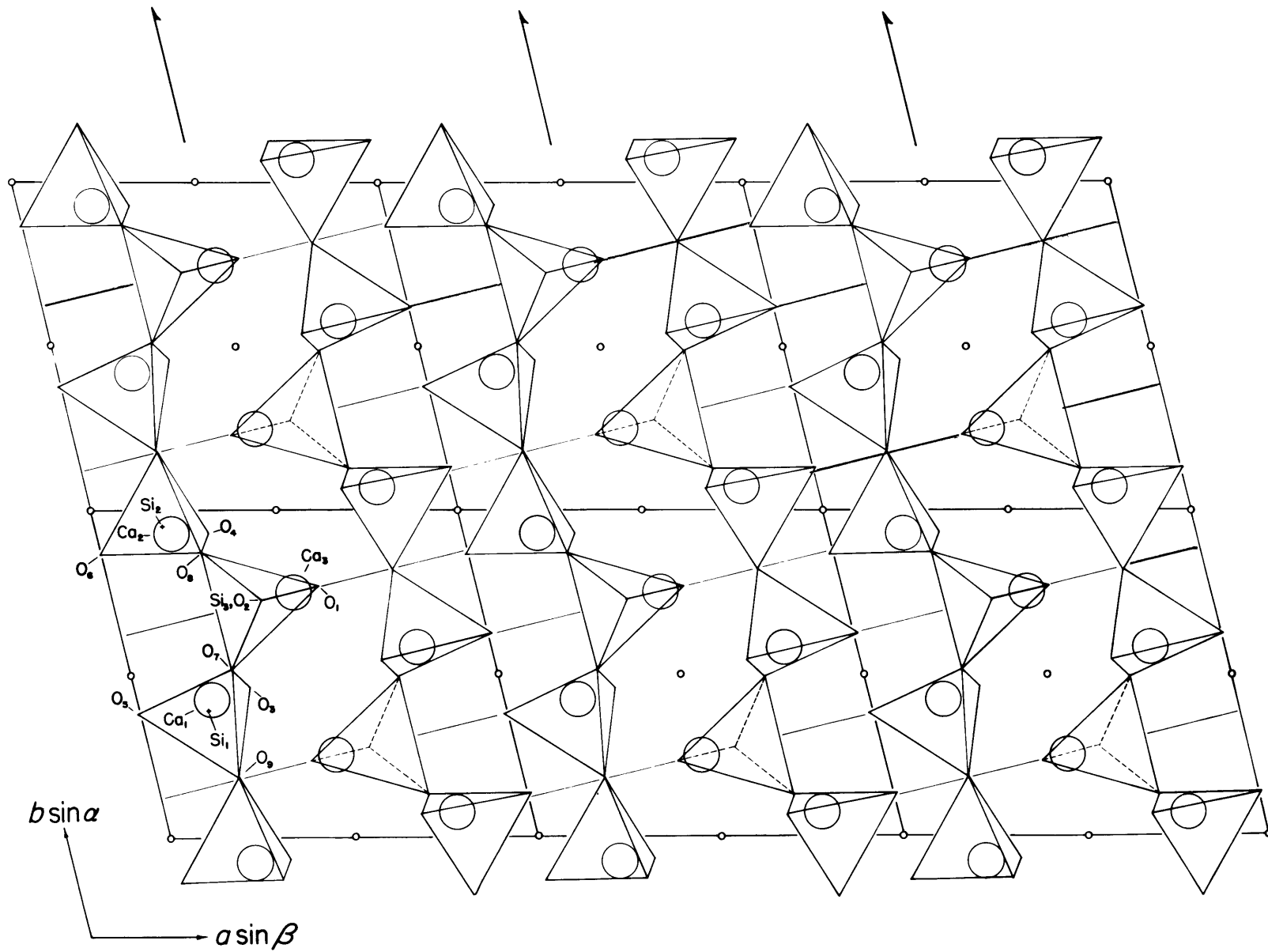
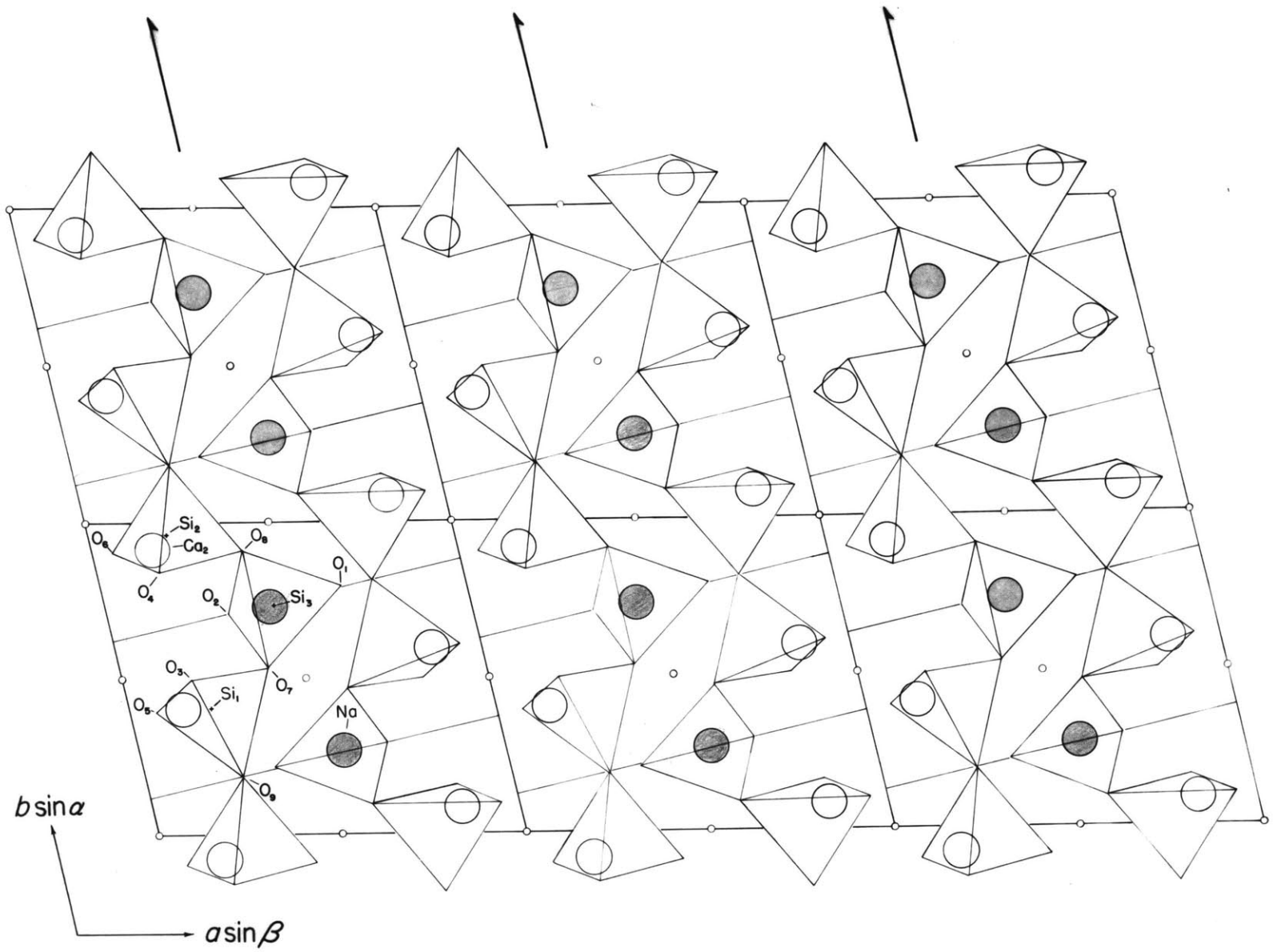


Figure 5.

Projection of pectolite along \underline{c} corresponding to that of wollastonite of Fig. 4. Note that the orientations of the silicate chains are different in the two structures.



The results of the different shifts which can be made are discussed in another section of this paper.

It is interesting to note how closely the refined atom coordinates conform to the monoclinic symmetry. The coordinates were refined in the space group $\underline{P}\bar{1}$ so that all atoms were in the general position with no restrictions on \underline{x} , \underline{y} or \underline{z} . Table 3 gives the wollastonite and pectolite coordinates transformed to the pseudomonoclinic cell using the cell transformation[†]

	Pseudomonoclinic		
	1	-	0
Triclinic	0	1	0
	0	0	1

and adding 0.125 to the transformed \underline{y} coordinates.

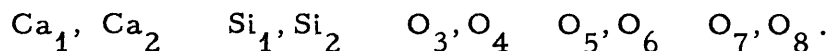
For the atoms Ca_3 , Si_3 , O_1 , O_2 and O_9 in wollastonite, which would be on the mirror plane in $\underline{P}2_1/\underline{m}$, the \underline{y} coordinates should be .250 or .750. The very small deviations of about .001 (or .007 Å) are within the expected accuracy of the measurements. The other atoms which are related by the mirror planes also show little deviation from the positions they would occupy if the mono-

[†] This transformation is not exact when there is a departure of α (triclinic) from 90° ; α in wollastonite is nearly 90° and departs from 90° by only $31'$ in pectolite.

Table 3. Atom Coordinates of Wollastonite and Pectolite referred to a Pseudomonoclinic Cell $\underline{P}2_1/\underline{m}$ (Origin at $\bar{1}$).

Pseudo- equipoint	Wollastonite				Pectolite			
	Atom	\underline{x}	\underline{y}	\underline{z}	Atom	\underline{x}	\underline{y}	\underline{z}
$\underline{4f}$	$2Ca_1$.1985	.4982	.7608	$2Ca_1$.857	.507	.146
	$2Ca_2$.2027	.0038	.7440	$2Ca_2$.843	-.002	.139
$\underline{2e}$	$2Ca_3$.5034	.7496	.5280	$2Na$.552	.252	.344
$\underline{4f}$	$2Si_1$.1852	.4657	.2687	$2Si_1$.221	.472	.337
	$2Si_2$.1849	.0333	.2692	$2Si_2$.210	1.026	.344
$\underline{2c}$	$2Si_3$.3970	.7492	.0560	$2Si_3$.451	.747	.148
$\underline{2e}$	$2O_1$.5709	.7509	.1981	$2O_1$.652	.750	.125
$\underline{2e}$	$2O_2$.4008	.7507	-.1698	$2O_2$.322	.746	-.057
$\underline{4f}$	$2O_3$.3037	.5126	.4641	$2O_3$.185	.575	.538
	$2O_4$.3017	.4870	.4655	$2O_4$.171	.921	.541
$\underline{4f}$	$2O_5$	-.0039	.5035	.2657	$2O_5$.070	.500	.175
	$2O_6$	-.0044	.9975	.2647	$2O_6$.053	1.008	.179
$\underline{4f}$	$2O_7$.2732	.5685	.0919	$2O_7$.396	.559	.275
	$2O_8$.2713	.9287	.0940	$2O_8$.402	.930	.275
$\underline{2e}$	$2O_9$.2188	.2487	.2228	$2O_9$.260	.242	.381

clinic symmetry held. If the space group $\underline{P}2_1/\underline{m}$ is assumed, then the following paired atoms are equivalent and occupy the general position:



$\text{Ca}_3, \text{Si}_3, \text{O}_1, \text{O}_2$ and O_9 are each in the special positions \underline{m} .

Although the atoms in pectolite have the same pseudo-equipoint distributions as do those in wollastonite, the refined coordinates for the pectolite atoms do not conform as closely to the monoclinic symmetry. For example, the \underline{y} coordinate of O_9 is .242 as compared with .250 if O_9 were on the mirror plane. This is a deviation of about 0.06\AA . A detailed refinement of pectolite now being carried out in this laboratory will determine whether these deviations in the pectolite coordinates are real.

The pseudosymmetry gives rise to the strong substructure along \underline{b} , since all the atoms except O_7 and O_8 in both wollastonite and pectolite and Na in pectolite have \underline{x} and \underline{z} coordinates similar to another atom of the same type located $\frac{1}{2}\underline{b}$ away. It is interesting that Ca_3 and its inversion equivalent in wollastonite have similar \underline{x} and \underline{z} coordinates and are approximately $\frac{1}{2}\underline{b}$ apart, while Na and its inversion equivalent in pectolite do not have similar \underline{x} and \underline{z} coordinates even though they are separated by $\frac{1}{2}\underline{b}$. This is one of

the major differences between these minerals.

The similarities and differences between wollastonite and pectolite brought out in this section seem to be more useful in describing the structures than do those in the last section where a special orientation of one of the structures was used to show how the silicate chains could be superposed. Because of this, the authors feel that the conventional orientation should be retained and that while the other aspect is interesting, it will not be useful except, for example, in a classification of metasilicates based on oxygen packing.

Distribution of Ca and Na

The main difference in the wollastonite and pectolite structures is in the way the large cations are distributed in the sheet parallel to (101). Figures 6 and 7 show parts of the wollastonite and pectolite structures projected onto (101) of the pseudomonoclinic cell. Only the silicate chains on the upper side of (101) are shown.

The Ca in wollastonite are arranged in a nearly planar hexagonal pattern which is separated into bands 3 Ca columns wide running in the \underline{b} direction and parallel to the silicate chains.

Fig. 6

Structure of wollastonite projected onto (101) of four adjacent pseudomonoclinic cells. Only the silicate chains on the near side of (101) are shown. The axial directions are for the pseudomonoclinic cell.

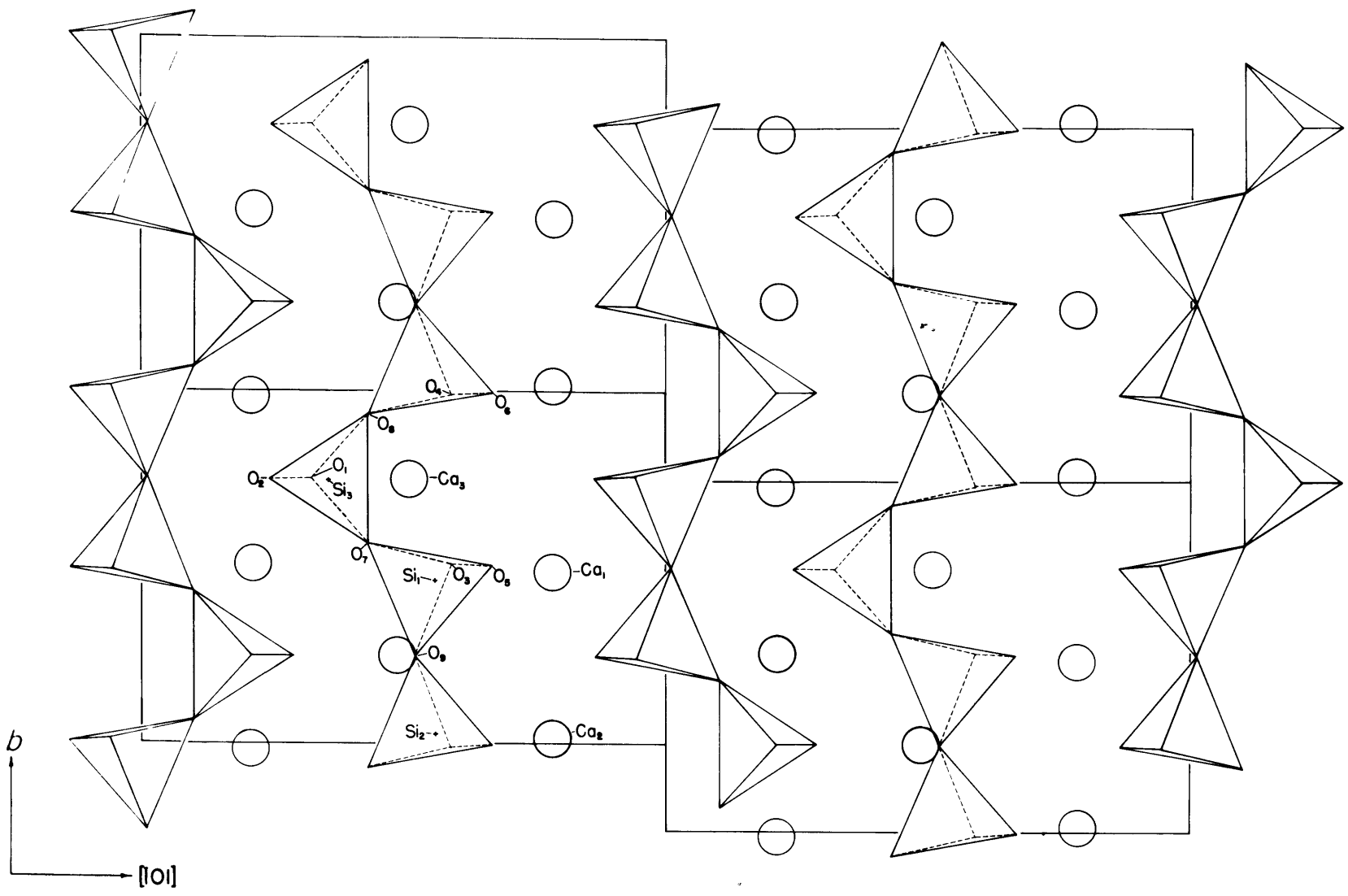
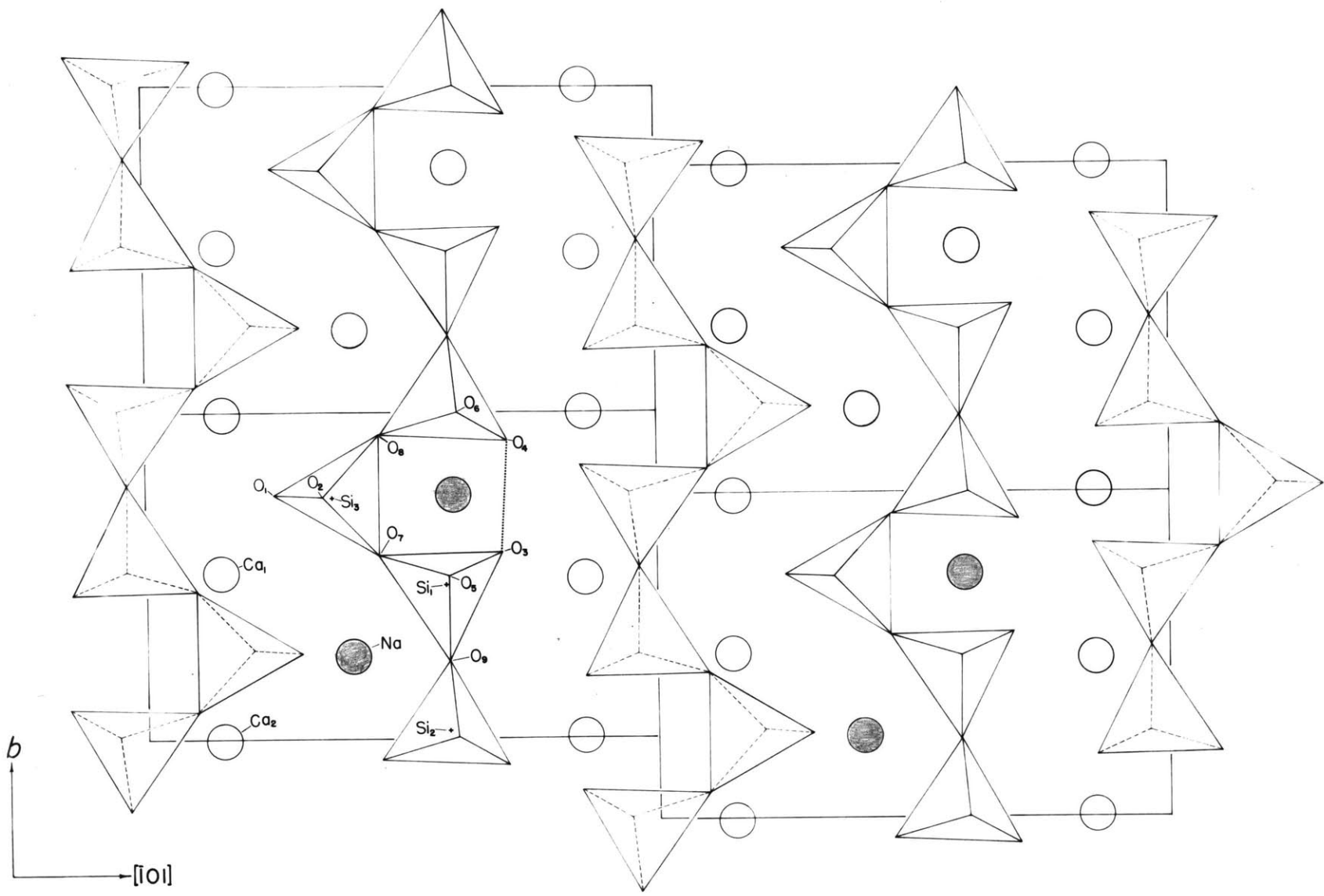


Figure 7 .

Structure of pectolite projected onto (101) of the four adjacent pseudomonoclinic cells. Only the silicate chains on the near side of (101) are shown. The most likely location for the hydrogen bond is indicated by the dotted line between the labeled O_3 and O_4 .



The Na and Ca in pectolite are also arranged in a hexagonal pattern with bands consisting of 2 Ca columns bounded on either side by a half-filled Na column. Because each of these bands is translated by $\frac{1}{4}b$ with respect to neighboring bands, every other Na in a particular Na column is missing. This is necessary because otherwise the Na-Na distances between neighboring Na columns would be much too small.

Interatomic Distances and Interbond Angles.

Interatomic distances and angles given in Table 4 were calculated for wollastonite and pectolite using a computer program written by Busing and Levy (1959)¹. The Si-O distances in both wollastonite and pectolite show a considerable variation, the lengths apparently being determined by the coordinations of the oxygens. Table 5 gives the coordination and distances of cations around the oxygens. It can be seen that, for O₁ through O₆ of wollastonite, the Si-O distances are longer when an oxygen is coordinated by 3 Ca than when coordinated by 2 Ca. The situation

¹ Busing, William R., and Henri A. Levy (1959). A crystallographic function and error program for the IBM 704/ Oak Ridge National Laboratory Central Files No. 59-12-3. Oak Ridge, Tenn. 1-95.

Table 4. Interatomic Distances and Interbond Angles in Wollastonite and Pectolite.

Atoms		Interatomic Distances	
		Wollastonite	Pectolite
Si ₁	O ₃	1.61 ₈ Å	1.63 Å
	O ₅	1.57 ₂	1.59
	O ₇	1.65 ₉	1.60
	O ₉	1.64 ₇	1.67
	O _{av}	1.62 ₄	1.62
Si ₂	O ₄	1.61 ₇	1.63
	O ₆	1.58 ₁	1.61
	O ₈	1.65 ₀	1.75
	O ₉	1.63 ₇	1.58
	O _{av}	1.62 ₁	1.64
Si ₃	O ₁	1.59 ₉	1.59
	O ₂	1.59 ₉	1.68
	O ₇	1.66 ₅	1.68
	O ₈	1.67 ₃	1.63
	O _{av}	1.63 ₄	1.65
Ca ₁	O ₁	2.30 ₂	2.33
	O ₂	2.27 ₂	2.31
	O ₃	2.32 ₄	2.35
	O ₅	2.30 ₂	2.35
	O ₅ ¹	-	2.44
	O ₆	2.27 ₂	2.34
	O ₇	2.41 ₂	-
	O _{av}	2.31 ₄	2.35

(Table 4 continued)

Atoms		Wollastonite	Pectolite
Ca ₂	O ₁	2.50 ₁	2.30
	O ₂	2.42 ₁	2.25
	O ₄	2.31 ₆	2.32
	O ₅	2.36 ₈	2.51
	O ₆	2.31 ₆	2.35
	O ₆ [†]	-	2.45
	O ₈	2.40 ₆	-
	O _{av}	2.38 ₈	2.36
Ca ₃	O ₁	2.43 ₉	
	O ₂	2.34 ₉	
	O ₃	2.42 ₉	
	O ₃ [†]	2.33 ₅	
	O ₄	2.44 ₁	
	O ₄ [†]	2.34 ₉	
	O ₉	2.64 ₂	
	O _{av}	2.39 ₀ (excluding Ca ₃ -O ₉)	
Na	O ₂		2.32
	O ₃		2.46
	O ₄		2.54
	O ₇		2.50
	O ₇ [†]		2.97
	O ₈		2.57
	O ₈ [†]		2.97
	O ₉		2.32
	O _{av}		2.45 (excluding Na-O ₇ [†] , Na-O ₈ [†])

(Table 4 continued)

Atoms		Wollastonite	Pectolite
Si ₁	Si ₂	3.16 ₅	3.10
	Si ₃	3.11 ₆	3.04
Si ₂	Si ₃	3.12 ₅	3.11
Interbond Angles			
Si ₁ - O ₉ - Si ₂		149.0°	149.5°
Si ₂ - O ₈ - Si ₃		140.0°	134.7°
Si ₃ - O ₇ - Si ₁		139.0°	136.1°

is different for O_7 through O_9 because these oxygens are coordinated by 2 Si as well as Ca, showing that Pauling's rule does not hold. The Si-O distances here are larger than in either of the examples above. The coordination of oxygens in wollastonite can thus be divided into three classes:

1. Oxygen coordinated by one Si and three Ca (O_1 , O_2 , O_3 , O_4);
2. Oxygen coordinated by one Si and two Ca (O_5 , O_6);
3. Oxygen coordinated by two Si and one Ca (O_7 , O_8 , O_9).

It is felt that an analysis of the pectolite interatomic distances before a detailed refinement is completed would be premature, particularly since the range in Si-O distances is so great, varying from 1.58\AA for Si_2-O_9 to 1.75\AA for Si_2-O_8 . This may be a real variation, however, since Morimoto, Appleman and Evans (1960)¹ reported a range of $1.58 - 1.74\text{\AA}$ for Si-O in clinoenstatite.

Ca_1 and Ca_2 in wollastonite are octahedrally coordinated by six oxygen atoms at average distances of 2.38_3\AA for Ca_1 and 2.38_8\AA for Ca_2 . Ca_3 is surrounded by six oxygen atoms at an average distance of 2.39_0\AA and by an additional oxygen (O_9) at

¹ Morimoto, N., D.E. Appleman and H. T. Evans (1960). The crystal structures of clinoenstatite and pigeonite. *Z. Krist.*, 114, 120-147.

Table 5. Coordination of Oxygens in Wollastonite and Pectolite.

Wollastonite			Pectolite		
Atoms		Interatomic Distances	Atoms		Interatomic Distances
O ₁	Si ₃	1.59 ₉ Å	O ₁	Si ₃	1.59 Å
	Ca ₁	2.30 ₂		Ca ₁	2.33
	Ca ₂	2.31 ₆		Ca ₂	2.30
	Ca ₃	2.43 ₉			
O ₂	Si ₃	1.59 ₉	O ₂	Si ₃	1.68
	Ca ₁	2.27 ₂		Ca ₁	2.31
	Ca ₂	2.36 ₉		Ca ₂	2.25
	Ca ₃	2.34 ₉		Na	2.32
O ₃	Si ₁	1.61 ₈	O ₃	Si ₁	1.63
	Ca ₁	2.32 ₄		Ca ₁	2.35
	Ca ₃	2.42 ₉		Na	2.46
	Ca ₃ [†]	2.33 ₅			
O ₄	Si ₂	1.61 ₇	O ₄	Si ₂	1.63
	Ca ₂	2.42 ₁		Ca ₂	2.32
	Ca ₃	2.44 ₁		Na	2.54
	Ca ₃ [†]	2.34 ₉			
O ₅	Si ₁	1.57 ₂	O ₅	Si ₁	1.59
	Ca ₁	2.30 ₂		Ca ₁	2.35
	Ca ₂	2.50 ₁		Ca ₁ [†]	2.44
		Ca ₂		2.51	

(Table 5 continued)

O ₆	Si ₂	1.58 ₁		O ₆	Si ₂	1.61
	Ca ₁	2.27 ₂			Ca ₁	2.34
	Ca ₂	2.50 ₁			Ca ₂	2.35
					Ca ₂ ^t	2.45
O ₇	Si ₁	1.65 ₉		O ₇	Si ₁	1.60
	Si ₃	1.66 ₅			Si ₃	1.68
	Ca ₁	2.41 ₂			Na	2.50
					Na ^t	
O ₈	Si ₂	1.65 ₀		O ₈	Si ₂	1.75
	Si ₃	1.67 ₃			Si ₃	1.63
	Ca ₂	2.40 ₆			Na	2.57
					Na ^t	
O ₉	Si ₁	1.64 ₇		O ₉	Si ₁	1.67
	Si ₂	1.63 ₇			Si ₂	1.58
	Ca ₃	2.64 ₂			O ₉	2.39

2.64₂ Å. The Ca-O sheet is similar to a brucite sheet separated into slabs running along \underline{b} and distorted by the presence of O₉.

The coordination of Ca₁ and Ca₂ in pectolite is similar to that of Ca₁ and Ca₂ in wollastonite with an average Ca₁-O distance of 2.35 Å and an average Ca₂-O distance of 2.36 Å. Na is surrounded by six oxygen atoms at an average distance of 2.45 Å, and two further oxygen atoms, both at 2.97 Å.

The most probable location for the hydrogen bond in pectolite is between O₃ and O₄. These atoms are separated by 2.44 Å which is short even for a hydrogen bond. This is represented by a dotted line between the labelled O₃ and O₄ in Fig. 7. This separation is much less than between similar atoms in the wollastonite chain as seen in Fig. 6. Buerger (1956)¹ attributed the presence of a shorter \underline{b} axis in pectolite than in wollastonite to the hydrogen bond. In both structures, the silicon-oxygen-silicon angles have the same distribution, with Si₁-O₉-Si₂ being larger than Si₂-O₈-Si₃ and Si₃-O₇-Si₁, which are approximately equal. This difference results from the somewhat abnormal location of O₉ in the oxygen sheet.

¹ Buerger, M.J., op. cit.

Twinning

One of the most interesting aspects of the pectolite and wollastonite structures is the way in which twinning can occur. Mention has already been made of the way in which pseudomonoclinic subcells are fitted together to give a triclinic structure. This is shown schematically in Fig. 8b. It is also possible to reverse the shift between successive pseudomonoclinic subcells to give the sequence shown in Fig. 8a, which corresponds to a twinned structure. If, however, the shift is reversed in each successive cell, the effect is as shown in Fig. 8c. This sequence was suggested by Ito (1950)¹ for parawollastonite² which was originally distinguished from wollastonite by Peacock (1935a)³.

Peacock (1935b)⁴ found that the twin law in pectolite is such that \underline{b} is the twin axis with (100) as the composition plane. This is consistent with Fig. 8a since a rotation of 180° around \underline{b} of one of the pseudomonoclinic units would be approximately equivalent to

¹ Ito, T., op. cit.

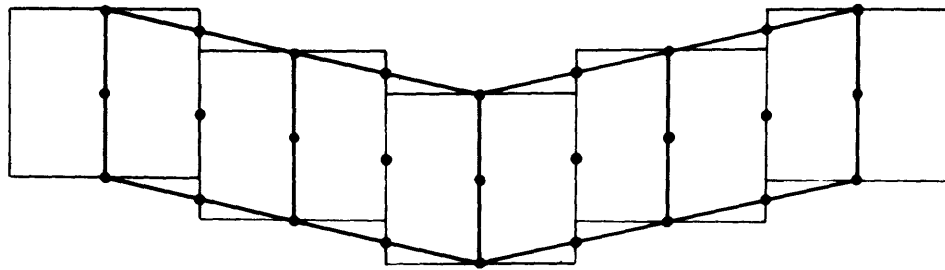
² The Commission on Mineral Data recommended at the meeting of the International Mineralogical Association in Washington, D. C., April 17-20, 1962, that wollastonite and parawollastonite be redesignated wollastonite-1T and wollastonite-2M, respectively.

³ Peacock, M. A. (1935a). On wollastonite and parawollastonite. *Am. J. Sci.*, 30., 495-529.

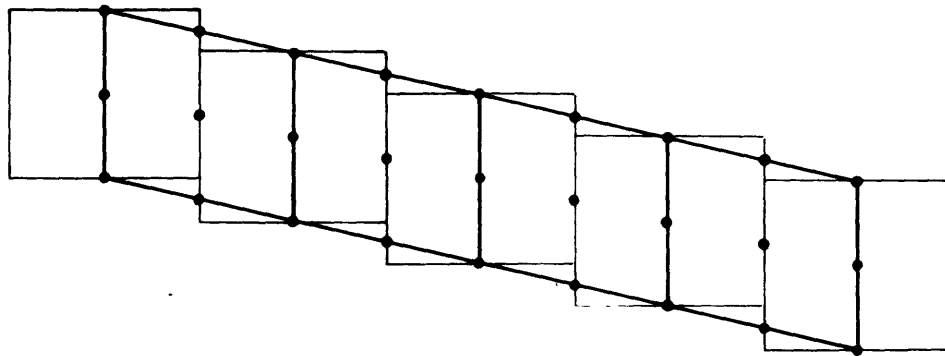
⁴ Peacock, M. A. (1935b). On pectolite. *Zeit. Krist.* 90, 97-111.

Figure 8.

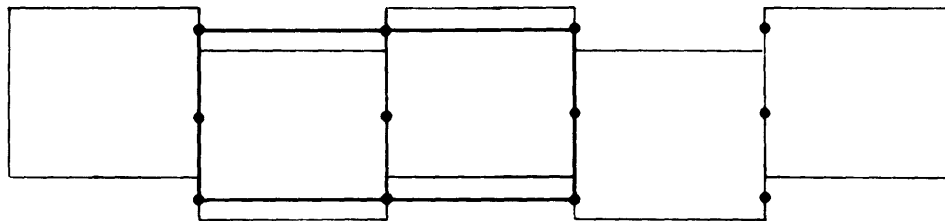
Fig. 8a (top), b (middle) and c (bottom). Three ways in which the pseudomonoclinic unit can be stacked on (100) to produce different overall diffraction effects.



TWINNED



TRICLINIC



MONOCLINIC

translating it by $\frac{1}{2}\underline{b}$ along a neighboring cell. This is not exactly true unless the cell is actually monoclinic, thus making α (triclinic) equal to 90° . The authors have taken x-ray photographs of several twinned pectolite crystals from various localities and have found that the diffraction effects substantiate the above ideas. Fig. 9a represents part of the composite reciprocal lattice of twinned pectolite. When the members of the twin are present in equal amount, oscillating crystal photographs around \underline{b} , as well as \underline{c} -axis precession photographs, show an apparent mirror plane normal to \underline{b} . Close examination of the films reveals, however, that the registry of superposed spots is not perfect and that the registry is slightly different in different specimens.

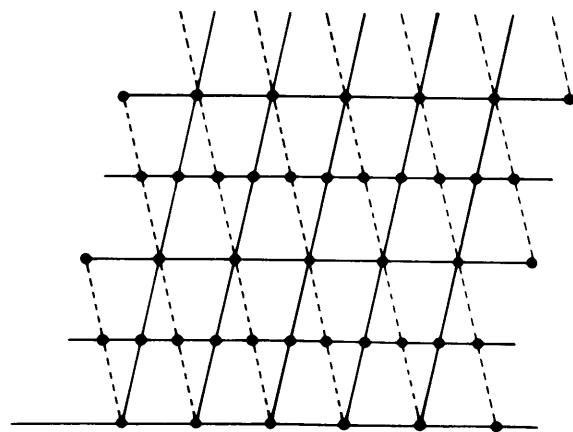
If the pseudomonoclinic cells are joined as in Fig. 8c, the parawollastonite structure is formed having an overall monoclinic symmetry with a doubling of the cell along \underline{a} . The symmetry of this monoclinic cell should be $\underline{P}2_1/\underline{a}$ with extra centers of symmetry, not required by the space group¹, being present. In an attempt to refine the structure of parawollastonite, however, Tolliday (1958)² found that the structure could not be refined using

¹ Tolliday (1958) gives the systematic absences in the parawollastonite diffraction pattern as: for \underline{hkl} , $2\underline{h} + \underline{k} = 4\underline{n} + 2$, and for $0\underline{k}0$ as $\underline{k} = 2\underline{n} + 1$.

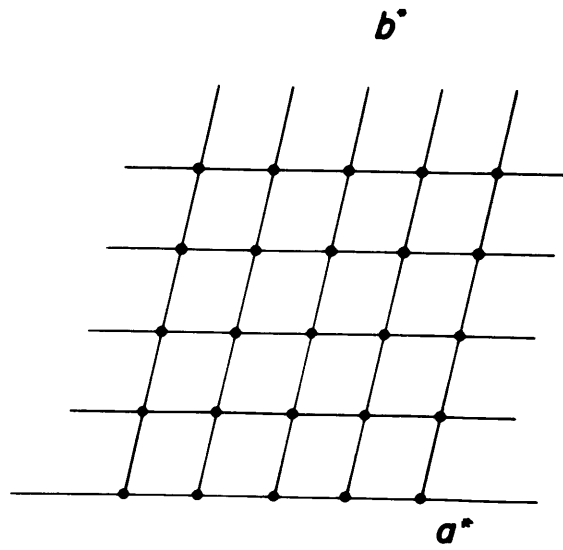
² Tolliday, Joan (1958). Crystal structure of β -wollastonite. Nature, 182, 1012-1013.

Figure 9

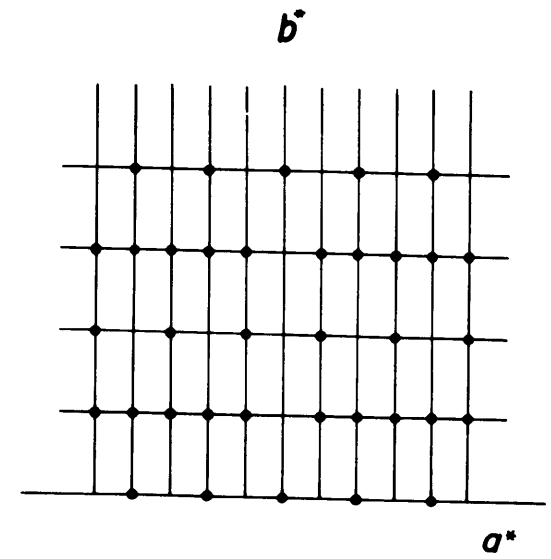
Figure 9a (left), 9b (middle) and 9c (right). Reciprocal lattices corresponding to the geometries shown in Figs. 8a, 8b, and 8c.



TWINNED



TRICLINIC



MONOCLINIC

the centrosymmetric space group $\underline{P}2_1/\underline{a}$ and that when the non-centrosymmetric space $\underline{P}2_1$ was assumed, the refinement proceeded satisfactorily. Since no coordinates, structure factors or \underline{R} -factors were published, the validity of this assumption cannot be evaluated. This is an extremely important point in the crystal chemistry of CaSiO_3 and one which should be resolved.

One of the interesting features of Figs. 9a, 9b, and 9c is that the reciprocal-lattice levels with \underline{k} even are identical (when $\alpha = 90^\circ$) and that the differences between triclinic, monoclinic and twinned composite reciprocal lattices occur in only the odd levels. It is simpler for wollastonite than for pectolite to alternate to form the parawollastonite type because α in wollastonite is 90° (within experimental error) and because the symmetry of the repeating unit in wollastonite is nearly monoclinic, i. e., the Si_1 and Si_2 tetrahedra, as well as Ca_1 and Ca_2 , are symmetrically equivalent. The authors examined several wollastonite specimens from the Monte Somma, Italy, Csiklova, Romania, and Crestmore, California, localities before finding one which gave a parawollastonite diffraction pattern.¹ Continuous radiation streaks along reciprocal lattice rows parallel to \underline{a}^* were observed in the \underline{b} -axis Weissenberg photographs with \underline{k} odd for the monoclinic as well as several triclinic specimens.

¹ The parawollastonite crystal (locality: Crestmore, California) was supplied by Professor A. Pabst from a specimen, 138-80, in the University of California collection.

This effect was interpreted by Jeffery (1953)¹ as a type of disorder due to the presence of regions of wollastonite and parawollastonite, but it could also be thought of as an irregular sequence of pseudo-monoclinic subcells.

Peacock (1935a)² was unable to find any twinned triclinic wollastonite in the material available to him. Spencer (1903)³, however, reported a twinned wollastonite crystal from Chiapas, Mexico, which would presumably give a diffraction pattern similar to our twinned pectolite. It is possible that some of the material reported in the literature as ordered parawollastonite is actually twinned wollastonite. One could be misled by diffraction photographs if the members of the twin were present in equal amounts.

One point which should be brought out here is that the way in which these pseudomonoclinic units fit together results in what Ito (1950)⁴ called "space-group twinning" and "structure twinning". The "space-group twinning" is seen in the joining of pseudomonoclinic cells to give an overall triclinic or a different monoclinic symmetry, while "structure twinning" corresponds to our twinned pectolite. This may be a valuable concept in an attempt to classify the triclinic metasilicates.

¹Jeffery, J. W. (1953). Unusual diffraction effects from a crystal of wollastonite. *Acta Cryst.*, 6, 821-825.

²Peacock, M. A. (1935a) op. cit.

³Spencer, L. J. (1903). see paper by Collins, H. F. *Min. Mag.*, 13, 356-362,

⁴Ito, T. (1950). op. cit.

Conclusions

It has been established that wollastonite and pectolite have many structural similarities, but yet must be classified as having different structures. Whether the pseudomonoclinic unit found in both wollastonite and pectolite will be of significance in an overall classification of the triclinic metasilicates will depend on the results of structural investigation of such minerals as bustamite, rhodonite and pyroxmangite. This pseudomonoclinic unit at present appears to be important in determining the relations between different modifications of a particular mineral in the wollastonite series. Its departure from actual monoclinic symmetry may also be a controlling factor in determining what forms of a particular triclinic metasilicate can occur. Certainly, any study of the stability relations of wollastonite and parawollastonite would have to be concerned with the details of the structures to a greater extent than is usual in such investigations, because the difference in energy between the two structures must be quite small.

Acknowledgements

The authors wish to express thanks to Professor Clifford Frondel and Dr. Alden Carpenter of Harvard University, Professor Adolf Pabst of the University of California and Dr. George Switzer of the U.S. National Museum for supplying much of the material used in this investigation, and to Donald R. Peacor for many helpful discussions. This work was supported by the National Science Foundation. The computations were carried out at the M. I. T. Computation Center.

Chapter III.

Drilling Coordinates for Crystal Structure Models

Abstract

Calculation of the spherical drilling coordinates, ρ and ϕ , for crystal structure models often requires a prohibitive amount of time, especially for structures of low symmetry. The coordinates are readily calculated using a vector algebraic method which is applicable to any crystal system. This method is designed for computation with a digital computer.

INTRODUCTION

Many papers have described the construction of crystal structure models¹. In those methods in which the structure is represented by balls connected with rigid pins, it is necessary to drill holes in the balls to maintain interatomic angles. Several drilling devices have been described²⁻⁴ which may be used to drill these holes if the spherical drilling coordinates are known. Calculation of these drilling coordinates, ρ and ϕ , may be the most time-consuming part of building a crystal structure model, especially when the structure is one of low symmetry. Because of this, the structure is often "idealized" to save computation time, thus obscuring important structural features.

A straightforward method of calculating drilling coordinates for any crystal system has been developed. This method is easily programmed for a digital computer and has been used in the construction of complex crystal structure models.

COORDINATE SYSTEMS

Computations are most easily carried out if atom positions are known relative to an orthogonal coordinate system in which coordinates are given directly in angstroms. The transformation

of coordinates from a general axial system to an orthogonal system is given by

$$\begin{aligned} p_i &= x_i a + y_i (b \cos \gamma) + z_i (c \cos \beta) \\ q_i &= y_i (b \sin \gamma) - z_i (c M) \\ r_i &= z_i [c(\sin^2 \beta - M^2)^{\frac{1}{2}}] \end{aligned} \quad (1)$$

where \underline{a} , \underline{b} , \underline{c} , α , β and γ are unit cell parameters of the original axial system; \underline{x}_i , \underline{y}_i and \underline{z}_i are fractional coordinates of atom \underline{i} relative to this system; \underline{p}_i , \underline{q}_i and \underline{r}_i are coordinates of atom \underline{i} based upon an orthogonal axial system, and

$$M = (\cos \beta \cos \gamma - \cos \alpha) / \sin \gamma.$$

The coordinate axes are fixed so that, if \underline{i} , \underline{j} and \underline{k} are unit vectors of the orthogonal coordinate system, \underline{i} and \underline{a} are colinear and \underline{i} , \underline{j} , \underline{a} and \underline{b} are coplanar.

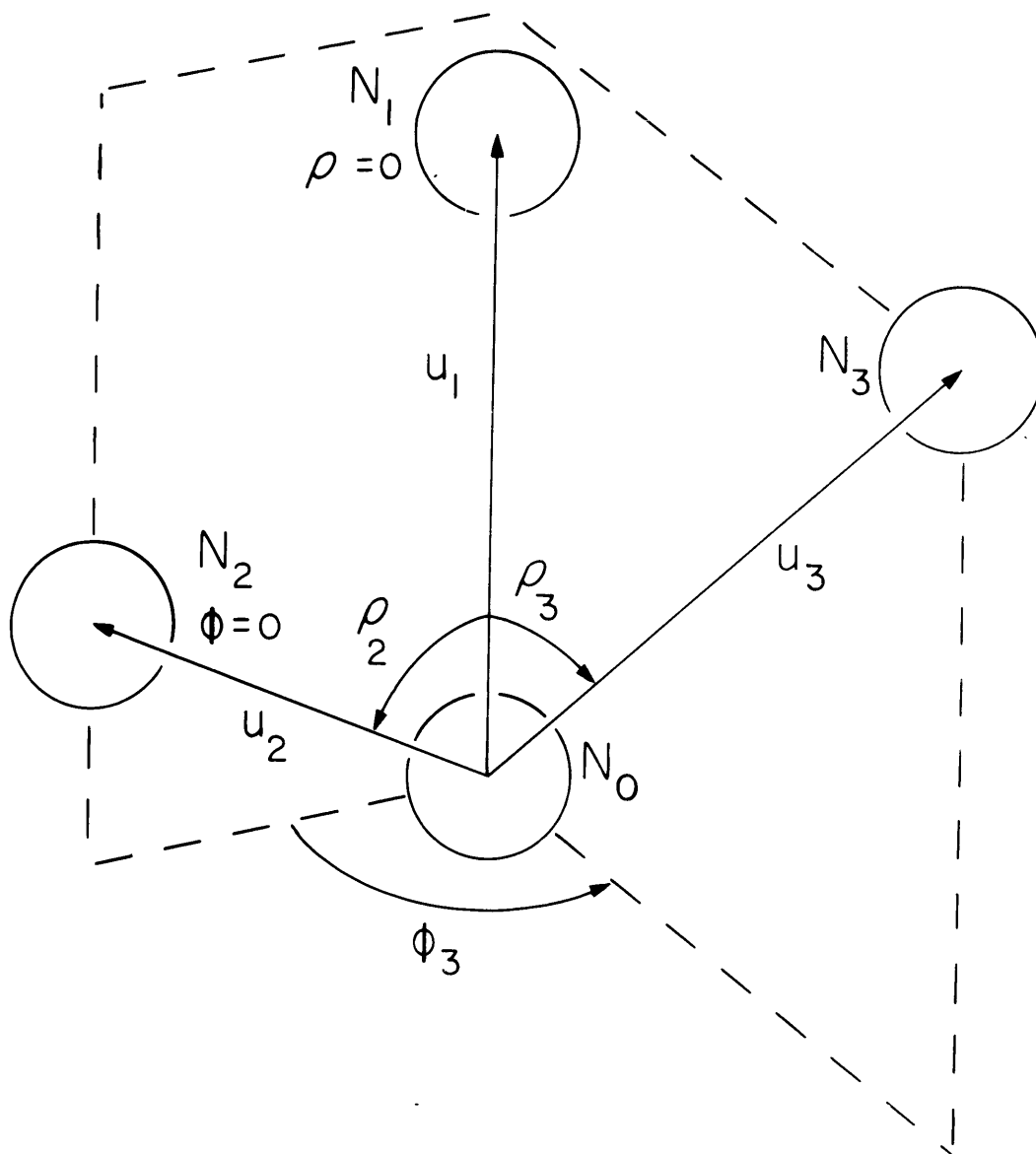
Consider a coordination group of \underline{n} atoms, designated by \underline{N}_i ($i = 1, 2, \dots, n$), which surrounds a central atom \underline{N}_0 . All atoms are at the ends of vectors \underline{s}_i from the unit cell origin, where

$$s_i = (p_i^2 + q_i^2 + r_i^2)^{\frac{1}{2}}. \quad (2)$$

The vector $\underline{u}_i = \underline{s}_i - \underline{s}_0$ is the vector from the central atom to one of the coordinating atoms. Figure 1 shows the spherical coordinate system used in computing the drilling angles. Atom \underline{N}_0 is at the origin, the vector \underline{u}_1 defines the direction $\rho = 0$, and the plane containing \underline{u}_1 and \underline{u}_2 defines the condition $\phi = 0$. The drilling coordinates of any atom \underline{N}_i , say \underline{N}_3 , are computed from these

Figure 1

Coordination group of atoms \underline{N}_1 , \underline{N}_2 , \underline{N}_3 and central atom \underline{N}_0 , and its relation to the spherical coordinate system.



fixed positions.

CALCULATION OF ρ AND ϕ

For all atoms \underline{N}_i ($i = 1, 2, \dots, n$) coordinating the central atom \underline{N}_0 ,

$$\rho_i = \cos^{-1} \frac{\underline{u}_1 \cdot \underline{u}_i}{u_1 u_i} \quad (3)$$

Figure 2 shows the vectors \underline{u}_2 and \underline{u}_3 projected onto a plane which is normal to \underline{u}_1 . Any angle ϕ_i , say ϕ_3 , is measured in this plane. Let $\text{proj. } \underline{u}_2$ define the direction $\phi = 0$ in this plane. Then ϕ_i is the angle, taken counterclockwise, from $\text{proj. } \underline{u}_2$ to $\text{proj. } \underline{u}_i$.

Consider a vector $\underline{v}_i = \underline{u}_1 \times \underline{u}_i$. All such vectors are normal to \underline{u}_1 and therefore lie in the plane of Fig. 2. Furthermore, the angle between \underline{v}_2 and \underline{v}_i is ϕ_i' , whose magnitude may be determined by

$$\phi_i' = \cos^{-1} \frac{\underline{v}_2 \cdot \underline{v}_i}{v_2 v_i} \quad (4)$$

where, since ϕ may vary from 0 to 2π , and since the cosine function is unique only in the region 0 to π ,

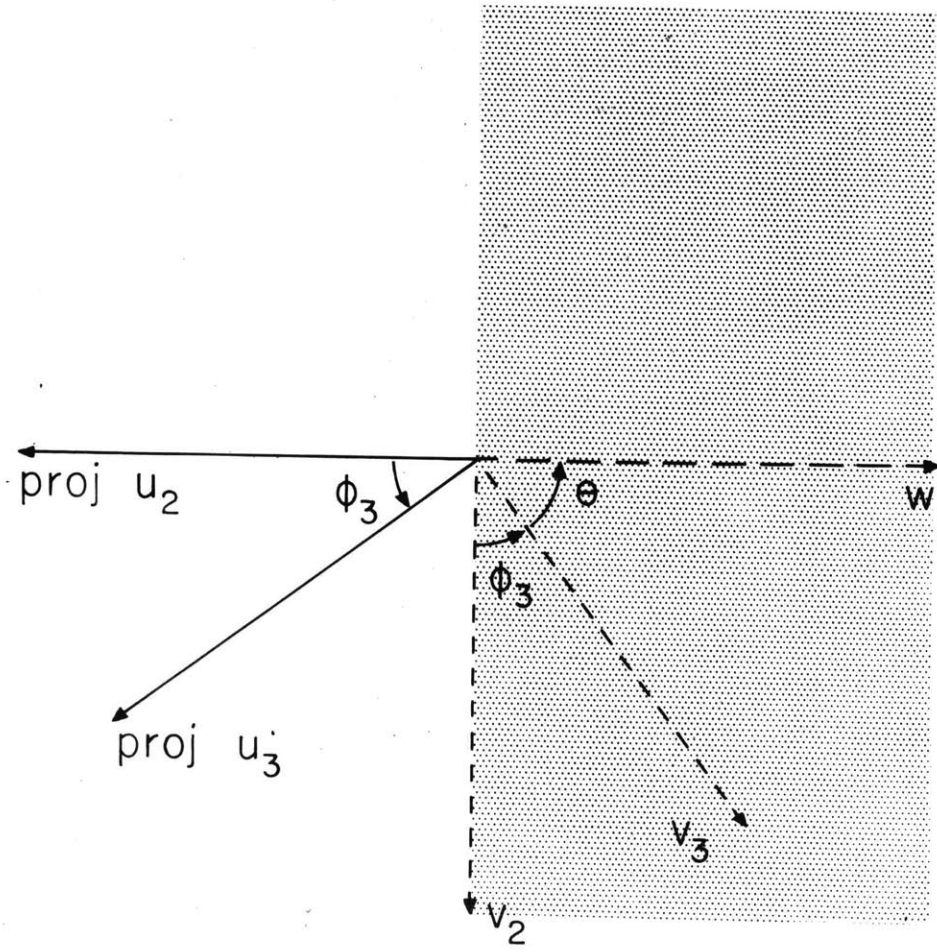
$$\phi_i = \phi_i'$$

$$\text{or} \quad \phi_i = 2\pi - \phi_i' \quad (5)$$

The ambiguity in the magnitude of ϕ_i may be resolved in the following way. Consider the vector $\underline{w} = \underline{u}_1 \times \underline{u}_2$. This vector lies

Figure 2

Vectors used in the calculation of angle ϕ_3 . Plane of the drawing is normal to vector \underline{u}_2 of Fig. 1.



in the plane of Fig. 2 and has a direction opposite to that of $\text{proj. } \underline{u}_2$.

The cosine of the angle θ between \underline{v}_i and \underline{w} is given by

$$\cos \theta = \frac{\underline{v}_i \cdot \underline{w}}{v_i w} \quad (6)$$

If $\cos \theta \geq 0$, \underline{v}_i lies in the shaded portion of Fig. 2 and $\phi_i = \phi_i^1$.

If $\cos \theta < 0$, \underline{v}_i lies in the unshaded portion and $\phi_i = 2\pi - \phi_i^1$.

DISCUSSION

This method was designed specifically for use with a digital computer although it is certainly possible to use it with a desk calculator. In programming the computations it has been found convenient to have the interatomic distances \underline{u}_i printed out as a check on the accuracy of input data. In addition, results may be obtained for enantiomorphically related coordination polyhedra. The drilling coordinates of two such polyhedra, \underline{N}_i and \underline{N}_j , are related by

$$\rho_i = \rho_j \quad (7)$$

$$\phi_i = 2\pi - \phi_j .$$

In this laboratory, open structure models are usually built on the scale of $\frac{1}{2}$ inch = 1 Å with the ball diameters at approximately half scale. Using half-scale balls permits the interiors of the models and the bonding directions to be seen more easily. The balls are

joined by $\frac{1}{8}$ inch brass rods cut so that the center-to-center distances are proportional to the bond lengths.

ACKNOWLEDGEMENTS

This work was supported by a grant from the National Science Foundation, and was done in part at the M.I. T. Computation Center, Cambridge, Massachusetts. The authors wish to thank Professor M.J. Buerger for his helpful review of the manuscript.

REFERENCES

- ¹ Deane K. Smith, Bibliography on molecular and crystal structure models, National Bureau of Standards, Monograph 14, Washington D.C., May 1960.
- ² M. J. Buerger, Rev. Sci. Instr. 6, 412 (1935)
- ³ B. F. Decker and R. T. Asp, J. Chem. Educ. 32, 75 (1955)
- ⁴ C. A. Haywood, J. Sci. Instr. 26, 379 (1949)

Chapter IV

Introduction

Although the gross details of the crystal structures of several of the triclinic metasilicates have been known for several years, the results of detailed refinements have just recently become available (Chapter I; Peacor, 1962). These refinement results are extremely useful for comparing related structures and are absolutely necessary if one is interested in deducing the physical and chemical principles upon which these structures are based. Chapter I describes a least-squares refinement of pectolite, $\text{Ca}_2\text{NaHSi}_3\text{O}_9$, which was carried out with relatively crude intensity data originally used by Buerger (1956) to solve the structure. It was not possible to refine \underline{R} below 17% using this data (sets of $\underline{hk0}$, $\underline{0kl}$, and $\underline{h0l}$ reflections). Because of the unusual interatomic distances which resulted from this refinement, and because of the high \underline{R} , it was felt that further work should be done to improve the pectolite situation. Furthermore, this would also provide another set of reliable data to be used in comparing the different triclinic metasilicates.

Selection of material

A problem which arises when working with pectolite is that it is quite hard to obtain a uniform single crystal. The mineral

occurs in needles which tend to "feather" when broken. The feathered end of a broken crystal consists of many smaller, somewhat mis-oriented crystals which cause the major diffraction spots on a Weissenberg film to be streaked parallel to the needle (when the needle axis is the rotation axis). When using a counter diffractometer, this is especially troublesome because the long tails on the diffraction peaks make the background corrections rather difficult.

A large number of pectolite samples from several localities were searched for a crystal which would be small enough to be entirely bathed by the x-ray beam and which would produce negligible streaking in the diffraction photographs. This was not achieved and, instead, a long needle which would extend out of the x-ray beam at all equi-inclination angles, μ_e , was chosen. This crystal* was transparent and bounded by distinct (100) and (001) faces with b as the needle axis. The crystal had the following dimensions:

between (100) and ($\bar{1}00$)	.110 mm
between (001) and ($00\bar{1}$)	.087 mm
needle length	3.68 mm

Even with this crystal, which was photographed with each end of the needle out of the x-ray beam, the Weissenberg photographs showed a slight streaking of the diffraction spots, indicating some mis-orientation of different regions of the crystal. These were, however,

* U. S. National Museum number 2452. Locality: Erie railroad cut, Bergen Hill, New Jersey. (Manchester, 1919).

by far the best photographs obtained from any of the pectolite crystals examined, although it appears that a penalty results from this in that large primary extinction is evident in the observed diffraction intensities (see the section on refinement).

An interesting result of the search for good single crystals was that many of those examined were twins. When the members of the twin were present in equal amounts, b-axis oscillation photographs showed an apparent mirror symmetry normal to b. This is discussed in Chapter II in a comparison of twinned pectolite and twinned wollastonite.

Apparently there are no published analyses of Bergen Hill pectolite. Schaller (1955), however, gives several analyses for pectolite including two for New Jersey pectolites, one from Paterson and the other from Franklin. Both of these analyses are given in Table 1 along with the stoichiometric composition. It is likely that the Bergen Hill material has a composition more like the Paterson pectolite than the Franklin pectolite.

Unit cell data

Buerger (1956) published unit cell data on pectolite which was obtained from precession films. An attempt was made in the present study to obtain precision Weissenberg photographs (Buerger, 1942) from which measurements could be made and then refined with a

Table 1

Compositions of two pectolites and the hypothetical composition
 computed from $\text{Ca}_2\text{NaHSi}_3\text{O}_9$ (data from Schaller, 1955)

	Paterson, N.J.	Franklin, N.J.	Hypothetical
CaO	33.20	31.15	33.74
MnO	.12	2.57*	-
FeO	1.00	1.29	-
Na ₂ O	9.01	7.97	9.32
SiO ₂	53.80	52.04	54.23
H ₂ O	2.94	3.07	2.71
Etc.	-	2.12	-
	<hr/>	<hr/>	<hr/>
	100.07	100.21	100.00

*Includes 0.26 % ZnO

least-squares program written by Burnham (1962b). Because of pectolite's needlelike habit, however, the only satisfactory photographs were ones taken with \underline{b} as the rotation axis, thus giving refined values of only \underline{a}^* , \underline{c}^* , and β^* . Since these reciprocal cell parameters compared very favorably with those of Buerger, the old values for \underline{b}^* , α^* , and γ^* were combined with the new for \underline{a}^* , \underline{c}^* , and β^* to give a slightly different direct cell. The old and new reciprocal and direct cells are given in Table 2.

Space group

All previous investigators have assumed that the pectolite space group is $\underline{P}\bar{1}$, although the author could find no experimental evidence for a center of symmetry. Peacock (1935b) does not report any doubly terminated crystals for pectolite as he does for wollastonite (Peacock, 1935a). Although the refinement proceeded satisfactorily assuming space group $\underline{P}\bar{1}$, it would be interesting to test pectolite for piezoelectricity and to try a cycle of refinement assuming space group $\underline{P}1$.

Intensity collection

Three-dimensional x-ray intensities were collected with a Weissenberg counter diffractometer using CuK_{α} radiation. Ni foils

Table 2

Results of least-squares refinement of pectolite cell constants.

	Buerger (1956)	Results of refinement	Adopted cell
a*	.12878 Å ⁻¹	0.128785 ± 0.000002 Å ⁻¹	
b*	.14549		
c*	.14310	0.143001 ± 0.000003	
α*	88.32°		
β*	84.58°	84.57808 ± 0.00106°	
γ*	77.43°		
a	7.99 Å	7.98818 ± 0.00011 Å	7.988 Å
b	7.04	7.03996	7.040
c	7.02	7.02468 ± 0.00013	7.025
α	90.52°	90.51984	90.52°
β	95.18°	95.18062	95.18°
γ	102.47°	102.46865	102.47°
V			383.98 Å ³

* Refinement using precision Weissenberg data (59 observations) and Burnham (1962b) IBM 7090 program LCLSQ III.

at the x-ray tube and at the proportional counter aperture were used in conjunction with a pulse height analyzer to discriminate against unwanted radiation. The proportional detector was a standard Philips Xe-filled tube with preamplifier. The largest counting rate observed was about 9×10^3 c.p.s. Background was counted for 50 seconds on each side of a peak and the total intensity plus background was obtained as the crystal rotated through a given angle, $\Delta\phi$. The integrated intensity, I , was obtained from

$$I = C - (B_1 + B_2) T/100$$

where C is the total count, B_1 and B_2 are backgrounds, and T is the time required to collect C .

Structure factors were obtained using data reduction programs written by Burnham (1962a) and Prewitt (1960). This included a prismatic crystal absorption correction in which path lengths for the zero level were computed for all reflections and then divided by $\cos \mu_e$. In addition, the linear absorption coefficient, μ_1 , was replaced by $\mu_1/\cos \mu_e$ to compensate for the increased scattering volume for upper levels due to the use of an "infinite" crystal. A total of 1357 structure factors were thus produced.

Refinement

All refinement was carried out using the IBM 7090 program, SFLSQ3, described in Appendix I. Starting coordinates were those

given in Table 1 of Chapter 1. Form factors for atoms assumed to be half-ionized were taken from Freeman (1959), and correction was made for both the real and imaginary anomalous scattering factors for Ca (International Tables (1962), Vol. III). The first cycles of refinement used only reflections from the reciprocal lattice levels 0, 1, 2, and 3 in order to save computing time. After an initial cycle to adjust the scale factor, the initial \underline{R} -factor was 0.174, which is, incidentally, about the same as was found using the original Buerger data and the same atom coordinates. In a further cycle in which all atom coordinates plus the overall scale factor were varied, the \underline{R} went up to 0.239. This result made the statistical weighting scheme (Burnham, 1962a) suspect, especially since $\sqrt{\underline{w}} (\underline{F}_o - \underline{F}_c)$ varied quite widely for different reflections. In the next two cycles, the original coordinates were used as a starting point and a weighting scheme recommended by Cruickshank (1961) was incorporated into the program where

$$\sqrt{\underline{w}} = 1/(a + F_o + C F_o^2)^{\frac{1}{2}}.$$

In this expression, $a = 2F_{\min}$ and $C = 2/F_{\max}$. At the end of the second cycle the \underline{R} was 0.085, thus supporting the assumption that the weighting in the original cycles was incorrect. In order to check whether the Burnham weighting scheme itself was causing trouble or whether the philosophy of weights based only on counting statistics alone was in error, two more cycles were tried using the Evans (1961) weighting scheme which is somewhat different from that of Burnham.

At the end of the two cycles, the \underline{R} had gone up to 0.148. After this, all weighting was carried out using the Cruickshank method. No analysis has been made of why trouble was encountered with the Burnham and Evans methods, but it appears that there must be systematic errors present in the data which are not accounted for in schemes based solely on counting statistics.

In the next cycle, temperature factors in addition to atom coordinates were varied, resulting in an \underline{R} of 0.079. There were, however, negative temperature factors for atoms Si_1 , Si_2 , Si_3 , and O_9 . Another cycle was run in which reflections were rejected from the refinement but included in the \underline{R} -factor. The \underline{R} was reduced to 0.075 and all temperature factors refined to positive values. A further cycle using all 1357 reflections but with the rejection test, left \underline{R} at 0.075.

It is noteworthy that for the strongest reflections, the calculated value is much larger than the observed, indicating the need for a primary extinction correction. Although none was made, it should be done before this work is published. A possible correction to the observed intensities is

$$I_c = I_o / (1 - t I_o)$$

where \underline{t} is a very small number determined by comparing the present \underline{I}_o and \underline{I}_c . The need for this correction is supported by the fact that removing the two strongest reflections (120 and $\bar{2}20$)

reduces \underline{R} to 0.070 and that removing the twenty strongest reduces \underline{R} to about 0.05. It is probable that inclusion of a hydrogen contribution in the calculated structure factor plus anisotropic temperature factor refinement will lower the \underline{R} even further.

The final atom coordinates and isotropic temperature factors are given in Table 3. It is doubtful that there will be any significant change in these coordinates in further refinement.

Evaluation of the structure

Figure 1 is a projection of the pectolite structure onto (101) of the pseudomonoclinic pectolite cell described in Chapter II. The structure is made up of double columns of edge-sharing Ca octahedra which extend in the \underline{b} -direction. Adjoining sets of octahedra are linked by single silicate chains and irregularly coordinated Na atoms. The silicate chains share only corners with the Ca octahedra, but five edges of the Na polyhedron are shared with the silicate tetrahedra. This is in contrast with the wollastonite structure where the Ca octahedra are found in columns of three edge-sharing octahedra wide with the Ca_1 and Ca_2 octahedra each sharing one edge with the Si_3 tetrahedron, and the Ca_3 octahedron sharing edges with only the other octahedra.

Table 4 is a compilation of the interatomic distances in pectolite, computed using the coordinates of Table 3. Each silicon

Table 3

Refined coordinates for pectolite

Atom	x	y	z	B
Ca ₁	.8549	.5939	.1449	.39
Ca ₂	.8465	.0837	.1404	.38
Na	.5520	.2591	.3430	.83
Si ₁	.2182	.4010	.3373	.20
Si ₂	.2152	.9553	.3446	.23
Si ₃	.4505	.7353	.1448	.06
O ₁	.6520	.7863	.1296	.45
O ₂	.3299	.7036	-.0524	.24
O ₃	.1861	.5010	.5385	.30
O ₄	.1782	.8433	.5406	.40
O ₅	.0626	.3853	.1742	.34
O ₆	.0598	.8958	.1775	.44
O ₇	.3987	.5411	.2720	.38
O ₈	.3952	.9044	.2750	.37
O ₉	.2630	.1934	.3861	.32

Figure 1

Pectolite structure projected onto (101). The Ca locations and coordination are represented by octahedra, but, because of its irregular coordination, Na is represented by both a shaded circle and, for a single sodium atom, an irregular polyhedron.

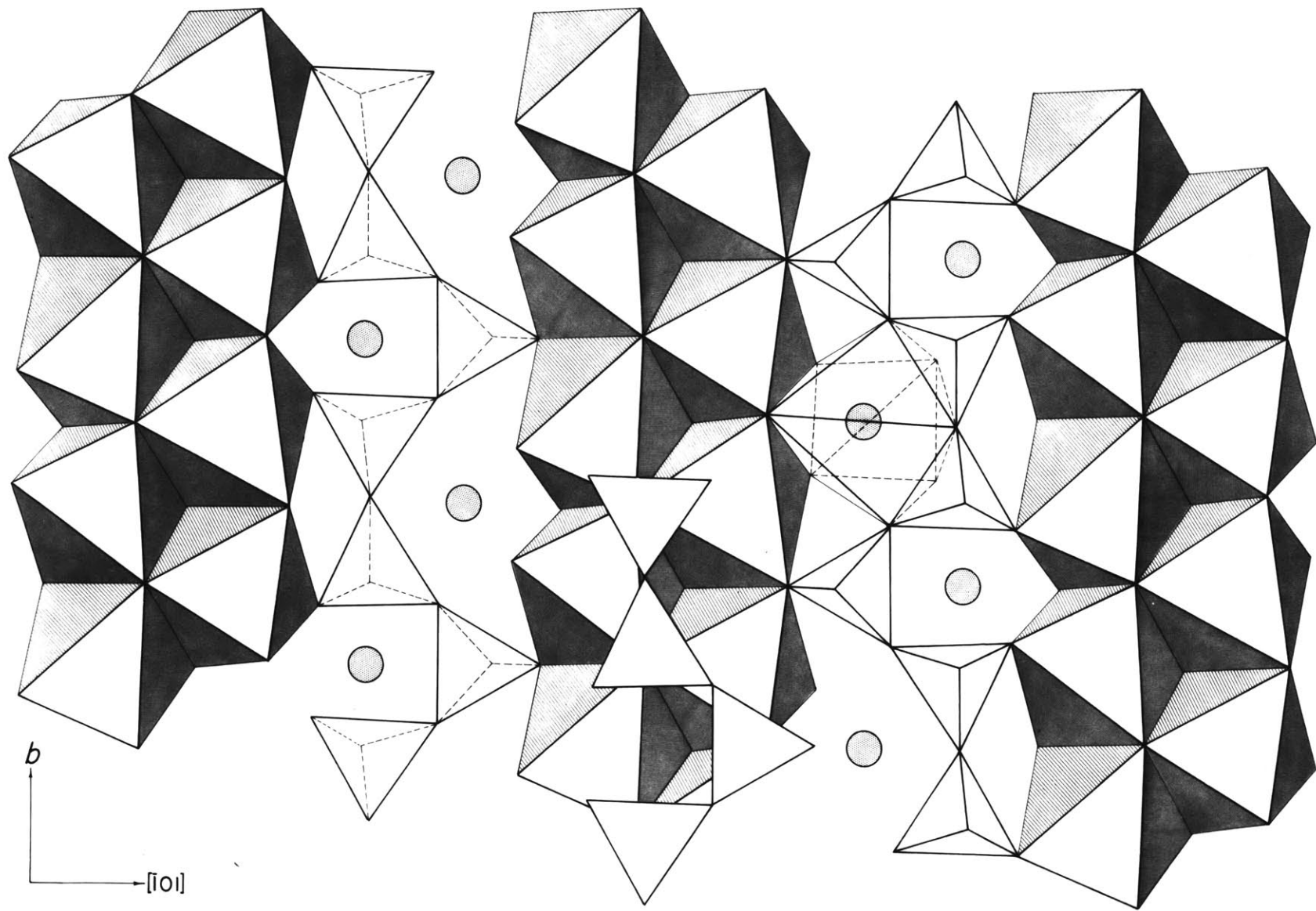


Table 4

Interatomic distances in pectolite

Si ₁	O ₃	1.638 Å
	O ₅	1.597
	O ₇	1.666
	O ₉	1.611
	Av.	1.628
Si ₂	O ₄	1.612
	O ₆	1.612
	O ₈	1.668
	O ₉	1.654
	Av.	1.637
Si ₃	O ₁	1.585
	O ₂	1.599
	O ₇	1.638
	O ₈	1.652
	Av.	1.619
Ca ₁	O ₁	2.322
	O ₂	2.336
	O ₃	2.359
	O ₅	2.439
	O ₅ '	2.390

	O ₆	2.381
	Av.	2.371
Ca ₂	O ₁	2.318
	O ₂	2.320
	O ₄	2.330
	O ₅	2.425
	O ₆	2.414
	O ₆ '	2.399
	Av.	2.368
Na	O ₂	2.319
	O ₃	2.461
	O ₄	2.489
	O ₇	2.578
	O ₇ '	2.991
	O ₈	2.560
	O ₈ '	2.961
	O ₉	2.303
	Av.	2.583 (2.452 excluding O ₇ ' and O ₈ ')
O ₁	O ₂	2.709
	O ₇	2.639
	O ₈	2.654

O ₂	O ₇	2.626
	O ₈	2.639
O ₃	O ₃ '	2.971
	O ₄	2.424
	O ₅	2.710
	O ₇	2.616
	O ₉	2.620
O ₄	O ₆	2.696
	O ₈	2.636
	O ₉	2.678
O ₅	O ₇	2.695
	O ₉	2.673
O ₆	O ₈	2.692
	O ₉	2.687
O ₇	O ₈	2.564
	O ₉	2.618
O ₈	O ₉	2.629

is coordinated by four oxygen atoms, the average Si-O distance being 1.628 Å, a little higher than the "ideal" metasilicate distance of about 1.622 given by Smith and Bailey (1962). The range from the smallest (1.585 Å) to the largest (1.668 Å) Si-O distance is 0.083 Å, as large a spread as Burnham (1962) found in sillimanite, where there is supposed to be "drastic" shortening of shared polyhedron edges. Ca₁ and Ca₂ are octahedrally coordinated by 6 oxygens at average distances of 2.371 Å and 2.368 Å, respectively. Na is irregularly surrounded by 6 oxygens at an average distance of 2.452 Å with two more at 2.991 Å and 2.961 Å.

Table 5 gives some of the interatomic distances rearranged to show how each oxygen is coordinated by cations. Because of the complicated way in which the Na polyhedron shares edges with the silicate tetrahedra, it is not as easy to divide the oxygen atoms into different "types" according to their coordination. In addition, until the hydrogen location is proven, a realistic division cannot be made. In general, however, O₁ through O₆ can be characterized by being coordinated by one Si and two or three cations while O₇ through O₉ are coordinated by two Si and one or two cations. When an oxygen is coordinated by two Si, the Si-O distances are considerably longer than when the oxygen is coordinated by only one Si.

As was stated in Chapter II, the most likely location for H is between O₃ and O₄ because of the anomalously short O₃-O₄ distance of 2.424 Å. This, however, is the edge of the Si₃

Table 5

Oxygen coordination in pectolite

O ₁	Si ₃	1.585	O ₆	Si ₂	1.612
	Ca ₁	2.322		Ca ₁	2.381
	Ca ₂	2.318		Ca ₂	2.414
O ₂	Si ₃	1.599	O ₇	Ca ₂ ¹	
	Ca ₁	2.322		Si ₁	1.666
	Ca ₂	2.320		Si ₃	1.638
	Na	2.319		Na	2.578
O ₃	Si ₁	1.638	O ₈	Na ¹	2.991
	Ca ₁	2.359		Si ₂	1.668
	Na	2.461		Si ₃	1.652
	H?	-		Na	2.560
O ₄	Si ₂	1.612	O ₉	Na ¹	2.961
	Ca ₂	2.330		Si ₁	1.611
	Na	2.489		Si ₂	1.654
	H?	-		Na	2.303
O ₅	Si ₁	1.597			
	Ca ₁	2.439			
	Ca ₁ ¹	2.390			
	Ca ₂	2.425			

tetrahedron shared by the Na polyhedron. Difference maps will have to be computed to show whether hydrogen is actually present between O_3 and O_4 .

It is interesting to note that all shared polyhedron edges are shorter than unshared ones, in accordance with Pauling's rules. The unshared tetrahedral edges are in the range of 2.673 Å to 2.710 Å while the shared edges range from 2.564 Å to 2.636 Å.

Conclusions

There is no doubt that we now have a reasonably accurate set of interatomic distances for pectolite, even though a few additional improvements could be made by including a correction for primary extinction and by refining anisotropic temperature factors. In addition, some investigation should be made of the possibility that the Na position contains more scattering power than has been assumed, i.e., a small percentage of heavier atoms. This is supported by the large temperature factor of Na ($B = 0.83$).

References

- Buerger, Martin J. (1942), X-ray Crystallography. John Wiley and Sons, New York.
- Buerger, M.J. (1956), The determination of the crystal structure of pectolite, $\text{Ca}_2\text{NaHSi}_3\text{O}_9$. *Z. Krist.*, 108, 248-261.
- Burnham, Charles W. (1962a), The structures and crystal chemistry of the aluminum-silicate minerals. Ph.D. Thesis, M. I. T., Cambridge, Mass.
- Burnham, Charles W. (1962b), Crystallographic lattice constant least-squares refinement program, LCLSQ (Mark III). Unpublished IBM 7090 computer program.
- Cruickshank, D.W.J., Deana E. Pilling, A. Bujosa, F.M. Lovell, and Mary R. Truter (1961), In Computing methods and the phase problem in x-ray crystal analysis. Pergamon Press, Oxford, 32-78.
- Evans, Howard T., Jr. (1961), Weighting factors for single-crystal x-ray diffraction intensity data. *Acta Cryst.* 14, 689-700.
- Freeman, A.S. (1959), Atomic scattering factors for spherical and aspherical charge distributions. *Acta Cryst.* 12, 261-271.
- International Tables for X-ray Crystallography, Vol. III (1962). The Kynoch Press, Birmingham, England.
- Manchester, James G. (1919), The minerals of the Bergen archways. *Am. Mineral.*, 4, 107-116.
- Peacock, M.A. (1935a), On wollastonite and parawollastonite. *Am. J. Sci.*, 30, 495-529.
- Peacock, M.A. (1935b), On pectolite. *Z. Krist.*, 90, 97-111.

- Peacor, Donald R. (1962), The structures and crystal chemistry of bustamite and rhodonite. Ph.D. Thesis, M.I.T., Cambridge, Mass.
- Prewitt, Charles T. (1960), The parameters Υ and ϕ for equi-inclination, with application to the single-crystal counter diffractometer. Z. Krist., 114, 356-360.
- Schaller, Waldemar T. (1955), The pectolite-schizolite-serandite series. Am. Mineral., 40, 1022-1031.

Part B

Chapter V

Review of the crystallographic investigation of metasilicates

The metasilicates are classically grouped together because of their characteristic chemical composition which is hypothetically derived from metasilic acid, H_2SiO_3 . This is not entirely satisfactory because the structures of the minerals classed as metasilicates can be quite different from one another. A classification based on structure was proposed by Strunz (1941) which uses Greek prefixes to describe the way in which the silicate tetrahedra are linked together. This classification divides metasilicates into two categories, cyclosilicates (rings of tetrahedra) and inosilicates (chains of tetrahedra). Inosilicates, however, contain additional members which are not metasilicates, e.g., amphiboles. The present chapter, therefore, discusses ino-metasilicates, which can be further defined as compounds of formula $\text{A}_m(\text{SiO}_3)_n$ containing single chains of silicate tetrahedra.

Table 1 is a compilation of the more common members of the ino-metasilicate group and shows the current status of structural work on each entry. Although only a few of these structures have been refined in detail, the gross relations between the minerals are much clearer today than they were just a few years ago.

Table 1

List of crystallographically interesting metasilicates

Name	Formula	Space group	Status of structure			
			A	B	C	D
enstatite	MgSiO_3	Pbca			x	x
clinoenstatite	MgSiO_3	$P2_1/c$			x	x
protoenstatite	MgSiO_3	Pbcn?	x			
pigeonite	$(\text{Ca}, \text{Mg}, \text{Fe})\text{SiO}_3$	$P2_1/c$			x	x
augite	$(\text{Ca}, \text{Mg}, \text{Fe})\text{SiO}_3$	$C2/c$	x			
diopside	$\text{CaMgSi}_2\text{O}_6$	"			x	
hedenbergite	$\text{CaFeSi}_2\text{O}_6$	"	x			
johannsenite	$\text{CaMnSi}_2\text{O}_6$	"	x			
acmite	$\text{NaFeSi}_2\text{O}_6$	"	x			
jadeite	$\text{NaAlSi}_2\text{O}_6$	"	x			
spodumene	$\text{LiAlSi}_2\text{O}_6$	"	x			
wollastonite	CaSiO_3	$P\bar{1}$			x	x
parawollastonite	CaSiO_3	$P2_1/a$	x			
bustamite	$\text{CaMnSi}_2\text{O}_6$	$A\bar{1}$			x	x
rhodonite	$\text{CaMn}_5\text{Si}_6\text{O}_{18}$	$P\bar{1}$			x	x
pyroxmangite	$(\text{Mn}, \text{Fe}, \text{Ca}, \text{Mg})\text{SiO}_3$	$P\bar{1}$	x			
pectolite	$\text{Ca}_2\text{NaHSi}_3\text{O}_9$	$P\bar{1}$			x	x
serandite	$\text{Mn}_2\text{NaHSi}_3\text{O}_9$	$P\bar{1}$			x	
babingtonite	$(\text{Ca}, \text{Fe}^{+2}, \text{Fe}^{+3})\text{SiO}_3$	$P\bar{1}$	x			

Key to status of structure:

A - not known

B - inferred or incomplete

C - structure correct

D - structure refined

Status of structural work. The first pyroxene structure to be solved by x-ray methods was that of diopside (Warren and Bragg, 1928). This was followed closely by two more papers on the structures of pyroxenes, the first on enstatite (Warren and Modell, 1930) and the other on the monoclinic pyroxenes (Warren and Bischoe, 1931). In the latter paper, Warren and Bischoe compared diffraction patterns of diopside with those of hedenbergite, augite, clinoenstatite, acmite, jadeite, and spodumene and concluded that they were all very similar in crystal structure. An attempt was also made to solve the structures of wollastonite and pectolite, but since their structures were quite unlike that of diopside, this attempt did not succeed.

A few years later Barnick (1935) proposed a ring structure for parawollastonite which has since been proven to be wrong. As will be pointed out in Chapter VI, this choice of material was unfortunate. He should have worked with the triclinic structure, wollastonite, instead, because parawollastonite is a twinned wollastonite.

Two important papers (Peacock, 1935a;1935b) on wollastonite and pectolite appeared at about the same time as Barnick's paper. Although these papers did not directly shed new light on the structures of these minerals, they have been proven to be very valuable as a source of morphological and optical data. Warren and Bischoe (1931) had shown that both the wollastonite and the pectolite they had examined were triclinic, and Peacock showed further that there

were actually two forms of wollastonite which were being confused. He called the triclinic phase wollastonite and the monoclinic one parawollastonite. He further named the high temperature form first described by Bourgeois (1882) and which was not being confused with wollastonite, pseudowollastonite.

No further structural work was done until Ito (1950) tried to explain the differences between wollastonite and parawollastonite. Since he based much of his argument on the assumption that the Barnick structure was correct, this work has not been given proper credit for the portion that really described the basis for distinguishing wollastonite and parawollastonite (Chapters II and VI).

In 1956, structures for pectolite and wollastonite were published which have subsequently been found to be correct (Chapters I and II). Shortly thereafter, reinvestigations of the Mg-Fe-Ca pyroxenes showed that the space groups of clinoenstatite and pigeonite were different from that of diopside ($\underline{P2}_1/\underline{c}$ instead of $\underline{C2}/\underline{c}$) and that protoenstatite was a distinct phase with an apparently different structure from the other enstatites. Morimoto, Appleman, and Evans (1960) refined the structures of clinoenstatite and pigeonite, and Lindemann (1961) refined enstatite, thus giving fairly reliable sets of coordinates for these pyroxenes. No refinements of diopside, acmite, spodumene, jadeite, hedenbergite, or johannsenite are known at the present time, but it is probable that these will be refined in the near future.

No minerals are known with the pectolite structure except schizolite and serandite, which involve substitution of Mn for Ca in pectolite. The ideal formula for schizolite is $\text{CaMnNaHSi}_3\text{O}_9$ and for serandite is $\text{Mn}_2\text{NaHSi}_3\text{O}_9$, but as far as has been determined, a continuous series exists from pectolite to a phase containing about 77% of the manganese end member (Schaller, 1955). There may be more to this problem than one might suppose, since Warren and Biscoe (1931) found that the \underline{c} axis in schizolite (locality not given) was double that of \underline{c} in pectolite. This is exactly the same relation as bustamite has to wollastonite and consequently bears further investigation. However, Ito (1939) and Liebau (1957) give cell constants which are approximately those of pectolite.

Peacor (1962) has refined the structures of bustamite and rhodonite, thus providing detailed information about these structures. This leaves the pyroxmangite type structure as the only category of Table 1 in which no detailed refinement has been done although Liebau (1959) proposed a structure but did not give any coordinates.

Future possibilities for ino-metasilicate investigations. One of the most probable things that will be found when metasilicates are further investigated is that additional phases will be found which are a result of space group twinning (Chapter VI). The hydrated calcium silicates will also be of considerable interest if any are shown to definitely have single silicate chains. Peacor (personal communication) thinks that babingtonite, $(\text{Ca}, \text{Fe}^{+2}, \text{Fe}^{+3})\text{SiO}_3$ may

have the rhodonite structure and it would be very interesting to see whether other structures like those of rhodonite and pyroxmangite could be found.

Another topic of interest for the future would be the relating of the physical and chemical properties of the minerals to their structures. This has already been done to some extent, but a number of things are left to be explained in terms of the structures. These include cleavage, optical properties, chemical bonding, mechanisms of phase changes, twinning, and crystal morphology. The ultimate as far as the mineralogist or petrologist is concerned is to be able to relate natural phase assemblages with conditions necessary for their formation. This, of course, involves much more than the ino-metasilicates and probably will require many years of work before a satisfactory solution is found.

References

- Barnick, Max A.W. (1935), Strukturuntersuchung des natürlichen Wollastonite. Mitt. Kaiser-Wilhelm-Inst. Silikatforsch., No. 172, 4-36.
- Bourgeois, L. (1882), Essai de production artificielle de wollastonite et de meionite. Bull. Soc. Min. France, 5, 13-16.
- Brown, W.L., N. Morimoto, and J.V. Smith (1961), A structural explanation of the polymorphism and transitions of $MgSiO_3$. J. Geol., 69, 609-616.
- Ito, T. (1939), The determination of lattice constants of triclinic crystals from one crystals setting- a special case. Z. Krist., 100, 437-439.
- Liebau, Friedrich (1957), Über die Struktur des Schizoliths. Neues Jb. Mineral., Mh., 10, 227-229.
- Lindemann, W. (1961), Beitrag zur Enstatitstruktur. Neues Jahrb. Min., 10, 226-233.
- Peacock, M.A. (1935a), On wollastonite and parawollastonite. Am. J. Sci., 30, 495-529.
- Peacock, M.A. (1935b), On pectolite. Z. Krist., 90, 7-111.
- Peacor, Donald R. (1962), Structures and crystal chemistry of bustamite and rhodonite. M.I.T. Ph.D. Thesis.
- Schaller, Waldemar T. (1955), The pectolite-schizolite-serandite series. Am. Min., 40, 1022-1031.
- Smith, J.V. (1959), The crystal structure of proto-enstatite, $MgSiO_3$. Acta Cryst., 12, 515-519.
- Strunz, Hugo (1941), Mineral. Tabellen. Akademische Verlagsgesellschaft Leipzig.

- Warren, B.E. and J. Biscoe (1931), The crystal structure of the monoclinic pyroxenes. *Z. Krist.*, 80, 391-401.
- Warren, B., and W. Lawrence Bragg (1928), The structure of diopside, $\text{CaMg}(\text{SiO}_3)_2$. *Z. Krist.*, 69, 168-193.
- Warren, B.E., and D.I. Modell (1930), The structure of enstatite MgSiO_3 . *Z. Krist.*, 75, 1-14.

Chapter VI

Twinning in silicate crystallography

The presence of twinning is probably the most common cause of experimental difficulty in the field of silicate crystallography. It is obvious that one can expect to have trouble solving or refining a crystal structure if the material being investigated is twinned, although techniques have been developed (Morimoto, Appleman, and Evans, 1960; Frueh, 1962) which will give reasonable results if the nature of the twinning is known. It is sometimes difficult, however, to establish what twin laws are operating in a crystal, or that twinning exists at all. It will be the purpose of this chapter to look into some of the aspects of twinning in silicate minerals, particularly in the light of experience gained in working with wollastonite and parawollastonite as described in Chapter II.

Structure and space group twinning. It is not generally realized that in addition to the macroscopic twinning of crystals there is another type which takes place on unit cell scale. This latter type produces a reduction or enhancement of the symmetry of the crystal over the symmetry of some basic repeating unit. Ito (1950) called these structure twinning and space group twinning. Structure twinning is represented by all examples of twinning given in, say, a standard mineralogy textbook. Space group twinning, however, manifests itself in a much more subtle way and

can usually only be detected as such by interpretation of x-ray diffraction patterns. Good and perhaps classic examples of space group twinning are found in wollastonite and parawollastonite as discussed in Chapter II. Other possibilities for space group twinning will be discussed below.

One problem which arises when space group twinning is considered is how one distinguishes very fine polysynthetic twinning from actual space group twinning, since the two are quite similar except for the scale of the repetition. The answer seems to be in the nature of the diffracted x-rays; that is, since our only tool for comparing these phenomena is x-ray diffraction, then the criteria for distinguishing between them are to be found in differences in diffraction effects. If, for example, the observed diffraction pattern is an apparent result of space group twinning, the resulting structure must be accepted as having the symmetry of the observed space group even though it is possible that polysynthetic twinning is present on a very fine scale. If, however, a method is devised which will distinguish between these two alternatives, then one or the other can be adopted. The exact nature of the space group twin does not concern us here. What is important is that the repetition is on a fine enough scale so that x-ray coherence is such that the diffraction pattern has an apparent symmetry and that this symmetry is representative of the crystal structure in question.

Implications of space group twinning. Aside from academic interest in this phenomena, the most important result of understanding the nature of space group twinning lies in the phase equilibria of a system containing a compound which exhibits space group twinning. Take CaSiO_3 , for example. Triclinic wollastonite has been demonstrated to have a definite stability field, but parawollastonite has not been synthesized and probably forms only under very unique conditions. From this standpoint, parawollastonite appears to be a metastable phase under most conditions and may not even have a stability field at all.

Figure 1 demonstrates the geometrical relationships between wollastonite and parawollastonite. In the upper left of the diagram, the wollastonite pseudomonoclinic subcell described in Chapter II is represented by a cell containing two triangles on mirror planes at $\underline{y} = \frac{1}{4}$ and $\underline{y} = \frac{3}{4}$. Each of these triangles represents a silicate chain in the actual structure. There are no symmetry elements other than the single center and the two mirror planes. If the other identical cells are added in the \underline{y} direction, then centers of symmetry and a 2_1 axis at $\underline{x} = \frac{1}{2}$ relate the cells to one another. Now, Fig. 2 shows that it is possible to join wollastonite cells on (100) in one of two ways which, as far as first coordination spheres are concerned, are geometrically identical (provided the symmetry of the subcell is truly monoclinic). This stacking involves a shift of $+\frac{1}{4}\underline{b}$, resulting in an overall triclinic

Figure 1

Schematic representations of the ways in which pseudomonoclinic subcells can be joined to give a different overall symmetry. The diagram in the upper left shows how the subcells can be stacked on (010) to give space group $\underline{P}2_1/\underline{m}$. On the right, the cells are joined on (100) in successive shifts of $+\frac{1}{4}\underline{b}$ or $-\frac{1}{4}\underline{b}$ to give obverse and reverse $\underline{P}\bar{1}$ symmetry (wollastonite). In the lower left, cells are joined with alternating shifts of $+$ and $-\frac{1}{4}\underline{b}$ to give overall $\underline{P}2_1/\underline{a}$ symmetry (parawollastonite).

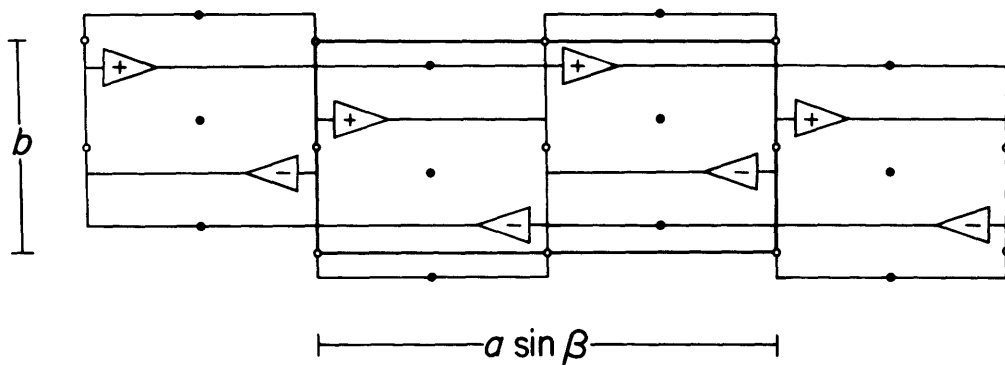
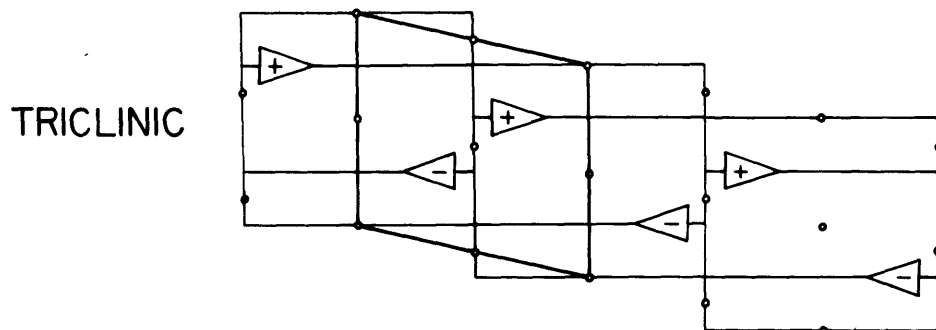
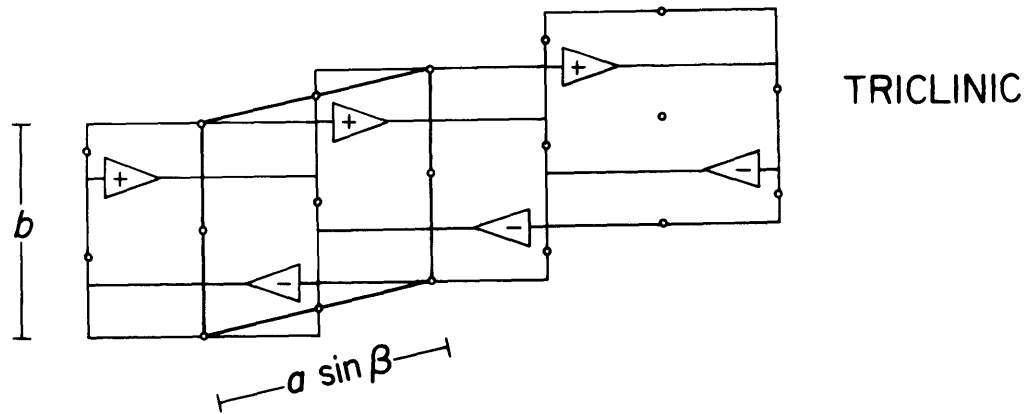
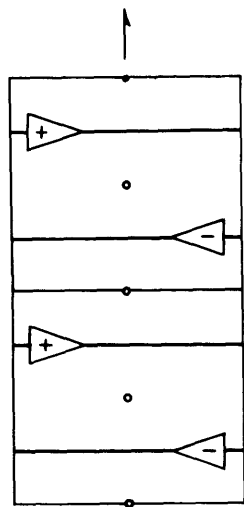
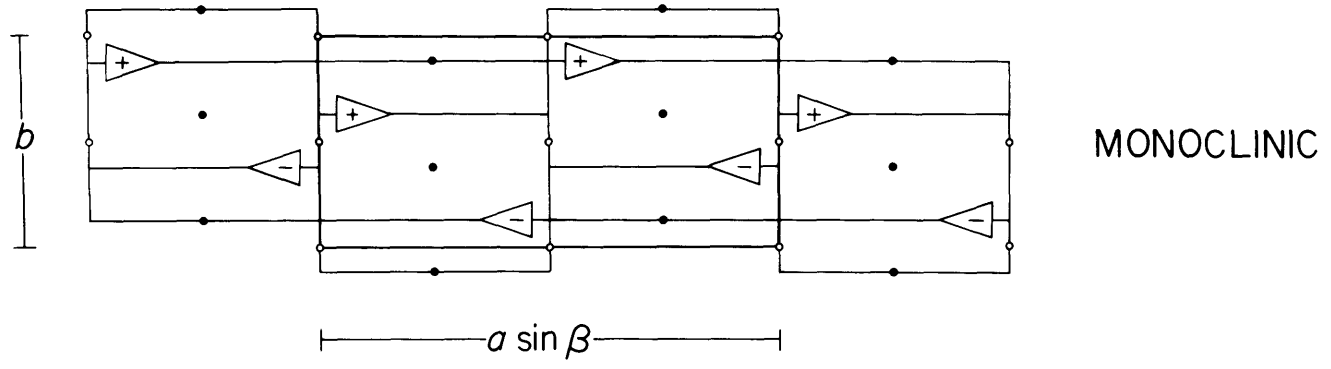
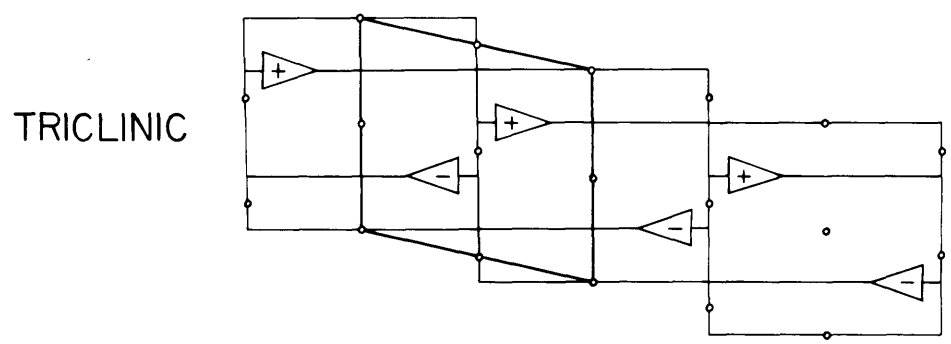
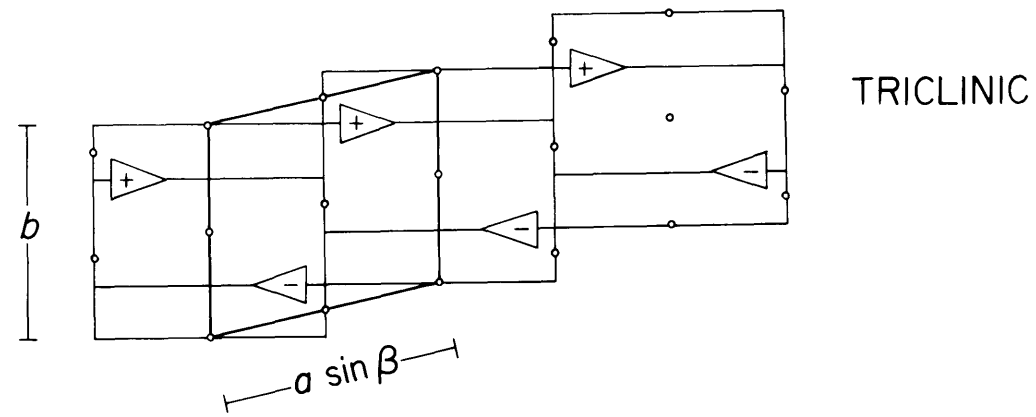
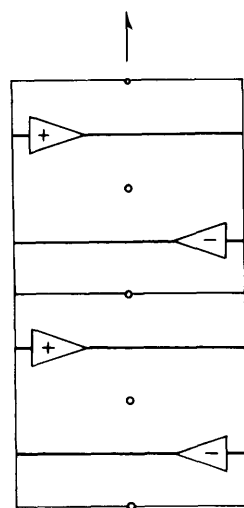


Figure 2

Pseudomonoclinic CaSiO_3 subcells joined on (100) to give wollastonite (top) and parawollastonite (bottom).



symmetry. Returning to Fig. 1, the stacking of subcells with successive shifts of $+\frac{1}{4}b$ gives the same triclinic cell as do shifts of $-\frac{1}{4}b$, except that the cells are oriented differently in space.

Parawollastonite is formed by adding cells on (100) with alternating shifts of $+\frac{1}{4}b$ and $-\frac{1}{4}b$. When this is done, the centers at $\underline{x} = \frac{1}{2}$ in the single cell still exist for the single cell, but do not relate adjoining cells with each other. Instead, the centers which arise between subcells define a new cell with symmetry $\underline{p}2_1/\underline{a}$.

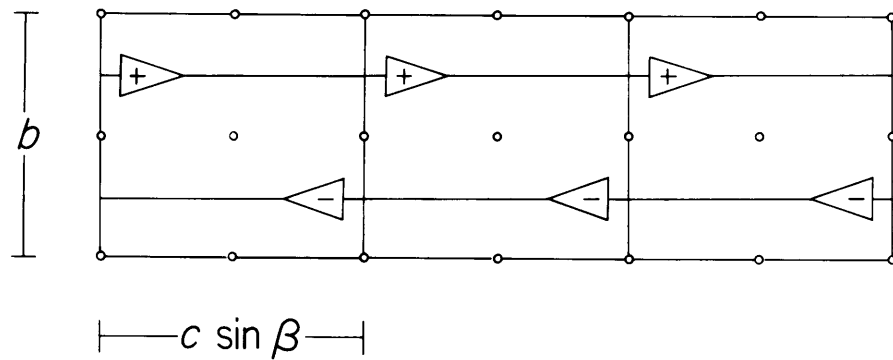
In order to check the validity of the above findings, structure factors were calculated for each structure with a single atom placed on the mirror plane of the subcell. The resulting patterns exactly duplicated the extinction rules observed in wollastonite and parawollastonite, respectively.

It is interesting to compare these results with the bustamite structure which has been solved by Peacor (1962). Figure 3 shows the two ways in which the wollastonite pseudomonoclinic subcells can be joined on (001) with shifts of either $+\frac{1}{2}b$ or $-\frac{1}{2}b$.

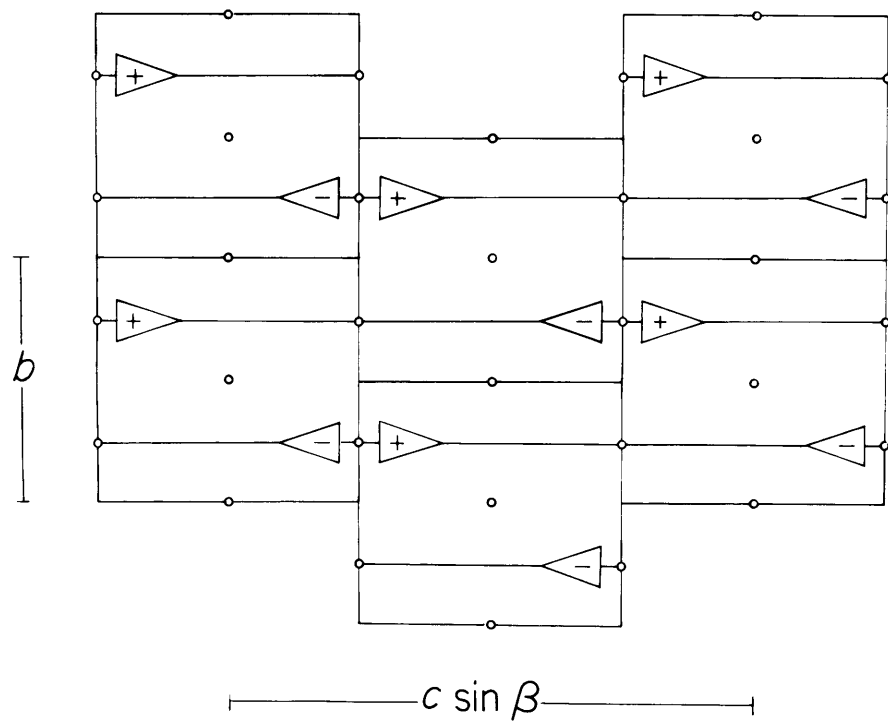
Here, because of the cell geometry, the mirror planes are continuous across the cells. The sequence in the upper part of the figure produces the wollastonite structure and the one in the lower part produces the bustamite structure. This is really the only difference between bustamite and wollastonite. This does result, however, in different coordinations for two-thirds of the large cations in each of the structures. Figure 4 shows how the actual

Figure 3

Schematic representations of the wollastonite (top) and bustamite (bottom) structure. The relation between wollastonite and bustamite is similar to that between wollastonite and parawollastonite except that successive pseudomonoclinic subcells are not shifted on (001) in wollastonite and are shifted by \pm or $-\frac{1}{2}\underline{b}$ in bustamite.



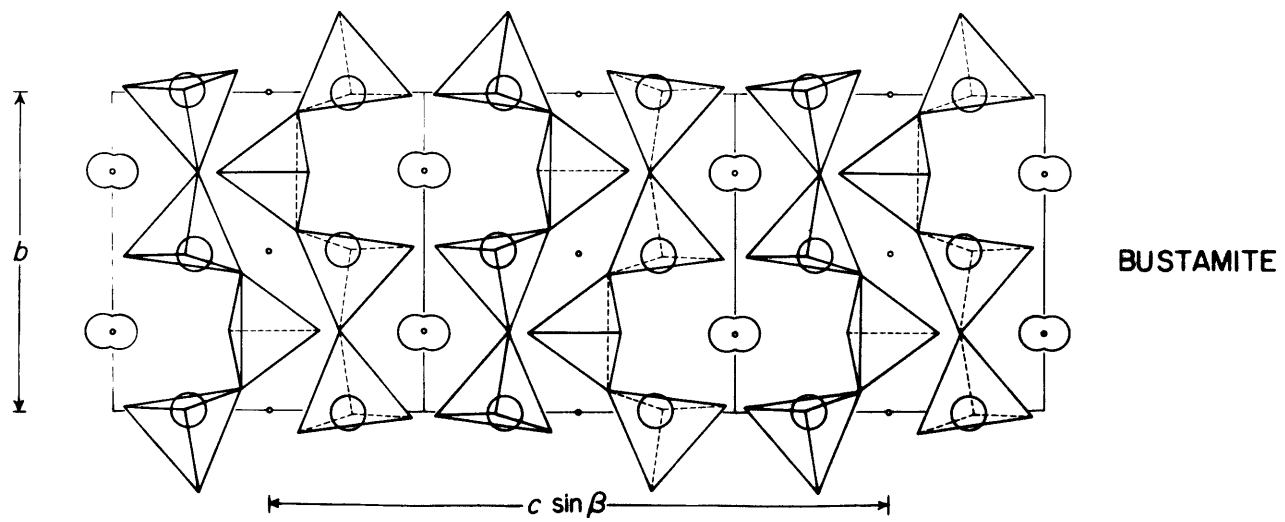
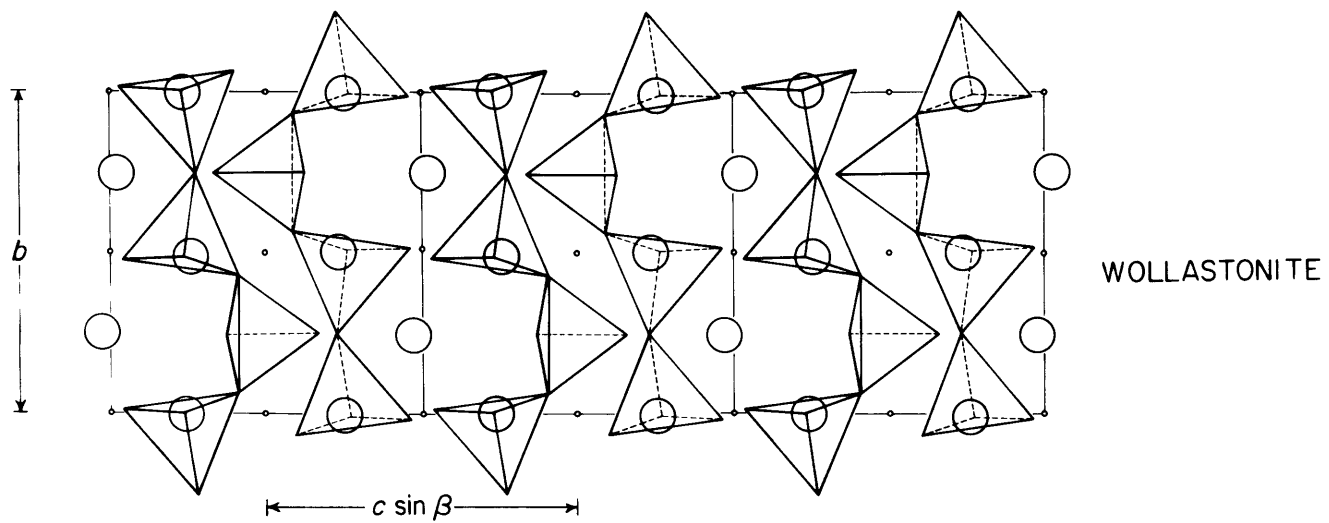
WOLLASTONITE



BUSTAMITE

Figure 4

Result of joining CaSiO_3 subcells as described in Figure 3 to give the wollastonite structure (top) and the bustamite structure (bottom).



structures look when joined in this way. It is interesting to note that although bustamite has an A-centered cell, the extinction rule is compatible with space group extinction rules, but this is not so with parawollastonite. This occurs because the bustamite structure does not contain the "leftover" centers of symmetry that are found in parawollastonite. Also the bustamite structure is much more different from wollastonite than is parawollastonite.

Energy relations in parawollastonite and bustamite. There must be some way of rationalizing the foregoing observations in terms of energy. To provide a means of describing the ways in which cells can be joined, the letter A can be assigned to an interface with a shift of, say, $+\frac{1}{4}b$, and B to one with a shift of $-\frac{1}{4}b$. Then wollastonite would be represented by AAAAA... or BBBBBB... and parawollastonite by ABABAB... . Now, ignoring the mechanism of twin formation, we can say that in the ideal case, there is no difference in energy between the interfaces A and B. The difference must be between AA and AB. It is probable that under most conditions, the condition AA or BB has a lower energy than AB, and therefore wollastonite is the stable phase. Other conditions, such as mechanical stress, could favor AB and parawollastonite would be formed. On the other hand, bustamite seems to favor the AB sequence to the exclusion of AA. It would be interesting to try calculating these different energies using just Coulombic interaction such as was done by Zoltai and Buerger (1960) on rings of tetrahedra.

Space group twinning in other silicates. There are other silicates which, although common, have not been successfully shown to have definite stability fields in the laboratory. Boyd (1959) states that conditions for stability of anthophyllite have not been found. Ito (1950) tried to show that the orthorhombic anthophyllite structure was the result of space group twinning of the tremolite (or cummingtonite) structure, but was unsuccessful. There are, however, certain relations between these structures which bear further investigation and which may shed light on the problems of the Mg-Fe amphiboles.

There is more evidence for a space group twinning relationship between the ortho and clino pyroxenes. Strunz (1958) states that the orthorhombic pyroxene structures arise from the monoclinic through a space lattice twinning on $\underline{a}(100)$. Brown, Morimoto, and Smith (1961) show that although the orientations with respect to the silicate chains are different, the structures of protoenstatite, clinoenstatite and rhombic enstatite differ in the same way as do wollastonite and parawollastonite. In the notation given above for the interfaces of adjoining cells, these pyroxenes are represented as

clinoenstatite	AAAAAA	(wollastonite)
protoenstatite	ABABAB	(parawollastonite)
enstatite	AABBAA	(no known equivalent)

It is interesting that the phase relations between these minerals are as yet unclear (Brown, Morimoto, and Smith, 1961) because of the

tendency for these minerals to exist metastably. Energy calculations could well be introduced here.

There are many parallels in the feldspar problem to what is found in wollastonite-parawollastonite, although apparently the feldspars are much more complex. Feldspar diffraction patterns contain extra spots, diffuse spots, and streaks which are also observed in the wollastonites. Although the feldspar situation is much too involved to be discussed here, it should be noted that there seems to be a common thread running through all of the structural discussions of feldspars which is not yet clearly defined. This, too, is a fruitful field for research.

One thing that is common to all silicate structures is that there is a tendency for the oxygen to form close-packed, although distorted, arrangements. This is more evident in olivine than in quartz, but it is to some extent true in all silicate structures. The analogy here is to stacking faults seen in close-packed structures such as those of the metals and the fact that a close-packed plane offers different sites for the location of adjoining atoms which differ little in energy. It may well be that the location of a twin boundary in the silicates will often be one of these close-packed planes. This point is not clear in parawollastonite because (100) is not strictly a plane of close packing, but the ease of demonstrating the twinning on (100) may be misleading and the real differences may occur elsewhere. It is true, however, that there is a definite boundary

in parawollastonite which is common to adjoining cells and that this boundary plane contains only oxygen atoms.

It is quite evident that while much work has been done on twinning of the silicates, not much of it has concerned the actual structures. There is much room for descriptive investigations to compare the similarities and differences among different twinned silicates and for analytical investigations which can justify why a particular twin occurs.

References

- Boyd, Francis R. (1959), Hydrothermal investigations of amphiboles. Researches in geochemistry, P.H.Abelson, Ed. John Wiley and Sons, New York.
- Brown, W.L., N. Morimoto, and J.V. Smith (1961), A structural explanation of the polymorphism and transitions of $MgSiO_3$. *J. Geol.*, 69, 609-616.
- Ito, T. (1950), X-Ray Studies in Polymorphism. Maruzen, Tokyo.
- Morimoto, Nobuo, Daniel E. Appleman, and Howard T. Evans, Jr. (1960), The crystal structures of clinoenstatite and pigeonite. *Z. Krist.*, 114, 120-147.
- Strunz, Hugo (1957), Mineralogische tabellen, Akademische Verlagsgesellschaft, Leipzig.
- Zoltai, Tibor, and M.J. Buerger (1960), The relative energies of rings of tetrahedra. *Z. Krist.*, 114, 1-8.

Chapter VII

Crystal structures related to wollastonite and pectolite

Liebau (1957;1961) has made extensive compilations of inorganic silicates, germanates, phosphates, arsenates, vanadates, and fluoberyllates whose structures contain chains of tetrahedra. Although there appears to be a great number of these compounds, all fall into relatively few classes, one of which is represented by the wollastonite structure. No attempt will be made here to reproduce or improve this extensive tabulated data except to give examples of each class and to comment briefly on the status of structural information for each of these classes.

Table 1 is a listing of the different structure types as proposed by Liebau. Each structure type in this table is characterized by the number of tetrahedra in the repeating unit of the chain. For example, the pyroxene and the wollastonite structures have repeats of two and three tetrahedra, respectively, whereas rhodonite and pyroxmangite contain five and seven tetrahedra, respectively. The pseudowollastonite structure contains chains of three tetrahedra linked together to form a three-membered ring.

Status of structural information. One of the most interesting aspects of the classification is that here is a series of compounds which vary in structure primarily because of differences in atom radii. With enough information about the structures, one

Table 1

Classification of compounds with formula ABX_3 (after Liebau, 1961)

Number of tetrahedra in repeat unit	Compound	Cation radius ratio	Remarks
1	$CuGeO_3$.99	$CuSiO_3$ not known
2	$MgSiO_3$ (enstatite)	1.60	well refined
	$CaMg(SiO_3)_2$ (diopside)	1.98	structure known but not refined
7	$(Ca,Mg)(Mn,Fe)_6(SiO_3)_7$ (pyroxmangite)	1.98	structure proposed but not refined
5	$CaMn_5(SiO_3)_6$ (rhodonite)	1.98	well refined
3	$CaSiO_3$ (wollastonite)	2.36	well refined
	$CaMn(SiO_3)_2$ (bustamite)	2.14	well refined
∞ (3-membered ring)	$CaSiO_3$ (pseudowollastonite)	2.36	structure proposed but not proven or refined
	$SrSiO_3$	2.67	
	$SrGeO_3$	1.53	
2	$BaSiO_3$	3.19	structure proposed but not proven
	$BaGeO_3$	1.84	

might be able to relate crystal chemistry with phase equilibria in a quantitative way. It might be possible, for instance, to predict the temperature at which wollastonite transforms to pseudowollastonite by knowing how the effective radii of Ca, Si, and O vary with temperature. The cation radius ratios given in Table 1 show that there is a considerable range in the radius ratio among the different structural types, although this is apparently not the only factor which controls the structure of a particular phase. Undoubtedly, quantitative work would require that the radii of all atoms be known accurately at different temperatures.

At present, only a few structures in the groups of Table 1 are known with any degree of accuracy, some are very poorly known, and no work at all has been done at other than room temperature. The status of the pyroxenes was discussed in Chapter V, there being refined coordinates for only enstatite, clinoenstatite, and pigeonite. In the other groups, only wollastonite, bustamite, and rhodonite have been adequately refined.

Structures have been proposed for CuGeO_3 (Ginetti, 1954), pseudowollastonite (Dornberger-Schiff, 1962), BaSiO_3 (Lazarev et al., 1962), and pyroxmangite (Liebau, 1959), but none have been refined and some may even be wrong. Certainly, there is much room for further work in this series of compounds.

Pseudowollastonite. Since pseudowollastonite is very closely related to the subject of this thesis, some important features of the

status of its structure should be noted here. It was originally intended that some experimental work would be done on this structure but, due to the difficulty of obtaining good single crystals for structure refinement, this was not done. Since Hilmer (1958) had published a note on the structure of SrGeO_3 which is thought to have about the same structure as pseudowollastonite, the prospect of publishing a proposed pseudowollastonite structure without a refinement was not too interesting. Dornberger-Schiff (1962) has subsequently done this very thing. The structure proposed is much like one the author picked in a study of the octahedral cation sheet in wollastonite.

The pseudowollastonite structure consists of layers of Ca octahedrally coordinated by oxygens. These octahedral layers are connected by rings of Si tetrahedra which share oxygens with the Ca octahedra in layers above and below the rings. Dornberger-Schiff (1962) reports the presence of diffuse reflections and radiation streaks in pseudowollastonite diffraction patterns which are indicative of disregistry between adjoining octahedral sheets.

The phase equilibria between pseudowollastonite and wollastonite are of interest. Pseudowollastonite, which was first synthesized by Bourgeois (1882), can be formed by heating CaO and SiO_2 above 1200°C . (melting point of pseudowollastonite: 1540°C .) and will persist in a metastable state if cooled to room temperature.

It can also be synthesized hydrothermally at as low as 600° C. (Flint, McMurdie, and Wells, 1938). Although wollastonite can be formed from pseudowollastonite under certain circumstances (Allen, White, and Wright, 1906), no evidence has been presented that this takes place in natural systems. Instead, wollastonite seems to form as a primary mineral. It is still probable, however, that whether wollastonite or parawollastonite occurs may have some connection with the temperature of formation, even if pseudowollastonite is not involved.

Hydrated calcium silicates. Many hydrated calcium silicates are known, most of which show some relationship with wollastonite, such as a transformation to wollastonite upon being heated. None of these have been shown to have a wollastonite-like silicate chain, however. Not too much work has been done in this area and some phases may have the wollastonite structure with hydrogen bonding as in pectolite, or with H₂O in the large holes which exist in the wollastonite structure.

There is one hydrated calcium silicate which bears mentioning here, and that is xonotolite, Ca₆Si₆O₁₇(OH)₂. Mamedov and Belov (1955) have published a structure for xonotolite which seems to be correct (R₂ ≈ 20%). This structure consists of silicate chains which are similar to those in wollastonite except that the chains are paired with the Si₃ tetrahedra in each pair sharing a corner. Although no investigation of xonotolite has been made in connection with this

thesis, there are certain aspects of the proposed structure which should be further studied. The primary reason for suspicion is the great similarity between the reported diffraction diagrams for xonotolite and those for parawollastonite. For example, \underline{a} in both xonotolite and parawollastonite is approximately double the wollastonite \underline{a} . Dent and Taylor (1956) report that the odd layers photographs of xonotolite are streaked and very weak. It could be that xonotolite does not have a really different structure from wollastonite and varies only in the way that the cells are put together. Whether this is true could probably be determined by computing interatomic distances from coordinates given by Mamedov and Belov (1955). Even if their structure is correct, there is no doubt that it should be refined.

References

- Allen, E. T., W. P. White, and F. E. Wright (1906), On wollastonite and pseudowollastonite, polymorphic forms of calcium metasilicate. *Am. J. Sci.*, 21, 89-108.
- Bourgeois, L. (1882), Essai de production artificielle de wollastonite et de meionite. *Bull Soc. Min. France*, 5, 13-16.
- Dent, L. S. and H. F. W. Taylor (1956), The dehydration of xonotolite, *Acta Cryst*, 9, 1002-1004.
- Dornberger-Schiff, K. (1962), The symmetry and structure of strontium germanate, $\text{Sr}(\text{GeO}_3)$, as a structure model for α -wollastonite, $\text{Ca}(\text{SiO}_3)$. *Soviet Physics--Crystallography*, 6, 694-700.
- Flint, E. P., H. F. McMurdie, and L. S. Wells (1938), Formation of hydrated calcium silicates at elevated temperatures and pressures. *Bur. Stand. J. Res.*, 21, 617-638.
- Ginetti, Y. (1954), Structure cristalline du métagermanate de cuivre. *Bull. Soc. Chim. Belg.*, 63, 209-216.
- Hilmer, Waltraud (1958), Zur strukturbestimmung von strontiumgermanat SrGeO_3 . *Naturwiss.* 10, 238-239.
- Lazaref, A. N., T. F. Tenisheva, and R. G. Grebenshchikov (1962), The structure of barium silicates. *Soviet Physics--Doklady*, 6, 847-850.
- Liebau, Friedrich (1956), Bemerkungen zur systematik der kristallstrukturen von silikaten mit hochkondensierten anionen. *Z. Phys. Chemie.*, 206, 73-92.
- Liebau, Friedrich (1959), Über die kristallstruktur des pyroxmangits $(\text{Mn, Fe, Ca, Mg})\text{SiO}_3$ *Acta Cryst.*, 12, 177-181.

Liebau, F. (1960), Zur kristallchemie der silikate, germanate und fluoberyllate des formeltyps ABX_3 . N. Jb. Miner., Abh., 94, 1209-1222.

Mamedov, Kh. C., and N. V. Belov (1955), Crystal structure of xonotolite, Doklady Akad. Nauk SSSR, 104, 615-618.

Chapter VIII

Crystal structure of larsenite, PbZnSiO_4

Experimental work

Although the structure of larsenite has no direct connection to those of wollastonite and pectolite, this account is presented because many of the experimental and computing techniques used by the author for wollastonite and pectolite were developed in the study of larsenite. As the structure of larsenite has not been completely solved, this chapter represents more of a progress report than a finished paper.

The solution of the larsenite structure is especially interesting in that it appears that it will be a structure unlike that of any of the olivines or other orthosilicates. This, however, will not be certain until the work is finished.

Occurrence. Larsenite has been reported only from Franklin, New Jersey. The specimens are found in veins cutting massive willemite-franklinite ore along with garnet, hodgkinsonite, calcite, zincite, willemite, and clinohedrite. The crystals are slender needles 10 to 20 times longer than they are thick. Although terminated crystals have been found (Palache, 1935), none are known to be doubly terminated. Larsenite has one good cleavage parallel to (120) of the morphological unit.

Unit cell and space group. The unit cell and space group of larsenite was published by Layman (1957). Table 1 compares Layman's cell data with that obtained in the present investigation and with forsterite. Layman stated that the larsenite cell apparently was that of olivine doubled along a and b. As will be shown below, this seems to be a fortuitous comparison. The space group given by Layman, Pnam or Pna, was confirmed by the author. Since no doubly terminated crystals have been found, it is difficult to establish to which of these space groups larsenite belongs. Because, however, of the large number of minerals reported in space group Pnam versus only one in Pna (Donnay and Nowacki, 1954), Pnam seems to be the more likely.

Intensity collection. Since absorption is quite large ($\mu_1 = 911 \text{ cm}^{-1}$ for CuK α radiation) in larsenite, a thin needle was selected for intensity determination. The absorption correction was made by assuming that the crystal approximated a cylinder with a radius of 0.0015 cm (15 microns), giving a $\mu_1 R$ of 1.37. The intensities were collected with a Weissenberg Geiger counter diffractometer (Buerger, 1960) using CuK α radiation. Care was taken that the linearity limits of the Geiger tube was not exceeded. The integrated intensities were obtained by measuring with a planimeter the peak areas above background as recorded on a strip chart recorder. In all, 822 intensities were recorded.

Solution of the structure. The three-dimensional Patterson function was computed using the Fourier program MIFRI1 (Sly and Shoemaker, 1960). At this point it was thought that the structure might be solved by inspection if it were similar to that of olivine. Table 2 gives the equipoint distribution of the atoms in forsterite (Belov and Belova, 1951) and the possible equipoints in \underline{Pnam} for larsenite.

Examination of the Patterson sections normal to \underline{c} shows that all of the strong peaks lie on $\underline{z} = 0$ and $\underline{z} = \frac{1}{2}$. It is relatively easy to determine whether Pb or Zn are located on centers of symmetry in $4\underline{a}$ or $4\underline{b}$. If $4\underline{a}$ and/or $4\underline{b}$ were filled with Pb or Zn, large peaks would occur in the Patterson at $00\frac{1}{2}$. Since there is a negative region at this point, $4\underline{a}$ and $4\underline{b}$ certainly do not contain Pb or Zn and probably not O. Si is excluded since it never is found on centers of symmetry in orthosilicates. This leaves only $4\underline{c}$ and $8\underline{d}$ to be filled.

Since all the strong peaks in the Patterson lie on sections which are separated by $\frac{1}{2}\underline{z}$ it is probable that the heavy atoms are in $4\underline{c}$ (the mirror planes at $\frac{1}{4}\underline{z}$ and $\frac{3}{4}\underline{z}$). With this in mind, inversion peaks for Pb_1 and Pb_2 with supporting satellites were located at $(.082, .465, \frac{1}{2})$ and $(.304, .118, \frac{1}{2})$, respectively. From these inversion peaks it was possible to construct an $Pb_1 + Pb_2 M_8(\underline{xy}\frac{1}{4})$ function of the crystal structure. This map is given in Fig. 1. The

Table 1

Comparison of larsenite and forsterite cells

	Larsenite ¹	Larsenite ²	Forsterite ³
a	8.23 \pm .01 Å	8.30 Å	4.765 Å
b	18.94 \pm .01	19.1	10.23
c	5.06 \pm .01	5.06	5.997
z	8	8	4
formula	PbZnSiO ₄	PbZnSiO ₄	Mg ₂ SiO ₄
space group	Pnam	Pnam	Pbnm

¹ Layman (1957)

² Prewitt (this work)

³ Belov and Belova (1951)

Table 2

The forsterite structure (Belov and Belova, 1951)

 $4\text{Mg}_2\text{SiO}_4$, space group $\underline{\underline{\text{Pbnm}}}$

<u>Atom</u>	<u>Equipoint</u>	<u>Symmetry</u>	<u>x</u>	<u>y</u>	<u>z</u>
Mg ₁	4 a	$\bar{1}$	0	0	0
Mg ₂	4 c	m	-.01	.218	1/4
Si	4 c	m	.415	.095	1/4
O ₁	4 c	m	-.229	.083	1/4
O ₂	4 c	m	.221	.430	1/4
O ₃	8 d	1	.262	.152	.027

The larsenite structure

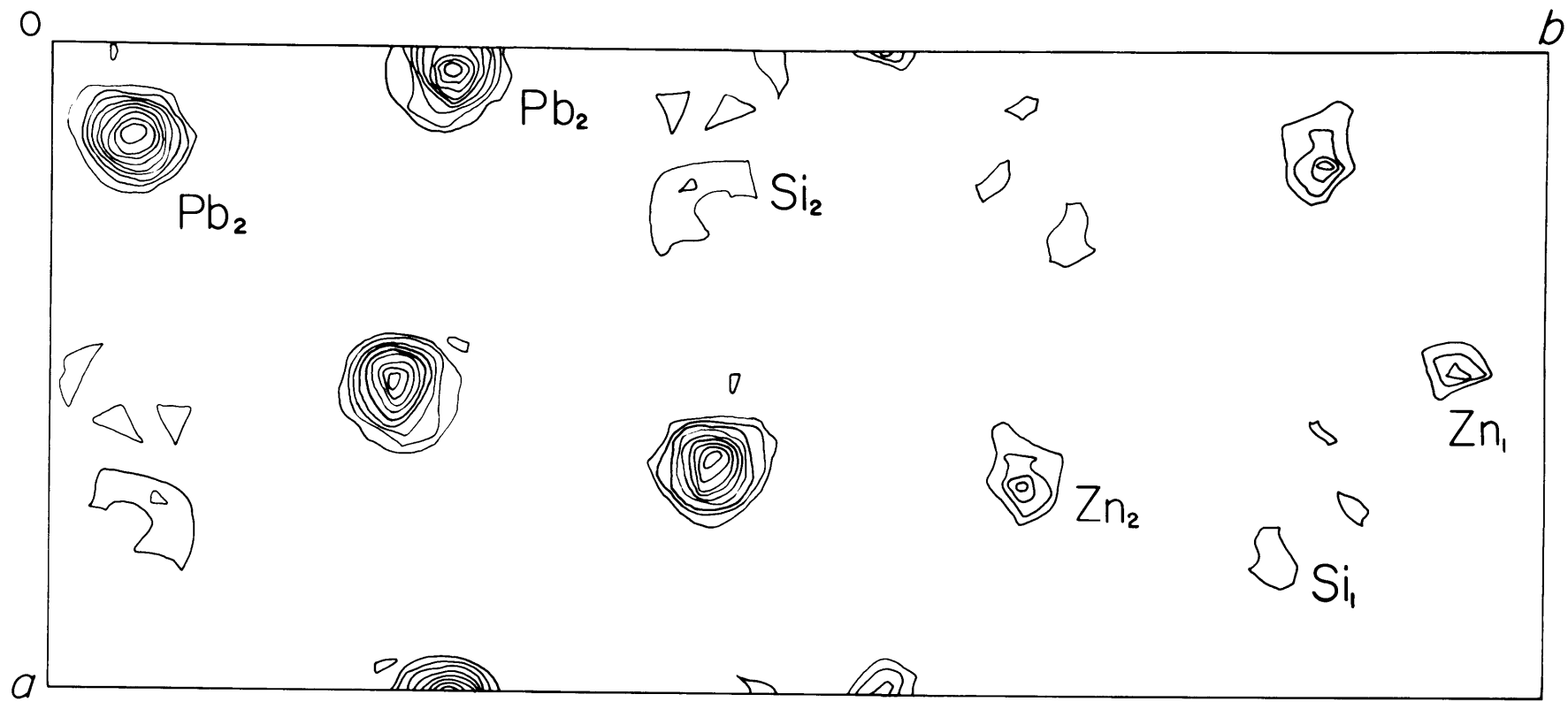
 8PbZnSiO_4 , space group $\underline{\underline{\text{Pnam}^*}}$

<u>Equipoint</u>	<u>Symmetry</u>	<u>Equivalent positions</u>
4 a	$\bar{1}$	$000; 00\frac{1}{2}; \frac{1}{2}\frac{1}{2}0; \frac{1}{2}\frac{1}{2}\frac{1}{2}$
4 b	$\bar{1}$	$\frac{1}{2}00; \frac{1}{2}0\frac{1}{2}; 0\frac{1}{2}0; 0\frac{1}{2}\frac{1}{2}$
4 c	m	$xy\frac{1}{4}; \bar{x}\bar{y}\frac{3}{4}; \frac{1}{2}-x, \frac{1}{2}+y, \frac{3}{4}; \frac{1}{2}+x, \frac{1}{2}-y, \frac{1}{4}$
8 d	1	$xyz; \frac{1}{2}+x, \frac{1}{2}-y, \frac{1}{2}-z; x, y, \frac{1}{2}+z;$ $\frac{1}{2}-x, \frac{1}{2}+y, \bar{z}; \bar{x}\bar{y}\bar{z}; \frac{1}{2}-x, \frac{1}{2}+y, \frac{1}{2}+z;$ $x, y, \frac{1}{2}-z; \frac{1}{2}+x, \frac{1}{2}-y, z$

*Equivalent positions for this orientation are not given in International Tables, Vol. I.

Figure 1

$Pb_1 + Pb_2 M_8(xy\frac{1}{4})$ map of larsenite



large peaks are Pb and the somewhat smaller ones correspond to Zn. It is almost certain that Si also lies on the mirror plane since the short c axis would require that if Si were not on the mirror plane, the silicate tetrahedra would have to be linked in chains across the mirror planes and this cannot be the case in orthosilicates. Accepting this, the most likely location for Si is at $(.24, .44, \frac{1}{4})$ and $(.28, .67, \frac{1}{4})$.

Although the cations are located rather easily, the oxygen positions present a problem. There is no information on the $M_g(xy\frac{1}{4})$ function which will give a consistent set of oxygen coordinates. An attempt to find these locations is discussed in the next section.

Refinement. A number of cycles of refinement were tried, using a computer program written by Prewitt (Appendix I). The lowest R -factor obtained was 19.7%. The final coordinates for this refinement are given in Table 3. It is evident that the oxygens are not located properly here since other refinement cycles in which the oxygen coordinates were completely different gave R -factors almost as low as 19.7%. A three-dimensional difference map using the coordinates of Table 3 was computed to assist in relocating the oxygen atoms, but apparently either enough signs were wrong or enough reflections were in error to produce a rather ambiguous map. Some changes were made according to a best guess of what information the map contained, but further refinement was unsuccessful. It is noteworthy that the difference map showed a depression

Table 3

Atom coordinates for larsenite

Atom	<u>x</u>	<u>y</u>	<u>z</u>
Pb ₁	.037	.270	$\frac{1}{4}$
Pb ₂	.148	.059	$\frac{1}{4}$
Zn ₁	.498	.943	$\frac{1}{4}$
Zn ₂	.674	.656	$\frac{1}{4}$
Si ₁	.796	.824	$\frac{1}{4}$
Si ₂	.226	.423	$\frac{1}{4}$
O ₁ *	.988	.877	$\frac{1}{4}$
O ₂	.649	.876	$\frac{1}{4}$
O ₃	.352	.475	$\frac{1}{4}$
O ₄	.091	.460	$\frac{1}{4}$
O ₅	.250	.353	.427
O ₆	.809	.775	.493

* The oxygen coordinates are provisional

in the region of Zn_2 which was not large enough to be the result of displacing one of the zinc atoms, but which indicates that something is wrong with the proposed structure.

Discussion of results

Since the least-squares refinement has reached a point where some modification of the larsenite structure has to be made, it is useful to review the facts and to recommend what procedures should be followed to reach a successful conclusion. It is believed that the answer will be forthcoming if a reasonable effort is put into the solution.

Oxygen packing. One of the first things that should be considered is whether the oxygen might have an olivine-like packing and consequently similar cation coordination, or whether the structure might be related to that of willemite, Zn_2SiO_4 , where the Zn is in tetrahedral coordination. The space group of forsterite and larsenite are the same, but attempts to fit the Pb and Zn of larsenite into the forsterite oxygen structure have not been successful. It also has not been possible to find a reasonable structure where the Zn are tetrahedrally coordinated. The tentative interpretation of this is that the larsenite structure is really a new one.

Other chemical and physical evidence should be collected and tabulated before any further work is done. This includes

refractivities, interatomic distances, and coordinations of Pb and Zn. One difficulty here is that there is very little reliable structural data available on Pb and Zn silicates. Because of this, the solution of larsenite becomes even more interesting and points the way to a much larger field of investigation.

Substructures and heavy atoms. Another approach to structure solution which comes to mind is the heavy atom method. Since, however, there are two crystallographically distinct Pb atoms in larsenite, this is not a foolproof approach because the structure factor amplitudes due to Pb cancel for many of the reflections. This technique was used to determine the signs of about one-fourth of the reflections after the lead positions were determined. This is discussed further below in connection with direct methods.

Although the cations lie on mirror planes at $z = \frac{1}{4}$ and $\frac{3}{4}$, and the oxygens probably lie on both the mirror plane and in the general position, there is no set of reflections which can be picked that contain contributions from only part of the atom population. The trigonometric formula for the general position in Pnam,

$$A = 8 \cos 2\pi \left(hx - \frac{h+k+l}{4} \right) \cos 2\pi \left(ky + \frac{h+k}{4} \right) \cos 2\pi \left(lz + \frac{l}{4} \right),$$

shows that for atoms with $z = \frac{1}{4}$, the third cosine is ± 1 regardless of the value of l . It is true that oxygen in the general position would contribute more heavily to the even levels, and an electron density calculation using only these reflections may be computed.

Direct methods. The most interesting and promising method for solving larsenite is with Harker-Kasper inequalities or through suitable application of sign relationships (Woolfson, 1961). As was stated above, the signs of about one-fourth or 200 reflections are known because if

$$F_{\text{Pb+Zn}} > 8f_{\text{Si}} + 32f_{\text{O}},$$

then the sign of $F_{\text{Pb+Zn}}$ must control the sign of the whole structure factor. Tests have shown that within these 200 strong reflections, the sign relationship,

$$s(H) s(H^*) s(H+H^*) \approx +1,$$

is always obeyed. This relation and others can be used to find signs for many other reflections.

References

- Belov, N. V., E. N. Belova, N. H. Andrianova, and P. F. Smirnova (1951), Determination of the parameters in the olivine (forsterite) structure with the harmonic three-dimensional synthesis. Doklady Akad. Nauk. SSSR, 81, 399-402.
- Buerger, Martin J. (1960), Crystal structure analysis. John Wiley and Sons, New York.
- Donnay, J. D. H. and Werner Nowacki (1954), Crystal data. Geol. Soc. Am. Memoir 60.
- Layman, Fredric G. (1957), Unit cell and space group of larsenite, PbZnSiO_4 . Am. Mineral., 42,
- Palache, Charles (1935), The minerals of Franklin and Sterling Hill, Sussex County, New Jersey. U.S.G.S. Prof. Paper, 180, 80-81.
- Sly, William G., and David P. Shoemaker (1960), MIFRI1: Two- and three-dimensional crystallographic Fourier summation program for the IBM 704 computer. Unpublished report.
- Woolfson, M. M. (1961), Direct methods in crystallography. Clarendon Press, Oxford.

Chapter IX

Automatic crystal structure analysis

Because of extremely rapid developments in the fields of automation, control, and digital computing, it is possible today to design a system for nearly automatic crystal structure determination and refinement. There are some tremendous advantages to such a setup, both philosophical and practical, and also some disadvantages. The advantages are that a great deal of useful, reliable structural information can be gained in a relatively short time and investigators can begin to spend more time interpreting results than in repeating the experimental details over and over again. One disadvantage is that the costs per unit time will be quite high even though the cost per crystal structure should be much lower than at present. Another disadvantage is that a few people will have to spend considerable time in setting up an automated system and in eliminating the deficiencies that are bound to be present.

Present capabilities. Considerable progress toward large-scale automation has been made in connection with this thesis, and also other theses by Burnham (1961) and Peacor (1962). Burnham outlined a series of data reduction programs for the IBM 7090 computer which have since been augmented and improved and which are listed below. In addition, the automatic diffractometer is now a reality and should be available soon in a number of forms. The

author has done considerable work on possible control systems for the Weissenberg diffractometer, including the writing of the diffractometer settings program described in Appendix III.

The following IBM 7090 programs are now in use in the Crystallographic Laboratory at M.I.T. and, with revisions, could be incorporated into an automated system.

1. Least-squares refinement of lattice constants (Burnham)
2. Weissenberg diffractometer settings (Prewitt)
3. Data reduction and prismatic absorption correction (Burnham)
4. Cylindrical and spherical absorption correction (Prewitt)
5. Fourier synthesis (Sly, Shoemaker and Van den Hende)
6. Structure factors and full-matrix least-squares refinement (Prewitt)
7. Structure factors and diagonal matrix least-squares refinement (Van den Hende)
8. Drilling coordinates for crystal structure models (Peacor and Prewitt)

This program is now under development.

General absorption correction (Wuensch and Prewitt)

Future capabilities. These programs need to be obtained or written before an automated system would be practical.

1. Diffractometer control
2. Processing of diffractometer output

3. Structure determination
 - (a) Minimum function
 - (b) Inequalities
 - (c) Statistics
4. Refinement - differential synthesis
5. Output
 - (a) Fourier plot - cathode ray tube
 - (b) Fourier plot - mechanical or electrostatic
 - (c) Structure drawing - mechanical or electrostatic
6. Interatomic distances and interbond angles

With an automatic diffractometer and the above programs working correctly, a structure analysis could be practically automatic except for selection, mounting, and cell determination of the crystal and the writing of the final paper. Some work would be required in the supervision of the equipment and in transferring data between the diffractometer and the computer, but this would be very small in comparison with what is now being done. Of course, many experimental difficulties can be expected before such a system is perfected, but it is not inconceivable that, once a typical mineral crystal is set up, the whole process from data collection to final refined structure and illustrations could be carried out in two weeks. The time required at present for the same thing can vary from a few months to over a year. This does

not include protein or other structures with especially large cells, or situations in which special problems arise. Time required for these latter investigations is often on the order of several years.

Expected results of automated crystal structure analysis. As was stated earlier, automation will allow the investigator much more time in which to evaluate the results of his work--that is, unless he spends the extra time working on more different structures. In either case, there will be opportunity to do more thinking about the physical rather than the mechanical aspects of the problem. As it is today, the pressure for turning out results may cause important concepts to be overlooked and poorer papers to be written.

Another, less obvious, result of automation is that the data and therefore the results will be much more reliable. Although the less expensive human operator can set an instrument as well as a machine for any individual diffraction intensity, he cannot possibly be as consistent over several hundreds or thousands of observations. Experience has shown that data from manually operated diffractometers have contained errors which could have caused the more difficult problem to fail completely.

Automation will enable the investigator to obtain reliable information on many related compounds such as different pyroxenes which would have been skipped previously as not being a good investment of time. From this work, much information about such

topics as bonding, polymorphism, and phase equilibria should be obtained, thus enabling the crystallographer to become more involved in what he is working on than in what he is working with.

Part C

Appendix I

SFLSQ3, a structure factor and least-squares refinement program
for the IBM 7090 digital computer

Introduction

The writing of this program was begun in the spring of 1961, a few months after the installation of an IBM 709 digital computer at the M. I. T. Computation Center. At that time this laboratory was using the crystallographic least-squares program, ORXLS, written by Busing and Levy (1959) for the IBM 704. Since many difficulties were encountered in using the 704 program on the 709 and since the running times were so long that many problems could not be undertaken, the author decided to write a program modeled after the one by Busing and Levy which would be very flexible, faster, and operable under the Fortran Monitor System. The resulting program, SFLSQ3, has been in use for over a year and has been used successfully by a number of people for both structure factor and least-squares calculations.

The programming of SFLSQ3 is in FORTRAN with the exception of the normal equation matrix storage routine, the Busing and Levy matrix inverter, and library routines, which are written in FAP. Much of the program is broken up into subroutines which

communicate with each other and with the main program through a large common storage. This enables the user to make many changes which would be impossible with most other similar programs. It is felt that by coding in FORTRAN and by providing a detailed writeup and references, the user should find this program no harder to set up and run than others of similar type which have been distributed.

Although the mathematical method in SFLSQ3 is similar in many respects to ORXLS of Busing and Levy (1959), the programming is completely new except for the matrix inversion routine ORSMI (Busing and Levy, 1962) which was obtained from Dr. Busing through Dr. Karl Fischer. As SFLSQ3 is now constituted, the full normal equation matrix is inverted to obtain the necessary parameter shifts. It would be quite possible to provide the option of refining using only the diagonal matrix, a feature which would considerably reduce the time required to run the program. Then, presumably, there would be an optimum procedure for carrying out a complete least-squares refinement, depending on the number of observations and the number of variable parameters. For example, in a problem involving a large number of observations and variable parameters, considerable time might be saved by first refining using the diagonal approximation until convergence is almost obtained and then switching to a few cycles of full matrix and anisotropic temperature refinement, so that as good a solution as possible is obtained. For smaller problems, the most advantageous approach would probably be to use the full

matrix in all the computations.

When run under the Fortran Monitor System (FMS), SFLSQ3 consists of a main program and 16 subroutines, plus subroutines called from the library tape. The program as distributed will refine up to 172 variables (full matrix refinement) and an essentially unlimited number of reflections. It was originally intended that subroutine CHLNK3 could be compiled as a main program so that it would be read in separately as a CHAIN LINK, thereby increasing the number of registers available for storing the matrix. This can still be done, but it might be more useful to consider the IBM 1301 Disk File which will soon be available as the means for storing larger matrices.

Common storage. Communication between the main program and the subroutines is principally through a large block of COMMON storage which is divided into six dummy arrays, CMA, CMB, CMC, CMD, CME, and CMF. Variable symbols are assigned to portions of these arrays by means of EQUIVALENCE statements. Table 1 is a list of the symbols which refer to COMMON storage.

Sense indicators. The array CMA contains the sense indicators which control much of the flow of the program. The definitions of these indicators are given in the section on running the program. They will be referred to frequently in the sections that follow.

Tape usage. The tape assignments for this program are given in Table 2. A copy of the M.I.T. IOU subprogram which

Table 1

Symbols assigned to COMMON storage

<u>Symbol</u>	<u>Dimension</u>	<u>Function</u>
CMA	50	Dummy array
CMB	507	" "
CMC	651	" "
CMD	700	" "
CME	419	" "
CMF	50	" "
AR	14969	Normal equation matrix
V	200	Vector matrix
TITLE	12	Title for printed output
MODE, INV, ISAN, NPU, NEW, NU, NS, NFOUR, NCOR, SUMDL, KARD, ID, NFSQ		See directions for preparing sense card.
A, B, C, ALPHA, BETA, GAMMA	1 each	Cell constants
SUMDL	1	$\sum_{hkl} (\sqrt{w} \Delta)^2$
NPAR	1	Total number of parameters
NVAR	1	Number of parameters varied
NCOUNT	1	Number of observations used in refinement
KSEL	504	Parameter selection words
S	50	Scale factors
BO	1	Overall temperature factor

Table 1 continued

MF	50	Form factor indicator
X, Y, Z	50 each	Atom coordinates
BI	50	Isotropic temperature factor
B11, B22, B33, B12, B13, B23	50 each	Anisotropic temperature factors
SYM	50	Atom "scale factor" or multiplicity
NAME	50	Atom name for printed output
NF	1	Number of form factor tables
FORM	32, 20	Form factor tables
F	20	f_i
ASTER	4	Asterisks for printed output
RHO, RHOSQ	1 each	$\sin\theta/\lambda$, $\sin^2\theta/\lambda^2$
ARG	32	Arguments for form factor tables
ISAVE	1	Indicator of last entry into form factor table arguments
FOBS	1	$F_o(hkl)$
FCAL	1	$F_c(hkl)$
AOBS, ACAL, BOBS, BCAL	1 each	A_o, A_c, B_o, B_c
DELTA	1	$(F_o - S_m F_c) \equiv \Delta$
SIGMA	1	Observation error
EXT1, EXT2	1 each	Optional extra input
SQRTW	1	\sqrt{w}
MS1	1	Scale factor subscript

Table 1 continued

MREJ	1	Rejection indicator
MH, MK, ML	1 each	Fixed point h, k, l
TH, TK, TL	1 each	Floating point h, k, l
DA, DB	200 each	Derivatives of A_c and B_c
SFC	1	$S_m F_c(hkl)$
SMSFC	1	$\sum_{hkl} S_m F_c(hkl)$
SQDL	1	$(\sqrt{w}\Delta)^2$
DELTA1	1	$\sum_{hkl} \Delta$ including zero F_o 's
SUMFO1	1	$\sum_{hkl} F_o$ including zero F_o 's
WDL1	1	$(\sum_{hkl} (\sqrt{w}\Delta)^2)^{\frac{1}{2}}$ including zero F_o 's
WFO1	1	$(\sum_{hkl} (\sqrt{w}F_o)^2)^{\frac{1}{2}}$ including zero F_o 's
DELTA2	1	
SUMFO2	1	Same as for preceding four symbols except without zero F_o 's
WDL2	1	
WFO2	1	

Table 2

Tape assignments for SFLSQ3 at M. I. T. Computation Center

<u>Logical</u>	<u>Physical</u>	<u>Use</u>
1	A1	Library
4	A2	Input
2	A3	Output
8	A4	Derivatives if CHAIN JOB is used
9	A5	Optional input for ERFR2 (Fourier synthesis)
5	B1	-
6	B2	Chain tape (optional)
7	B3	Scratch
3	B4	Punched output
10	B5	Binary output tape used as input to next cycle

correlates the logical and physical tape designations is provided with the program deck. If the physical designations do not correspond with the usage of a particular computing center, it is generally easier to change the IOU rather than the logical tape numbers in the FORTRAN input-output statements. One should, however, check with the computing center if he is uncertain as to how to proceed.

Punched output. At the M. I. T. Computation Center, punched output may be produced from a tape or on-line depending on whether sense switch 4 is down. The FORTRAN statements, PUNCH N, List, in subprograms PRSF and CARD may have to be replaced by WRITE OUTPUT TAPE M, N, List, if punched output is desired at a particular center where the sense switch option is not available. Otherwise, all card punching will be done on-line.

A subprogram from the M. I. T. library, MIFLIP, is provided with the program which will cause identification cards to be punched along with any off-line punched output. If this feature is not desired, a dummy subprogram, SUBROUTINE PILF1 (FLP, N), may be compiled or statements 16 and 17 in READ1 removed.

Description of the main program and its subroutines

MAIN. Although the main program is primarily used as a means of connecting the various subroutines, it does perform some essential computational functions. For example, the statements from 500 to 504 convert temperature factors from isotropic to anisotropic form when so requested by the sense card. At statement 8, the program tests whether reflection data is to be read from A2 or B5 and then reads and processes one reflection at a time until all are read in. For each reflection, the value of $\sin \theta / \lambda$ is computed or read from B5. When this quantity is computed, the program evaluates

$$\rho^2 = (\sin^2 \theta / \lambda^2) = (h^2 a^2 + k^2 b^2 + l^2 c^2 + 2hka^* b^* + 2klb^* c^* + 2lhc^* a^*) / 4. \quad (1)$$

The main program also computes the derivatives of $\frac{F}{c}(\underline{hkl})$ or $\frac{F^2}{c}(\underline{hkl})$ with respect to varied parameters beginning at statement 38. These relations are given in Table 3.

In order to be able to run consecutive structure factor calculations or cycles of refinement with a minimum of difficulty, all input data with the exception of title and sense cards is written on B5 at the end of a structure factor or least-squares calculation. The main program (or subroutine CHAIN) has to put some of this information first on B3 so that B5 can be updated on each cycle.

Table 3

Derivatives of $F_c(\text{hkl})$ or $F_c^2(\text{hkl})$ with respect to varied parameters (After Busing and Levy, 1959)

Computed Quantity	$F_c(\text{hkl})$	
	Centrosymmetric	Non-centrosymmetric
$s_m F_c$	$2 s_m \exp(-B_o \rho^2) A_c$	$s_m \exp(-B_o \rho^2) (A_c^2 + B_c^2)^{\frac{1}{2}}$
$\frac{\partial(s_m F_c)}{\partial s_m}$	$(s_m F_c)/s_m$	$(s_m F_c)/s_m$
$\frac{\partial(s_m F_c)}{\partial B_o}$	$-\rho^2 (s_m F_c)$	$-\rho^2 (s_m F_c)$
$\frac{\partial(s_m F_c)}{\partial p}$	$2 s_m \exp(-B_o \rho^2) \left(\frac{\partial A_c}{\partial p}\right)$	$s_m \exp(-B_o \rho^2) (A_c^2 + B_c^2)^{-\frac{1}{2}} \left[A_c \left(\frac{\partial A_c}{\partial p}\right) + B_c \left(\frac{\partial B_c}{\partial p}\right) \right]$

Table 3 continued

$$F_c^2(hkl)$$

Computed Quantity	Centrosymmetric	Non-centrosymmetric
$(s_m F_c)^2$	$4 s_m^2 \exp(-2B_o \rho^2) A c^2$	$s_m^2 \exp(-2B_o \rho^2) (A c^2 + B c^2)$
$\frac{\partial (s_m F_c)^2}{\partial s_m}$	$2 (s_m F_c)^2 / s_m$	$2 (s_m F_c)^2 / s_m$
$\frac{\partial (s_m F_c)^2}{\partial B_o}$	$-2 \rho^2 (s_m F_c)^2$	$-2 \rho^2 (s_m F_c)^2$
$\frac{\partial (s_m F_c)^2}{\partial p}$	$8 s_m^2 \exp(-2B_o \rho^2) A \left(\frac{\partial A c}{\partial p}\right)$	$2 s_m^2 \exp(-2B_o \rho^2) [A c \left(\frac{\partial A c}{\partial p}\right) + B c \left(\frac{\partial B c}{\partial p}\right)]$

The following symbols not listed in Table 1 are used in the main program.

<u>Symbol</u>	<u>Dimension</u>	<u>Function</u>
DF	200	Storage for derivatives
ALPHA 1, BETA 1, GAMMA 1	1 each	Reciprocal cell angles in radians
AA, BB, CC, ABC, BCA, CAB	1 each	Functions of cell parameters
I, J, K	1 each	Variable subscripts
N, NT	1 each	Number of storage registers in normal equation matrix
PI	1	π
RAD	1	$\pi/180.0$
TO	1	Exponential of B_0
C 1, C 2, Q	1	Terms used in calculating derivatives
LAST	1	Indicator of last reflection card
IEND	1	Indicator of the end of run
MS	1	Scale factor subscript
WDEL	1	$\sqrt{w} \Delta$

READ 1. The title, sense, and cell cards are read from A2. If data is available from a previous calculation, all but the reflection data is read in from B5. PILF 1 is called, if requested, to write identification of off-line punched output on B4.

The only symbol defined in READ 1 is FLP, an array of four registers used for storing the punched output identification.

READ 2. Reads and stores form factor tables unless the f's were read from B5 and are not to be altered.

READ 3. Reads and stores scale factors, overall temperature factor, atom coordinates and temperature factors, atom multiplicities, atom names, number of parameters, and parameter selection card. If this data was read in from B5 in READ 1 and is to be used without change, the program does not attempt to read A2.

SET. See STMAT.

LOOKUP. If f 's have not already been computed in a previous calculation, this routine performs a linear interpolation in the form factor tables. The program "looks" both ways in a table of arguments (array ARG) to find the location of $\sin \theta / \lambda$ for a particular hkl and then computes and stores interpolated f 's for all different types of atoms in array F. Each succeeding entry to the argument table will be at the point of last exit so that the program is more efficient if reflections with similar $\sin \theta / \lambda$ are grouped together.

It should be noted that it would be relatively easy to change the interpolation scheme to a more sophisticated one or to substitute a subroutine which would compute the form factors directly. The only requirement is that the f 's are stored in array F in the proper order.

WEIGHT. Weighting for least-squares is accomplished by either reading $\sigma(\sqrt{w} = \frac{1}{\sigma})$ from reflection data cards or by calculating σ in this subroutine. If σ is read from cards, WEIGHT must be a dummy subroutine. The main program computes $\sqrt{w} = 0$ if $\sigma = 0$.

If a weighting scheme requires the calculated structure factor, \sqrt{w} could be computed in REJECT.

Possible weighting schemes are given in International Tables (1959), Vol. II, p.328, Cruickshank (1961), Evans (1961), and Burnham and Buerger (1961).

SPGRP. Since this is the only subroutine which will require alterations for most routine work, considerable space will be devoted to its details. Many arguments have been advanced for coding space group manipulations in one way or another. In order to avoid this problem and because there are definite advantages in having particular space group routines for specific applications, the choice is left up to the user. The main program requires that SPGRP compute ACAL and, if the space group is non-centrosymmetric, BCAL. It also requires computation of derivatives of ACAL and BCAL with respect to the parameters that are to be varied. Two space group routines, however, are provided with the program. One is a general routine which can be easily adapted for any space group and with which anisotropic temperature factors can be refined. The other is written for space group $\underline{P1}$ only and is representative of routines which can be written for other specific space groups by using the Lonsdale formulas for the general position (International Tables, 1952, Vol. I). Unfortunately, except for $\underline{P1}$ and $\underline{P1}$, it is not easy to refine anisotropic temperature factors using this approach.

The remaining part of this section will be used to describe the two subroutines distributed with the program. Those interested in other approaches to the problem are referred to papers by Rollett and Davies (1955), Trueblood (1956), Cruickshank (1961), Hybl and Marsh (1961), and International Tables (1959), Vol. II, p.326-328.

Table 4 gives the quantities which are calculated by the general space group routine. SPGRP is entered once for each reflection. $\underline{A}_{\underline{c}}(hkl)$ and $\underline{B}_{\underline{c}}(hkl)$ are computed and stored in ACAL and BCAL respectively, while derivatives of $\underline{A}_{\underline{c}}$ and $\underline{B}_{\underline{c}}$ are stored in arrays DA and DB, respectively. The only changes which must be made to allow for different space groups are in the 300 group of statements unless modifications for atoms in special positions are required.

The general space group routine computes the contribution to the structure factor of each atom in the cell exclusive of atoms related by translations or centers of symmetry. For these latter groups of atoms, the contribution of one atom is computed and multiplied by a multiplicity factor \underline{M} (designated SYM in the program). The transformation of symmetry related atoms is accomplished by transforming indices instead of atom coordinates. This is done mainly so that anisotropic temperature factors can be handled properly.

The symmetry considerations are resolved by supplying the routine with the transformed indices. As an example, consider

Table 4
 Quantities evaluated by general space group subroutine
 Atoms i are transformed through j equivalent positions

Computed Quantity	Isotropic temperature factor	Anisotropic temperature factor
Ac(hkl)	$\sum_i M_i f_i \exp(-T_i) \sum_j \cos 2\pi(h_j x_i + k_j y_i + l_j z_i)$	$\sum_i M_i f_i \sum_j \exp(-T_{ij}) \cos 2\pi(h_j x_i + k_j y_i + l_j z_i)$
Bc(hkl)	$\sum_i M_i f_i \exp(-T_i) \sum_j \sin 2\pi(h_j x_i + k_j y_i + l_j z_i)$	$\sum_i M_i f_i \sum_j \exp(-T_{ij}) \sin 2\pi(h_j x_i + k_j y_i + l_j z_i)$
$T_{i(j)}$	$B_i \rho^2$	$h_j^2 \beta_{11i} + k_j^2 \beta_{22i} + l_j^2 \beta_{33i} + 2h_j k_j \beta_{12i} + 2h_j l_j \beta_{13i} + 2k_j l_j \beta_{23i}$
$\frac{\partial Ac}{\partial M_i}$	$f_i \exp_i \sum_j \cos_{ij}$	$f_i \sum_j \exp_{ij} \cos_{ij}$
$\frac{\partial Bc}{\partial M_i}$	$f_i \exp_i \sum_j \sin_{ij}$	$f_i \sum_j \exp_{ij} \sin_{ij}$
$\frac{\partial Ac}{\partial x_i}$	$-2\pi M_i f_i \exp_i \sum_j h_j \sin_{ij}$	$-2\pi M_i f_i \sum_j h_j \exp_{ij} \sin_{ij}$
$\frac{\partial Bc}{\partial x_i}$	$2\pi M_i f_i \exp_i \sum_j h_j \cos_{ij}$	$2\pi M_i f_i \sum_j h_j \exp_{ij} \cos_{ij}$

Table 4 continued

Computed Quantity	Isotropic temperature factor	Anisotropic temperature factor
$\frac{\partial A_c}{\partial B_i}$	$-\rho^2 M_i f_i \exp_i \sum_j \cos_{ij}$	—
$\frac{\partial B_c}{\partial B_i}$	$-\rho^2 M_i f_i \exp_i \sum_j \sin_{ij}$	—
$\frac{\partial A_c}{\partial \beta_{11i}}$	—	$- M_i f_i \sum_j h_j^2 \exp_{ij} \cos_{ij}$
$\frac{\partial B_c}{\partial \beta_{11i}}$	—	$- M_i f_i \sum_j h_j^2 \exp_{ij} \sin_{ij}$

$$\rho = \sin\theta/\lambda$$

M_i is atom multiplicity

B_i is the isotropic temperature factor

$B_c(hkl)$ is the imaginary component of the structure factor

space group Pnam. The general position in Pnam is represented by the coordinates

$$x, y, z; \frac{1}{2}+x, \frac{1}{2}-y, \frac{1}{2}-z; \bar{x}, \bar{y}, \frac{1}{2}+z; \frac{1}{2}-x, \frac{1}{2}+y, \bar{z}$$

plus their centrosymmetric equivalents. It is evident that

$$\cos 2\pi(h^1x + k^1y + l^1z + t) = \cos 2\pi(h(\frac{1}{2}+x) + k(\frac{1}{2}-y) + l(\frac{1}{2}-z)) \quad (2)$$

where $\underline{h}^1 = \underline{h}$, $\underline{k}^1 = -\underline{k}$, $\underline{l}^1 = -\underline{l}$, and $\underline{t} = (\underline{h} + \underline{k} + \underline{l})/2$. In SPGRP, \underline{h} , \underline{k} , and \underline{l} are stored in TH, TK, and TL, and \underline{h}^1 , \underline{k}^1 , \underline{l}^1 , and \underline{t} in RH, RK, RL, and T. The only requirement for Pnam is that RH, RK, RL, and T be transformed to correspond to each of the four equivalent positions above. This is accomplished by writing the following sequence of FORTRAN instructions and compiling them into SPGRP. Note that only those indices which are different from the previous loop have to be computed.

```

300   DO 413 J= 1, 4

301   GO TO (302, 303, 304, 305), J

302   RH = TH
      RK = TK
      RL = TL
      T = 0.0
      GO TO 400

303   RK = -TK
      RL = -TL
      T = (TH + TK + TL)/2.0
      GO TO 400

```

```

304   RH = -TH
      RL = TL
      T = TL/2.0
      GO TO 400
305   RK = TK
      RL = -TL
      T = (TH + TK)/2.0
400   PHI = TPI*(RH*X(I)+RK*Y(I)+RL*Z(I)+T)
      :
413   CONTINUE

```

This is the only change required for most situations. Extra modification may be necessary, however, when computing anisotropic temperature factors for atoms in special positions, for atoms with redundant coordinates, and for anomalous dispersion corrections.

Anisotropic temperature factor computations for atoms in special positions of Pnam are not difficult because the only restraints are that for atoms lying on the mirror plane in equipoint 4c, $\beta_{13} = \beta_{23} = 0$ (Levy, 1956). This can be taken care of by simply not varying β_{13} and β_{23} . When refining structures in space groups of higher symmetry, however, the constraints on the anisotropic temperature factor lead to special coding problems. Take, for example, the space group P6₃/mmc discussed in this regard by Levy (1956). He finds that for equipoint 12k with symmetry m,

$$\beta_{12} = \frac{1}{2}\beta_{22}, \beta_{13} = \frac{1}{2}\beta_{23}.$$

These restrictions would be handled in SPGRP in the following way. SPGRP normally evaluates the anisotropic temperature factor as given in Table 4. Since β_{12} and β_{31} are redundant, they must not be varied. The expression which is evaluated is then

$$\exp\{-[h_j^2\beta_{11i} + (k_j^2 + h_j k_j)\beta_{22i} + l_j^2\beta_{33i} + (2h_j k_j + k_j l_j)\beta_{23i}]\}. \quad (3)$$

This would be accomplished by substituting the following statements for those in SPGRP from 407 to 407 + 5.

```

407   RHH = RH**2
      RKK = RK**2+RH*RK
      RLL = RLL**2
      RHK = 0.0
      RHL = 0.0
      RKL = 2.0*RH*RK+RK*RL

```

In the event that different types of special positions are present, a statement at 407,

```
GO TO (N1, N2, ..., Ni), I,
```

where I is number of the atom being considered, would direct the program to the proper index transformation.

After a cycle of refinement is completed, the redundant β 's should be set to their proper values in TEST before the test for negative temperature factors is made. Redundant positional parameters which are handled similarly in the 300 group of statements can also be reset at this point.

If any particular difficulty is encountered in determining what to do about anisotropic temperatures or atom coordinates in specific space groups reference to Levy (1956), Trueblood (1956), Cruickshank (1961), Busing and Levy (1959), or International Tables (1959), Vol. II, might be helpful.

Anomalous dispersion can easily be allowed for in any version of SPGRP. In the general space group routine, the dispersion terms are added in the 500 series of statements. One way of doing this is to compute the contributions to the structure factor for the real and imaginary scattering factor terms separately and then add the components of the structure factor vectorially. For example, if the total scattering factor is

$$f = f_o + \Delta f' + i\Delta f'' \quad (4)$$

then (neglecting temperature factors),

$$A_c = \sum \{ (f_o + \Delta f') \cos\phi - \Delta f'' \sin\phi \} \quad (5)$$

and

$$B_c = \sum \{ (f_o + \Delta f') \sin\phi + \Delta f'' \cos\phi \} \quad (6)$$

for non-centrosymmetric space groups. In centrosymmetric space groups, $\sin\phi = 0$. For atoms in the cell which do not exhibit appreciable anomalous scattering, $\Delta f' = \Delta f'' = 0$. Since centrosymmetric structures are treated as though they are non-centrosymmetric, the user must remember to run the program with $INV = 2$ and to adjust the multiplicity to account for the fact that the main program will not multiply ACAL by two (see Table 3). As an example,

the following sequence of statements is suggested for a problem with two atoms, the first being an anomalous scatterer and the other not.

Data for the first atom, Fe in CuK_α radiation, is taken from International Tables (1962), Vol. III.

```

500   GO TO (501, 502, 502), ISAN
501   TMP = EXPF(-BI(I)*RHOSQ)*SYM(I)
      GO TO 503
502   TMP = SYM(I)
503   GO TO (504, 505), I
504   TMPA = (F(JJ)-1.1)*TMP
      TMPB = 3.4*TMP
      GO TO 506
505   TMPA = F(JJ)*TMP
      TMPB = 0.0
506   AR = TMPA*SMCP
      AI = TMPB*SMCP
      BR = TMPA*SMSP
      BI = TMPB*SMSP
507   ACAL = ACAL + AR - BI
      BCAL = BCAL + BR + AI
508   GO TO (700, 600), MODE

```

Statements 600 to 600 + 3 compute constants required for the derivatives. If no anomalous scattering correction is used, TMPB should be made equivalent to TMPA with a statement, $\text{TMPB} = \text{TMPA}$,

or EQUIVALENCE (TMPA, TMPB).

Derivatives are calculated in the general SPGRP routine as noted in Table 4. For each atom in turn, the program computes the contributions to \underline{A}_c , \underline{B}_c , and derivatives of \underline{A}_c and \underline{B}_c with respect to the atom parameters that are to be varied. If the number of derivatives calculated exceeds the number of parameters to be varied the program skips to the calculations for the next atom in the list.

Space group calculations which evaluate the Lonsdale formulas differ **only** in that the expression for the general position is used instead of finding the contribution of each symmetry equivalent atom separately. The computation time for this method is probably somewhat less than for the general routine, but there are two drawbacks. One is that anisotropic temperature factors cannot be handled conveniently except in $\underline{P1}$ or $\underline{P\bar{1}}$, and the other is that the expressions for the derivatives have to be worked out separately for each space group. An example for $\underline{P\bar{1}}$ coded in this way is supplied with the program deck.

There are undoubtedly many variations in the methods of calculation of structure factors which could be profitably used in SPGRP. Considerable machine time could be saved in special problems if the coding were done especially for those problems. One obvious way to cut down on the running time would be to program SPGRP in FAP. It is estimated that the number of machine instructions

in the general SPGRP routine could be reduced by at least one-half if the routine were written in FAP.

Symbols unique to the general SPGRP routine are listed below.

<u>Symbol</u>	<u>Dimension</u>	<u>Function</u>
K	1	Subscript for derivatives DA and DB
L	1	Subscript for KSEL, the parameter selection words 2π
TPI	1	2π
PHI		$\phi_j = (h_j x_i + k_j y_i + l_j z_i)$
CP		$\cos\phi_j$ or $\exp_j \cos\phi_j$
SP		$\sin\phi_j$ or $\exp_j \sin\phi_j$
SMCP		$\sum_j \cos\phi_j$
SMSP		$\sum_j \sin\phi_j$
RH, RK, RL, T		$\frac{h_j}{-j}, \frac{k_j}{-j}, \frac{l_j}{-j}, \frac{t}{-}$
RHH		$\frac{h_j^2}{-j}$
E		Exponential of anisotropic temperature factor expression
CPH		$\sum_j \frac{h_j}{-j} \cos\phi_j$
TMP, TMPA, TMPB		Temporary storage
AR, AI, BR, BI		Contribution of 1 atom to structure factor
TA, TB, RA, RB		Derivative multipliers

REJECT. Any reflection not wanted in the refinement can be rejected here by storing zero in MREJ. Otherwise, all reflections

except those for which \underline{F}_c is identically zero will be included in the refinement. The criterion for rejection can either be computed from data available in COMMON or can be sensed from information punched in the EXT 1 and/or EXT 2 fields of the reflection data cards. EXT 1 and EXT 2 are stored in COMMON also.

STAT. This subroutine accumulates statistical data for R-factor calculations or any other desired reliability indicators. Several registers in addition to those used in the distributed routine are available in array CMF for transmitting this data to PRST, the routine which prints statistical results after all structure factors have been computed.

The quantity

$$\Delta(hkl) = F_o - s_m F_c \quad (7)$$

is computed in this routine, where \underline{F}_o is given the sign of \underline{F}_c . This differs from many refinement programs which compute the difference of the absolute magnitudes of \underline{F}_o and \underline{F}_c . Of course, in non-centrosymmetric structures, \underline{F}_c is always positive.

The only symbol unique to STAT is SQFO which contains $(\sqrt{w} \Delta)^2$.

PRSF. This routine controls the structure factor output, both printed and punched. For each reflection the following is written on the output tape:

$\underline{h}, \underline{k}, \underline{l}, |\underline{F}_o|, s_m \underline{F}_c, \underline{A}_o, \underline{A}_c, \underline{B}_o, \underline{B}_c, \Delta, \Delta/\sigma$, asterisks where

$\underline{A}_o = |\underline{F}_o|(\underline{A}_c/\underline{s}_m\underline{F}_c)$ and $\underline{B}_o = |\underline{F}_o|(\underline{B}_c/\underline{s}_m\underline{F}_c)$. \underline{B}_o and \underline{B}_c are not written on tape for centrosymmetric structures in SPGRP unless an anomalous dispersion correction has been made. One asterisk is written if the reflection has been rejected from the refinement and two are written if $\Delta/\sigma > 2.0$.

Provision is made for punching of cards for input to ERFR2 (Sly, Shoemaker, and Van den Hende, 1962). In this option, $\underline{h}, \underline{k}, \underline{l}, \underline{A}_o, \underline{A}_c, (\underline{B}_o, \underline{B}_c), |\underline{F}_o/\underline{s}_m|$ are either punched on-line or written on B4 for off-line punching, depending on whether sense switch 5 is up or down. Since the option of on- or off-line punching may not be available at a particular computing center, PUNCH statements, 8 and 64, may have to be changed. This same information may, however, be written on A5 so that input to ERFR2 does not have to go through the punched card state.

Enough information is available in COMMON to enable the user to tailor the output to suit almost any requirement. One might, for example, substitute new SPGRP and PRSF routines which would calculate and put out unitary structure factors.

Special symbols used in PRSF are listed below. All have a dimension of 1.

<u>Symbol</u>	<u>Function</u>
C 1	$\underline{F}_o/(\underline{s}_m\underline{F}_c)$
DS	Δ/σ
FOSC	$ \underline{F}_o/\underline{s}_m $
I	Indicator for asterisks

STMAT and SET. Since the storage of the normal equation and vector matrices is the most time-consuming single operation in large problems, this routine is written in FAP. The entry point SET is used to set up the indexing and addresses needed in STMAT. The storage loops are about as efficient as possible for this type of program. STMAT is entered once for each reflection accepted in the refinement.

PRST. The statistics accumulated in STAT are written on A3. These include various R-factors and an error of fit given in Table 5. Extra symbols used in PRST are as follows:

R1, R2, WR1, WR2	R-factors
RSUMDL	$\sqrt{(\sum w\Delta)^2}$
TEST	Error of fit

CHLNK3. Presently constituted as SUBROUTINE CHAIN. It may be compiled as a main program and run as a chain link with SFLSQ3 which would then call the FMS subroutine CHAIN instead of CHLNK3. This requires several modifications in the main program and STMAT as well as CHLNK3.

CHLNK3 calls the matrix inverter SMI, writes the Geller correlation matrix (Geller, 1961) on A3, computes and applies the parameter shifts, and writes the refinement results on A3.

Following the notation of Busing and Levy (1959) and Geller (1961), Table 5 lists the various relations evaluated by CHLNK3. Only the binary deck of the matrix inversion routine, ORSMI, is

supplied with this program. However, a description of the numerical methods used has been published by Busing and Levy (1962).

Three other subroutines are called by CHLNK3 which will be discussed below. One of these, TEST, tests whether the temperature factors are positive-definite. If the user so desires, the symbol K in the calling sequence to TEST can be made non-zero if one or more temperature factors are not positive-definite and the run will be stopped regardless of how many cycles are left to be run. If K is zero, however, the program will attempt to go through another cycle if requested to do so.

If a singular matrix occurs, CHLNK3 will list the offending elements on A3 and terminate the run. A singular matrix is generally the result of trying to vary parameters for which derivatives have not been computed. This can occur, however, when an attempt is made to vary atoms in special positions or when varying coordinates of overlapping atoms using two-dimensional data.

The following symbols not in COMMON are used in CHLNK3.

<u>Symbol</u>	<u>Dimension</u>	<u>Function</u>
ART	20	Line of correlation matrix
EP	1	Parameter change
ERFIT	1	FIT/(m-n)
FIT	1	$\sqrt{\sum(\sqrt{w}\Delta)^2 - \sum \Delta p_i v_i}$
I1, I2, IT, MT, NV	1 each	Subscripts used in generating correlation matrix output

Table 5

Expressions evaluated in CHLNK3 (after Busing and Levy, 1959)

Quantity	Relation
Normal equation matrix	$a_{ij} = \sum_{hkl} (\sqrt{w} D_i) (\sqrt{w} D_j)$
Vector	$v_i = \sum_{hkl} (\sqrt{w} D_i) (\sqrt{w} \Delta)$
Inverse matrix	$b_{ij} = A_{ji}/d$
Parameter shift	$\Delta p_i = \sum_j b_{ij} v_j$
Error of fit	$E = \left\{ \sum_{hkl} (\sqrt{w} \Delta)^2 - \sum_{k=1}^m \Delta p_k v_k \right\} / (m-m)^{\frac{1}{2}}$
Standard error of Δp_i	$\sigma(p_i) = \sqrt{b_{ii}} E$
Correlation coefficient	$\rho_{ij} = b_{ij} / [(\sqrt{b_{ii}}) (\sqrt{b_{jj}})]$

Definitions

Δ	$[(\text{sign of } F_c) F_o] - s_m F_c$
s_m	scale factor
D_i	derivatives
A_{ji}	cofactor of a_{ij}
d	det a
p_i	parameters

LJD, LJ, NM, N, NT	1 each	Subscripts used in manipulating least-squares matrices
I, J, K	1 each	Subscripts
KA	1	Positive-definite temperature factor indicator
SUMCH	1	$\sum_i \Delta p_i v_i$

TEST. This subroutine is used to test whether the new temperature factors are positive-definite and may also be used to reset relations between parameters. If the overall temperature factor \underline{B}_o is non-zero, it is added to the individual atom temperature factors and the following tests are made.

For isotropic temperature factors, if $\underline{B}_i < 0$, \underline{B}_i will be set to .01 and K is left at zero. For anisotropic temperature factors the following relations must be satisfied. Otherwise K will be non-zero and the program will stop upon return to CHLNK.

$$\beta_{11i} > 0, \beta_{22i} > 0, \beta_{33i} > 0$$

$$\begin{vmatrix} \beta_{11} & \beta_{12} & \beta_{13} \\ \beta_{12} & \beta_{22} & \beta_{23} \\ \beta_{13} & \beta_{23} & \beta_{33} \end{vmatrix} \geq 0$$

$$\begin{vmatrix} \beta_{22} & \beta_{23} \\ \beta_{23} & \beta_{33} \end{vmatrix} \geq 0 \quad \begin{vmatrix} \beta_{11} & \beta_{13} \\ \beta_{13} & \beta_{33} \end{vmatrix} \geq 0 \quad \begin{vmatrix} \beta_{11} & \beta_{12} \\ \beta_{12} & \beta_{22} \end{vmatrix} \geq 0$$

The program can be changed so that after these tests are made, the offending elements are altered so that they will pass the positive-definite tests. Another feature that could be added is to

compute an equivalent isotropic \underline{B} for each set of anisotropic β 's.
See Hamilton (1959) or Lipscomb et al. (1956) for relations between \underline{B} and β 's.

CARD. This subroutine will write the new atom parameters on B4 for off-line punching. This is particularly useful if a large number of atoms are being refined.

DIST. A subroutine, not written as yet, which will compute interatomic distances and angles after the end of a cycle.

Running the program

Data deck. The data cards are prepared according to the directive below. An understanding of FORTRAN format statements is assumed.

FORMAT

1. TITLE: Any identification in cols. 1-72
2. FLP: Information for identifying punched output.
May be blank if NPU below is zero. The problem and programmer numbers are for use at M. I. T.
Actually any Hollerith characters may be used. 4A6

Col.

1-6	Program number
7-12	Programmer number
13-24	Blank

3. Sense card.

Col.

1	MODE:	1 - structure factors only	I1
		2 - structure factors plus least-squares	
2	INV:	1 - centrosymmetric	I1
		2 - non-centrosymmetric	
3	ISAN:	1 - isotropic temperature factors	I1
		2 - anisotropic temperature factors	
		3 - change from isotropic to an- isotropic before refining	
4	NPU:	0 - no punched card structure factor output	I1
		1 - punched card structure factor output (writes tape B4)	
	NEW(5):	0 for old values and 1 for new values of:	5I1
5		(a) number of form factors and cell constants	
6		(b) form factor tables	
7		(c) atom parameters	
8		(d) key card and parameter selection cards	
9		(e) reflection data	

This allows the user to select whether the old values from a previous structure factor or least squares calculation (written in binary on B5), or new values in the input deck are to be used. There are restrictions on the changing of certain of these, e.g., the number of form factor tables may not be altered without changing the card corresponding to (a) above.

These values must all be 1 unless the binary output tape (B5) from a previous run is available to the program. If data from B5 is used, the corresponding cards must not be in the input deck.

10-11	NU:	number of atoms in the asymmetric unit	I2
12-13	NS:	number of scale factors	I2
14	NFOUR:	0 - no BCD output tape (A5) will be written 1 - BCD output tape (A5) will be written with end of data card for ERFR2 (1 in col. 1) and rewind 2 - BCD output tape with end of data card and <u>not</u> rewind	I1

This option permits writing a tape with the title above as the first record and with $h, k, l, A_o, A_c,$ and B_o and B_c , if necessary, plus $|F_o/s_m|$ in succeeding records for input to ERFR2.

15	NCOR:	0 - no correlation matrix 1 - will write the Geller correlation matrix on A3 for off-line printing (Used only in mode 2)	I1
16	KARD:	0 - no punched card output of atom parameters 1 - the new scale factors, overall temperature factor, and atom coordinates and temperature factors will be written on B4 for off-line punching	I1
17	ID:	0 - no interatomic distances and interbond angles	I1

1 - will compute and put out inter-atomic distances and interbond angles after end of cycle. Subroutine DIST which computes these functions is not available at this time.

I1

18 NFSQ: 0 - refine on F_o I1
 1 - refine on F_o^2

4. Cell card (note that angles are used and not cosines as in ORXLS)

Col.

1-2	Number of form factor tables	I2
3-9	Blank	7X
10-18	a^* ($\frac{1}{a}$, not $\frac{\lambda}{a}$)	F9.4
19-27	b^*	"
28-36	c^*	"
37-45	α^* (in degrees)	"
46-54	β^*	"
55-63	γ^*	"

5. Form factor tables (same format as ORXLS). One set of four cards for each different kind of atom. 7F9.2, F8.2

<u>Col.</u>	<u>Card 1</u>	<u>Card 2</u>	<u>Card 3</u>	<u>Card 4</u>
1-9 f for $\frac{\sin \theta}{\lambda} =$	1.55	1.15	.75	.35
.
.
64-71	1.20	.80	.40	0

6. Scale factors (1 per card). There must be NS cards.

Col.

1-9 F9.4

7. Overall temperature factor
- Col.
- 1-9 F9.4
8. Atom parameters (may be used in ORXLS)
(One card for each atom in asymmetric unit)
- Col.
- | | | |
|-------|------------------------------|------|
| 1-2 | Form factor table to be used | I2 |
| 3-7 | Blank | 5X |
| 8-14 | x | F7.4 |
| 15-21 | y | " |
| 22-28 | z | " |
| 29-35 | B or β_{11} | " |
| 36-42 | β_{22} | " |
| 43-49 | β_{33} | " |
| 50-56 | β_{12} | " |
| 57-63 | β_{13} | " |
| 64-72 | β_{23} | " |
9. 'Multiplicity.' This is the quantity M_i in Table 4. 12F6.4
- Col.
- | | |
|-------|---------|
| 1-6 | Atom 1 |
| 7-12 | Atom 2 |
| . | |
| . | |
| 67-72 | Atom 12 |
10. Atom name 12A6
- Col.
- | | |
|------|--|
| 1-6 | Any BCD characters desired to correspond to atom 1, etc. |
| 7-12 | Any BCD characters desired to correspond to atom 2, etc. |

67-72 Any BCD characters desired to correspond to atom 12, etc.

Use as many of cards 9 and 10 as are needed to describe all atoms.

11. Key card

Col.

1-3	NPAR: Total number of parameters	I3
4-6	Blank	3X
7-9	NVAR: Number of parameters varied	I3

NVAR must always be less than the number of non-zero weight, non-rejected reflections.

12. Parameter selection card 72I1

Col.

1-72 0 if the corresponding parameter is not to be varied, 1 if it is to be varied. The following order is to be observed: $s_1, s_2, \dots, s_m, B_o, M_1, x_1, y_1, z_1, B_1^i, \dots, M_v, x_v, y_v, z_v, B_v^i$. B^i represents either B_i or $\beta_{11i}, \beta_{22i}, \beta_{33i}, \beta_{12i}, \beta_{13i}, \beta_{23i}$. Use as many cards as necessary to describe NPAR above. 1's need not be punched for mode 1 calculation.

13. Reflection data (may be used in ORXLS)

Col.

1-3	h	I3
4-9	blank	6X
10-12	k	I3
13-18	blank	6X
19-21	l	I3

22-27	blank	6X
28-36	F_o or F_o^2	F9.2
37-45	sigma (program computes $\sqrt{w} = \frac{1}{\sigma}$)	"
46-47	number of scale factor to be used for this reflection	I2
48-54	blank	7X
55-63	extra input 1	F9.2
64-70	extra input 2	F7.2
71	blank	1X
72	blank	I1

Use one card for each reflection. Note that identifying letters in col. 72 sometimes used in ORXLS will cause this program to stop.

14. End of reflection deck

Col.

1-71	blank	71X
72	1	I1

15. Run termination card

Col.

1-71	blank	71X
72	Mode 1: If 0, the program will stop. If 1, the program will attempt to read a new set of data.	I1

Mode 2: If 0, the program will stop.

If 1, a new cycle will be begun either by returning to the main program from subroutine CHAIN or by calling in SFLSQ2 as a chain link, depending on the way the run is set up.

Submitting a run. The following main program and subroutine decks (left) should be included in the run deck (right).

SFSLQ3 (main program)	* ID card
READ1	* XEQ
READ2	SFSLQ3
READ3	Subroutines
LOOKUP	* DATA
WEIGHT	Data deck
SPGRP	Data deck for additional cycles.
REJECT	
STAT	
PRSF	
STMAT/SET	
CHLNK3	
SMI	
TEST	
CARD	
DIST	
MIFLIP	
MIIOU	

Tape B5 is always used by the program and may be saved as input to further computations.

References

- Busing, William R., and Henri A. Levy (1959), A Crystallographic Least-squares Program for the IBM 704. (Oak Ridge National Laboratory, Central Files No. 59-4-37, Oak Ridge, Tenn.)
- Busing, William R., and Henri A. Levy (1962), A Procedure for Inverting Large Symmetric Matrices. Comm. Assoc. Computing Mach. In press.
- Burnham, Charles W., and M. J. Buerger (1964), Refinement of the crystal structure of andalusite. Zeit. Krist. 115, 269-290.
- Cruickshank, D.W.J., Deana E. Pilling, A. Bujosa, F.M. Lovell, and Mary R. Truter (1964), In Computing Methods and the Phase Problem in X-Ray Crystal Analysis, Pergamon Press, Oxford, 32-78.
- Evans, Howard T., Jr. (1961), Weighting factors for single-crystal x-ray diffraction intensity data. Acta Cryst. 14, 689.
- Geller, S. (1961), Parameter interaction in least squares structure refinement. Acta Cryst. 14, 1026-1035.
- Hamilton, W. C. (1959), On the isotropic temperature factor equivalent to a given anisotropic temperature factor. Acta Cryst. 12, 609-610.
- Hybl, Albert, and Richard E. Marsh (1961), Structure factor and least-squares calculation for orthorhombic systems with anisotropic vibrations. Acta Cryst. 14, 1046-1051.
- International Tables for X-Ray Crystallography. Vol. I (1952), Vol. II (1959), Vol. III (1962). The Kynoch Press, Birmingham, England.
- Levy, Henri A. (1956), Symmetry relations among coefficients of the anisotropic temperature factor. Acta Cryst. 9, 679.

- Rollett, J. S., and David R. Davies (1955), The calculation of structure factors for centrosymmetric monoclinic systems with anisotropic atomic vibrations. *Acta Cryst.* 8, 125-128.
- Rossmann, Michael G., Robert A. Jacobson, F. L. Hirshfeld, and William N. Lipscomb (1959), An account of some computing experiences. *Acta Cryst.* 12, 530-535.
- Sly, W. G., D. P. Shoemaker, and J. H. Van den Hende (1962), Two- and Three-dimensional Crystallographic Fourier Summation Program for the IBM 7090 Computer. (Massachusetts Institute of Technology, Esso Research and Engineering Company).
- Trueblood, Kenneth N. (1956), Symmetry transformations of general anisotropic temperature factors. *Acta Cryst.*, 9, 359-361.

```

*      LIST
*      LABEL
CSFLSQ3
C      MAIN PROGRAM FOR STRUCTURE FACTOR AND LEAST SQUARES REFINEMENT
C      THIS VERSION STORES THE NORMAL EQUATION MATRIX DIRECTLY IN CORE
C      6/7/62
COMMON CMA,CMB,CMC,CMD,CME,CMF,AR,V
EQUIVALENCE (CMA,TITLE),(CMA(13),MODE),(CMA(14),INV),(CMA(15),ISAN
1),(CMA(16),NPU),(CMA(17),NEW),(CMA(22),NU),(CMA(23),NS),(CMA(24),A
2),(CMA(25),B),(CMA(26),C),(CMA(27),ALPHA),(CMA(28),BETA),(CMA(29),
3GAMMA),(CMA(30),NFOUR),(CMA(31),NCOR),(CMA(32),SUMDL),(CMA(33),KAR
4D),(CMA(34),ID),(CMA(35),NFSQ)
EQUIVALENCE (CMB,NPAR),(CMB(2),NVAR),(CMB(3),NCOUNT),(CMB(4),KSEL)
EQUIVALENCE (CMC,S),(CMC(51),BO),(CMC(52),MF),(CMC(102),X),(CMC
1(152),Y),(CMC(202),Z),(CMC(252),B11,BI),(CMC(302),B22),(CMC(352),
2B33),(CMC(402),B12),(CMC(452),B23),(CMC(502),B13),(CMC(552),SYM),(
3CMC(602),NAME)
EQUIVALENCE (CMD,NF),(CMD(2),FORM),(CMD(642),F),(CMD(662),ASTER),(
1CMD(666),RHO),(CMD(667),RHOSQ),(CMD(668),ARG),(CMD(700),ISAVE)
EQUIVALENCE (CME,FOBS),(CME(2),FCAL),(CME(3),AOBS),(CME(4),ACAL),(
1CME(5),BOBS),(CME(6),BCAL),(CME(7),DELTA),(CME(8),SIGMA),(CME(9),E
2XT1),(CME(10),EXT2),(CME(11),SQRTW),(CME(12),MS1),(CME(13),MREJ),(
3CME(14),MH),(CME(15),MK),(CME(16),ML),(CME(17),TH),(CME(18),TK),(
4CME(19),TL),(CME(20),DA),(CME(220),DB)
EQUIVALENCE (CMF,SFC),(CMF(2),SMSFC),(CMF(3),SQDL),(CMF(4),DELTA1)
1,(CMF(5),SUMFO1),(CMF(6),WDL1),(CMF(7),WFO1),(CMF(8),DELTA2),(CMF(
29),SUMFO2),(CMF(10),WDL2),(CMF(11),WFO2)
DIMENSION CMA(50),CMB(507),CMC(651),CMD(700),CME(419),CMF(50)
DIMENSION TITLE(12),NEW(5)
DIMENSION FORM(32,20),F(20),ASTER(4),ARG(32)
DIMENSION S(50),MF(50),X(50),Y(50),Z(50),BI(50),B11(50),B22(50),B3
13(50),B12(50),B23(50),B13(50),SYM(50),NAME(50)
DIMENSION DA(200),DB(200),DF(200)
DIMENSION AR(14969),V(200)
DIMENSION KSEL(504)
1      CALL READ1
      IF(NEW(2))2,3,2
2      CALL READ2
B3     ASTER(1)=605454735460
B      ASTER(2)=605460606060
B      ASTER(3)=605454606060
B      ASTER(4)=606060606060
      CALL READ3
      ARG(32)=0.0
      DO 4 I=1,31
      J=32-I
      K=33-I
      ARG(J)=ARG(K)+.05
4      CONTINUE
      ISAN=ISAN
      MODE=MODE
      INV=INV
      ISAVE=1
      NCOUNT=0
      SUMDL=0.0

```



```
DO 400 I=1,50
400 CMF(I)=0.0
401 GO TO (407,402),MODE
402 NT=NVAR+1
   N=NVAR*NT
   N=N/2
403 DO 404 I=1,N
404 AR(I)=0.0
405 DO 406 I=1,NVAR
406 V(I)=0.0
   CALL SET(N,DF,WDEL)
407 PI=3.1415927
   RAD=PI/180.0
   ALPHA1=ALPHA*RAD
   BETA1=BETA*RAD
   GAMMA1=GAMMA*RAD
   AA=A*A/4.0
   BB=B*B/4.0
   CC=C*C/4.0
   ABG=A*B*COSF(GAMMA1)/2.0
   BCA=B*C*COSF(ALPHA1)/2.0
   CAB=C*A*COSF(BETA1)/2.0
   GO TO(6,6,500),ISAN
500 DO 501 I=1,NU
   B22(I)=BI(I)*BB
   B33(I)=BI(I)*CC
   B12(I)=BI(I)*ABG/2.0
   B13(I)=BI(I)*CAB/2.0
   B23(I)=BI(I)*BCA/2.0
   B11(I)=BI(I)*AA
501 CONTINUE
6 REWIND 7
8 IF(NEW(5))10,9,10
9 READ TAPE 10,MH,MK,ML,FOBS,SIGMA,MS1,EXT1,EXT2,LAST,RHO,RHOSQ,F
   GO TO 15
10 READ INPUT TAPE 4,11,MH,MK,ML,FOBS,SIGMA,MS,EXT1,EXT2,LAST
11 FORMAT(3(I3,6X),2F9.2,I2,7X,F9.2,F7.2,1X,I1)
   FREQUENCY 12(1,5,1),13(1,5,1),15(1,100,1)
12 IF(MS)13,15,13
13 IF(MS-MS1)14,15,14
14 MS1=MS
15 IF(LAST)55,16,55
16 TH=MH
   TK=MK
   TL=ML
180 IF(NEW(5))182,181,182
181 IF(NEW(2))182,183,182
182 RHOSQ=TH*TH*AA+TK*TK*BB+TL*TL*CC+TH*TK*ABG+TK*TL*BCA+TL*TH*CAB
   RHO=SQRTF(RHOSQ)
   CALL LOOKUP
183 WRITE TAPE 7,MH,MK,ML,FOBS,SIGMA,MS1,EXT1,EXT2,LAST,RHO,RHOSQ,F
21 CALL WEIGHT
   FREQUENCY 22(1,25,1)
22 IF(SIGMA)23,24,23
23 SQRTW=1.0/SIGMA
```

```
GO TO 25
24  SQRTW=0.0
25  TO=EXPF(-BO*RHOSQ)
    CALL SPGRP
    MS1=MS1
26  GO TO(27,30),INV
27  Q=2.0*S(MS1)*TO
    SFC=Q*ACAL
    Q=SFC*SQRTW
28  IF(NFSQ)29,34,29
29  SFC=SFC**2
    Q=2.0*SFC*SQRTW
    GO TO 34
30  Q=S(MS1)*TO
    FCSQ=ACAL**2+BCAL**2
    FCAL=SQRTF(FCSQ)
    SFC=Q*FCAL
    Q=SFC*SQRTW
31  IF(NFSQ)29,34,29
34  CALL REJECT
    FREQUENCY 340(10,0,10)
340 IF(SFC)342,341,342
341 MREJ=0
342 CALL STAT
    CALL PRSF
    FREQUENCY 35(0,1,25),36(0,1,20)
35  IF(MREJ)36,8,36
36  IF(SQRTW)37,8,37
37  NCOUNT=NCOUNT+1
    SUMDL=SUMDL+SQDL
    GO TO(8,38),MODE
38  K=0
39  DO 43 J=1,NS
    IF(KSEL(J))40,43,40
40  K=K+1
    IF(MS1-J)41,42,41
41  DF(K)=0.0
    GO TO 43
42  DF(K)=Q/S(MS1)
43  CONTINUE
    J=NS+1
    IF(KSEL(J))44,450,44
44  K=K+1
    DF(K)=-RHOSQ*Q
    FREQUENCY 450(1,1,50)
450 IF(NVAR-K)52,52,451
451 I=1
    K=K+1
46  GO TO(47,49),INV
47  C1=Q/ACAL
    DO 48 J=K,NVAR
    DF(J)=DA(I)*C1
    I=I+1
48  CONTINUE
    GO TO 52
```

```

49  C1=Q/FCSQ
50  DO 51 J=K,NVAR
    DF(J)=(ACAL*DA(I)+BCAL*DB(I))*C1
    I=I+1
51  CONTINUE
52  WDEL=SQRW*DELTA
    CALL STMAT
53  GO TO 8
55  WRITE TAPE 7,MH,MK,ML,FOBS,SIGMA,MS1,EXT1,EXT2,LAST,RHO,RHOSQ,F
550 REWIND 7
    REWIND 10
551 GO TO(552,56),MODE
552 WRITE TAPE 10,NF,A,B,C,ALPHA,BETA,GAMMA,S,BO,MF,X,Y,Z,B11,B22,B33,
    1B12,B13,B23,SYM,NAME,NPAR,NVAR,KSEL
553 READ TAPE 7,MH,MK,ML,FOBS,SIGMA,MS1,EXT1,EXT2,LAST,RHO,RHOSQ,F
    WRITE TAPE 10,MH,MK,ML,FOBS,SIGMA,MS1,EXT1,EXT2,LAST,RHO,RHOSQ,F
554 IF(LAST)555,553,555
555 REWIND 7
    REWIND 10
56  CALL PRST
560 IF(NPU)57,580,57
57  END FILE 3
580 IF(NFOUR)581,584,581
581 WRITE OUTPUT TAPE 9,582
582 FORMAT(1H171X)
    IF(NFOUR-1)583,583,584
583 REWIND 9
584 GO TO(59,61),MODE
59  READ INPUT TAPE 4,60,IEND
60  FORMAT(71X,I1)
    IF(IEND)1,62,1
61  CALL CHAIN(2,B2)
    GO TO 1
62  CALL EXIT
    END

```

```

*  LIST
*  LABEL
SUBROUTINE READ1
C  READ INITIAL INPUT DATA AND WRITE HEADINGS ON OUTPUT TAPE
COMMON CMA,CMB,CMC,CMD
EQUIVALENCE (CMA,TITLE),(CMA(13),MODE),(CMA(14),INV),(CMA(15),ISAN
1),(CMA(16),NPU),(CMA(17),NEW),(CMA(22),NU),(CMA(23),NS),(CMA(24),A
2),(CMA(25),B),(CMA(26),C),(CMA(27),ALPHA),(CMA(28),BETA),(CMA(29),
3GAMMA),(CMA(30),NFOUR),(CMA(31),NCOR),(CMA(32),SUMDL),(CMA(33),KAR
4D),(CMA(34),ID),(CMA(35),NFSQ)
EQUIVALENCE (CMB,NPAR),(CMB(2),NVAR),(CMB(3),NCOUNT),(CMB(4),KSEL)
EQUIVALENCE (CMC,S),(CMC(51),BO),(CMC(52),MF),(CMC(102),X),(CMC
1(152),Y),(CMC(202),Z),(CMC(252),B11,B1), (CMC(302),B22),(CMC(352),
2B33),(CMC(402),B12),(CMC(452),B23),(CMC(502),B13),(CMC(552),SYM),(
3CMC(602),NAME)
EQUIVALENCE (CMD,NF),(CMD(2),FORM),(CMD(642),F),(CMD(662),ASTER),(
1CMD(666),RHO),(CMD(667),RHOSQ),(CMD(668),ARG),(CMD(700),ISAVE)
DIMENSION CMA(50),CMB(507),CMC(651),CMD(700)

```

```

DIMENSION TITLE(12),NEW(5)
DIMENSION S(50),MF(50),X(50),Y(50),Z(50),BI(50),B11(50),B22(50),B3
13(50),B12(50),B23(50),B13(50),SYM(50),NAME(50)
DIMENSION KSEL(504)
DIMENSION FLP(4)
1 READ INPUT TAPE 4,1,TITLE
  FORMAT(12A6)
2 READ INPUT TAPE 4,2,FLP(3),FLP(4),FLP(1),FLP(2)
  FORMAT(4A6)
3 WRITE OUTPUT TAPE 2,3,TITLE
  FORMAT(1H112A6)
4 READ INPUT TAPE 4,4,MODE,INV,ISAN,NPU,NEW,NU,NS,NFOUR,NCOR,KARD,ID
  1,NFSQ
  FORMAT(9I1,2I2,5I1)
  WRITE OUTPUT TAPE 2,5
5 FORMAT(30HOSENSE CARD AS READ BY PROGRAM)
  WRITE OUTPUT TAPE 2,6,MODE,INV,ISAN,NPU,NEW,NU,NS,NFOUR,NCOR,KARD,
  1ID,NFSQ
6 FORMAT(1H09I1,2I2,5I1)
  WRITE OUTPUT TAPE 2,3,TITLE
  REWIND 10
7 IF(NEW(1))8,12,8
8 IF(NEW(2))9,12,9
9 IF(NEW(3))10,12,10
10 IF(NEW(4))11,12,11
11 IF(NEW(5))14,12,14
12 READ TAPE 10,NF,A,B,C,ALPHA,BETA,GAMMA,S,BO,MF,X,Y,Z,B11,B22,B33,B
  112,B13,B23,SYM,NAME,NPAR,NVAR,KSEL
13 IF(NEW(1))14,16,14
14 READ INPUT TAPE 4,15,NF,A,B,C,ALPHA,BETA,GAMMA
15 FORMAT(I2,7X,6F9.4)
16 IF(NPU+KARD)17,18,17
17 CALL PILF1(FLP,4)
18 IF(NFSQ)181,180,181
B180 OBS=602646226260
B CAL=602623214360
  GO TO 182
B181 OBS=462262545402
B CAL=232143545402
182 GO TO (I9,21),INV
19 WRITE OUTPUT TAPE 2,20,OBS,CAL
20 FORMAT(18H0 H K L A6,7H A6,57H AOBS
  1 ACAL OBS-CAL (OBS-CAL)/SIGMA)
  GO TO 23
21 WRITE OUTPUT TAPE 2,22,OBS,CAL
22 FORMAT(18H0 H K L A6,7H A6,83H AOBS
  1 ACAL BOBS BCAL OBS-CAL (OBS-CAL)/SIGMA)
23 IF(NFOUR)24,25,24
24 WRITE OUTPUT TAPE 9,1,TITLE
25 RETURN
  END

```

```

* LIST
* LABEL

```

C READ2

```

SUBROUTINE READ2
C   READ FORM FACTOR FACTOR TABLES
COMMON CMA,CMB,CMC,CMD
EQUIVALENCE (CMA,TITLE),(CMA(13),MODE),(CMA(14),INV),(CMA(15),ISAN
2),(CMA(25),B),(CMA(26),C),(CMA(27),ALPHA),(CMA(28),BETA),(CMA(29),
3GAMMA),(CMA(30),NFOUR),(CMA(31),NCOR),(CMA(32),SUMDL)
EQUIVALENCE (CMB,NPAR)
EQUIVALENCE (CMC,S)
EQUIVALENCE (CMD,NF),(CMD(2),FORM),(CMD(642),F),(CMD(662),ASTER),(
1CMD(666),RHO),(CMD(667),RHOSQ),(CMD(668),ARG),(CMD(700),ISAVE)
DIMENSION CMA(50),CMB(507),CMC(651),CMD(700)
DIMENSION FORM(32,20),F(20),ASTER(4),ARG(32)
DO 6 J=1,NF
READ INPUT TAPE 4,5,(FORM(I,J),I=1,32)
5  FORMAT(7F9.2,F8.2)
6  CONTINUE
RETURN
END

```

```

*   LIST
*   LABEL

```

```

SUBROUTINE READ3
C   SUBROUTINE FOR READING ATOM PARAMETERS
COMMON CMA,CMB,CMC
EQUIVALENCE (CMA,TITLE),(CMA(13),MODE),(CMA(14),INV),(CMA(15),ISAN
1),(CMA(16),NPU),(CMA(17),NEW),(CMA(22),NU),(CMA(23),NS),(CMA(24),A
2),(CMA(25),B),(CMA(26),C),(CMA(27),ALPHA),(CMA(28),BETA),(CMA(29),
3GAMMA),(CMA(30),NFOUR),(CMA(31),NCOR),(CMA(32),SUMDL),(CMA(33),KAR
4D),(CMA(34),ID)
EQUIVALENCE (CMB,NPAR),(CMB(2),NVAR),(CMB(3),NCOUNT),(CMB(4),KSEL)
EQUIVALENCE (CMC,S),(CMC(51),BO),(CMC(52),MF),(CMC(102),X),(CMC
1(152),Y),(CMC(202),Z),(CMC(252),B11,BI),(CMC(302),B22),(CMC(352),
2B33),(CMC(402),B12),(CMC(452),B23),(CMC(502),B13),(CMC(552),SYM),(
3CMC(602),NAME)
DIMENSION TITLE(12),NEW(5)
DIMENSION S(50),MF(50),X(50),Y(50),Z(50),BI(50),B11(50),B22(50),B3
13(50),B12(50),B23(50),B13(50),SYM(50),NAME(50)
DIMENSION KSEL(504)
DIMENSION CMA(50),CMB(507),CMC(651)
1  IF(NEW(3))2,9,2
2  DO 4 I=1,NS
READ INPUT TAPE 4,3,S(I)
3  FORMAT(F9.4)
4  CONTINUE
READ INPUT TAPE 4,5,BO
5  FORMAT(F9.4)
READ INPUT TAPE 4,6,(MF(I),X(I),Y(I),Z(I),B11(I),B22(I),B33(I),B12
1(I),B13(I),B23(I),I=1,NU)
6  FORMAT(I2,5X,9F7.4)
READ INPUT TAPE 4,7,(SYM(I),I=1,NU)
7  FORMAT(12F6.4)
READ INPUT TAPE 4,8,(NAME(I),I=1,NU)
8  FORMAT(12A6)

```

```

9   IF(NEW(4))10,14,10
10  READ INPUT TAPE 4,11,NPAR,NVAR
11  FORMAT(I3,3X,I3)
12  READ INPUT TAPE 4,13,(KSEL(J),J=1,NPAR)
13  FORMAT(72I1)
14  RETURN
    END

```

```

*   LIST
*   LABEL
SUBROUTINE LOOKUP
C   TABLE LOOK-UP FOR FORM FACTORS
COMMON CMA,CMB,CMC,CMD
EQUIVALENCE (CMA,TITLE)
EQUIVALENCE (CMB,NPAR)
EQUIVALENCE (CMC,S)
EQUIVALENCE (CMD,NF),(CMD(2),FORM),(CMD(642),F),(CMD(662),ASTER),(
1  CMD(666),RHO),(CMD(667),RHOSQ),(CMD(668),ARG),(CMD(700),ISAVE)
DIMENSION FORM(32,20),F(20),ASTER(4),ARG(32)
DIMENSION CMA(50),CMB(507),CMC(651),CMD(700)
FREQUENCY 1(0,0,1),2(0,0,1),4(1,0,1),6(1,0,10),8(5),12(5),21(10,0,
1  11),22(5),30(5),37(5)
1   IF(RHO)32,30,2
2   IF(1.55-RHO)35,37,3
3   I=ISAVE
4   IF(RHO-ARG(I))20,12,5
5   I=I-1
6   IF(RHO-ARG(I))8,12,5
8   DO 10 J=1,NF
    F(J)=(FORM(I+1,J)-FORM(I,J))*(ARG(I)-RHO)/.05+FORM(I,J)
10  CONTINUE
    ISAVE=I
11  RETURN
12  DO 13 J=1,NF
    F(J)=FORM(I,J)
13  CONTINUE
    ISAVE=I
    RETURN
20  I=I+1
21  IF(RHO-ARG(I))20,12,22
22  DO 23 J=1,NF
    F(J)=(FORM(I,J)-FORM(I-1,J))*(ARG(I-1)-RHO)/.05+FORM(I-1,J)
23  CONTINUE
    ISAVE=I
24  RETURN
30  DO 31 J=1,NF
    F(J)=FORM(32,J)
31  CONTINUE
    RETURN
C   NEGATIVE RHO
32  WRITE OUTPUT TAPE 2,33
33  FORMAT(30HNEGATIVE RHO - RUN TERMINATED)
34  CALL EXIT
C   RHO GREATER THAN 1.55

```

```

35 WRITE OUTPUT TAPE 2,36
36 FORMAT(39HORHO GREATER THAN 1.55 - RUN TERMINATED)
   CALL EXIT
37 DO 38 J=1,NF
   F(J)=FORM(1,J)
38 CONTINUE
   RETURN
   END

```

```

* LIST
* LABEL
* SYMBOL TABLE
SUBROUTINE SPGRP
C GENERAL SPACE GROUP ROUTINE
COMMON CMA,CMB,CMC,CMD,CME
EQUIVALENCE (CMA,TITLE),(CMA(13),MODE),(CMA(14),INV),(CMA(15),ISAN
1),(CMA(16),NPU),(CMA(17),NEW),(CMA(22),NU),(CMA(23),NS),(CMA(24),A
2),(CMA(25),B),(CMA(26),C),(CMA(27),ALPHA),(CMA(28),BETA),(CMA(29),
3GAMMA),(CMA(30),NFOUR),(CMA(31),NCOR),(CMA(32),SUMDL),(CMA(33),KAR
4D),(CMA(34),ID)
EQUIVALENCE (CMB,NPAR),(CMB(2),NVAR),(CMB(3),NCOUNT),(CMB(4),KSEL)
EQUIVALENCE (CMC,S),(CMC(51),BO),(CMC(52),MF),(CMC(102),X),(CMC
1(152),Y),(CMC(202),Z),(CMC(252),B11,BI),(CMC(302),B22),(CMC(352),
2B33),(CMC(402),B12),(CMC(452),B23),(CMC(502),B13),(CMC(552),SYM),(
3CMC(602),NAME)
EQUIVALENCE (CMD,NF),(CMD(2),FORM),(CMD(642),F),(CMD(662),ASTER),(
1CMD(666),RHO),(CMD(667),RHOSQ),(CMD(668),ARG),(CMD(700),ISAVE)
EQUIVALENCE (CME,FOBS),(CME(2),FCAL),(CME(3),AOBS),(CME(4),ACAL),(
1CME(5),BOBS),(CME(6),BCAL),(CME(7),DELTA),(CME(8),SIGMA),(CME(9),E
2XT1),(CME(10),EXT2),(CME(11),SQRTW),(CME(12),MS1),(CME(13),MREJ),(
3CME(14),MH),(CME(15),MK),(CME(16),ML),(CME(17),TH),(CME(18),TK),(C
4ME(19),TL),(CME(20),DA),(CME(220),DB)
DIMENSION TITLE(12),NEW(5)
DIMENSION FORM(32,20),F(20),ASTER(4),ARG(32)
DIMENSION S(50),MF(50),X(50),Y(50),Z(50),BI(50),B11(50),B22(50),B3
13(50),B12(50),B23(50),B13(50),SYM(50),NAME(50)
DIMENSION KSEL(504)
DIMENSION DA(200),DB(200)
DIMENSION CMA(50),CMB(507),CMC(651),CMD(700),CME(419)
100 INV=INV
   ISAN=ISAN
   MODE=MODE
   ACAL=0.0
   BCAL=0.0
   K=1
   L=NS+2
   TPI=6.2831854
200 DO 700 I=1,NU
   JJ=MF(I)
201 SMCP=0.0
   SMSP=0.0
202 GO TO(300,203),MODE
203 CPH=0.0
   CPK=0.0

```

```

CPL=0.0
SPH=0.0
SPK=0.0
SPL=0.0
204 GO TO(300,205,205),ISAN
205 CPHH=0.0
CPKK=0.0
CPLL=0.0
CPHK=0.0
CPHL=0.0
CPKL=0.0
SPHH=0.0
SPKK=0.0
SPLL=0.0
SPHK=0.0
SPHL=0.0
SPKL=0.0
C LOOP FOR EACH ATOM IN ASYMMETRIC UNIT
300 DO 414 J=1,6
C INDEX TRANSFORMATION SECTION
C SPACE GROUP R 3BAR C
301 GO TO(302,303,304,305,306,307),J
302 RH=TH
RK=TK
RL=TL
T=0.0
GO TO 400
303 RH=TK
RK=-(TH+TK)
GO TO 400
304 RH=-(TH+TK)
RK=TH
GO TO 400
305 RH=TK
RK=TH
RL=-TL
T=TL/2.0
GO TO 400
306 RH=-(TH+TK)
RK=TK
GO TO 400
307 RH=TH
RK=-(TH+TK)
400 PHI=TPI*(RH*X(I)+RK*Y(I)+RL*Z(I)+T)
401 GO TO(402,407,407),ISAN
402 CP=COSF(PHI)
SP=SINF(PHI)
EQUIVALENCE (CPH,SPH),(CPK,SPK),(CPL,SPL),(SMCP,SMSP)
EQUIVALENCE(CPHH,SPHH),(SPKK,SPKK),(CPLL,SPLL),(CPHK,SPHK)
EQUIVALENCE(CPHL,SPHL),(CPKL,SPKL)
403 GO TO (413,404),MODE
404 SPH=SPH+SP*RH
SPK=SPK+SP*RK
SPL=SPL+SP*RL
405 GO TO (413,406),INV

```



```
406  CPH=CPH+CP*RH
      CPK=CPK+CP*RK
      CPL=CPL+CP*RL
      GO TO 413
407  GO TO(4070,4071),I
4070  RHH=RH**2
      RKK=RK**2+RH*RK
      RLL=RL**2
      RHK=0.0
      RHL=0.0
      RKL=2.0*RK*RL+RH*RL
      GO TO 408
4071  RHH=RH**2+RK**2+RH*RK
      RKK=0.0
      RLL=RL**2
      RHK=0.0
      RHL=0.0
      RKL=0.0
408  E=EXPF(-(RHH*B11(I)+RKK*B22(I)+RLL*B33(I)+RHK*B12(I)+RHL*B13(I)+RK
      1L*B23(I)))
      CP=COSF(PHI)*E
      SP=SINF(PHI)*E
409  GO TO(413,410),MODE
410  SPH=SPH+SP*RH
      SPK=SPK+SP*RK
      SPL=SPL+SP*RL
      CPHH=CPHH+CP*RHH
      CPKK=CPKK+CP*RKK
      CPLL=CPLL+CP*RLL
      CPHK=CPHK+CP*RHK
      CPHL=CPHL+CP*RHL
      CPKL=CPKL+CP*RKL
411  GO TO (413,412),INV
412  CPH=CPH+CP*RH
      CPK=CPK+CP*RK
      CPL=CPL+CP*RL
      SPHH=SPHH+SP*RHH
      SPKK=SPKK+SP*RKK
      SPLL=SPLL+SP*RLL
      SPHK=SPHK+SP*RHK
      SPHL=SPHL+SP*RHL
      SPKL=SPKL+SP*RKL
413  SMCP=SMCP+CP
      SMSP=SMSP+SP
414  CONTINUE
500  GO TO(501,502,502),ISAN
501  TMP=EXPF(-BI(I)*RHOSQ)*SYM(I)
      GO TO 503
502  TMP=SYM(I)
503  GO TO(504,505),I
504  TMPA=(F(JJ)-1.1)*TMP
      TMPB=3.4*TMP
      GO TO 506
505  TMPA=F(JJ)*TMP
      TMPB=0.0
```

```
506 AR=TMPA*SMCP
    AI=TMPB*SMCP
507 ACAL=ACAL+AR
    BCAL=BCAL+AI
508 GO TO(700,600),MODE
600 TA=TPI*TMPA
    TB=TPI*TMPB
    RA=-RHOSQ*TMPA
    RB=-RHOSQ*TMPB
    IF(NVAR-K)700,601,601
601 IF(KSEL(L))602,606,602
602 DA(K)=AR/SYM(I)
603 GO TO(605,604),INV
604 DB(K)=BR/SYM(I)
605 K=K+1
606 L=L+1
    IF(KSEL(L))607,610,607
607 DA(K)=-TA*SPH
    GO TO(609,608),INV
608 DB(K)=TB*CPH
609 K=K+1
610 L=L+1
    IF(KSEL(L))611,615,611
611 DA(K)=-TA*SPK
612 GO TO(614,613),INV
613 DB(K)=TB*CPK
614 K=K+1
615 L=L+1
    IF(KSEL(L))616,620,616
616 DA(K)=-TA*SPL
617 GO TO(619,618),INV
618 DB(K)=TB*CPL
619 K=K+1
620 L=L+1
621 GO TO(622,628,628),ISAN
622 IF(KSEL(L))623,627,623
623 DA(K)=RA*SMCP
624 GO TO(626,625),INV
625 DB(K)=RB*SMSP
626 K=K+1
627 L=L+1
    GO TO 700
628 IF(KSEL(L))629,633,629
629 DA(K)=-TMPA*CPHH
630 GO TO(632,631),INV
631 DB(K)=-TMPB*SPHH
632 K=K+1
633 L=L+1
    IF(KSEL(L))634,638,634
634 DA(K)=-TMPA*CPKK
635 GO TO(637,636),INV
636 DB(K)=-TMPB*SPKK
637 K=K+1
638 L=L+1
    IF(KSEL(L))639,643,639
```

```

639 DA(K)=-TMPA*CPLL
640 GO TO(642,641),INV
641 DB(K)=-TMPB*SPLL
642 K=K+1
643 L=L+1
      IF(KSEL(L))644,648,644
644 DA(K)=-TMPA*CPHK
645 GO TO(647,646),INV
646 DB(K)=-TMPB*SPHK
647 K=K+1
648 L=L+1
      IF(KSEL(L))649,653,649
649 DA(K)=-TMPA*CPHL
650 GO TO(652,651),INV
651 DB(K)=-TMPB*SPHL
652 K=K+1
653 L=L+1
      IF(KSEL(L))654,658,654
654 DA(K)=-TMPA*CPKL
655 GO TO(657,656),INV
656 DB(K)=-TMPB*SPKL
657 K=K+1
658 L=L+1
700 CONTINUE
      RETURN
      END

```

```
* LIST
```

```
* LABEL
```

```
  SUBROUTINE SPGRP
```

```
  C SPACE GROUP P1 BAR WITH DISPERSION CORRECTION FOR 2 CA.
```

```
  COMMON CMA,CMB,CMC,CMD,CME
```

```
  EQUIVALENCE (CMA,TITLE),(CMA(13),MODE),(CMA(14),INV),(CMA(15),ISAN
1),(CMA(16),NPU),(CMA(17),NEW),(CMA(22),NU),(CMA(23),NS),(CMA(24),A
2),(CMA(25),B),(CMA(26),C),(CMA(27),ALPHA),(CMA(28),BETA),(CMA(29),
3GAMMA),(CMA(30),NFOUR),(CMA(31),NCOR),(CMA(32),SUMDL),(CMA(33),KAR
4D),(CMA(34),ID)
```

```
  EQUIVALENCE (CMB,NPAR),(CMB(2),NVAR),(CMB(3),NCOUNT),(CMB(4),KSEL)
  EQUIVALENCE (CMC,S),(CMC(51),B0),(CMC(52),MF),(CMC(102),X),(CMC
1(152),Y),(CMC(202),Z),(CMC(252),B11,BI),(CMC(302),B22),(CMC(352),
2B33),(CMC(402),B12),(CMC(452),B23),(CMC(502),B13),(CMC(552),SYM),(
3CMC(602),NAME)
```

```
  EQUIVALENCE (CMD,NF),(CMD(2),FORM),(CMD(642),F),(CMD(662),ASTER),(
1CMD(666),RHO),(CMD(667),RHOSQ),(CMD(668),ARG),(CMD(700),ISAVE)
```

```
  EQUIVALENCE (CME,FOBS),(CME(2),FCAL),(CME(3),AOBS),(CME(4),ACAL),(
1CME(5),BOBS),(CME(6),BCAL),(CME(7),DELTA),(CME(8),SIGMA),(CME(9),E
2XT1),(CME(10),EXT2),(CME(11),SQRTW),(CME(12),MS1),(CME(13),MREJ),(
3CME(14),MH),(CME(15),MK),(CME(16),ML),(CME(17),TH),(CME(18),TK),(C
4ME(19),TL),(CME(20),DA),(CME(220),DB)
```

```
  DIMENSION TITLE(12),NEW(5)
```

```
  DIMENSION FORM(32,20),F(20),ASTER(4),ARG(32)
```

```
  DIMENSION S(50),MF(50),X(50),Y(50),Z(50),BI(50),B11(50),B22(50),B3
13(50),B12(50),B23(50),B13(50),SYM(50),NAME(50)
```

```
  DIMENSION KSEL(504)
```

```

DIMENSION DA(200),DB(200)
DIMENSION CMA(50),CMB(507),CMC(651),CMD(700),CME(419)
1  ACAL=0.0
   BCAL=0.0
   IP=1
   ISAN=ISAN
   MODE=MODE
   L=NS+2
   K=1
   C2=6.2831854
   DO 27 I=1,NU
     J=MF(I)
100  GO TO(101,102,102),ISAN
101  TMP=EXPF(-BI(I)*RHOSQ)*SYM(I)*2.0
1010 IF(IP-2)1011,1011,1012
1011 C1=(F(J)+0.2)*TMP
     D1=1.4*TMP
     GO TO 103
1012 C1=F(J)*TMP
     D1=0.0
     GO TO 103
102  THS=TH*TH
     TKS=TK*TK
     TLS=TL*TL
     THKS=TH*TK
     TKLS=TK*TL
     THLS=TH*TL
     TMP=EXPF(-(THS*B11(I)+TKS*B22(I)+TLS*B33(I)+2.0*(THKS*B12(I)+THLS*
1B13(I)+TKLS*B23(I))))*SYM(I)*2.0
     GO TO 1010
103  C3=C2*(TH*X(I)+TK*Y(I)+TL*Z(I))
     C4=COSF(C3)
     C5=SINF(C3)
     AR=C1*C4
     AJ=D1*C4
     ACAL=ACAL+AR
     BCAL=BCAL+AJ
     GO TO(26,200),MODE
200  IF(NVAR-K)26,201,201
201  IF(KSEL(L))202,203,202
202  DA(K)=AR/SYM(I)
     DB(K)=AJ/SYM(I)
     K=K+1
203  L=L+1
     IF(KSEL(L))3,4,3
3    DT=-C2*TH*C5
     DA(K)=DT*C1
     DB(K)=DT*D1
     K=K+1
4    L=L+1
     IF(KSEL(L))5,6,5
5    DT=-C2*TK*C5
     DA(K)=DT*C1
     DB(K)=DT*D1
     K=K+1

```

```
6   L=L+1
    IF(KSEL(L))7,8,7
7   DT=-C2*TL*C5
    DA(K)=DT*C1
    DB(K)=DT*D1
    K=K+1
8   L=L+1
9   GO TO(10,13,13),ISAN
10  IF(KSEL(L))11,12,11
11  DT=-RHOSQ*C4
    DA(K)=DT*C1
    DB(K)=DT*D1
    K=K+1
12  L=L+1
    GO TO 26
13  IF(KSEL(L))14,15,14
14  DT=-THS*C4
    DA(K)=C1*DT
    DB(K)=D1*DT
    K=K+1
15  L=L+1
    IF(KSEL(L))16,17,16
16  DT=-TKS*C4
    DA(K)=C1*DT
    DB(K)=D1*DT
    K=K+1
17  L=L+1
    IF(KSEL(L))18,19,18
18  DT=-TLS*C4
    DA(K)=C1*DT
    DB(K)=D1*DT
    K=K+1
19  L=L+1
    IF(KSEL(L))20,21,20
20  DT=-THKS*C4
    DA(K)=C1*DT
    DB(K)=D1*DT
    K=K+1
21  L=L+1
    IF(KSEL(L))22,23,22
22  DT=-THLS*C4
    DA(K)=C1*DT
    DB(K)=D1*DT
    K=K+1
23  L=L+1
    IF(KSEL(L))24,25,24
24  DT=-TKLS*C4
    DA(K)=C1*DT
    DB(K)=D1*DT
    K=K+1
25  L=L+1
26  IP=IP+1
27  CONTINUE
    RETURN
    END
```

```

* LIST
* LABEL
SUBROUTINE WEIGHT
C STORE STANDARD DEVIATION IN LOCATION SIGMA IF DIFFERENT THAN ON
C DATA CARD. MAIN PROGRAM COMPUTES SQRT WEIGHT=1/SIGMA.
COMMON CMA,CMB,CMC,CMD,CME
EQUIVALENCE (CMA,TITLE)
EQUIVALENCE (CMB,NPAR)
EQUIVALENCE (CMC,S)
EQUIVALENCE (CMD,NF),(CMD(2),FORM),(CMD(642),F),(CMD(662),ASTER),(
1CMD(666),RHO),(CMD(667),RHOSQ),(CMD(668),ARG),(CMD(700),ISAVE)
EQUIVALENCE (CME,FOBS),(CME(2),FCAL),(CME(3),AOBS),(CME(4),ACAL),(
1CME(5),BOBS),(CME(6),BCAL),(CME(7),DELTA),(CME(8),SIGMA),(CME(9),E
2XT1),(CME(10),EXT2),(CME(11),SQRTW),(CME(12),MS1),(CME(13),MREJ),(
3CME(14),MH),(CME(15),MK),(CME(16),ML),(CME(17),TH),(CME(18),TK),(C
4ME(19),TL),(CME(20),DA),(CME(220),DB)
DIMENSION CMA(50),CMB(507),CMC(651),CMD(700),CME(419)
FREQUENCY 1(0,1,10),2(2,0,1)
1 IF(FOBS)2,5,2
2 SIGMA=SQRTF(3.02+FOBS+.0193*FOBS**2)
GO TO 6
5 SIGMA=0.0
6 RETURN
END

```

```

* LIST
* LABEL
SUBROUTINE REJECT
C REJECTION TEST FOR REFLECTION DATA. REJECT IF MREJ=0.
COMMON CMA,CMB,CMC,CMD,CME,CMF
EQUIVALENCE (CMA,TITLE)
EQUIVALENCE (CMB,NPAR)
EQUIVALENCE (CMC,S)
EQUIVALENCE (CMD,NF)
EQUIVALENCE (CME,FOBS),(CME(2),FCAL),(CME(3),AOBS),(CME(4),ACAL),(
1CME(5),BOBS),(CME(6),BCAL),(CME(7),DELTA),(CME(8),SIGMA),(CME(9),E
2XT1),(CME(10),EXT2),(CME(11),SQRTW),(CME(12),MS1),(CME(13),MREJ),(
3CME(14),MH),(CME(15),MK),(CME(16),ML),(CME(17),TH),(CME(18),TK),(C
4ME(19),TL),(CME(20),DA),(CME(220),DB)
EQUIVALENCE (CMF,SFC),(CMF(2),SMSFC),(CMF(3),SQDL),(CMF(4),DELTA1)
1,(CMF(5),SUMFO1),(CMF(6),WDL1),(CMF(7),WFO1),(CMF(8),DELTA2),(CMF(
29),SUMFO2),(CMF(10),WDL2),(CMF(11),WFO2)
DIMENSION CMA(50),CMB(507),CMC(651),CMD(700),CME(419),CMF(50)
10 IF(FOBS)1,4,1
1 IF(.333*FOBS-ABSF(SFC))2,4,4
2 IF(((ABSF(FOBS-ABSF(SFC)))/FOBS)-.20)3,4,4
3 MREJ=1
GO TO 5
4 MREJ=0
5 RETURN
END

```

```

*      LIST
*      LABEL
SUBROUTINE STAT
C      ACCUMULATION OF STATISTICAL DATA
COMMON CMA,CMB,CMC,CMD,CME,CMF
EQUIVALENCE (CMA,TITLE),(CMA(13),MODE),(CMA(14),INV),(CMA(15),ISAN
1),(CMA(16),NPU),(CMA(17),NEW),(CMA(22),NU),(CMA(23),NS),(CMA(24),A
2),(CMA(25),B),(CMA(26),C),(CMA(27),ALPHA),(CMA(28),BETA),(CMA(29),
3GAMMA),(CMA(30),NFOUR),(CMA(31),NCOR),(CMA(32),SUMDL)
EQUIVALENCE (CMB,NPAR)
EQUIVALENCE (CMC,S)
EQUIVALENCE (CMD,NF)
EQUIVALENCE (CME,FOBS),(CME(2),FCAL),(CME(3),AOBS),(CME(4),ACAL),(
1CME(5),BOBS),(CME(6),BCAL),(CME(7),DELTA),(CME(8),SIGMA),(CME(9),E
2XT1),(CME(10),EXT2),(CME(11),SQRTW),(CME(12),MS1),(CME(13),MREJ),(
3CME(14),MH),(CME(15),MK),(CME(16),ML),(CME(17),TH),(CME(18),TK),(C
4ME(19),TL),(CME(20),DA),(CME(220),DB)
EQUIVALENCE (CMF,SFC),(CMF(2),SMSFC),(CMF(3),SQDL),(CMF(4),DELTA1)
1,(CMF(5),SUMFO1),(CMF(6),WDL1),(CMF(7),WFO1),(CMF(8),DELTA2),(CMF(
29),SUMFO2),(CMF(10),WDL2),(CMF(11),WFO2)
DIMENSION CMA(50),CMB(507),CMC(651),CMD(700),CME(419),CMF(50)
1      SMSFC=SMSFC+ABSF(SFC)
      INV=INV
10     GO TO(11,12),INV
11     DELTA=SIGNF(FOBS,ACAL)-SIGNF(SFC,ACAL)
      GO TO 13
12     DELTA=FOBS-SFC
13     SQDL=(SQRTW*DELTA)**2
      SQFO=(SQRTW*FOBS)**2
      DELTA1=DELTA1+ABSF(DELTA)
      SUMFO1=SUMFO1+ABSF(FOBS)
      WDL1=WDL1+SQDL
      WFO1=WFO1+SQFO
3      IF(FOBS)4,5,4
4      DELTA2=DELTA2+ABSF(DELTA)
      SUMFO2=SUMFO2+ABSF(FOBS)
      WDL2=WDL2+SQDL
      WFO2=WFO2+SQFO
5      RETURN
      END

```

```

*      LIST
*      LABEL
SUBROUTINE PRSF
C      SUBROUTINE FOR PRINTING STRUCTURE FACTORS
COMMON CMA,CMB,CMC,CMD,CME,CMF
EQUIVALENCE (CMA,TITLE),(CMA(13),MODE),(CMA(14),INV),(CMA(15),ISAN
1),(CMA(16),NPU),(CMA(17),NEW),(CMA(22),NU),(CMA(23),NS),(CMA(24),A
2),(CMA(25),B),(CMA(26),C),(CMA(27),ALPHA),(CMA(28),BETA),(CMA(29),
3GAMMA),(CMA(30),NFOUR),(CMA(31),NCOR),(CMA(32),SUMDL)
EQUIVALENCE (CMB,NPAR)
EQUIVALENCE (CMC,S)

```

```

EQUIVALENCE (CMD,NF),(CMD(2),FORM),(CMD(642),F),(CMD(662),ASTER),(
1CMD(666),RHO),(CMD(667),RHOSQ),(CMD(668),ARG),(CMD(700),ISAVE)
EQUIVALENCE (CME,FOBS),(CME(2),FCAL),(CME(3),AOBS),(CME(4),ACAL),(
1CME(5),BOBS),(CME(6),BCAL),(CME(7),DELTA),(CME(8),SIGMA),(CME(9),E
2XT1),(CME(10),EXT2),(CME(11),SQRTW),(CME(12),MS1),(CME(13),MREJ),(
3CME(14),MH),(CME(15),MK),(CME(16),ML),(CME(17),TH),(CME(18),TK),(C
4ME(19),TL),(CME(20),DA),(CME(220),DB)
EQUIVALENCE (CMF,SFC),(CMF(2),SMSFC),(CMF(3),SQDL),(CMF(4),DELTA1)
1,(CMF(5),SUMFO1),(CMF(6),WDL1),(CMF(7),WFO1),(CMF(8),DELTA2),(CMF(
29),SUMFO2),(CMF(10),WDL2),(CMF(11),WFO2)
DIMENSION TITLE(12),NEW(5)
DIMENSION CMA(50),CMB(507),CMC(651),CMD(700),CME(419),CMF(50)
DIMENSION FORM(32,20),F(20),ASTER(4),ARG(32)
DIMENSION S(50)
FREQUENCY 21(10,1,10),22(1,1,5),25(1,1,5)
1  INV=INV
   MS1=MS1
18  GO TO(18,19),INV
   AOBS=FOBS/S(MS1)
   FOSC=AOBS
   AOBS=SIGNF(AOBS,ACAL)
   GO TO 20
19  C1=FOBS/SFC
   FOSC=FOBS/S(MS1)
   AOBS=C1*ACAL
   BOBS=C1*BCAL
20  DS=DELTA/SIGMA
   IF DIVIDE CHECK 21,21
21  IF(MREJ)25,22,25
22  IF(2.0-ABSF(DS))31,31,32
25  IF(2.0-ABSF(DS))33,33,34
31  I=1
   GO TO 5
32  I=2
   GO TO 5
33  I=3
   GO TO 5
34  I=4
5   GO TO(51,61),INV
51  WRITE OUTPUT TAPE 2,6,MH,MK,ML,FOBS,SFC,AOBS,ACAL,DELTA,DS,ASTER(I
1)
6   FORMAT(3I4,3X,4(F9.2,4X),F9.2,3X,F9.2,A6)
7   IF(NPU)8,10,8
8   PUNCH 9,MH,MK,ML,AOBS,ACAL,FOSC,ASTER(I)
9   FORMAT(3I4,12X,2F8.2,16X,F8.2,8X,A6)
10  IF(NFOUR)11,13,11
11  WRITE OUTPUT TAPE 9,12,MH,MK,ML,AOBS,ACAL,FOSC
12  FORMAT(3I4,12X,2F8.2,16X,F8.2,8X)
13  RETURN
61  WRITE OUTPUT TAPE 2,62,MH,MK,ML,FOBS,SFC,AOBS,ACAL,BOBS,BCAL,DELTA
1,DS,ASTER(I)
62  FORMAT(3I4,3X,6(F9.2,4X),F9.2,3X,F9.2,A6)
63  IF(NPU)64,66,64
64  PUNCH 65,MH,MK,ML,AOBS,ACAL,BOBS,BCAL,FOSC,ASTER(I)
65  FORMAT(3I4,12X,5F8.2,8X,A6)

```



```

66 IF(NFOUR)67,69,67
67 WRITE OUTPUT TAPE 9,68,MH,MK,ML,AOBS,ACAL,BOBS,BCAL,FOSC
68 FORMAT(3I4,12X,5F8.2,8X)
69 GO TO 13
END

```

```

*      FAP
      COUNT    50
      REM      ROUTINE FOR STORING NORMAL EQUATION MATRIX
      ENTRY    SET
      ENTRY    STMAT
SET    CLA      1,4          STORE ADDRESSES FOR ARGUMENTS
      STA      TA
      CLA      2,4
      ADD      =1
      STA      BA
      STA      BA+1
      STA      BB+1
      CLA      3,4
      STA      BB+2
      CLA      NVAR
      STD      BB
      STD      BC
      TRA      4,4
STMAT  SXD      SA,1
      SXD      SA+1,2
      SXD      SA+2,4
TA     CLA      N
      SUB      ONE
      PDX      0,4
      LXD      ONE,1
AA     PDX      0,1
      PDX      0,2
      REM      LOOP TO FORM AND STORE MATRIX ELEMENTS
BA     LDQ      0,1          DF+1
      FMP      0,2          DF+1
      FAD      AR,4
      STO      AR,4
      TXI      *+1,2,1
      TXI      *+1,4,-1
BB     TXL      BA,2
      REM      LOOP TO FORM AND STORE VECTOR ELEMENTS
      LDQ      0,1          DF+1
      FMP      WDEL
      FAD      V+1,1
      STO      V+1,1
      TXI      *+1,1,1
BC     TXL      AA,1
      LXD      SA,1
      LXD      SA+1,2
      LXD      SA+2,4
      TRA      1,4
ONE   PZE      0,0,1
SA    BSS      3

```

```

COMMON 51
NVAR COMMON 2326          FOR SFLSQ3 AND CHLNK3
AR COMMON 14969
V COMMON 1
END

```

```

* LIST
* LABEL
SUBROUTINE PRST
C PRINT STATISTICAL RESULTS
COMMON CMA,CMB,CMC,CMD,CME,CMF
EQUIVALENCE (CMA,TITLE),(CMA(32),SUMDL)
EQUIVALENCE (CMB,NPAR),(CMB(2),NVAR),(CMB(3),NCOUNT),(CMB(4),KSEL)
EQUIVALENCE (CMC,S)
EQUIVALENCE (CMD,NF)
EQUIVALENCE (CME,FOBS)
EQUIVALENCE (CMF,SFC),(CMF(2),SMSFC),(CMF(3),SQDL),(CMF(4),DELTA1)
1,(CMF(5),SUMFO1),(CMF(6),WDL1),(CMF(7),WFO1),(CMF(8),DELTA2),(CMF(
29),SUMFO2),(CMF(10),WDL2),(CMF(11),WFO2)
DIMENSION CMA(50),CMB(507),CMC(651),CMD(700),CME(419),CMF(50)
DIMENSION TITLE(12)
30 WRITE OUTPUT TAPE 2,31,TITLE
31 FORMAT(1H112A6)
WRITE OUTPUT TAPE 2,33
33 FORMAT(79HODISCREPANCY FACTORS BASED ON INPUT PARAMETERS. NUMERAT
1OR DENOMINATOR R)
R1=DELTA1/SUMFO1
WDL1=SQRTF(WDL1)
WFO1=SQRTF(WFO1)
WR1=WDL1/WFO1
R2=DELTA2/SUMFO2
WDL2=SQRTF(WDL2)
WFO2=SQRTF(WFO2)
WR2=WDL2/WFO2
RSUMDL=SQRTF(SUMDL)
TEST=RSUMDL/SQRTF(FLOATF(NCOUNT-NVAR))
WRITE OUTPUT TAPE 2,34,DELTA1,SUMFO1,R1
34 FORMAT(48HOR FACTOR INCLUDING ZEROS F10.3,3H
1 F10.3,5H F5.3)
WRITE OUTPUT TAPE 2,35,DELTA2,SUMFO2,R2
35 FORMAT(48HOR FACTOR OMITTING ZEROS F10.3,3H
1 F10.3,5H F5.3)
WRITE OUTPUT TAPE 2,36,WDL1,WFO1,WR1
36 FORMAT(48HOWEIGHTED R FACTOR INCLUDING ZEROS F10.3,3H
1 F10.3,5H F5.3)
WRITE OUTPUT TAPE 2,37,WDL2,WFO2,WR2
37 FORMAT(48HOWEIGHTED R FACTOR OMITTING ZEROS F10.3,3H
1 F10.3,5H F5.3)
WRITE OUTPUT TAPE 2,38,RSUMDL,NCOUNT,NVAR,TEST
38 FORMAT(48HOSQUARE ROOT (SUM W(OBS-CALC)**2/(M-N)) F10.3,6H
1 SQRT(I4,1H-13,3H) F6.3)
WRITE OUTPUT TAPE 2,39,SMSFC
39 FORMAT(48HOSUM FCAL F10.3)
RETURN

```

END

```
* LIST
* LABEL
```

CCHLNK3

SUBROUTINE CHAIN(KXX,KZZ)

COMMON CMA,CMB,CMC,V,DIAG,EPS

```
EQUIVALENCE (CMA,TITLE),(CMA(13),MODE),(CMA(14),INV),(CMA(15),ISAN
1),(CMA(16),NPU),(CMA(17),NEW),(CMA(22),NU),(CMA(23),NS),(CMA(24),A
2),(CMA(25),B),(CMA(26),C),(CMA(27),ALPHA),(CMA(28),BETA),(CMA(29),
3GAMMA),(CMA(30),NFOUR),(CMA(31),NCOR),(CMA(32),SUMDL),(CMA(33),KAR
4D),(CMA(34),ID)
```

```
EQUIVALENCE (CMB,NPAR),(CMB(2),NVAR),(CMB(3),NCOUNT),(CMB(4),KSEL)
EQUIVALENCE (CMC,S),(CMC(51),BO),(CMC(52),MF),(CMC(102),X),(CMC
1(152),Y),(CMC(202),Z),(CMC(252),B11,BI),(CMC(302),B22),(CMC(352),
2B33),(CMC(402),B12),(CMC(452),B23),(CMC(502),B13),(CMC(552),SYM),(
3CMC(602),NAME)
```

```
EQUIVALENCE (CMC(652),SN),(CMC(702),BON),(CMC(703),XN),(CMC(753),Y
1N),(CMC(803),ZN),(CMC(853),BIN,B11N),(CMC(903),B22N),(CMC(953),B33
2N),(CMC(1003),B12N),(CMC(1053),B23N),(CMC(1103),B13N),(CMC(1153),S
3YMN),(CMC(1203),CHG),(CMC(1403),STD)
```

EQUIVALENCE (CMC(652),NFA),(CMC(1821),AR)

DIMENSION CMA(50),CMB(507),CMC(2403)

DIMENSION AR(14969),V(200),DIAG(200)

DIMENSION TITLE(12),NEW(5)

```
DIMENSION S(50),MF(50),X(50),Y(50),Z(50),BI(50),B11(50),B22(50),B3
13(50),B12(50),B23(50),B13(50),SYM(50),NAME(50)
```

```
DIMENSION SN(50),XN(50),YN(50),ZN(50),BIN(50),B11N(50),B22N(50),B3
13N(50),B12N(50),B23N(50),B13N(50)
```

DIMENSION SYMN(50)

DIMENSION CHG(200),STD(200),EPS(200)

DIMENSION KSEL(504)

DIMENSION ART(20)

DIMENSION F(20)

1 ISAN=ISAN

NF=NFA

ISING=0

2 N=((NVAR+1)*NVAR)/2

NM=N

400 DO 406 I=1,NVAR

401 DO 405 J=I,NVAR

402 IF(J-I)404,403,404

403 IF(AR(N))404,56,404

404 N=N-1

405 CONTINUE

406 CONTINUE

5 CALL SMI(AR(NM),NVAR,ISING)

C IF ISING = 0, MATRIX IS NON-SINGULAR

IF(ISING)52,6,52

6 DO 12 I=1,NVAR

EP=0.0

IJ=NM-I+1

IJD=NVAR-1

7 DO 11 J=1,NVAR

```

      EP=EP+AR(IJ)*V(J)
      IF(J-I)8,9,10
8     IJ=IJ-IJD
      IJD=IJD-1
      GO TO 11
9     DIAG(I)=SQRTF(AR(IJ))
10    IJ=IJ-1
11    CONTINUE
      EPS(I)=EP
12    CONTINUE
1200  IF(NCOR)120,136,120
120   N=NM
      FREQUENCY 121(50),122(25)
121   DO 124 I=1,NVAR
122   DO 123 J=I,NVAR
      AR(N)=AR(N)/(DIAG(I)*DIAG(J))
      N=N-1
123   CONTINUE
124   CONTINUE
      I1=1
      I2=20
      NV=NM+1
125   WRITE OUTPUT TAPE 2,126,TITLE
126   FORMAT(1H112A6)
      WRITE OUTPUT TAPE 2,127
127   FORMAT(31HOPRINTOUT OF CORRELATION MATRIX)
128   DO 135 K=1,25
129   WRITE OUTPUT TAPE 2,130,I1
130   FORMAT(1H 15)
      IT=1
      FREQUENCY 1310(50)
1310  DO 1315 I=I1,I2
      MT=NV-I
      FREQUENCY 1311(0,0,1)
1311  IF(MT)1312,1312,1313
1312  ART(IT)=0.0
      GO TO 1314
1313  ART(IT)=AR(MT)
1314  IT=IT+1
1315  CONTINUE
1316  WRITE OUTPUT TAPE 2,132,(ART(IT),IT=1,20)
132   FORMAT(1H F5.2,19F6.2)
133   IF(NM-I2)136,136,134
134   I1=I2+1
      I2=I1+19
135   CONTINUE
      GO TO 125
136   SUMCH=0.0
      DO 13 I=1,NVAR
      SUMCH=SUMCH+EPS(I)*V(I)
13    CONTINUE
      FIT=SQRTF(SUMDL-SUMCH)
      ERFIT=FIT/SQRTF(FLOATF(NCOUNT-NVAR))
      J=1
14    DO 17 I=1,NPAR

```

```

IF(KSEL(I))15,16,15
15  CHG(I)=EPS(J)
    STD(I)=DIAG(J)*ERFIT
    J=J+1
    GO TO 17
16  CHG(I)=0.0
    STD(I)=0.0
17  CONTINUE
    DO 18 J=1,NS
    SN(J)=S(J)+CHG(J)
18  CONTINUE
    J=NS+1
    BON=BO+CHG(J)
    J=J+1
19  DO 22 I=1,NU
    SYMN(I)=SYM(I)+CHG(J)
    J=J+1
    XN(I)=X(I)+CHG(J)
    J=J+1
    YN(I)=Y(I)+CHG(J)
    J=J+1
    ZN(I)=Z(I)+CHG(J)
    J=J+1
    GO TO (20,21,21),ISAN
20  BIN(I)=BI(I)+CHG(J)
    J=J+1
    GO TO 22
21  B11N(I)=B11(I)+CHG(J)
    J=J+1
    B22N(I)=B22(I)+CHG(J)
    J=J+1
    B33N(I)=B33(I)+CHG(J)
    J=J+1
    B12N(I)=B12(I)+CHG(J)
    J=J+1
    B13N(I)=B13(I)+CHG(J)
    J=J+1
    B23N(I)=B23(I)+CHG(J)
    J=J+1
22  CONTINUE
220 WRITE OUTPUT TAPE 2,126,TITLE
23  WRITE OUTPUT TAPE 2,24
24  FORMAT(79H0ESTIMATE OF                                NUMERAT
10R  DENOMINATOR      R)
    WRITE OUTPUT TAPE 2,25,FIT,NCOUNT,NVAR,ERFIT
25  FORMAT(50HOSQUARE ROOT (SUM W(OBS-CALC)**2/(M-N))      F9.3,6
1H  SQRT(I4,1H-I3,3H)  F6.3)
    WRITE OUTPUT TAPE 2,26
26  FORMAT(28H0BASED ON OUTPUT PARAMETERS.)
    WRITE OUTPUT TAPE 2,27
27  FORMAT(57H0PARAMETER          OLD          CHANGE          NEW          ERRO
1R)
28  DO 30 J=1,NS
    WRITE OUTPUT TAPE 2,29,J,S(J),CHG(J),SN(J),STD(J)
29  FORMAT(14H0SCALE FACTOR I2,F9.4,3H  F8.4,2H  F8.4,4H  F7.4)

```

```
30 CONTINUE
   J=NS+1
   WRITE OUTPUT TAPE 2,31,B0,CHG(J),BON,STD(J)
31 FORMAT(16H00OVERALL B      F9.4,3X,F8.4,2X,F8.4,4X,F7.4)
   J=J+1
32 DO 47 I=1,NU
   WRITE OUTPUT TAPE 2,33,I,NAME(I)
33 FORMAT(6H0ATOM I2,3X,A6)
   WRITE OUTPUT TAPE 2,34,MF(I)
34 FORMAT(19H FORM FACTOR      I2)
   WRITE OUTPUT TAPE 2,340,SYM(I),CHG(J),SYMN(I),STD(J)
340 FORMAT(15H ATOM S.F.      4(F10.7,1X))
   J=J+1
   WRITE OUTPUT TAPE 2,35,X(I),CHG(J),XN(I),STD(J)
35 FORMAT(15H X                4(F10.7,1X))
   J=J+1
   WRITE OUTPUT TAPE 2,36,Y(I),CHG(J),YN(I),STD(J)
36 FORMAT(15H Y                4(F10.7,1X))
   J=J+1
   WRITE OUTPUT TAPE 2,37,Z(I),CHG(J),ZN(I),STD(J)
37 FORMAT(15H Z                4(F10.7,1X))
   J=J+1
   GO TO (38,40,40),ISAN
38 WRITE OUTPUT TAPE 2,39,BI(I),CHG(J),BIN(I),STD(J)
39 FORMAT(15H ATOMIC B        4(F10.7,1X))
   J=J+1
   GO TO 47
40 WRITE OUTPUT TAPE 2,41,B11(I),CHG(J),B11N(I),STD(J)
41 FORMAT(15H BETA(1,1)      4(F10.7,1X))
   J=J+1
   WRITE OUTPUT TAPE 2,42,B22(I),CHG(J),B22N(I),STD(J)
42 FORMAT(15H BETA(2,2)      4(F10.7,1X))
   J=J+1
   WRITE OUTPUT TAPE 2,43,B33(I),CHG(J),B33N(I),STD(J)
43 FORMAT(15H BETA(3,3)      4(F10.7,1X))
   J=J+1
   WRITE OUTPUT TAPE 2,44,B12(I),CHG(J),B12N(I),STD(J)
44 FORMAT(15H BETA(1,2)      4(F10.7,1X))
   J=J+1
   WRITE OUTPUT TAPE 2,45,B13(I),CHG(J),B13N(I),STD(J)
45 FORMAT(15H BETA(1,3)      4(F10.7,1X))
   J=J+1
   WRITE OUTPUT TAPE 2,46,B23(I),CHG(J),B23N(I),STD(J)
46 FORMAT(15H BETA(2,3)      4(F10.7,1X))
   J=J+1
47 CONTINUE
   CALL TEST(KA)
   WRITE TAPE 10,NF,A,B,C,ALPHA,BETA,GAMMA,SN,BON,MF,XN,YN,ZN,B11N,B2
12N,B33N,B12N,B13N,B23N,SYM,NAME,NPAR,NVAR,KSEL
470 READ TAPE 7,MH,MK,ML,FOBS,SIGMA,MS1,EXT1,EXT2,LAST,RHO,RHOSQ,F
   WRITE TAPE 10,MH,MK,ML,FOBS,SIGMA,MS1,EXT1,EXT2,LAST,RHO,RHOSQ,F
471 IF(LAST)472,470,472
472 IF(KARD)473,474,473
473 CALL CARD
474 IF(ID)475,476,475
```

```

475 CALL DIST
476 REWIND 10
      REWIND 7
      IF(KA)51,48,51
48  READ INPUT TAPE 4,49,IEND
49  FORMAT(71X,I1)
      IF(IEND)50,51,50
50  RETURN
51  CALL EXIT
52  WRITE OUTPUT TAPE 2,53
53  FORMAT(19H0MATRIX IS SINGULAR)
      WRITE OUTPUT TAPE 2,54
54  FORMAT(39H0LISTING OF DIAGONAL OF INVERTED MATRIX)
      WRITE OUTPUT TAPE 2,55,(DIAG(I),I=1,NVAR)
55  FORMAT(10E10,3)
      GO TO 58
56  WRITE OUTPUT TAPE 2,53
      WRITE OUTPUT TAPE 2,57,I
57  FORMAT(22H0DIAGONAL TERM NUMBER I3,38H IN THE NORMAL EQUATION MATR
1IX IS ZERO)
      ISING=1
      GO TO 404
58  CALL EXIT
      END

```

```

* LIST
* LABEL
SUBROUTINE TEST(K)
C TEST FOR NEGATIVE TEMPERATURE FACTORS
COMMON CMA,CMB,CMC
EQUIVALENCE (CMA,TITLE),(CMA(13),MODE),(CMA(14),INV),(CMA(15),ISAN
1),(CMA(16),NPU),(CMA(17),NEW),(CMA(22),NU),(CMA(23),NS),(CMA(24),A
2),(CMA(25),B),(CMA(26),C),(CMA(27),ALPHA),(CMA(28),BETA),(CMA(29),
3GAMMA),(CMA(30),NFOUR),(CMA(31),NCOR),(CMA(32),SUMDL),(CMA(33),KAR
4D),(CMA(34),ID)
EQUIVALENCE (CMB,NPAR)
EQUIVALENCE (CMC,S),(CMC(51),BO),(CMC(52),MF),(CMC(102),X),(CMC
1(152),Y),(CMC(202),Z),(CMC(252),B11,BI),(CMC(302),B22),(CMC(352),
2B33),(CMC(402),B12),(CMC(452),B23),(CMC(502),B13),(CMC(552),SYM),(
3CMC(602),NAME)
EQUIVALENCE (CMC(652),SN),(CMC(702),BON),(CMC(703),XN),(CMC(753),Y
1N),(CMC(803),ZN),(CMC(853),BIN,B11N),(CMC(903),B22N),(CMC(953),B33
2N),(CMC(1003),B12N),(CMC(1053),B23N),(CMC(1103),B13N),(CMC(1603),C
3HG),(CMC(2103),STD),(CMC(2203),EPS)
DIMENSION CMA(50),CMB(507),CMC(2403)
DIMENSION S(50),MF(50),X(50),Y(50),Z(50),BI(50),B11(50),B22(50),B3
13(50),B12(50),B23(50),B13(50),SYM(50),NAME(50)
DIMENSION SN(50),XN(50),YN(50),ZN(50),BIN(50),B11N(50),B22N(50),B3
13N(50),B12N(50),B23N(50),B13N(50)
1 K=0
ISAN=ISAN
GO TO(3,5,5),ISAN
3 DO 4 I=1,NU
BI(I)=BIN(I)+BON

```

```

4   CONTINUE
    GO TO 7
5   AA=BON*A*A/4.0
    BB=BON*B*B/4.0
    CC=BON*C*C/4.0
    AB=BON*A*B*COSF(GAMMA)/4.0
    BC=BON*B*C*COSF(ALPHA)/4.0
    AC=BON*A*C*COSF(BETA)/4.0
    DO 6 I=1,NU
    B11(I)=B11N(I)+AA
    B22(I)=B22N(I)+BB
    B33(I)=B33N(I)+CC
    B12(I)=B12N(I)+AB
    B23(I)=B23N(I)+BC
    B13(I)=B13N(I)+AC
6   CONTINUE
7   GO TO(8,12,12),ISAN
8   DO 11 I=1,NU
    IF(BI(I))9,11,11
9   WRITE OUTPUT TAPE 2,10,I
10  FORMAT(28H0TEMPERATURE FACTOR OF ATOM I2,25H IS NOT POSITIVE-DEFIN
    1ITE)
    BIN(I)=.01
11  CONTINUE
    GO TO 20
12  DO 19 I=1,NU
13  IF(B11(I))18,14,14
14  IF(B22(I))18,15,15
15  IF(B33(I))18,16,16
16  IF(B11(I)*B22(I)*B33(I)+2.0*B12(I)*B23(I)*B13(I)-(B13(I)*B13(I)*B2
    12(I)+B12(I)*B12(I)*B33(I)+B11(I)*B23(I)*B23(I)))18,160,160
160 IF(B22(I)*B33(I)-B23(I)**2)18,161,161
161 IF(B11(I)*B33(I)-B13(I)**2)18,162,162
162 IF(B11(I)*B22(I)-B12(I)**2)18,17,17
17  GO TO 19
18  WRITE OUTPUT TAPE 2,10,I
    K=K+1
19  CONTINUE
20  RETURN
    END

```

```

*   LIST8
*   LABEL
    SUBROUTINE CARD
C   PUNCH ATOM PARAMETER CARDS
    COMMON CMA,CMB,CMC,V,DIAG,EPS
    EQUIVALENCE (CMA,TITLE),(CMA(13),MODE),(CMA(14),INV),(CMA(15),ISAN
1) ,(CMA(16),NPU),(CMA(17),NEW),(CMA(22),NU),(CMA(23),NS),(CMA(24),A
2) ,(CMA(25),B),(CMA(26),C),(CMA(27),ALPHA),(CMA(28),BETA),(CMA(29),
3) GAMMA),(CMA(30),NFOUR),(CMA(31),NCOR),(CMA(32),SUMDL),(CMA(33),KAR
4) D),(CMA(34),ID)
    EQUIVALENCE (CMB,NPAR),(CMB(2),NVAR),(CMB(3),NCOUNT),(CMB(4),KSEL)
    EQUIVALENCE (CMC,S),(CMC(51),BO),(CMC(52),MF),(CMC(102),X),(CMC
1) (152),Y),(CMC(202),Z),(CMC(252),B11,BI),(CMC(302),B22),(CMC(352),

```



```

2B33),(CMC(402),B12),(CMC(452),B23),(CMC(502),B13),(CMC(552),SYM),(
3CMC(602),NAME)
EQUIVALENCE (CMC(652),SN),(CMC(702),BON),(CMC(703),XN),(CMC(753),Y
1N),(CMC(803),ZN),(CMC(853),BIN,B11N),(CMC(903),B22N),(CMC(953),B33
2N),(CMC(1003),B12N),(CMC(1053),B23N),(CMC(1103),B13N),(CMC(1603),C
3HG),(CMC(2103),STD)
EQUIVALENCE (AR,CMC(652),NFA)
EQUIVALENCE (CMC(1153),SYMN)
DIMENSION CMA(50),CMB(507),CMC(2403)
DIMENSION AR(14969),V(200),DIAG(200)
DIMENSION TITLE(12),NEW(5)
DIMENSION S(50),MF(50),X(50),Y(50),Z(50),BI(50),B11(50),B22(50),B3
13(50),B12(50),B23(50),B13(50),SYM(50),NAME(50)
DIMENSION SN(50),XN(50),YN(50),ZN(50),BIN(50),B11N(50),B22N(50),B3
13N(50),B12N(50),B23N(50),B13N(50)
DIMENSION SYMN(50)
DIMENSION CHG(200),STD(200),EPS(200)
DIMENSION DF(200)
DIMENSION KSEL(504)
DIMENSION ART(20)
DIMENSION F(20)
ISAN=ISAN
1 DO 3 I=1,NS
PUNCH 2,SN(I)
2 FORMAT (F9.4)
3 CONTINUE
PUNCH 4,BON
4 FORMAT (F9.4)
5 DO 11 I=1,NU
6 GO TO (7,9,9),ISAN
7 PUNCH 8,MF(I),XN(I),YN(I),ZN(I),BIN(I)
8 FORMAT (I2,5X,3F7.5,F7.4)
GO TO 11
9 PUNCH 10,MF(I),XN(I),YN(I),ZN(I),B11N(I),B22N(I),B33N(I),B12N(I),B
X13N(I),B23N(I)
10 FORMAT (I2,5X6F7.5,3F7.4)
11 CONTINUE
12 END FILE 3
13 RETURN
END

```

```

*      FAP
      COUNT      2
      ENTRY      DIST
      REM        DUMMY SUBROUTINE DIST
DIST   TRA       1,4
      END

```

Appendix II

Program for computation of drilling coordinates for crystal structure models

Chapter III gives a mathematical account of the procedures for calculating drilling coordinates for crystal structure models. This contains some details of a program written for the IBM 7090 computer which will compute these drilling coordinates. As it is written, the program is a rather elementary one, since it contains no provision for generating coordinates of symmetry-related atoms. It works well, however, and its use not only saves time in calculation of drilling coordinates, but it reduces the possibility of computational errors which could cause considerable trouble in putting a model together.

Since the computational methods are very similar, an obvious extension of this program would be to compute interbond angles as well as drilling coordinates and interatomic distances. In such a program, symmetry transformations could be included so that only the coordinates of atoms of the asymmetric unit would have to be submitted with the program. In addition, although they are not required for the drilling coordinates, the errors in interatomic and interbond angles could also be computed.

Directions for running the program DRILL

This program computes the drilling angles ϕ and ρ for all atoms \underline{N}_j coordinating atom \underline{N}_i , given cell parameters, atom coordinates, and information defining coordination polyhedra. No symmetry transformations are performed on input atom coordinates. Therefore all transformations must be performed by the program user and all atoms with unique coordinates must be supplied to the program. The program is designed to be run under the Fortran Monitor System and is coded entirely in FORTRAN.

DATA CARDS FOR DRILL

1. TITLE CARD. Format (I2A6) Cols. 1-72; Any identification information may be included.
2. CELL PARAMETER CARD. Format (3(F7.4, 3X), 3(F6.2, 4X), I2)

<u>cols.</u>	<u>Parameter</u>	<u>Format</u>
1-7	$a(\overset{\circ}{\text{A}})$	F7.4
11-17	$b(\overset{\circ}{\text{A}})$	"
21-27	$c(\overset{\circ}{\text{A}})$	"
31-36	alpha (in degrees)	F6.4
41-46	beta (in degrees)	"
51-56	gamma (in degrees)	"
61-62	NT	I2

NT is the number of atoms and is equal to the number of atom parameter cards or atom coordination cards. NT must not be greater than 72.

3. ATOM PARAMETER CARDS. Format (I2, 2X, A6, 2X, 3(I2, 2X), 3F6.4)

<u>Cols.</u>	<u>Parameter</u>	<u>Format</u>
1-2	atom number, n_i	I2
5-10	atom name	A6
13-14	no. of atoms coordinating atom n_i	I2
17-18	no. of the atom with $\rho = 0.0$	"
21-22	no. of the atom with $\phi = 0.0$	"
25-30	x_i	F6.4
31-36	y_i	"
37-42	z_i	"

Columns 13-14, 17-18, and 21-22 are left blank if no atoms coordinate atom $\underline{n_i}$. (i.e. Atom $\underline{n_i}$ is only coordinated to some other atom in this case.)

\underline{x} , \underline{y} , and \underline{z} may be negative or greater than 1.0

There are NT such cards, one card for each atom with unique coordinates.

4. ATOM COORDINATION CARDS. Format(72I1)

NT cards, one for each atom. These cards designate the numbers of the atoms which coordinate atom $\underline{n_i}$. A blank card must be used if no atoms coordinate atom $\underline{n_i}$.

Cols. 1-72: Punch 1 in the columns whose numbers correspond to the atom numbers coordinating atom $\underline{n_i}$.

Cards of type 3 and 4 are arranged such that $\underline{n_i}$ increases uniformly. The two cards of types 3 and 4 for atom $\underline{n_i}$ are placed together with that of type 3 first.

DESCRIPTION OF DATA DECK

* DATA

Title card

Cell parameter card

Atom parameter card for atom 1

Atom coordination card for atom 1

Atom parameter card for atom 2

Atom coordination card for atom 2

· ·
· ·

Atom parameter card for atom NT

Atom coordination card for atom NT

DESCRIPTION OF OUTPUT

The numbers, names and angles phi and rho of all atoms coordinating some atom \underline{n}_1 are printed out for each coordination group and its enantiomorphic equivalent, i. e., for atoms related by a mirror plane or an inversion center.

In addition, interatomic distances are printed out and may be used as a check on the correctness of the input data.

FORTRAN LISTING OF PROGRAM DRILL

```

C   ROUTINE TO COMPUTE DRILLING COORDINATES PHI AND RHO + INT DIST
      DIMENSION TITLE(12),N(72),NAME(72),NCRD(72),NRHO(72),NPHI(72),
1X(72),Y(72),Z(72),NC(72,72),DX(72),DY(72),DZ(72),DIST(72),RHO(72),
2ARHO(72),U(72),V(72),W(72),SIZE(72),PHI(72),PHIN(72),XP(72),YP(72)
3,ZP(72),T(3,3)
      FREQUENCY 11(0,3,1),13(0,10,1),23(0,10,1),31(0,10,1),33(5,1,5)
      READ INPUT TAPE 4,1,(TITLE(I),I=1,12)
1   FORMAT(12A6)
      WRITE OUTPUT TAPE 2,2,(TITLE(I),I=1,12)
2   FORMAT(1H112A6)
      WRITE OUTPUT TAPE 2,3
3   FORMAT(88HOCENTER ATOM      COORDINATING ATOM      PHI      RHO      *
1   ENANTIOMORPH      PHI      RHO)
      READ INPUT TAPE 4,4,A,B,C,ALPHA,BETA,GAMMA,NT
4   FORMAT(3(F7.4,3X),3(F6.2,4X),I2)
      DO 7 I=1,NT
      READ INPUT TAPE 4,5,N(I),NAME(I),NCRD(I),NRHO(I),NPHI(I),X(I),Y(I)
1,Z(I)
5   FORMAT(I2,2X,A6,2X,3(I2,2X),3F6.4)
      READ INPUT TAPE 4,6,(NC(I,J),J=1,72)
6   FORMAT(72I1)
7   CONTINUE
      PI =3.1415927
      RAD =PI/180.0
      ALPHA=ALPHA*RAD
      BETA=BETA*RAD
      GAMMA=GAMMA*RAD
      ONE=(COSF(ALPHA)-COSF(BETA)*COSF(GAMMA))/SINF(GAMMA)
      T(1,1)=A
      T(1,2)=B*COSF(GAMMA)
      T(1,3)=C*COSF(BETA)
      T(2,1)=0.0
      T(2,2)=B*SINF(GAMMA)
      T(2,3)=C*ONE
      T(3,1)=0.0
      T(3,2)=0.0
      T(3,3)=C*SQRTF(SINF(BETA)**2-ONE**2)
      DO 8 I=1,NT
      XP(I)=X(I)*T(1,1)+Y(I)*T(1,2)+Z(I)*T(1,3)
      YP(I)=X(I)*T(2,1)+Y(I)*T(2,2)+Z(I)*T(2,3)
      ZP(I)=X(I)*T(3,1)+Y(I)*T(3,2)+Z(I)*T(3,3)
8   CONTINUE
10  DO 50 I=1,NT
11  IF(NCRD(I))50,50,12
12  WRITE OUTPUT TAPE 2,121,N(I),NAME(I)
121 FORMAT(1H0I2,2X,A6)
      DO 21 J=1,72
13  IF(NC(I,J))21,21,14
14  DX(J)=XP(I)-XP(J)

```

```

        DY(J)=YP(I)-YP(J)
        DZ(J)=ZP(I)-ZP(J)
19      DIST(J)=DX(J)**2+DY(J)**2+DZ(J)**2
        DIST(J)=SQRTF(DIST(J))
21      CONTINUE
22      DO 28 J=1,72
23      IF(NC(I,J))28,28,24
24      K=NRHO(I)
        SCALA=DX(K)*DX(J)+DY(K)*DY(J)+DZ(K)*DZ(J)
        RHC(J)=SCALA/(DIST(K)*DIST(J))
241     IF(RHO(J)-1.0)243,242,242
242     RHO(J)=0.0
        GO TO 246
243     IF(RHO(J)+1.0)244,244,245
244     RHO(J)=3.1415927
        GO TO 246
245     RHO(J)=ACOSF(RHO(J))
246     ARHO(J)=RHO(J)/RAD
        U(J)=(DY(K)*DZ(J))-(DZ(K)*DY(J))
        V(J)=(DZ(K)*DX(J))-(DX(K)*DZ(J))
        W(J)=(DX(K)*DY(J))-(DY(K)*DX(J))
        SIZE(J)=SINF(RHO(J))*DIST(K)*DIST(J)
28      CONTINUE
29      L=NPHI(I)
        UU=(DY(K)*W(L))-(DZ(K)*V(L))
        VV=(DZ(K)*U(L))-(DX(K)*W(L))
        WW=(DX(K)*V(L))-(DY(K)*U(L))
30      DO 49 J=1,72
31      IF(NC(I,J))49,49,32
32      SCALA=U(L)*U(J)+V(L)*V(J)+W(L)*W(J)
        PHI(J)=SCALA/(SIZE(L)*SIZE(J))
321     IF(PHI(J)-1.0)323,322,322
322     PHI(J)=0.0
        GO TO 36
323     IF(PHI(J)+1.0)324,324,329
324     PHI(J)=180.0
        GO TO 36
329     PHI(J)=ACOSF(PHI(J))
        PHI(J)=PHI(J)/RAD
        SCALE=UU*U(J)+VV*V(J)+WW*W(J)
33      IF(SCALE)35,36,36
35      PHI(J)=360.0-PHI(J)
36      PHIN(J)=360.0-PHI(J)
        WRITE OUTPUT TAPE 2,41,J,NAME(J),PHI(J),ARHO(J),PHIN(J),ARHO(J),
1DIST(J)
41      FORMAT(19X,I2,2X,A6,6X,F6.1,3X,F6.1,24X,F6.1,3X,F6.1,5X,F7.3)
49      CONTINUE
50      CONTINUE
        CALL EXIT
        END

```

Appendix III

Computation of diffractometer settings

In recent years many laboratories engaged in single-crystal x-ray diffraction work have begun to use counter diffractometers to measure diffraction intensities. Many of the difficulties which were first encountered in this area have been overcome, and, with the advent of complete automation of the equipment, this method should be much better than the conventional film methods. Prewitt (1960) published the relations needed to compute the angular settings for the equi-inclination Weissenberg diffractometer (Buerger, 1960) which is being used in a number of laboratories in the U. S. A. and abroad. This appendix describes an IBM 7090 program written to compute these settings.

Program description. This program, which is designed to operate under the Fortran Monitor System, consists of a main program DFSET and several subroutines. After a brief description of each section of the program, instructions for setting up a run will be given.

DFSET. The main program reads the input data from A2, computes necessary constants, writes headings on the output tape A3 and transfers to the selected hkl generation subroutine INDEX1 or INDEX2. Upon return from one or the other of these subroutines, a selected hkl has been stored in COMMON. The main program computes $\sin\theta$ and compares it to a maximum allowable $\sin\theta$ prescribed

by the input data. If the computed $\sin \theta$ is too large, one of the indexing routines is called again and a new hkl generated; otherwise the main program goes on to compute τ , ϕ , and $1/L_p$ as given by Prewitt (1960). Also computed are the precision Weissenberg coordinates, ξ and ψ (Buerger, 1942; Prewitt, 1960), which are very useful in indexing precision Weissenberg films. OUTPUT is then called to write tapes for printing and/or punching. Upon the return from OUTPUT, the main program again calls one of the indexing routines.

INDEX1. This subroutine will read hkl's from cards in the data deck. Upon reading a termination card as described below, the subroutine TERM will be called.

INDEX2. This routine is coded in FAP and generates hkl's according to extinction rules given in International Tables (1952), Vol. I, pp. 53-54. Input data to the program contains lower and upper limits for hkl and INDEX2 examines all combinations between these limits for compliance with the extinction rules. If a particular hkl passes, it is stored in COMMON and control is returned to the main program.

INDEX2 could be used in conjunction with any program which requires the generation of hkl's according to a particular extinction rule. All communication with the main program is through COMMON. The information needed by INDEX2 to operate successfully is found at the end of the program listing in the COMMON section. These

symbols are defined in the instructions for running the program.

Upon exceeding the upper limits of \underline{hkl} , TERM will be called to terminate the run. If for some reason \underline{h} , \underline{k} , or \underline{l} is accidentally exceeded, sense light 1 will be turned on before TERM is called.

OUTPUT. \underline{h} , \underline{k} , \underline{l} , τ , ϕ , $1/\underline{Lp}$, $\sin \theta$, and (with their addition to the calling sequence) ξ and ψ , are written on A3 and/or B4 for printing and/or punching^{*}, respectively. Note that statement 24 is a PUNCH statement which might have to be changed if this would cause on-line punching at a particular computing center.

MIFLIP. An M. I. T. subroutine which writes punched output identification records on B4. May be eliminated by removing statements 131 and 131-1 in the main program.

TERM. Depending on the end of run indicators, this routine will either call EXIT and stop the run or will call CHAIN (2, A4) which will cause the program to be read in from A4 and a new set of data evaluated.

Speed of computation. Settings are computed at a rate of 30-45 per second, depending on the extinction rules and the speed of the tape drives being used.

* The punched cards produced by this program may be used as input to the Burnham (1961) program DTRDA.

Running the program

Data deck. The cards of the data deck are assembled in the following order:

		FORMAT
1. TITLE:	Any identification in cols. 1-72.	12A6
2. FLP:	Information for identifying punched output. May be blank if no punched output is requested.	4A6

Col.

1-6	Problem number (at M. I. T.)
7-12	Programmer number
13-24	Blank

3. Sense card

Col.

1	LSQ:	1 - cell constants are to be read from data cards	I1
		2 - if this is a chain link with the Burnham (1964) lattice parameter least-squares program.	
4	IKL:	1 - <u>hkl</u> are to be read from data cards	I1
		2 - internal generation of <u>hkl</u> is to be used	
7	NPRNT	1 - print output	I1
		2 - punch output	
16-20	SINTHO:	upper limit of $\sin \theta$ for which settings are to be computed.	F5.4
		When computing for all reflections, this probably should be .99999	

rather than 1.0 because of possible trouble in the arcsin routine.

23-25	MH1:	lower limit for \underline{h}	I3
28-30	MH2:	upper " " "	"
33-35	MK1:	lower " " \underline{k}	"
38-40	MK2:	upper " " "	"
43-45	ML1:	lower " " \underline{l}	"
48-50	ML2:	upper " " "	"
53	ISET:	1 - rotation axis is c	I1
		2 - " " " b	
		3 - " " " a	
72	LAST:	0 - if this is the last (or only) group of settings to be computed	I1
		1 - if there is another set of data and chain cards are in their proper places	

4. Reciprocal cell data and space group extinction selection.
The cell data is not needed if the program is operated with the Burnham lattice constant refinement program.

<u>Col.</u>			
1-7	A1:	a^* ($1/\underline{a}$, not λ/\underline{a})	F7.6
8-14	B1:	b^*	"
15-21	C1:	c^*	"
22-28	ALPHA1:	α^* (in degrees)	F7.4
29-35	BETA1:	β^*	"
36-42	GAMMA1:	γ^*	"
43-49	WVLNG:	λ (\AA)	"

61-69 Extinction rules

911

- 61 LHKL: 1 - $h + k = 2n$
 2 - $k + l = 2n$
 3 - $l + h = 2n$
 4 - hkl all odd or all even
 5 - $h + k + l = 2n$
 6 - $h + k + l = 3n$
 7 - $h - k + l = 3n$
 8 - $h - k = 3n$
 0 - no restrictions
- 62 LHKO: 1 - $h = 2n$
 2 - $k = 2n$
 3 - $h + k = 2n$
 4 - $h + k = 4n$
- 63 LOKL: 1 - $h = 2n$
 2 - $l = 2n$
 3 - $k + l = 2n$
 4 - $k + l = 4n$
- 64 LHOL: 1 - $l = 2n$
 2 - $h = 2n$
 3 - $l + h = 2n$
 4 - $l + h = 4n$
- 65 LHHL: 1 - $l = 2n$
 2 - $2h + l = 4n$
- 66 LHML: 1 - $l = 2n$ ($h\bar{l}$)
- 67 LHOO: 1 - $h = 2n$
 2 - $h = 4n$
- 68 LHOKO: 1 - $k = 2n$

69 LOOL: 1 - 1 = 2n
 2 - 1 = 3n
 3 - 1 = 4n
 4 - 1 = 6n

5. hkl cards--needed only if there is a 1 in col. 4 of the sense card. If this option is used, diffractometer settings will be computed for all reflections for which $\sin \theta$ is less than the allowable maximum.

<u>Col.</u>			
1-3	MH:	h	I3
5-7	MK:	k	"
9-11	ML:	l	"
72	IEOF:	End of <u>hkl</u> deck indicator.	I1
		Blank except on last card which is blank except for 1 in col. 72.	

The deck should be composed as follows:

- * I.D. card
- * XEQ card
- * CHAIN(2,A4) --include this card if more than one set of data is to be run and col. 72 of the same card contains a one. Also include this card if the program is being run as a chain link with the Burnham (1961) lattice constant refinement program.
- DFSET (main program)
- Subroutines
- * DATA
- Data deck for 1st set of reflections
- " " " 2nd " " "
- .
- .
- Data deck for nth set of reflections

References

- Buerger, M. J. (1942), X-Ray Crystallography. John Wiley and Sons, New York.
- Buerger, M. J. (1960), Crystal Structure Analysis. John Wiley and Sons, New York.
- Burnham, Charles W. (1961), The Structures and Crystal Chemistry of the Aluminum-silicate Minerals. Ph.D. thesis, M. I. T., Cambridge, Mass.
- Prewitt, Charles T. (1960), The parameters τ and ϕ for equi-inclination, with application to the single-crystal diffractometer. Z. Krist. 114, 355-360.

```

*      LIST8
*      LABEL
CDFSET
C      PROGRAM FOR COMPUTING EQUI-INCLINATION SINGLE-CRYSTAL
C      DIFFRACTOMETER SETTINGS PLUS 1/LP AND SIN THETA      1/11/62
COMMON A1,B1,C1,ALPHA1,BETA1,GAMMA1,NTEST,
1MH,MK,ML,LAST,NPRNT,MH1,MH2,MK1,MK2,ML1,ML2,ISET,
2LHKL,LHK0,LOKL,LH0L,LHHL,LHML,LH00,LOK0,LOOL
FREQUENCY 25(1,50,1),28(5,0,1),31(8,0,1)
DIMENSION FLP(4),TITLE(12)
50     READ INPUT TAPE 4,1,(TITLE(I),I=1,12)
1      FORMAT(12A6)
      READ INPUT TAPE 4,2,FLP(3),FLP(4),FLP(1),FLP(2)
2      FORMAT(4A6)
3      READ INPUT TAPE 4,4,LSQ,IKL,NPRNT,SINTHO,MH1,MH2,MK1,MK2,ML1,ML2,
1ISET,LAST
4      FORMAT(I1,2X,I1,2X,I1,8X,F5.4,2X,6(I3,2X),I1,18X,I1)
41     GO TO(5,7),LSQ
5      READ INPUT TAPE 4,6,A1,B1,C1,ALPHA1,BETA1,GAMMA1,WVLNG,LHKL,LHK0,L
1OKL,LH0L,LHHL,LHML,LH00,LOK0,LOOL
6      FORMAT(3F7.6,3F7.3,F7.4,11X,9I1)
      NTEST=1
      GO TO 9
7      READ INPUT TAPE 4,8,WVLNG,LHKL,LHK0,LOKL,LH0L,LHHL,LHML,LH00,LOK0,
1LOOL
8      FORMAT(42X,F7.4,11X,9I1)
81     IF(NTEST-1)35,9,35
9      PI=3.1415927
      RAD=PI/180.0
      GO TO(10,11,12),ISET
10     A=A1*WVLNG
      B=B1*WVLNG
      C=C1*WVLNG
      ALPHA=ALPHA1*RAD
      BETA=BETA1*RAD
      GAMMA=GAMMA1*RAD
      GO TO 13
11     A=C1*WVLNG
      B=A1*WVLNG
      C=B1*WVLNG
      ALPHA=GAMMA1*RAD
      BETA=ALPHA1*RAD
      GAMMA=BETA1*RAD
      GO TO 13
12     A=B1*WVLNG
      B=C1*WVLNG
      C=A1*WVLNG
      ALPHA=BETA1*RAD
      BETA=GAMMA1*RAD
      GAMMA=ALPHA1*RAD
13     COSA=COSF(ALPHA)
      COSB=COSF(BETA)
      COSG=COSF(GAMMA)
      SING=SINF(GAMMA)
      ABG=A*B*COSG

```



```

BCA=B*C*COSA
CAB=C*A*COSB
AA=A*A
BB=B*B
CC=C*C
BCOSG=B*COSG
CCOSB=C*COSB
BSING=B*SING
CNST1=(COSA*COSA+COSB*COSB-2.0*COSA*COSB*COSG)/(SING*SING)
CNST2=CNST1/4.0
CNST3=C*(COSA-COSB*COSG)/SING
TLTST=100
GO TO(14,131,131),NPRNT
131 CALL PILF1(FLP,4)
14 GO TO(141,18,141),NPRNT
141 WRITE OUTPUT TAPE 2,142,(TITLE(I),I=1,12)
142 FORMAT(1H112A6)
WRITE OUTPUT TAPE 2,15,A1,B1,C1,WVLNG
15 FORMAT(7H A* = F7.6,7H B* = F7.6,7H C* = F7.6,11H LAMBDA = F7.
14)
WRITE OUTPUT TAPE 2,16,ALPHA1,BETA1,GAMMA1
16 FORMAT(11H ALPHA* = F8.4,10H BETA* = F8.4,11H GAMMA* = F8.4)
WRITE OUTPUT TAPE 2,17
17 FORMAT(63H0 H K L UPSILON PHI 1/LP SIN
1(THETA))
18 DO 34 I=1,50
181 GO TO(19,20),IKL
19 CALL INDEX1
GO TO 21
20 CALL INDEX2
21 GO TO(22,23,24),ISET
22 TH=FLOATF(MH)
TK=FLOATF(MK)
TL=FLOATF(ML)
GO TO 25
23 TH=FLOATF(ML)
TK=FLOATF(MH)
TL=FLOATF(MK)
GO TO 25
24 TH=FLOATF(MK)
TK=FLOATF(ML)
TL=FLOATF(MH)
25 IF(TL-TLTST)26,27,26
26 TLTST=TL
TLLCC=TL*TL*CC
27 SIG=TH*TH*AA+TK*TK*BB+2.0*(TH*TK*ABG+TK*TL*BCA+TL*TH*CAB)
SINTH=(SQRTF(SIG+TLLCC))/2.0
28 IF(SINTH-SINTH0)29,29,181
29 XISQ=SIG+TLLCC*CNST1
XI=SQRTF(XISQ)
RSQ=1.0-TLLCC*(.25-CNST2)
OMEGA=ASINF(SQRTF(XISQ/(4.0*RSQ)))
XIX=TH*A+TK*BCOSG+TL*CCOSB
XIY=TK*BSING+TL*CNST3
FREQUENCY 291(50,1,50),292(1,0,1)

```

```

291 IF(XIX)295,292,295
292 IF(XIY)293,295,294
293 PSI=-PI/2.0
    XIX=1.0
    GO TO 296
294 PSI=PI/2.0
    XIX=1.0
    GO TO 296
295 PSI=ATANF(XIY/XIX)
296 PHI=PI-(XIX/ABS(XIX))*PI/2.0-PSI+OMEGA
    UPSILN=2.0*OMEGA
30  VLP=(2.0*RSQ*SINF(UPSILN))/(1.0+(COSF(2.0*ASINF(SINTH)))**2)
    PHI=PHI/RAD
    UPSILN=UPSILN/RAD
    PSI=PSI/RAD
31  IF(PHI-360.0)33,32,32
32  PHI=PHI-360.0
    GO TO 31
33  CALL OUTPUT(UPSILN,PHI,VLP,SINTH)
34  CONTINUE
    GO TO 14
35  WRITE OUTPUT TAPE 2,36
36  FORMAT(4I1H1LEAST-SQUARES REFINEMENT BAD. TERMINATE.)
37  CALL EXIT
    END

```

```

* LIST8
* LABEL
  SUBROUTINE OUTPUT(UPSILN,PHI,VLP,SINTH)
  COMMON A1,B1,C1,ALPHA1,BETA1,GAMMA1,NTEST,
1MH,MK,ML,LAST,NPRNT
21 GO TO(22,23,22),NPRNT
22 WRITE OUTPUT TAPE 2, 26, MH,MK,ML,UPSILN,PHI,VLP,SINTH
23 GO TO(25,24,24),NPRNT
24 PUNCH 27,MH,MK,ML,UPSILN,PHI,VLP,SINTH
25 RETURN
26 FORMAT(2H I3,2X,I3,2X,I3,2F12.2,F12.4,F11.4)
27 FORMAT(3I3,2X,2(F6.2,1X),2(F6.4,1X))
    END

```

```

* LIST8
* LABEL
  SUBROUTINE INDEX1
C  SUBROUTINE FOR READING HKL FROM DATA CARDS
  COMMON A1,B1,C1,ALPHA1,BETA1,GAMMA1,NTEST,
1MH,MK,ML,LAST
1  READ INPUT TAPE 4,2,MH,MK,ML,IEOF
2  FORMAT(I3,1X,I3,1X,I3,59X,I1)
3  IF(IEOF)5,4,5
4  RETURN
5  CALL TERM
    END

```

```

*      LIST8
*      LABEL
      SUBROUTINE TERM
      COMMON A1,B1,C1,ALPHA1,BETA1,GAMMA1,NTEST,
1MH,MK,ML,LAST,NPRNT
1      IF(SENSE LIGHT 1)9,2
2      GO TO(4,3,3),NPRNT
3      END FILE 3
4      IF(LAST)5,6,5
5      CALL CHAIN(2,A4)
6      WRITE OUTPUT TAPE 2,7
7      FORMAT(11HOEND OF RUN)
8      CALL EXIT
9      WRITE OUTPUT TAPE 2,10
10     FORMAT(116H1AN ERROR HAS OCCURRED IN THE INDEXING SUBROUTINE. ONE
1OF THE INDICES HAS EXCEEDED ITS STATED LIMIT. RUN TERMINATED.)
      GO TO 8
      END

```

```

*      FAP
      COUNT      405
      ENTRY      INDEX2
      REM        SUBROUTINE TO GENERATE HKL AND TO REJECT HKL WHICH DO NOT
      REM        CONFORM TO SPACE GROUP EXTINCTION RULES.
INDEX2  SXD      SAVE,1
      SXA      SAVE,2
      NOP
      CLA      TRABA
      STO      *-2
      CLA      MH1          ENTER INITIAL INDICES
      STO      MH
      CLA      MK1
      STO      MK
      CLA      ML1
      STO      ML
      REM      CHECK FOR ZEROES IN EXTINCTION RULE REQUESTS
NOEXT  ZET      LHKL
      TRA      AA
      ZET      LHK0
      TRA      AA
      ZET      LOKL
      TRA      AA
      ZET      LH0L
      TRA      AA
      ZET      LHHL
      TRA      AA
      ZET      LHML
      TRA      AA
      ZET      LH00
      TRA      AA
      ZET      LOK0
      TRA      AA
      ZET      L00L

```

	TRA	AA	
	CLA	TRAEA	BYPASS EXTINCTION RULES
	STO	TRNS	
	TRA	AM	
	REM	CHOOSE EXTINCTION RULES	
AA	CLA	L00L	HKL
	TZE	AB	
	PDX	0,1	
	CLA	XA+4,1	
	STO	TRNS	
AB	CLA	LOK0	
	TZE	AC	
	PDX	0,1	
	CLA	XB+2,1	
	STO	TRNS+1	
AC	CLA	LH00	
	TZE	AD	
	PDX	0,1	
	CLA	XC+2,1	
	STO	TRNS+2	
AD	CLA	LH0L	
	TZE	AE	
	PDX	0,1	
	CLA	XD+4,1	
	STO	TRNS+3	
AE	CLA	LOKL	
	TZE	AF	
	PDX	0,1	
	CLA	XE+4,1	
	STO	TRNS+4	
AF	CLA	LHK0	
	TZE	AG	
	PDX	0,1	
	CLA	XF+4,1	
	STO	TRNS+5	
AG	CLA	LHHL	
	TZE	AH	
	PDX	0,1	
	CLA	XG+2,1	
	STO	TRNS+6	
AH	CLA	LHML	
	TZE	AK	
	CLA	XH	
	STO	TRNS+7	
AK	CLA	LHKL	
	TZE	AM	
	PDX	0,1	
	CLA	XK+8,1	
	STO	TRNS+8	
AM	LXD	ISET,1	ROTATION AXIS IS C, B, OR A
	XEC	SETTR+3,1	
AN	CLA	TRABD	ROTATION AXIS IS B
	STO	BA	
	CLA	TRABB	
	STO	BD1	

	CLA	TRAEX	
	STO	BC1	
	TRA	CA	
AO	CLA	TRABC	ROTATION AXIS IS A
	STO	BA	
	CLA	TRABB	
	STO	BD1	
	CLA	TRAEX	
	STO	BB1	
	TRA	CA	
BA	NOP		
BB	CLA	MH	INCREMENT H
	CAS	MH2	
	TRA	ERROR	
	TRA	BB2	
	ADD	ONE	
	TZE	*+2	
	TRA	*+2	
	SSP		
	STO	MH	
	TRA	CA	
BB1	NOP		
BC	CLA	MK	INCREMENT K
	CAS	MK2	
	TRA	ERROR	
	TRA	BC2	
	ADD	ONE	
	TZE	*+2	
	TRA	*+2	
	SSP		
	STO	MK	
	TRA	CA	
BC1	NOP		
BD	CLA	ML	INCREMENT L
	CAS	ML2	
	TRA	ERROR	
	TRA	BD2	
	ADD	ONE	
	TZE	*+2	
	TRA	*+2	
	SSP		
	STO	ML	
	TRA	CA	
BD1	TRA	EX	
BB2	CLA	MH1	
	STO	MH	
	TRA	BB1	
BC2	CLA	MK1	
	STO	MK	
	TRA	BC1	
BD2	CLA	ML1	
	STO	ML	
	TRA	BD1	
	REM	PLACE H, K, AND L IN INDICATOR REGISTER	
CA	CLA	ML	

	SSP		
	ARS	18	
	ADM	MH	
	ALS	9	
	ADM	MK	
	PAI		
	TRA	TRNS	
	REM	EXTINCTION RULE ROUTINES	
DA1	OFT	YA	00L
	TRA	1,2	
	CLA	ML	
DA2	TRA	TEST2	
	OFT	YA	
	TRA	1,2	
	CLA	ML	
DA3	TRA	TEST3	
	OFT	YA	
	TRA	1,2	
	CLA	ML	
DA4	TRA	TEST4	
	OFT	YA	
	TRA	1,2	
	CLA	ML	
DR1	TRA	TEST6	
	OFT	YB	OKO
	TRA	1,2	
	CLA	MK	
DB2	TRA	TEST2	
	OFT	YB	
	TRA	1,2	
	CLA	MK	
DC1	TRA	TEST4	
	OFT	YC	HOO
	TRA	1,2	
	CLA	MH	
DC2	TRA	TEST2	
	OFT	YC	
	TRA	1,2	
	CLA	MH	
DD1	TRA	TEST4	
	OFT	YD	HOL
	TRA	1,2	
	CLA	ML	
DD2	TRA	TEST2	
	OFT	YD	
	TRA	1,2	
	CLA	MH	
DD3	TRA	TEST2	
	OFT	YD	
	TRA	1,2	
	CLA	ML	
	ADD	MH	
DD4	TRA	TEST2	
	OFT	YD	
	TRA	1,2	

	CLA	ML	
	ARS	18	
	LBT		
	TRA	*+2	
	TRA	BA	
	CLA	MH	
	ARS	18	
	LBT		
	TRA	*+2	
	TRA	BA	
	CLA	ML	
	ADD	MH	
	TRA	TEST4	
DE1	OFT	YE	OKL
	TRA	1,2	
	CLA	MK	
	TRA	TEST2	
DE2	OFT	YE	
	TRA	1,2	
	CLA	ML	
	TRA	TEST2	
DE3	OFT	YE	
	TRA	1,2	
	CLA	MK	
	ADD	ML	
	TRA	TEST2	
DE4	OFT	YE	
	TRA	1,2	
	CLA	MK	
	ARS	18	
	LBT		
	TRA	*+2	
	TRA	BA	
	CLA	MH	
	ARS	18	
	LBT		
	TRA	*+2	
	TRA	BA	
	CLA	MK	
	ADD	ML	
	TRA	TEST4	
DF1	OFT	YF	HKO
	TRA	1,2	
	CLA	MH	
	TRA	TEST2	
DF2	OFT	YF	
	TRA	1,2	
	CLA	MK	
	TRA	TEST2	
DF3	OFT	YF	
	TRA	1,2	
	CLA	MH	
	ADD	MK	
	TRA	TEST2	
DF4	OFT	YF	

	TRA	1,2	
	CLA	MH	
	ARS	18	
	LBT		
	TRA	*+2	
	TRA	BA	
	CLA	MK	
	ARS	18	
	LBT		
	TRA	*+2	
	TRA	BA	
	CLA	MH	
	ADD	MK	
	TRA	TEST4	
DG1	CLA	MH	HHL
	SUB	MK	
	TZE	*+2	
	TRA	1,2	
	CLA	ML	
	TRA	TEST2	
DG2	CLA	MH	
	SUB	MK	
	TZE	*+2	
	TRA	1,2	
	CLA	MH	
	ADD	MH	
	ADD	ML	
	TRA	TEST4	
DH1	CLA	MH	H(-H)L
	ADD	MK	
	TZE	*+2	
	TRA	1,2	
	CLA	ML	
	TRA	TEST2	
DK1	CLA	MH	HKL
	ADD	MK	
	TRA	TEST2	
DK2	CLA	MK	
	ADD	ML	
	TRA	TEST2	
DK3	CLA	ML	
	ADD	MH	
	TRA	TEST2	
DK4	OFT	YK	
	TRA	*+2	
	TRA	EA	
	ONT	YK	
	TRA	BA	
	TRA	EA	
DK5	CLA	MH	
	ADD	MK	
	ADD	ML	
	TRA	TEST2	
DK6	CLA	MH	
	CHS		


```

      ADD      MK
      ADD      ML
      TRA      TEST3
DK7   CLA      MH
      SUB      MK
      ADD      ML
      TRA      TEST3
DK8   CLA      MH
      SUB      MK
      TRA      TEST3
EA    LXD      SAVE,1
      LXA      SAVE,2
      TRA      1,4
      REM      SECTION FOR ASSEMBLING TRANSFER INSTRUCTIONS
TRNS  NOP      OOL
      NOP      OKO
      NOP      HOO
      NOP      HOL
      NOP      OKL
      NOP      HKO
      NOP      HHL
      NOP      H(-H)L
      NOP      HKL
      TRA      EA          TO EXIT
      REM      ROUTINES FOR TESTING WHETHER INDICES FIT EXTINCTION RULE
TEST2 SSP
      ARS      18
      LBT
      TRA      EA
      TRA      BA
TEST3 SSP
      LRS      36
      DVP      THREE
      TZE      EA
      TRA      BA
TEST4 SSP
      LRS      36
      DVP      FOUR
      TZE      EA
      TRA      BA
TEST6 SSP
      LRS      36
      DVP      SIX
      TZF      EA
      TRA      BA
THREE OCT      000000000003
FOUR  OCT      000000000004
SIX   OCT      000000000006
      REM      TRANSFER INSTRUCTIONS FOR EXTINCTION RULE SELECTION
XA    TSX      DA4,2          OOL
      TSX      DA3,2
      TSX      DA2,2
      TSX      DA1,2
XB    TSX      DB2,2          OKO
      TSX      DB1,2

```

XC	TSX	DC2,2	H00
	TSX	DC1,2	
XD	TSX	DD4,2	H0L
	TSX	DD3,2	
	TSX	DD2,2	
	TSX	DD1,2	
XE	TSX	DE4,2	OKL
	TSX	DE3,2	
	TSX	DE2,2	
	TSX	DE1,2	
XF	TSX	DF4,2	HK0
	TSX	DF3,2	
	TSX	DF2,2	
	TSX	DF1,2	
XG	TSX	DG2,2	HHL
	TSX	DG1,2	
XH	TSX	DH1,2	H(-H)L
XX	TSX	DK8,2	HKL
	TSX	DK7,2	
	TSX	DK6,2	
	TSX	DK5,2	
	TSX	DK4,2	
	TSX	DK3,2	
	TSX	DK2,2	
	TSX	DK1,2	
TRABA	TRA	BA	
TRABB	TRA	BB	
TRABC	TRA	BC	
TRABD	TRA	BD	
TRAEA	TRA	EA	
TRAEX	TRA	EX	
SETTR	TRA	AO	ROTATION AXIS IS A
	TRA	AN	ROTATION AXIS IS B
	TRA	CA	ROTATION AXIS IS C
	REM	MASKS FOR IDENTIFYING SPECIAL REFLECTIONS	
YA	OCT	777777000000	00L
YB	OCT	777000777000	OK0
YC	OCT	000777777000	H00
YD	OCT	000777000000	H0L
YE	OCT	777000000000	OKL
YF	OCT	000000777000	HK0
YK	OCT	001001001000	HKL(ODD OR EVEN)
SAVE	PZE		
ONE	OCT	000001000000	
EX	CALL	TERM	
ERROR	PSE	141	TURN ON SENSE LIGHT 1
	TRA	EX	
	COMMON	7	
MH	COMMON	1	
MK	COMMON	1	
ML	COMMON	3	
MH1	COMMON	1	
MH2	COMMON	1	
MK1	COMMON	1	
MK2	COMMON	1	

```
ML1    COMMON  1
ML2    COMMON  1
ISET   COMMON  1
LHKL   COMMON  1
LHKO   COMMON  1
LOKL   COMMON  1
LHOL   COMMON  1
LHHL   COMMON  1
LHML   COMMON  1
LHOO   COMMON  1
LOKO   COMMON  1
LOOL   COMMON  1
      END
```

Appendix IV

Observed and calculated structure factors for wollastonite and pectolite

Wollastonite structure factors

The FCAL's for wollastonite were computed using the coordinates and isotropic temperature factors given in Chapter I. Separate scale factors assigned to each reciprocal lattice level were varied in the last refinement cycles. The scale factors used for Appendix IV FCAL's were 2.2127, 2.4003, 2.1966, 2.3820, 2.2853, 2.3164, 2.3359, 2.4079, and 2.4977, for levels zero through eight, respectively.

The contribution to the structure factors due to the imaginary component of the anomalous scattering of Ca is listed under BOBS and BCAL for both wollastonite and pectolite.

H	K	L	FOBS	FCAL	AOBS	ACAL	BOBS	BCAL
-0	-0	-1	20.03	6.67	-18.78	-6.25	-6.98	-2.32
1	-0	-0	37.96	22.19	-37.92	-22.17	-1.87	-1.09
2	-0	-0	59.94	64.73	-59.92	-64.71	-1.61	-1.74
3	-0	-0	52.44	60.14	-52.07	-59.72	-6.21	-7.12
4	-0	-0	52.65	57.36	52.49	57.19	4.08	4.45
5	-0	-0	61.94	70.31	61.90	70.26	2.30	2.62
6	-0	-0	35.53	33.79	35.28	33.55	4.22	4.01
7	-0	-0	27.31	24.95	-26.34	-24.07	-7.19	-6.57
8	-0	-0	28.13	26.89	-28.09	-26.85	-1.41	-1.34
9	-0	-0	25.62	23.32	-25.61	-23.31	-0.79	-0.72
-1	-0	-1	16.04	14.69	13.35	12.22	8.90	8.15
1	-0	-1	15.75	10.46	15.33	10.18	-3.62	-2.41
-4	-0	-1	46.40	48.90	-45.86	-48.32	-7.12	-7.50
4	-0	-1	16.22	14.86	-15.98	-14.64	2.73	2.50
-2	-0	-1	26.68	24.84	-26.68	-24.84	0.16	0.15
2	-0	-1	24.43	30.02	-23.89	-29.35	-5.12	-6.30
-3	-0	-1	40.00	42.50	39.99	42.49	-0.87	-0.93
3	-0	-1	5.78	5.66	0.00	0.00	5.78	5.66
-5	-0	-1	57.97	62.61	57.91	62.53	2.83	3.05
5	-0	-1	28.29	27.57	28.13	27.41	3.01	2.93
-7	-0	-1	22.36	20.28	21.72	19.70	5.29	4.80
7	-0	-1	16.07	15.15	16.06	15.14	-0.60	-0.57
-6	-0	-1	23.78	22.29	-23.63	-22.15	2.67	2.50
6	-0	-1	60.82	68.47	-60.47	-68.08	-6.54	-7.36
-8	-0	-1	17.20	15.30	-16.07	-14.30	-6.13	-5.45
8	-0	-1	13.78	13.23	13.77	13.23	0.21	0.20
-9	-0	-1	1.79	2.84	-1.31	-2.09	-1.21	-1.93
9	-0	-1	9.83	8.95	6.47	5.89	7.40	6.74
-1	-0	-2	82.64	94.51	-82.58	-94.45	-3.00	-3.43
1	-0	-2	82.40	100.67	-82.29	100.54	-4.17	-5.09
-4	-0	-2	25.31	25.37	-25.31	-25.37	-0.05	-0.05
4	-0	-2	10.25	11.76	10.14	11.64	1.44	1.65
-2	-0	-2	64.77	64.52	64.34	64.09	7.44	7.42
2	-0	-2	46.71	52.81	46.35	52.40	5.80	6.56
-3	-0	-2	61.62	65.46	61.61	65.44	1.21	1.29
3	-0	-2	46.34	50.73	46.30	50.68	1.99	2.17
-5	-0	-2	94.98	114.54	-94.78	114.30	-6.15	-7.42
5	-0	-2	85.29	102.69	-85.05	102.39	-6.43	-7.74
-7	-0	-2	39.51	39.25	39.45	39.19	2.21	2.20
7	-0	-2	2.97	1.90	2.37	1.51	1.79	1.14
-6	-0	-2	18.56	15.59	-18.46	-15.51	1.90	1.59
6	-0	-2	25.02	24.14	-25.02	-24.14	0.37	0.35
-8	-0	-2	44.57	41.86	44.21	41.53	5.59	5.25
8	-0	-2	58.80	63.59	58.49	63.25	6.04	6.53
9	-0	-2	15.81	15.51	-15.46	-15.17	-3.29	-3.23
-0	-0	-2	91.71	80.35	-91.65	-80.30	-3.27	-2.86
-1	-0	-3	16.54	13.23	-16.08	-12.87	-3.84	-3.07
1	-0	-3	90.89	103.00	90.67	102.75	6.24	7.07
-4	-0	-3	28.86	27.51	-28.76	-27.42	2.35	2.24
4	-0	-3	23.26	24.88	-22.13	-23.68	-7.16	-7.66
-2	-0	-3	27.43	22.46	26.92	22.04	-5.28	-4.32
2	-0	-3	29.65	29.54	-29.61	-29.50	1.65	1.65
-3	-0	-3	23.60	20.45	22.47	19.46	7.25	6.28
3	-0	-3	8.70	8.24	8.69	8.23	0.29	0.28

-5	-0	-3	0.	0.89	-0.	-0.37	0.	0.81
5	-0	-3	49.51	53.60	49.49	53.59	1.23	1.33
-7	-0	-3	18.69	18.17	18.69	18.17	0.20	0.20
7	-0	-3	5.78	5.92	0.33	0.34	5.78	5.91
-6	-0	-3	18.65	16.47	-16.94	-14.96	-7.80	-6.89
6	-0	-3	5.55	4.53	4.98	4.06	2.46	2.01
-8	-0	-3	11.08	9.36	-10.88	-9.19	2.07	1.75
8	-0	-3	3.97	4.32	0.73	0.79	-3.90	-4.25
9	-0	-3	4.64	5.15	-4.17	-4.63	-2.04	-2.26
-0	-0	-3	58.84	54.54	-58.71	-54.42	-3.90	-3.62
-1	-0	-4	21.57	19.16	-21.45	-19.06	-2.26	-2.00
1	-0	-4	55.78	58.64	55.77	58.63	0.94	0.98
-4	-0	-4	64.00	70.44	63.85	70.27	4.41	4.85
4	-0	-4	12.18	10.91	-11.91	-10.66	2.55	2.28
-2	-0	-4	20.79	18.51	-20.51	-18.26	-3.41	-3.04
2	-0	-4	33.08	32.49	-33.06	-32.48	-1.08	-1.06
-3	-0	-4	66.81	70.28	-66.64	-70.10	-4.67	-4.91
3	-0	-4	48.01	50.98	-47.54	-50.48	-6.70	-7.11
-5	-0	-4	46.74	47.96	46.66	47.87	2.85	2.93
5	-0	-4	46.06	51.71	45.99	51.64	2.42	2.72
-7	-0	-4	27.06	27.28	-26.39	-26.61	-5.95	-6.00
7	-0	-4	47.07	46.51	-46.79	-46.23	-5.13	-5.07
-6	-0	-4	23.06	22.17	23.00	22.11	1.63	1.57
6	-0	-4	62.52	71.31	62.37	71.14	4.29	4.90
8	-0	-4	18.96	16.76	-18.79	-16.61	-2.56	-2.27
-0	-0	-4	98.99	114.70	98.80	114.47	6.17	7.15
-1	-0	-5	15.59	13.61	-13.51	-11.79	7.79	6.80
1	-0	-5	21.82	19.14	21.67	19.00	-2.57	-2.26
-4	-0	-5	18.78	17.31	-17.93	-16.52	-5.60	-5.16
4	-0	-5	17.92	17.89	-17.63	-17.59	3.23	3.22
-2	-0	-5	27.28	26.72	27.28	26.71	-0.40	-0.39
2	-0	-5	34.17	32.90	-33.57	-32.32	-6.38	-6.14
-3	-0	-5	18.11	16.51	-17.85	-16.27	-3.05	-2.78
3	-0	-5	17.96	15.95	17.61	15.64	3.51	3.12
-5	-0	-5	31.34	29.80	31.15	29.62	3.43	3.26
5	-0	-5	12.49	11.73	11.89	11.17	3.81	3.58
-7	-0	-5	5.97	5.45	5.49	5.01	2.36	2.15
7	-0	-5	16.69	13.59	-16.49	-13.43	-2.55	-2.07
-6	-0	-5	5.17	5.86	-4.26	-4.82	2.94	3.33
6	-0	-5	35.49	36.10	-35.06	-35.67	-5.52	-5.62
8	-0	-5	13.03	12.74	13.02	12.73	-0.56	-0.54
-0	-0	-5	29.38	26.08	-29.37	-26.08	0.28	0.25
-1	-0	-6	2.42	0.53	0.97	0.21	-2.22	-0.48
1	-0	-6	61.92	69.23	-61.76	-69.06	-4.33	-4.84
-4	-0	-6	27.18	28.03	-27.09	-27.93	-2.27	-2.34
4	-0	-6	7.99	6.42	7.56	6.07	2.58	2.07
-2	-0	-6	59.14	63.06	58.86	62.77	5.67	6.05
2	-0	-6	32.21	31.28	31.98	31.05	3.86	3.75
-3	-0	-6	4.58	1.20	-1.92	-0.50	4.15	1.08
3	-0	-6	47.22	48.29	47.10	48.17	3.39	3.47
-5	-0	-6	45.79	51.93	-45.58	-51.68	-4.46	-5.06
5	-0	-6	47.96	51.23	-47.65	-50.90	-5.45	-5.82
7	-0	-6	18.12	16.83	-18.10	-16.81	0.81	0.75
-6	-0	-6	12.08	10.09	-11.91	-9.95	1.99	1.66
6	-0	-6	11.99	10.18	-11.82	-10.04	-2.01	-1.71

-0	-0	-6	54.84	59.49	-54.76	-59.41	-2.96	-3.21
-0	-0	-7	20.09	18.32	-19.75	-18.01	-3.66	-3.33
-1	-0	-7	10.84	10.40	10.06	9.65	-4.03	-3.87
-2	-0	-7	4.27	3.97	4.09	3.81	-1.22	-1.14
-3	-0	-7	6.68	7.09	4.75	5.03	4.71	4.99
-4	-0	-7	5.32	4.31	-4.49	-3.64	2.86	2.32
1	-0	-7	31.49	32.65	31.24	32.39	3.98	4.12
2	-0	-7	5.58	4.00	2.81	2.02	4.82	3.46
3	-0	-7	0.	0.60	-0.	-0.32	0.	0.50
4	-0	-7	9.54	8.86	-7.33	-6.81	-6.11	-5.67
5	-0	-7	0.	2.88	0.	2.61	-0.	-1.21
6	-0	-7	28.44	29.10	28.37	29.03	1.93	1.98
-1	-0	-8	12.19	10.87	12.03	10.73	-1.96	-1.75
1	-0	-8	37.05	40.86	36.94	40.73	2.91	3.21
4	-0	-8	16.29	16.01	-16.28	-16.00	-0.64	-0.63
-2	-0	-8	37.47	43.53	-37.29	-43.32	-3.62	-4.20
2	-0	-8	2.81	1.20	-1.57	-0.67	-2.33	-1.00
3	-0	-8	32.23	32.82	-31.83	-32.41	-5.08	-5.17
-0	-0	-8	22.68	25.12	22.36	24.77	3.80	4.21
-9	-1	-0	3.94	3.50	3.94	3.49	0.19	0.17
-8	-1	-0	17.60	16.35	17.59	16.34	0.62	0.58
-7	-1	-0	31.02	30.86	-31.01	-30.84	-0.88	-0.88
-6	-1	-0	6.59	5.70	6.59	5.70	-0.04	-0.04
-5	-1	-0	1.14	0.49	-1.11	-0.48	-0.26	-0.11
-4	-1	-0	18.17	18.31	18.16	18.30	0.64	0.65
-3	-1	-0	6.37	6.10	6.37	6.09	-0.13	-0.13
-2	-1	-0	34.59	40.63	-34.59	-40.63	-0.09	-0.10
-1	-1	-0	13.75	12.61	13.75	12.61	-0.23	-0.21
-0	-1	-0	0.	1.77	0.	1.77	0.	0.06
1	-1	-0	0.	0.10	-0.	-0.01	0.	0.10
2	-1	-0	28.66	30.20	28.66	30.20	-0.12	-0.12
3	-1	-0	23.94	26.63	-23.94	-26.63	0.25	0.27
4	-1	-0	9.08	8.41	-9.08	-8.41	-0.13	-0.12
5	-1	-0	9.18	8.87	9.18	8.87	0.18	0.17
6	-1	-0	4.27	4.09	-4.21	-4.04	-0.67	-0.64
7	-1	-0	20.98	20.54	20.98	20.54	0.37	0.36
8	-1	-0	21.58	22.17	-21.58	-22.17	-0.05	-0.05
9	-1	-0	7.08	7.44	7.04	7.40	0.73	0.77
1	-1	1	18.31	16.31	-18.30	-16.30	-0.61	-0.54
-1	-1	-1	11.88	10.73	11.86	10.70	0.78	0.70
-1	-1	1	36.14	37.90	36.14	37.90	-0.49	-0.52
1	-1	-1	20.02	19.08	-20.02	-19.07	0.44	0.42
4	-1	-1	4.09	4.58	-4.08	-4.57	-0.28	-0.31
4	-1	1	21.91	24.00	21.90	23.98	0.80	0.88
-4	-1	-1	6.75	7.61	-6.72	-7.57	-0.64	-0.72
-4	-1	1	7.55	6.57	-7.54	-6.56	0.33	0.28
2	-1	-1	41.60	42.67	41.60	42.67	-0.37	-0.38
2	-1	1	10.99	6.94	10.96	6.93	0.81	0.51
-2	-1	-1	19.39	18.63	-19.38	-18.61	-0.81	-0.77
-2	-1	1	22.70	23.93	-22.69	-23.92	0.41	0.43
3	-1	-1	4.91	5.10	-4.90	-5.09	0.31	0.32
3	-1	1	26.48	28.92	-26.48	-28.91	-0.64	-0.70
-3	-1	-1	26.68	27.83	26.68	27.83	0.27	0.28
-3	-1	1	5.65	3.91	-5.65	-3.91	-0.00	-0.00
5	-1	-1	12.53	11.83	-12.53	-11.83	-0.00	-0.00

5	-1	1	6.63	4.78	6.60	4.75	-0.69	-0.50
-5	-1	-1	0.	1.37	0.	0.62	0.	1.22
-5	-1	1	0.	1.57	0.	1.48	-0.	-0.52
7	-1	-1	27.85	28.57	27.84	28.57	0.35	0.35
7	-1	1	7.38	7.47	-7.28	-7.37	-1.21	-1.22
-7	-1	-1	6.19	5.49	-6.17	-5.47	0.52	0.46
-7	-1	1	22.16	22.47	-22.15	-22.47	0.20	0.20
6	-1	-1	10.76	9.59	-10.76	-9.59	-0.07	-0.07
6	-1	1	1.50	2.10	1.42	1.98	0.49	0.68
-6	-1	-1	4.75	4.07	-4.73	-4.05	-0.51	-0.44
-6	-1	1	21.79	21.64	21.79	21.64	-0.24	-0.24
8	-1	-1	13.46	13.59	-13.46	-13.59	0.17	0.18
8	-1	1	10.88	10.07	-10.86	-10.05	0.75	0.70
-8	-1	-1	7.15	6.88	6.99	6.73	-1.51	-1.45
-8	-1	1	10.91	9.98	10.89	9.97	0.58	0.53
9	-1	-1	2.15	2.19	2.12	2.16	-0.36	-0.36
9	-1	1	6.58	7.14	6.57	7.12	-0.42	-0.45
-9	-1	1	0.	0.23	0.	0.16	0.	0.16
-0	-1	1	4.52	4.01	4.50	3.99	0.47	0.42
-0	-1	-1	9.87	16.01	-9.87	-16.01	-0.20	-0.32
1	-1	2	10.19	7.30	-10.09	-7.22	1.47	1.05
-1	-1	-2	19.43	16.56	19.41	16.54	-0.88	-0.75
-1	-1	2	44.93	48.46	44.92	48.45	0.86	0.93
4	-1	-2	22.06	21.61	22.05	21.60	0.65	0.64
4	-1	2	7.76	7.91	7.66	7.81	-1.26	-1.28
-4	-1	-2	13.51	14.19	-13.50	-14.18	0.60	0.63
-4	-1	2	23.91	24.71	-23.89	-24.69	-0.93	-0.96
2	-1	-2	24.56	25.04	24.54	25.03	0.78	0.80
2	-1	2	4.95	3.83	4.76	3.68	-1.35	-1.05
-2	-1	-2	10.48	10.46	10.40	10.37	1.34	1.34
-2	-1	2	4.98	4.41	-4.92	-4.36	-0.75	-0.66
3	-1	-2	2.14	2.51	-2.04	-2.39	-0.65	-0.76
3	-1	2	6.72	6.21	6.65	6.15	0.96	0.89
-3	-1	-2	1.80	1.65	-1.19	-1.09	-1.35	-1.24
-3	-1	2	11.20	11.14	11.17	11.11	0.73	0.73
5	-1	-2	13.55	12.81	-13.54	-12.80	-0.60	-0.56
5	-1	2	3.49	3.08	-3.12	-2.75	1.55	1.37
-5	-1	-2	5.47	5.23	-5.29	-5.06	-1.36	-1.30
-5	-1	2	0.	1.45	-0.	-1.39	0.	0.41
7	-1	-2	9.17	9.32	9.16	9.31	-0.41	-0.42
7	-1	2	6.37	5.50	6.22	5.38	1.35	1.17
-7	-1	-2	3.00	1.59	-2.70	-1.43	-1.30	-0.69
-7	-1	2	0.	1.60	-0.	-1.32	0.	0.89
6	-1	-2	10.50	9.29	-10.47	-9.26	0.85	0.75
6	-1	2	8.62	8.39	-8.58	-8.35	-0.83	-0.81
-6	-1	-2	13.16	12.65	13.04	12.54	1.75	1.68
-6	-1	2	15.54	14.82	15.53	14.82	-0.28	-0.26
8	-1	-2	4.02	4.20	-4.02	-4.20	0.13	0.13
8	-1	2	12.54	11.60	-12.41	-11.47	-1.83	-1.69
-8	-1	-2	16.74	15.57	16.71	15.54	1.00	0.93
-8	-1	2	2.84	1.82	2.76	1.76	-0.69	-0.44
9	-1	-2	0.	0.62	0.	0.10	-0.	-0.62
9	-1	2	16.39	18.07	16.37	18.04	0.84	0.93
-9	-1	2	2.47	1.68	-2.45	-1.66	-0.31	-0.21
-0	-1	-2	14.03	12.68	13.99	12.65	0.97	0.88

-0	-1	2	39.73	40.99	-39.72	-40.98	-0.91	-0.94
1	-1	-3	6.81	6.35	-6.67	-6.22	1.38	1.29
1	-1	3	3.02	2.21	2.39	1.75	-1.85	-1.35
-1	-1	-3	21.22	20.36	21.18	20.32	1.28	1.23
-1	-1	3	17.36	16.00	-17.31	-15.95	-1.38	-1.27
4	-1	-3	2.37	2.28	-2.08	-1.99	-1.15	-1.10
4	-1	3	14.89	14.61	14.84	14.56	1.25	1.22
-4	-1	-3	23.44	25.10	-23.40	-25.05	-1.46	-1.56
-4	-1	3	7.63	7.34	7.55	7.27	1.06	1.02
2	-1	-3	25.01	24.62	-24.99	-24.59	-1.15	-1.13
2	-1	3	38.43	36.26	38.39	36.22	1.73	1.63
-2	-1	-3	30.92	30.79	-30.89	-30.77	-1.17	-1.17
-2	-1	3	24.18	23.56	24.15	23.53	1.23	1.20
3	-1	-3	9.64	9.96	9.57	9.88	1.19	1.23
3	-1	3	23.04	22.59	-22.99	-22.55	-1.46	-1.43
-3	-1	-3	18.13	18.09	18.03	17.99	1.92	1.91
-3	-1	3	1.88	2.44	-1.58	-2.05	-1.03	-1.34
5	-1	-3	17.76	18.62	17.73	18.59	1.07	1.12
5	-1	3	30.87	32.58	-30.82	-32.53	-1.71	-1.80
-5	-1	-3	22.28	23.75	22.26	23.74	0.87	0.93
-5	-1	3	17.99	18.24	-17.98	-18.22	-0.77	-0.78
7	-1	-3	6.52	6.22	6.48	6.18	0.72	0.69
7	-1	3	1.93	1.85	-1.60	-1.53	-1.09	-1.05
-7	-1	-3	7.57	7.02	7.26	6.73	2.15	1.99
-7	-1	3	8.77	7.42	-8.69	-7.36	-1.18	-1.00
6	-1	-3	16.90	16.20	-16.87	-16.17	-1.02	-0.97
6	-1	3	19.90	20.09	19.83	20.02	1.71	1.72
-6	-1	-3	11.44	11.41	-11.29	-11.27	-1.83	-1.82
-6	-1	3	15.32	15.09	15.27	15.04	1.26	1.24
8	-1	-3	5.51	4.76	-5.39	-4.66	-1.11	-0.96
8	-1	3	6.01	6.18	5.80	5.97	1.57	1.61
-8	-1	3	4.33	3.78	-4.32	-3.77	0.38	0.33
9	-1	-3	2.78	2.71	-2.61	-2.54	0.96	0.93
-0	-1	-3	18.73	15.40	18.63	15.32	-1.98	-1.63
-0	-1	3	22.96	21.42	-22.91	-21.38	1.42	1.32
1	-1	-4	11.89	12.53	-11.82	-12.45	-1.35	-1.42
1	-1	4	43.56	45.49	43.53	45.46	1.54	1.60
-1	-1	-4	38.80	39.43	-38.75	-39.38	-2.07	-2.11
-1	-1	4	8.63	8.97	8.48	8.81	1.60	1.67
4	-1	-4	5.68	5.63	-5.49	-5.44	1.46	1.45
4	-1	4	7.67	8.02	-7.51	-7.84	-1.60	-1.67
-4	-1	-4	15.66	15.66	15.48	15.48	2.38	2.37
-4	-1	4	11.08	11.13	11.00	11.06	-1.29	-1.30
2	-1	-4	12.28	12.33	12.16	12.21	1.70	1.71
2	-1	4	18.04	16.75	-17.94	-16.66	-1.87	-1.74
-2	-1	-4	3.95	3.18	-3.51	-2.83	1.82	1.47
-2	-1	4	16.59	15.92	-16.50	-15.84	-1.72	-1.65
3	-1	-4	13.55	13.24	-13.45	-13.14	-1.67	-1.63
3	-1	4	3.84	3.11	-2.83	-2.29	2.60	2.11
-3	-1	-4	0.	1.61	0.	0.43	-0.	-1.55
-3	-1	4	5.60	5.25	5.35	5.02	1.64	1.54
5	-1	-4	9.46	8.92	9.33	8.80	-1.52	-1.44
5	-1	4	4.35	4.88	4.14	4.64	1.34	1.51
-5	-1	-4	0.	2.55	0.	1.86	-0.	-1.74
-5	-1	4	6.80	6.57	-6.61	-6.38	1.61	1.55

7	-1	-4	3.27	2.69	-2.86	-2.36	-1.59	-1.31
7	-1	4	8.88	8.84	8.67	8.63	1.92	1.92
-7	-1	-4	18.94	19.49	-18.81	-19.36	-2.18	-2.25
-7	-1	4	8.12	6.73	8.05	6.68	1.07	0.89
6	-1	-4	3.15	3.25	-2.91	-3.01	1.20	1.24
6	-1	4	2.66	3.57	2.08	2.79	-1.66	-2.23
-6	-1	-4	5.96	6.03	-5.84	-5.92	1.17	1.18
-6	-1	4	2.21	1.82	-1.29	-1.06	-1.80	-1.48
8	-1	-4	16.18	14.46	16.11	14.40	1.51	1.35
8	-1	4	15.89	16.23	-15.85	-16.18	-1.19	-1.21
-8	-1	4	20.32	19.95	-20.28	-19.91	-1.19	-1.17
9	-1	-4	17.32	19.73	-17.31	-19.71	-0.76	-0.87
-0	-1	-4	41.98	42.64	41.95	42.60	1.73	1.76
-0	-1	4	28.20	28.86	-28.15	-28.80	-1.74	-1.78
1	-1	-5	6.70	6.21	6.33	5.86	2.20	2.04
1	-1	5	9.27	8.42	8.96	8.15	-2.36	-2.15
-1	-1	-5	12.37	11.19	-12.13	-10.97	2.41	2.18
-1	-1	5	5.31	5.28	-4.96	-4.93	-1.89	-1.88
4	-1	-5	27.13	29.17	-27.08	-29.12	-1.65	-1.78
4	-1	5	31.13	32.67	31.05	32.57	2.32	2.44
-4	-1	-5	19.36	19.49	-19.27	-19.40	-1.86	-1.87
-4	-1	5	27.61	28.29	27.55	28.23	1.78	1.83
2	-1	-5	7.63	7.12	-7.29	-6.80	-2.26	-2.11
2	-1	5	10.70	10.24	-10.54	-10.08	1.85	1.77
-2	-1	-5	8.80	8.64	-8.44	-8.30	-2.47	-2.43
-2	-1	5	15.22	14.06	15.08	13.93	2.07	1.92
3	-1	-5	20.43	21.23	20.37	21.16	1.67	1.74
3	-1	5	22.16	22.25	-22.06	-22.16	-2.06	-2.07
-3	-1	-5	27.73	28.59	27.68	28.54	1.54	1.58
-3	-1	5	26.51	26.30	-26.45	-26.24	-1.80	-1.78
5	-1	-5	26.14	28.04	26.09	27.98	1.63	1.75
5	-1	5	12.15	11.84	-12.02	-11.71	-1.81	-1.76
-5	-1	-5	16.08	16.45	15.87	16.23	2.62	2.68
-5	-1	5	28.51	29.59	-28.46	-29.53	-1.78	-1.85
7	-1	-5	17.58	16.74	17.49	16.66	1.76	1.68
7	-1	5	23.96	24.98	-23.83	-24.85	-2.42	-2.52
-7	-1	5	8.38	7.34	-8.21	-7.19	-1.69	-1.48
6	-1	-5	26.44	27.99	-26.39	-27.95	-1.55	-1.64
6	-1	5	16.36	15.76	16.27	15.67	1.80	1.73
-6	-1	-5	20.03	21.27	-19.96	-21.20	-1.67	-1.77
-6	-1	5	23.96	23.14	23.92	23.10	1.46	1.41
8	-1	-5	0.	1.48	-0.	-0.53	-0.	-1.38
-0	-1	-5	2.99	3.29	2.60	2.86	-1.48	-1.63
-0	-1	5	7.10	6.27	6.70	5.91	2.36	2.08
1	-1	-6	29.55	31.18	-29.46	-31.08	-2.36	-2.49
1	-1	6	26.56	25.55	26.44	25.44	2.51	2.41
-1	-1	-6	22.16	22.85	-22.09	-22.78	-1.71	-1.76
-1	-1	6	23.13	23.96	23.03	23.87	2.06	2.14
4	-1	-6	8.52	8.23	8.22	7.94	2.24	2.16
4	-1	6	1.48	2.48	-0.52	-0.86	-1.39	-2.32
-4	-1	-6	7.26	7.02	-7.07	-6.83	1.65	1.60
-4	-1	6	3.09	2.69	-1.95	-1.70	-2.40	-2.09
2	-1	-6	16.35	16.13	16.23	16.01	1.99	1.97
2	-1	6	29.25	30.90	-29.16	-30.81	-2.21	-2.34
-2	-1	-6	29.17	30.94	29.07	30.84	2.37	2.51

-2	-1	6	13.87	14.05	-13.70	-13.88	-2.15	-2.18
3	-1	-6	8.52	8.65	-8.29	-8.42	-1.95	-1.98
3	-1	6	20.06	20.03	19.98	19.94	1.84	1.84
-3	-1	-6	12.61	12.48	-12.34	-12.21	-2.60	-2.57
-3	-1	6	10.43	9.72	10.19	9.50	2.21	2.06
5	-1	-6	2.61	2.81	1.88	2.02	-1.81	-1.95
5	-1	6	2.42	3.28	1.48	2.01	1.92	2.60
-5	-1	-6	5.55	6.61	-5.26	-6.26	-1.78	-2.12
-5	-1	6	5.44	5.86	-5.16	-5.56	1.71	1.85
7	-1	-6	8.19	8.58	-8.01	-8.39	-1.72	-1.80
-7	-1	6	14.81	14.52	14.67	14.38	2.08	2.04
6	-1	-6	2.51	2.37	-1.50	-1.41	2.02	1.90
6	-1	6	8.22	8.62	-8.06	-8.45	-1.65	-1.74
-6	-1	6	4.30	4.00	-3.85	-3.59	-1.91	-1.78
-0	-1	-6	25.88	26.73	25.80	26.64	2.14	2.21
-0	-1	6	26.93	26.42	-26.85	-26.34	-2.07	-2.03
1	-1	-7	13.16	12.17	12.95	11.98	2.31	2.13
1	-1	7	3.78	3.95	-3.19	-3.33	-2.02	-2.11
-1	-1	-7	6.22	6.48	5.85	6.09	2.12	2.21
-1	-1	7	19.73	18.53	-19.55	-18.36	-2.61	-2.45
4	-1	-7	15.47	17.31	-15.35	-17.17	-1.97	-2.20
4	-1	7	9.16	9.80	9.00	9.63	1.70	1.81
-4	-1	-7	19.25	20.78	-19.11	-20.62	-2.35	-2.54
-4	-1	7	18.39	18.99	18.27	18.87	2.09	2.16
2	-1	-7	17.39	17.02	-17.26	-16.89	-2.09	-2.04
2	-1	7	10.55	10.44	10.21	10.11	2.66	2.63
-2	-1	-7	6.13	6.12	-5.86	-5.84	-1.82	-1.82
-2	-1	7	16.69	15.68	16.52	15.52	2.37	2.23
3	-1	-7	14.51	14.47	14.31	14.26	2.45	2.44
3	-1	7	6.67	7.02	-6.29	-6.62	-2.24	-2.35
-3	-1	-7	9.47	9.66	9.09	9.26	2.67	2.72
-3	-1	7	14.66	14.61	-14.50	-14.45	-2.19	-2.19
5	-1	-7	16.05	17.42	15.94	17.30	1.86	2.02
5	-1	7	22.86	25.34	-22.75	-25.22	-2.24	-2.48
-5	-1	7	15.31	13.59	-15.14	-13.43	-2.29	-2.03
6	-1	-7	9.58	10.03	-9.37	-9.80	-2.01	-2.10
-6	-1	7	7.57	7.05	7.21	6.71	2.33	2.16
-0	-1	-7	7.16	7.18	-6.62	-6.64	-2.73	-2.74
-0	-1	7	7.57	7.32	7.22	6.99	2.27	2.20
1	-1	-8	1.44	2.26	-0.70	-1.10	-1.25	-1.97
1	-1	8	15.72	16.75	15.60	16.62	1.98	2.11
-1	-1	-8	23.22	25.58	-23.07	-25.42	-2.57	-2.84
-1	-1	8	4.24	5.01	3.75	4.44	1.97	2.33
4	-1	-8	3.08	3.84	2.61	3.26	1.63	2.03
-4	-1	8	7.30	6.72	-6.89	-6.34	-2.41	-2.22
2	-1	-8	7.88	7.93	7.46	7.51	2.54	2.56
2	-1	8	20.19	20.70	-20.09	-20.59	-2.07	-2.12
-2	-1	-8	16.02	17.43	15.91	17.30	1.90	2.06
-2	-1	8	7.24	7.52	-6.93	-7.20	-2.08	-2.16
3	-1	-8	6.40	6.44	-5.95	-5.98	-2.37	-2.39
-3	-1	8	5.41	5.35	4.87	4.82	2.35	2.32
-0	-1	-8	10.57	11.82	10.38	11.61	1.99	2.23
-0	-1	8	6.27	6.89	-5.81	-6.39	-2.34	-2.58
-8	-2	-0	55.83	53.86	-55.39	-53.43	-7.00	-6.75
-7	-2	-0	31.73	30.37	31.64	30.29	2.31	2.21

-6	-2	-0	36.39	34.44	36.32	34.38	2.26	2.14
-5	-2	-0	5.13	5.73	0.15	0.16	5.12	5.73
-4	-2	-0	32.98	32.62	-32.49	-32.14	-5.65	-5.59
-3	-2	-0	52.56	57.59	-52.51	-57.54	-2.23	-2.44
-2	-2	-0	54.93	61.07	-54.88	-61.01	-2.56	-2.85
-1	-2	-0	94.79	153.42	94.66	153.21	4.92	7.96
-0	-2	-0	5.54	5.93	5.52	5.91	0.50	0.54
1	-2	-0	4.80	5.17	-4.79	-5.15	-0.41	-0.44
2	-2	-0	94.90	153.35	-94.77	153.14	-4.95	-8.00
3	-2	-0	53.93	61.47	53.88	61.41	2.40	2.74
4	-2	-0	51.57	57.26	51.52	57.21	2.19	2.43
5	-2	-0	33.27	33.29	32.78	32.80	5.69	5.69
6	-2	-0	5.28	5.68	0.46	0.49	-5.26	-5.66
7	-2	-0	36.23	34.70	-36.16	-34.63	-2.31	-2.21
8	-2	-0	33.44	30.53	-33.34	-30.45	-2.52	-2.30
9	-2	-0	55.83	53.71	55.38	53.28	7.02	6.76
1	-2	-1	24.18	18.21	22.06	16.62	-9.90	-7.45
1	-2	1	3.93	1.71	-1.83	-0.80	3.48	1.52
-1	-2	-1	8.53	6.49	8.50	6.47	-0.69	-0.52
-1	-2	1	32.96	34.72	-32.73	-34.48	-3.90	-4.11
4	-2	-1	49.48	54.99	49.30	54.79	4.23	4.71
4	-2	1	30.86	32.14	30.83	32.11	1.32	1.37
-4	-2	-1	28.56	27.54	28.48	27.47	-2.05	-1.97
-4	-2	1	46.76	48.47	46.30	48.00	6.50	6.74
2	-2	-1	30.42	32.25	30.18	32.00	3.78	4.00
2	-2	1	7.16	5.79	-7.12	-5.76	0.76	0.61
-2	-2	-1	81.71	93.60	81.41	93.25	7.02	8.05
-2	-2	1	25.79	24.27	-25.62	-24.12	-2.89	-2.72
3	-2	-1	25.88	24.85	25.73	24.70	2.83	2.71
3	-2	1	82.28	93.30	-81.97	-92.95	-7.11	-8.06
-3	-2	-1	31.93	33.49	-31.89	-33.45	-1.42	-1.49
-3	-2	1	49.22	53.26	-49.04	-53.06	-4.24	-4.59
5	-2	-1	45.50	48.63	-45.06	-48.17	-6.26	-6.69
5	-2	1	29.40	28.11	-29.33	-28.04	2.04	1.95
-5	-2	-1	30.12	29.19	-29.43	-28.52	-6.42	-6.22
-5	-2	1	21.67	19.05	-21.58	-18.98	1.89	1.66
7	-2	-1	11.39	10.55	11.31	10.47	-1.37	-1.26
7	-2	1	53.04	51.85	-52.85	-51.66	-4.46	-4.36
-7	-2	-1	4.43	2.89	2.49	1.62	3.67	2.40
-7	-2	1	48.53	44.94	-47.90	-44.35	-7.82	-7.24
6	-2	-1	19.94	18.03	19.85	17.95	-1.93	-1.74
6	-2	1	31.30	29.80	30.59	29.12	6.62	6.30
-6	-2	-1	53.28	53.02	53.09	52.83	4.47	4.45
-6	-2	1	11.27	10.91	-11.20	-10.85	1.21	1.17
8	-2	-1	82.39	45.39	81.32	44.81	13.19	7.27
8	-2	1	4.44	2.92	-2.40	-1.58	-3.73	-2.46
-8	-2	-1	3.23	3.12	-0.61	-0.59	3.17	3.06
-8	-2	1	27.01	24.11	26.99	24.10	0.93	0.83
9	-2	-1	26.22	24.28	-26.21	-24.27	-0.79	-0.73
9	-2	1	3.48	3.23	-0.77	-0.72	-3.40	-3.15
-0	-2	-1	4.77	2.75	4.08	2.35	-2.48	-1.43
-0	-2	1	25.21	18.99	-23.22	-17.50	9.81	7.39
1	-2	-2	32.26	31.96	31.86	31.56	5.11	5.06
1	-2	2	64.64	64.91	64.33	64.60	6.36	6.38
-1	-2	-2	42.37	39.78	-42.30	-39.72	-2.40	-2.25

-1	-2	2	37.49	38.50	-37.40	-38.40	-2.69	-2.77
4	-2	-2	70.99	82.13	-70.71	-81.80	-6.36	-7.36
4	-2	2	75.76	86.41	-75.46	-86.07	-6.70	-7.64
-4	-2	-2	43.07	43.89	43.07	43.89	-0.15	-0.15
-4	-2	2	49.40	53.58	49.39	53.57	0.93	1.00
2	-2	-2	37.55	37.82	37.45	37.72	2.75	2.77
2	-2	2	45.29	40.66	45.22	40.60	2.60	2.34
-2	-2	-2	33.98	31.38	-33.94	-31.34	-1.69	-1.56
-2	-2	2	52.05	56.40	-51.96	-56.31	-3.05	-3.30
3	-2	-2	53.92	57.54	53.83	57.43	3.21	3.43
3	-2	2	34.74	32.17	34.70	32.13	1.78	1.65
-3	-2	-2	73.47	85.28	73.18	84.93	6.59	7.65
-3	-2	2	71.17	82.31	70.89	81.97	6.39	7.39
5	-2	-2	54.07	54.68	-54.06	-54.66	-1.07	-1.08
5	-2	2	44.62	44.96	-44.62	-44.96	0.03	0.03
-5	-2	-2	28.60	29.01	-28.57	-28.98	-1.34	-1.36
-5	-2	2	13.99	13.30	13.99	13.30	0.03	0.03
7	-2	-2	67.28	66.08	66.86	65.67	7.49	7.36
7	-2	2	56.61	57.57	56.24	57.21	6.39	6.50
-7	-2	-2	26.07	22.49	25.84	22.29	3.50	3.02
-7	-2	2	10.73	8.42	10.45	8.21	2.40	1.88
6	-2	-2	16.74	14.03	-16.74	-14.03	-0.15	-0.12
6	-2	2	29.54	29.32	29.51	29.29	1.34	1.33
-6	-2	-2	54.41	57.13	-54.06	-56.76	-6.13	-6.44
-6	-2	2	64.38	65.81	-63.98	-65.41	-7.14	-7.30
8	-2	-2	9.21	7.42	-8.93	-7.21	-2.22	-1.79
8	-2	2	25.86	22.38	-25.64	-22.19	-3.37	-2.92
-8	-2	-2	23.22	19.90	23.04	19.75	2.84	2.44
-8	-2	2	11.51	8.44	11.23	8.24	2.52	1.85
9	-2	-2	11.76	8.82	-11.50	-8.63	-2.44	-1.83
9	-2	2	23.31	20.82	-23.15	-20.67	-2.78	-2.49
-0	-2	-2	65.70	66.16	-65.39	-65.84	-6.42	-6.47
-0	-2	2	34.59	33.16	-34.17	-32.76	-5.37	-5.15
1	-2	-3	7.90	6.97	-7.33	-6.46	2.95	2.60
1	-2	3	33.14	30.01	-32.50	-29.43	-6.49	-5.88
-1	-2	-3	59.40	60.08	-59.18	-59.86	-5.08	-5.14
-1	-2	3	6.27	3.66	5.42	3.16	-3.15	-1.84
4	-2	-3	46.39	50.87	46.38	50.87	-0.27	-0.29
4	-2	3	3.80	3.56	2.63	2.47	2.74	2.56
-4	-2	-3	8.52	8.76	5.34	5.49	6.64	6.82
-4	-2	3	0.	1.14	-0.	-0.25	-0.	-1.11
2	-2	-3	5.72	3.66	-4.83	-3.08	3.08	1.97
2	-2	3	62.20	58.80	61.97	58.59	5.32	5.03
-2	-2	-3	24.15	21.84	-23.94	-21.65	-3.16	-2.85
-2	-2	3	89.37	100.95	89.11	100.66	6.73	7.60
3	-2	-3	85.78	100.70	-85.53	100.42	-6.47	-7.60
3	-2	3	25.30	22.34	25.08	22.15	3.31	2.93
-3	-2	-3	3.14	2.99	-1.76	-1.68	-2.60	-2.48
-3	-2	3	47.56	50.28	-47.55	-50.28	0.20	0.21
5	-2	-3	0.	1.33	-0.	-0.84	0.	1.03
5	-2	3	8.51	8.40	-5.00	-4.93	-6.89	-6.79
-5	-2	-3	23.69	22.26	-23.66	-22.24	1.12	1.05
-5	-2	3	7.54	8.58	4.47	5.08	-6.08	-6.92
7	-2	-3	27.46	24.24	-27.27	-24.08	-3.21	-2.84
7	-2	3	2.82	1.66	-2.60	-1.53	1.10	0.65

-7	-2	-3	35.96	33.44	-35.33	-32.85	-6.72	-6.25
-7	-2	3	16.61	13.26	16.34	13.05	2.97	2.37
6	-2	-3	7.10	8.73	-4.25	-5.22	5.69	6.99
6	-2	3	24.65	21.35	24.61	21.32	-1.36	-1.18
-6	-2	-3	0.	1.44	0.	1.27	-0.	-0.68
-6	-2	3	27.56	24.94	27.37	24.76	3.23	2.92
8	-2	-3	15.19	11.98	-14.89	-11.74	-3.00	-2.36
8	-2	3	36.03	33.46	35.39	32.86	6.78	6.29
-8	-2	3	4.00	4.45	0.74	0.82	3.93	4.37
9	-2	-3	5.06	4.72	-1.61	-1.51	-4.79	-4.48
-0	-2	-3	32.60	29.66	31.97	29.08	6.38	5.80
-0	-2	3	9.61	7.96	9.08	7.53	-3.12	-2.59
1	-2	-4	3.64	2.41	3.57	2.36	0.68	0.45
1	-2	4	40.73	37.66	-40.66	-37.60	-2.39	-2.21
-1	-2	-4	85.61	93.61	85.43	93.41	5.65	6.17
-1	-2	4	52.09	51.70	51.56	51.18	7.41	7.35
4	-2	-4	42.56	45.14	42.52	45.09	1.95	2.07
4	-2	4	25.71	22.76	25.45	22.53	3.67	3.25
-4	-2	-4	33.48	33.70	-33.33	-33.55	-3.18	-3.20
-4	-2	4	69.65	71.96	-69.40	-71.70	-5.90	-6.10
2	-2	-4	48.61	52.06	-48.12	-51.53	-6.88	-7.37
2	-2	4	89.05	93.84	-88.85	-93.63	-5.91	-6.23
-2	-2	-4	61.65	65.41	-61.55	-65.31	-3.38	-3.59
-2	-2	4	39.22	36.54	39.21	36.53	-0.68	-0.64
3	-2	-4	37.99	37.53	-37.99	-37.53	0.56	0.56
3	-2	4	63.49	65.23	63.40	65.14	3.37	3.47
-3	-2	-4	24.63	22.47	-24.38	-22.24	-3.50	-3.19
-3	-2	4	44.72	44.96	-44.67	-44.91	-2.14	-2.15
5	-2	-4	64.26	73.45	64.03	73.19	5.42	6.19
5	-2	4	36.29	34.42	36.12	34.26	3.45	3.28
-5	-2	-4	33.11	33.67	32.64	33.19	5.56	5.65
-5	-2	4	5.20	4.63	2.91	2.59	4.31	3.84
7	-2	-4	23.96	23.42	-23.80	-23.26	-2.78	-2.71
7	-2	4	35.96	35.10	-35.89	-35.03	-2.22	-2.16
-7	-2	-4	5.93	5.07	-5.93	-5.07	-0.01	-0.01
-7	-2	4	51.07	46.60	50.94	46.48	3.58	3.26
6	-2	-4	4.72	4.59	-2.69	-2.62	-3.87	-3.77
6	-2	4	35.00	33.30	-34.50	-32.83	-5.89	-5.60
-6	-2	-4	35.31	34.56	35.25	34.50	2.09	2.04
-6	-2	4	24.65	22.24	24.47	22.07	3.01	2.71
8	-2	-4	46.45	46.33	-46.33	-46.21	-3.39	-3.38
8	-2	4	6.22	4.67	6.22	4.67	-0.05	-0.04
-8	-2	4	55.65	52.28	-55.30	-51.96	-6.15	-5.77
9	-2	-4	47.56	53.31	47.29	53.00	5.14	5.76
-0	-2	-4	39.59	37.43	39.52	37.36	2.36	2.23
-0	-2	4	2.63	0.48	-1.97	-0.36	-1.74	-0.32
1	-2	-5	10.14	8.16	5.77	4.64	-8.34	-6.71
1	-2	5	9.90	8.52	9.81	8.45	1.29	1.11
-1	-2	-5	8.72	7.22	8.47	7.02	2.06	1.71
-1	-2	5	41.28	40.45	-41.25	-40.42	-1.49	-1.46
4	-2	-5	36.80	36.96	36.46	36.62	5.00	5.02
4	-2	5	20.52	20.19	-20.43	-20.11	1.85	1.82
-4	-2	-5	10.33	9.99	-9.76	-9.44	-3.38	-3.26
-4	-2	5	35.15	32.06	34.80	31.73	4.99	4.55
2	-2	-5	39.36	39.36	39.33	39.34	1.39	1.39

2	-2	5	8.29	7.12	-8.06	-6.92	-1.95	-1.67
-2	-2	-5	24.75	23.68	23.90	22.87	6.42	6.15
-2	-2	5	13.78	12.13	13.35	11.75	-3.41	-3.00
3	-2	-5	14.16	13.66	-13.83	-13.35	3.04	2.93
3	-2	5	25.07	23.93	-24.22	-23.12	-6.48	-6.18
-3	-2	-5	20.11	19.12	20.01	19.02	-2.05	-1.95
-3	-2	5	37.71	36.00	-37.36	-35.66	-5.15	-4.92
5	-2	-5	31.74	30.90	-31.40	-30.57	-4.61	-4.49
5	-2	5	11.01	10.29	10.43	9.74	3.54	3.31
-5	-2	-5	13.65	12.33	-13.03	-11.78	-4.05	-3.66
-5	-2	5	4.59	3.52	2.71	2.08	3.71	2.84
7	-2	-5	18.38	16.93	18.25	16.81	-2.23	-2.06
7	-2	5	47.87	46.95	-47.68	-46.76	-4.28	-4.20
-7	-2	5	29.71	26.31	-28.91	-25.61	-6.85	-6.07
6	-2	-5	5.07	3.54	-3.00	-2.10	-4.08	-2.85
6	-2	5	13.96	12.67	13.34	12.11	4.11	3.73
-6	-2	-5	29.47	47.55	29.35	47.36	2.64	4.27
-6	-2	5	21.00	18.67	-20.88	-18.57	2.18	1.94
8	-2	-5	27.91	26.01	27.14	25.29	6.52	6.08
-0	-2	-5	8.36	7.73	-8.29	-7.66	-1.07	-0.98
-0	-2	5	8.18	7.88	-4.35	-4.19	6.92	6.67
1	-2	-6	6.73	5.70	-6.25	-5.29	2.49	2.11
1	-2	6	70.68	73.92	70.48	73.71	5.37	5.62
-1	-2	-6	16.42	14.42	-16.22	-14.24	-2.54	-2.23
-1	-2	6	55.03	54.22	-54.90	-54.10	-3.65	-3.60
4	-2	-6	48.07	50.32	-47.84	-50.08	-4.72	-4.94
4	-2	6	48.37	50.22	-48.05	-49.89	-5.55	-5.76
-4	-2	-6	3.40	1.80	3.32	1.76	-0.71	-0.38
-4	-2	6	37.59	35.69	37.47	35.58	2.90	2.75
2	-2	-6	53.59	54.79	53.48	54.67	3.46	3.54
2	-2	6	17.41	15.20	17.20	15.02	2.70	2.36
-2	-2	-6	14.25	13.18	14.20	13.14	1.18	1.09
-2	-2	6	34.79	32.10	-34.58	-31.91	-3.76	-3.47
3	-2	-6	31.84	31.70	31.64	31.50	3.61	3.59
3	-2	6	14.35	12.89	-14.30	-12.85	-1.17	-1.05
-3	-2	-6	47.70	49.61	47.38	49.28	5.52	5.74
-3	-2	6	49.28	49.60	49.03	49.35	4.95	4.98
5	-2	-6	35.65	35.17	-35.54	-35.06	-2.81	-2.77
5	-2	6	4.12	2.47	-4.10	-2.46	0.41	0.25
-5	-2	-6	29.58	29.74	-29.42	-29.58	-3.08	-3.10
-5	-2	6	25.51	22.66	25.50	22.66	0.56	0.50
7	-2	-6	37.87	36.37	37.35	35.87	6.27	6.02
6	-2	-6	24.24	22.42	-24.23	-22.41	-0.67	-0.62
6	-2	6	29.61	30.17	29.45	30.01	3.07	3.13
-6	-2	6	40.69	36.87	-40.15	-36.38	-6.62	-6.00
-0	-2	-6	69.52	75.24	-69.32	-75.02	-5.24	-5.68
-0	-2	6	6.44	5.82	5.97	5.40	-2.41	-2.18
-0	-2	8	5.69	4.13	5.67	4.11	-0.43	-0.31
-3	-2	8	3.13	3.76	-2.53	-3.04	-1.84	-2.21
-2	-2	8	29.72	28.58	29.65	28.51	2.09	2.01
2	-2	8	26.96	26.37	-26.78	-26.19	-3.12	-3.05
-1	-2	8	17.42	16.83	16.66	16.10	5.07	4.89
1	-2	8	46.46	50.36	-46.32	-50.21	-3.62	-3.93
1	-2	7	22.74	19.42	-22.51	-19.23	-3.19	-2.73
-1	-2	7	4.92	4.93	4.54	4.56	-1.89	-1.89

4	-2	7	1.27	1.96	1.24	1.92	-0.26	-0.41
-4	-2	7	18.97	17.20	-18.94	-17.17	-1.02	-0.92
2	-2	7	25.18	22.68	24.73	22.27	4.77	4.30
-2	-2	7	30.24	28.66	29.75	28.20	5.38	5.10
3	-2	7	7.92	8.11	7.22	7.40	3.24	3.32
-3	-2	7	3.76	3.78	-2.85	-2.87	2.44	2.46
-5	-2	7	6.51	5.94	-2.29	-2.09	-6.09	-5.56
-0	-2	7	10.84	10.76	10.10	10.03	-3.94	-3.91
-8	-3	-0	20.89	20.17	-20.86	-20.14	-0.96	-0.92
-7	-3	-0	2.07	2.39	2.05	2.37	-0.26	-0.30
-6	-3	-0	5.89	4.85	-5.88	-4.85	-0.35	-0.29
-5	-3	-0	38.03	40.27	38.02	40.26	0.89	0.94
-4	-3	-0	12.40	12.25	-12.40	-12.25	0.06	0.06
-3	-3	-0	35.36	38.63	-35.36	-38.62	-0.16	-0.17
-2	-3	-0	17.25	17.87	17.24	17.86	-0.56	-0.58
-1	-3	-0	3.46	4.25	3.45	4.25	0.10	0.13
-0	-3	-0	3.30	1.17	3.17	1.13	0.92	0.33
1	-3	-0	0.	1.09	0.	1.08	0.	0.09
2	-3	-0	2.95	3.25	2.95	3.25	-0.03	-0.03
3	-3	-0	7.43	1.63	7.31	1.60	-1.30	-0.29
4	-3	-0	32.77	35.89	-32.77	-35.89	0.21	0.23
5	-3	-0	14.80	14.90	14.80	14.90	-0.30	-0.30
6	-3	-0	32.39	34.30	32.39	34.30	0.29	0.31
7	-3	-0	21.44	20.94	-21.43	-20.94	-0.27	-0.26
8	-3	-0	0.	1.19	0.	1.03	0.	0.60
9	-3	-0	16.97	16.90	-16.96	-16.89	-0.54	-0.53
1	-3	-1	7.71	5.90	-7.66	-5.86	-0.92	-0.70
1	-3	1	2.66	0.72	0.20	0.05	2.65	0.72
-1	-3	-1	10.67	10.58	-10.67	-10.58	-0.07	-0.07
-1	-3	1	14.95	14.97	-14.95	-14.97	0.03	0.03
4	-3	-1	31.73	36.75	-31.72	-36.75	0.30	0.35
4	-3	1	14.19	14.74	-14.17	-14.72	-0.66	-0.68
-4	-3	-1	16.81	15.64	16.81	15.64	0.16	0.15
-4	-3	1	26.53	26.61	-26.53	-26.61	0.30	0.30
2	-3	-1	4.65	4.57	4.65	4.57	0.17	0.17
2	-3	1	5.50	6.03	-5.48	-6.02	-0.43	-0.47
-2	-3	-1	13.51	13.50	13.49	13.48	0.78	0.78
-2	-3	1	37.20	45.54	37.19	45.54	-0.44	-0.54
3	-3	-1	31.47	35.46	31.47	35.46	-0.21	-0.24
3	-3	1	12.93	14.10	12.91	14.09	0.55	0.60
-3	-3	-1	25.92	26.51	-25.90	-26.48	-1.10	-1.12
-3	-3	1	2.30	2.85	-2.25	-2.78	0.49	0.61
5	-3	-1	17.90	18.35	-17.90	-18.35	-0.15	-0.16
5	-3	1	26.07	27.83	26.07	27.83	0.67	0.72
-5	-3	-1	15.33	14.34	15.32	14.33	-0.56	-0.52
-5	-3	1	5.84	5.93	5.84	5.93	0.05	0.05
7	-3	-1	2.94	2.47	2.94	2.47	0.01	0.01
7	-3	1	21.39	21.53	-21.38	-21.52	0.68	0.69
-7	-3	-1	13.95	11.89	-13.94	-11.88	-0.64	-0.55
-7	-3	1	22.78	20.79	22.78	20.79	-0.32	-0.29
6	-3	-1	20.80	22.15	20.80	22.15	0.14	0.15
6	-3	1	5.98	5.73	-5.90	-5.66	-0.93	-0.90
-6	-3	-1	9.95	8.81	-9.80	-8.68	1.71	1.51
-6	-3	1	6.64	5.78	-6.59	-5.74	-0.84	-0.73
8	-3	-1	16.54	14.51	16.54	14.51	-0.10	-0.09

8	-3	1	0.	1.70	-0.	-1.56	-0.	-0.67
-8	-3	1	3.82	3.78	-3.77	-3.73	0.56	0.55
9	-3	-1	19.85	18.75	-19.85	-18.75	-0.17	-0.16
9	-3	1	14.55	13.26	14.49	13.21	1.25	1.14
-0	-3	-1	2.08	1.70	-1.95	-1.60	0.72	0.59
-0	-3	1	10.63	9.55	-10.62	-9.54	-0.54	-0.49
1	-3	-2	14.16	12.01	-14.14	-11.99	0.76	0.65
1	-3	2	4.05	4.85	-3.96	-4.74	-0.85	-1.02
-1	-3	-2	21.90	20.01	21.87	19.99	1.10	1.00
-1	-3	2	41.42	43.62	-41.41	-43.61	-0.88	-0.93
4	-3	-2	11.14	11.29	-11.12	-11.27	-0.67	-0.68
4	-3	2	12.34	11.96	-12.28	-11.91	1.16	1.13
-4	-3	-2	4.00	4.77	3.78	4.52	-1.29	-1.54
-4	-3	2	1.42	1.15	1.30	1.05	0.56	0.46
2	-3	-2	14.65	14.89	-14.64	-14.88	-0.63	-0.65
2	-3	2	32.80	31.37	32.78	31.35	1.14	1.09
-2	-3	-2	25.62	17.84	25.61	17.83	-0.67	-0.47
-2	-3	2	35.73	39.60	35.72	39.59	0.99	1.10
3	-3	-2	47.43	54.15	47.42	54.14	0.86	0.98
3	-3	2	2.37	1.93	-2.00	-1.63	-1.27	-1.04
-3	-3	-2	6.68	6.30	-6.51	-6.14	1.51	1.42
-3	-3	2	9.33	8.97	9.32	8.96	-0.39	-0.37
5	-3	-2	7.81	8.29	-7.79	-8.27	0.51	0.54
5	-3	2	6.75	7.34	6.69	7.27	-0.94	-1.02
-5	-3	-2	3.32	2.44	-3.26	-2.40	0.59	0.43
-5	-3	2	9.51	8.80	-9.43	-8.73	-1.22	-1.13
7	-3	-2	6.75	6.60	-6.74	-6.59	0.45	0.44
7	-3	2	14.79	15.26	-14.73	-15.19	-1.35	-1.39
-7	-3	-2	17.67	16.75	17.55	16.64	2.06	1.95
-7	-3	2	6.24	4.99	6.24	4.98	0.15	0.12
6	-3	-2	10.02	9.19	-10.00	-9.18	-0.63	-0.58
6	-3	2	6.56	7.06	-6.46	-6.95	1.12	1.21
-6	-3	-2	22.99	23.95	-22.97	-23.93	-1.05	-1.09
-6	-3	2	17.20	16.19	-17.20	-16.19	0.39	0.37
8	-3	-2	14.52	12.59	14.51	12.58	-0.60	-0.52
8	-3	2	22.49	22.84	22.47	22.82	0.96	0.97
-8	-3	2	11.05	9.91	11.00	9.88	0.98	0.88
9	-3	-2	7.77	7.11	7.76	7.10	0.42	0.38
9	-3	2	1.55	1.06	-0.08	-0.06	-1.55	-1.06
-0	-3	-2	27.32	26.39	-27.29	-26.36	-1.41	-1.36
-0	-3	2	7.26	6.55	-7.22	-6.51	0.74	0.67
1	-3	-3	18.25	16.51	-18.21	-16.48	-1.08	-0.97
1	-3	3	33.64	32.68	33.61	32.66	1.30	1.26
-1	-3	-3	5.20	4.31	4.64	3.85	-2.34	-1.94
-1	-3	3	22.02	21.12	-21.97	-21.07	1.56	1.50
4	-3	-3	20.82	22.48	20.81	22.46	0.84	0.90
4	-3	3	29.67	29.28	-29.63	-29.24	-1.59	-1.57
-4	-3	-3	23.18	25.94	23.11	25.86	1.78	2.00
-4	-3	3	14.16	14.27	-14.09	-14.19	-1.47	-1.48
2	-3	-3	21.15	21.55	-21.09	-21.49	1.52	1.54
2	-3	3	9.58	9.27	-9.46	-9.16	-1.49	-1.44
-2	-3	-3	12.53	11.48	12.45	11.41	1.42	1.30
-2	-3	3	17.23	16.80	-17.20	-16.77	-1.03	-1.00
3	-3	-3	2.68	2.92	2.43	2.65	-1.13	-1.23
3	-3	3	6.90	5.61	-6.68	-5.42	1.75	1.42

-3	-3	-3	28.46	30.54	-28.44	-30.53	-0.79	-0.85
-3	-3	3	17.54	17.36	17.52	17.34	0.91	0.90
5	-3	-3	9.24	9.64	-9.18	-9.58	-1.06	-1.10
5	-3	3	27.93	30.68	27.90	30.64	1.39	1.53
-5	-3	-3	19.29	19.30	-19.20	-19.22	-1.81	-1.82
-5	-3	3	21.74	20.76	21.72	20.73	1.03	0.98
7	-3	-3	19.24	17.78	-19.22	-17.76	-0.96	-0.88
7	-3	3	19.59	18.66	19.51	18.59	1.73	1.65
-7	-3	-3	9.67	7.98	9.48	7.82	-1.94	-1.60
-7	-3	3	10.43	9.27	-10.34	-9.19	1.32	1.17
6	-3	-3	17.11	16.45	17.08	16.42	1.05	1.01
6	-3	3	17.43	17.01	-17.38	-16.96	-1.32	-1.29
-6	-3	-3	21.31	6.19	21.18	6.15	2.30	0.67
-6	-3	3	2.40	0.50	-1.55	-0.32	-1.83	-0.38
8	-3	-3	9.73	8.61	-9.68	-8.57	0.97	0.86
8	-3	3	1.21	2.12	-0.68	-1.19	-1.00	-1.76
9	-3	-3	3.59	2.88	3.51	2.81	-0.77	-0.62
-0	-3	-3	27.37	26.03	27.35	26.00	1.20	1.14
-0	-3	3	6.95	6.75	6.82	6.62	-1.36	-1.32
1	-3	-4	38.63	40.61	38.59	40.56	1.89	1.99
1	-3	4	26.25	24.64	-26.18	-24.59	-1.80	-1.69
-1	-3	-4	13.91	13.13	13.81	13.03	1.70	1.60
-1	-3	4	8.47	7.84	-8.31	-7.68	-1.67	-1.54
4	-3	-4	7.82	8.00	-7.67	-7.85	-1.50	-1.53
4	-3	4	15.62	14.89	15.51	14.79	1.80	1.71
-4	-3	-4	16.39	16.57	16.35	16.53	-1.18	-1.19
-4	-3	4	17.09	16.77	-17.02	-16.70	1.55	1.52
2	-3	-4	27.46	28.43	-27.41	-28.37	-1.71	-1.77
2	-3	4	4.50	4.99	4.21	4.67	1.59	1.77
-2	-3	-4	33.73	33.96	-33.65	-33.88	-2.39	-2.40
-2	-3	4	0.	1.38	-0.	-0.23	0.	1.36
3	-3	-4	4.11	3.80	-3.89	-3.60	1.32	1.22
3	-3	4	27.49	27.12	-27.43	-27.06	-1.75	-1.73
-3	-3	-4	7.58	7.73	-7.44	-7.59	1.44	1.46
-3	-3	4	6.90	6.37	-6.62	-6.11	-1.92	-1.77
5	-3	-4	6.47	7.09	-6.31	-6.91	1.43	1.57
5	-3	4	14.72	14.74	14.59	14.60	-2.00	-2.01
-5	-3	-4	14.82	14.70	14.62	14.49	2.47	2.45
-5	-3	4	7.36	6.69	7.29	6.62	-0.99	-0.90
7	-3	-4	13.69	12.96	13.63	12.90	1.33	1.26
7	-3	4	12.31	11.46	-12.20	-11.36	-1.60	-1.49
-7	-3	4	7.42	6.35	-7.18	-6.14	-1.88	-1.61
6	-3	-4	18.97	19.42	18.93	19.38	-1.22	-1.25
6	-3	4	2.26	2.14	-1.26	-1.20	1.88	1.78
-6	-3	-4	12.27	12.01	-12.11	-11.86	-1.97	-1.93
-6	-3	4	23.45	22.68	23.40	22.64	1.50	1.45
8	-3	-4	18.26	17.60	-18.22	-17.56	-1.21	-1.17
8	-3	4	9.39	10.29	9.21	10.09	1.83	2.01
-0	-3	-4	4.42	4.71	-4.27	-4.55	-1.14	-1.22
-0	-3	4	40.73	41.26	40.69	41.22	1.78	1.80
1	-3	-5	4.90	4.27	4.17	3.63	-2.58	-2.25
1	-3	5	10.63	9.94	-10.41	-9.74	2.13	1.99
-1	-3	-5	15.42	14.29	-15.34	-14.22	-1.48	-1.37
-1	-3	5	6.56	4.94	6.12	4.61	2.36	1.77
4	-3	-5	22.84	23.15	22.75	23.06	2.04	2.07

4	-3	5	5.23	4.26	4.69	3.82	-2.30	-1.88
-4	-3	-5	30.55	31.72	30.51	31.68	1.45	1.51
-4	-3	5	36.29	37.91	-36.26	-37.88	-1.34	-1.40
2	-3	-5	6.85	6.47	6.67	6.30	1.56	1.48
2	-3	5	11.16	9.54	-10.91	-9.33	-2.36	-2.02
-2	-3	-5	3.65	4.34	3.23	3.84	1.70	2.02
-2	-3	5	7.07	6.66	-6.74	-6.35	-2.12	-2.00
3	-3	-5	1.94	1.88	-0.45	-0.43	-1.89	-1.83
3	-3	5	16.96	16.11	16.81	15.97	2.24	2.13
-3	-3	-5	8.53	8.47	-8.09	-8.03	-2.72	-2.70
-3	-3	5	40.70	43.65	40.66	43.61	1.79	1.92
5	-3	-5	44.03	49.17	-44.01	-49.15	-1.42	-1.59
5	-3	5	19.82	18.59	19.71	18.49	2.07	1.95
-5	-3	-5	24.28	26.43	-24.24	-26.39	-1.37	-1.49
-5	-3	5	4.38	3.63	3.87	3.21	2.05	1.70
7	-3	-5	1.08	1.82	-0.44	-0.74	-0.99	-1.66
7	-3	5	12.57	13.91	12.46	13.78	1.69	1.87
6	-3	-5	18.94	19.10	18.88	19.04	1.54	1.56
6	-3	5	36.44	39.97	-36.38	-39.90	-2.11	-2.32
-6	-3	5	14.05	12.69	-13.88	-12.54	-2.18	-1.97
8	-3	-5	22.03	21.94	21.98	21.89	1.47	1.46
-0	-3	-5	2.98	3.68	-2.34	-2.89	1.85	2.28
-0	-3	5	4.00	4.26	-3.56	-3.79	-1.83	-1.95
1	-3	-6	16.17	15.66	16.08	15.57	1.74	1.68
1	-3	6	23.10	23.32	-23.00	-23.22	-2.17	-2.19
-1	-3	-6	24.81	26.14	24.71	26.03	2.27	2.39
-1	-3	6	32.90	32.96	-32.83	-32.89	-2.14	-2.15
4	-3	-6	17.54	18.08	17.44	17.98	-1.83	-1.89
4	-3	6	9.48	9.36	9.18	9.06	2.37	2.33
-4	-3	-6	13.64	14.16	-13.37	-13.88	-2.70	-2.81
-4	-3	6	18.51	18.30	18.41	18.20	1.94	1.92
2	-3	-6	29.83	31.12	-29.77	-31.05	-1.89	-1.97
2	-3	6	30.94	31.51	30.87	31.44	2.04	2.08
-2	-3	-6	0.	1.46	-0.	-0.16	-0.	-1.45
-2	-3	6	17.24	2.47	-8.16	-1.17	15.18	2.18
3	-3	-6	23.41	25.05	23.30	24.93	2.31	2.47
3	-3	6	13.35	12.56	-13.13	-12.35	-2.42	-2.28
-3	-3	-6	16.41	17.20	16.26	17.04	2.24	2.35
-3	-3	6	20.34	16.51	20.22	16.41	-2.24	-1.82
5	-3	-6	0.	2.56	-0.	-1.87	0.	1.75
5	-3	6	16.62	17.05	-16.51	-16.94	-1.85	-1.90
7	-3	-6	2.96	2.91	-2.30	-2.26	1.86	1.83
6	-3	-6	22.60	23.47	-22.52	-23.38	-1.98	-2.06
6	-3	6	3.03	2.53	-1.67	-1.40	2.52	2.11
-0	-3	-6	31.48	32.51	-31.38	-32.41	-2.54	-2.63
-0	-3	6	24.35	23.66	24.26	23.56	2.18	2.12
1	-3	-7	3.30	2.72	-2.27	-1.87	-2.40	-1.97
1	-3	7	16.50	16.60	16.34	16.43	2.35	2.36
-1	-3	-7	5.45	5.78	-4.73	-5.01	-2.71	-2.87
-1	-3	7	12.78	12.52	12.57	12.31	2.33	2.28
4	-3	-7	23.81	25.95	23.75	25.88	1.67	1.82
4	-3	7	14.21	14.08	-13.99	-13.86	-2.46	-2.44
-4	-3	7	2.83	2.88	-1.67	-1.70	-2.28	-2.32
2	-3	-7	2.27	3.35	-1.32	-1.95	1.84	2.72
2	-3	7	11.74	12.48	-11.55	-12.27	-2.13	-2.26

-2	-3	-7	6.21	5.68	5.66	5.18	2.56	2.34
-2	-3	7	33.67	36.35	-33.61	-36.29	-1.97	-2.13
3	-3	-7	27.39	29.83	-27.32	-29.75	-1.97	-2.14
3	-3	7	2.25	3.16	-1.70	-2.39	1.48	2.08
-3	-3	-7	12.62	13.51	-12.55	-13.43	-1.36	-1.46
-3	-3	7	10.03	9.07	9.76	8.83	2.30	2.08
5	-3	-7	1.77	2.66	0.86	1.29	-1.54	-2.32
6	-3	-7	10.67	11.53	10.48	11.32	1.99	2.15
-0	-3	-7	16.73	17.51	16.63	17.41	1.75	1.83
-0	-3	7	5.57	6.73	5.26	6.35	-1.85	-2.23
1	-3	-8	28.14	32.16	28.04	32.04	2.46	2.81
1	-3	8	25.07	26.99	-24.98	-26.90	-2.08	-2.24
-1	-3	8	15.34	15.39	15.17	15.22	-2.29	-2.29
2	-3	-8	2.04	2.33	0.12	0.14	-2.04	-2.32
3	-3	-8	15.41	16.56	-15.32	-16.46	1.67	1.79
-0	-3	-8	11.41	12.13	-11.27	-11.99	-1.73	-1.84
-0	-3	8	16.65	17.69	16.52	17.54	2.10	2.24
-6	-4	-0	29.87	29.04	29.15	28.34	6.51	6.32
-7	-4	-0	22.05	19.59	22.01	19.56	1.32	1.17
-5	-4	-0	31.49	29.38	-31.23	-29.14	-4.02	-3.75
-4	-4	-0	54.99	57.81	-54.94	-57.76	-2.33	-2.44
-3	-4	-0	27.90	27.84	-27.56	-27.49	-4.37	-4.36
-2	-4	-0	44.50	49.31	44.08	48.85	6.09	6.75
-1	-4	-0	18.48	18.47	18.40	18.39	1.69	1.69
-0	-4	-0	14.72	15.29	14.68	15.25	1.13	1.17
1	-4	-0	101.08	166.96	-100.96	166.76	-4.87	-8.04
2	-4	-0	14.20	15.11	14.18	15.08	0.90	0.96
3	-4	-0	17.66	17.77	17.59	17.70	1.58	1.59
4	-4	-0	46.07	50.52	45.64	50.05	6.29	6.90
5	-4	-0	28.07	27.92	-27.75	-27.61	-4.19	-4.17
6	-4	-0	54.07	57.93	-54.02	-57.88	-2.34	-2.51
7	-4	-0	31.44	29.22	-31.15	-28.95	-4.25	-3.95
8	-4	-0	29.52	28.58	28.81	27.89	6.47	6.26
9	-4	-0	21.27	20.29	21.22	20.24	1.42	1.36
1	-4	-1	19.84	16.90	19.68	16.76	2.51	2.14
1	-4	1	22.69	19.47	22.53	19.33	2.73	2.34
-1	-4	-1	3.55	1.32	3.55	1.32	-0.03	-0.01
-1	-4	1	11.00	11.50	9.42	9.85	5.68	5.94
3	-4	-1	13.47	14.34	12.18	12.97	5.75	6.13
3	-4	1	5.40	1.70	-5.35	-1.68	-0.73	-0.23
-3	-4	-1	47.66	50.64	47.18	50.14	6.71	7.13
-3	-4	1	21.93	21.80	21.80	21.67	-2.35	-2.33
4	-4	-1	13.51	13.40	-12.39	-12.29	-5.38	-5.34
4	-4	1	13.42	12.00	-13.39	-11.97	0.90	0.81
-4	-4	-1	54.83	59.32	-54.76	-59.24	-2.81	-3.04
-4	-4	1	27.64	25.83	-27.49	-25.69	-2.90	-2.71
2	-4	-1	11.67	10.50	11.40	10.26	2.48	2.23
2	-4	1	30.86	30.60	-29.85	-29.60	-7.84	-7.78
-2	-4	-1	12.73	11.07	-12.69	-11.03	1.06	0.92
-2	-4	1	15.97	16.97	-15.11	-16.06	-5.17	-5.50
5	-4	-1	19.86	19.91	19.72	19.77	-2.40	-2.41
5	-4	1	47.29	49.96	46.79	49.43	6.85	7.24
-5	-4	-1	15.46	11.64	15.15	11.40	-3.12	-2.35
-5	-4	1	48.94	48.75	48.43	48.23	7.09	7.06
7	-4	-1	49.55	50.35	49.06	49.86	6.93	7.04

7	-4	1	12.58	12.52	12.35	12.29	-2.40	-2.39
-7	-4	-1	14.51	14.68	13.54	13.70	5.21	5.28
-7	-4	1	2.73	3.60	-2.72	-3.59	-0.17	-0.23
6	-4	-1	28.58	28.55	-28.43	-28.40	-2.93	-2.92
6	-4	1	52.96	57.27	-52.90	-57.20	-2.61	-2.82
-6	-4	-1	17.09	14.73	-16.27	-14.02	-5.24	-4.51
-6	-4	1	5.00	4.38	-4.97	-4.35	0.49	0.43
8	-4	-1	3.28	2.86	-3.20	-2.79	0.70	0.61
8	-4	1	18.80	17.25	-18.09	-16.60	-5.11	-4.69
9	-4	-1	3.06	3.45	-3.06	-3.45	-0.10	-0.11
9	-4	1	14.34	13.28	13.21	12.24	5.58	5.17
-0	-4	-1	31.65	30.19	-30.57	-29.16	-8.20	-7.82
-0	-4	1	12.52	11.87	12.28	11.64	2.45	2.32
1	-4	-2	53.44	50.51	53.37	50.44	2.83	2.67
1	-4	2	54.13	51.34	54.05	51.26	2.90	2.75
-1	-4	-2	53.53	53.41	-53.05	-52.93	-7.16	-7.15
-1	-4	2	45.83	48.40	-45.43	-47.98	-6.01	-6.34
3	-4	-2	44.49	48.79	-44.13	-48.39	-5.67	-6.22
3	-4	2	53.40	53.23	-52.93	-52.76	-7.08	-7.05
-3	-4	-2	16.87	16.29	16.87	16.29	0.09	0.09
-3	-4	2	5.15	5.31	4.95	5.10	-1.44	-1.48
4	-4	-2	41.04	44.11	-41.00	-44.06	-1.95	-2.10
4	-4	2	26.83	26.70	-26.80	-26.66	-1.33	-1.32
-4	-4	-2	64.24	71.96	63.93	71.61	6.31	7.07
-4	-4	2	72.95	80.10	72.64	79.76	6.74	7.40
2	-4	-2	74.14	78.99	74.00	78.83	4.68	4.99
2	-4	2	47.21	46.84	47.08	46.72	3.42	3.39
-2	-4	-2	26.40	25.50	-26.38	-25.48	-1.14	-1.10
-2	-4	2	41.01	44.66	-40.97	-44.62	-1.84	-2.01
5	-4	-2	5.28	4.72	4.92	4.40	-1.91	-1.70
5	-4	2	16.27	15.52	16.27	15.52	-0.04	-0.03
-5	-4	-2	14.02	12.75	13.90	12.65	-1.82	-1.65
-5	-4	2	6.11	4.13	6.08	4.11	-0.66	-0.45
7	-4	-2	7.70	5.19	7.69	5.18	-0.39	-0.26
7	-4	2	15.16	13.66	15.08	13.59	-1.57	-1.42
-7	-4	2	44.13	43.10	-43.68	-42.66	-6.33	-6.18
6	-4	-2	69.53	78.78	69.22	78.43	6.55	7.43
6	-4	2	66.97	73.37	66.65	73.02	6.51	7.13
-6	-4	-2	23.04	22.93	-22.94	-22.84	-2.08	-2.07
-6	-4	2	3.70	2.84	-3.40	-2.61	-1.46	-1.12
8	-4	-2	3.51	2.18	-3.11	-1.93	-1.64	-1.02
8	-4	2	25.13	24.54	-25.03	-24.45	-2.15	-2.10
9	-4	-2	38.35	44.27	-37.95	-43.82	-5.49	-6.33
-0	-4	-2	47.53	45.95	47.42	45.84	3.31	3.20
-0	-4	2	72.71	78.04	72.58	77.89	4.45	4.77
1	-4	-3	36.07	34.49	35.87	34.31	3.76	3.59
1	-4	3	33.20	32.22	33.02	32.05	3.45	3.35
-1	-4	-3	8.35	7.78	-7.13	-6.64	4.36	4.06
-1	-4	3	18.44	17.40	18.37	17.33	-1.59	-1.50
3	-4	-3	16.54	14.94	16.44	14.86	-1.78	-1.61
3	-4	3	6.35	5.69	-4.25	-3.81	4.72	4.23
-3	-4	-3	8.32	7.74	8.03	7.47	-2.17	-2.02
-3	-4	3	32.67	32.90	31.86	32.08	7.25	7.30
4	-4	-3	22.45	22.69	-22.44	-22.69	-0.39	-0.40
4	-4	3	11.30	9.99	-9.08	-8.03	-6.72	-5.94

-4	-4	-3	8.24	7.02	-8.20	-6.98	-0.85	-0.72
-4	-4	3	28.93	28.29	-28.90	-28.25	-1.41	-1.38
2	-4	-3	57.41	58.57	-57.03	-58.18	-6.60	-6.73
2	-4	3	4.41	4.11	3.08	2.87	3.15	2.95
-2	-4	-3	13.15	12.16	-11.39	-10.54	-6.57	-6.08
-2	-4	3	21.85	21.51	-21.85	-21.51	-0.18	-0.17
5	-4	-3	32.16	33.58	31.38	32.76	7.06	7.37
5	-4	3	6.59	5.75	6.08	5.30	-2.55	-2.22
-5	-4	-3	30.08	28.61	29.27	27.84	6.92	6.58
-5	-4	3	14.86	12.87	-14.69	-12.73	-2.24	-1.94
7	-4	-3	13.08	11.34	-12.91	-11.19	-2.14	-1.85
7	-4	3	29.75	28.93	28.96	28.16	6.79	6.61
-7	-4	3	5.21	5.94	3.74	4.27	3.62	4.13
6	-4	-3	27.82	28.38	-27.79	-28.36	-1.18	-1.20
6	-4	3	8.86	7.62	-8.81	-7.57	-0.99	-0.85
-6	-4	-3	9.41	9.30	-9.40	-9.29	-0.33	-0.33
-6	-4	3	17.16	13.55	-15.65	-12.35	-7.05	-5.56
8	-4	-3	17.68	14.68	-16.27	-13.51	-6.93	-5.75
8	-4	3	7.91	8.07	-7.91	-8.07	-0.08	-0.08
9	-4	-3	4.19	4.86	2.37	2.74	3.46	4.01
-0	-4	-3	5.04	4.58	3.91	3.56	3.18	2.89
-0	-4	3	56.39	58.54	-56.01	-58.14	-6.56	-6.81
1	-4	-4	83.17	89.25	-82.92	-88.99	-6.36	-6.82
1	-4	4	81.95	90.41	-81.71	-90.15	-6.22	-5.87
-1	-4	-4	20.30	17.76	20.03	17.53	3.28	2.87
-1	-4	4	31.82	31.72	31.80	31.71	1.11	1.11
3	-4	-4	29.19	29.00	29.17	28.99	0.89	0.89
3	-4	4	20.77	19.19	20.53	18.97	3.14	2.90
-3	-4	-4	56.78	63.89	-56.62	-63.71	-4.20	-4.73
-3	-4	4	2.99	2.93	1.88	1.84	-2.33	-2.28
4	-4	-4	26.23	24.81	25.21	23.84	7.25	6.86
4	-4	4	56.09	56.92	55.89	56.72	4.71	4.78
-4	-4	-4	33.12	35.28	-33.02	-35.18	-2.53	-2.69
-4	-4	4	29.45	28.47	-29.33	-28.35	-2.71	-2.62
2	-4	-4	30.16	28.46	-30.14	-28.44	-1.04	-0.98
2	-4	4	10.15	8.64	9.93	8.45	2.11	1.80
-2	-4	-4	53.14	56.83	52.96	56.64	4.33	4.63
-2	-4	4	26.09	23.91	25.03	22.93	7.37	6.75
5	-4	-4	4.14	4.48	3.65	3.95	-1.96	-2.12
5	-4	4	67.57	64.21	-67.40	-64.05	-4.80	-4.56
-5	-4	-4	9.02	8.40	-8.89	-8.27	-1.55	-1.44
-5	-4	4	54.04	54.30	-53.84	-54.11	-4.56	-4.58
7	-4	-4	53.56	55.38	-53.35	-55.17	-4.64	-4.80
7	-4	4	10.24	9.24	-10.09	-9.10	-1.75	-1.58
6	-4	-4	27.45	29.17	-27.35	-29.06	-2.39	-2.54
6	-4	4	34.43	35.29	-34.32	-35.17	-2.81	-2.88
-6	-4	4	36.01	34.13	35.64	33.78	5.17	4.90
8	-4	-4	37.29	35.08	36.94	34.75	5.12	4.81
-0	-4	-4	12.08	9.66	11.80	9.44	2.57	2.06
-0	-4	4	29.00	29.40	-28.99	-29.38	-0.85	-0.87
1	-4	-5	6.23	5.20	6.22	5.19	-0.34	-0.28
1	-4	5	7.19	6.41	7.19	6.41	-0.18	-0.16
-1	-4	-5	12.44	11.13	-12.42	-11.12	0.58	0.52
-1	-4	5	42.24	42.90	41.85	42.51	5.71	5.80
3	-4	-5	43.66	44.03	43.26	43.62	5.90	5.95

3	-4	5	13.87	13.09	-13.86	-13.09	0.27	0.25
-3	-4	-5	12.61	12.23	11.57	11.22	5.03	4.88
-3	-4	5	2.95	3.36	1.15	1.31	-2.72	-3.09
4	-4	-5	20.57	19.41	-20.34	-19.19	-3.09	-2.92
4	-4	5	18.28	17.12	18.06	16.92	2.82	2.65
-4	-4	-5	23.10	23.73	-22.89	-23.51	-3.14	-3.22
-4	-4	5	8.62	7.76	-7.80	-7.01	-3.69	-3.32
2	-4	-5	9.38	8.00	-9.07	-7.73	2.39	2.04
2	-4	5	6.06	6.50	0.03	0.03	-6.06	-6.50
-2	-4	-5	18.61	18.11	18.41	17.92	2.71	2.64
-2	-4	5	22.14	20.92	-21.90	-20.70	-3.24	-3.06
5	-4	-5	2.95	3.94	1.89	2.52	-2.27	-3.03
5	-4	5	13.14	12.43	12.03	11.38	5.29	5.00
-5	-4	5	36.30	35.59	35.88	35.18	5.51	5.40
7	-4	-5	36.31	34.75	35.88	34.34	5.59	5.35
6	-4	-5	11.09	9.96	-10.36	-9.31	-3.95	-3.55
6	-4	5	22.17	21.46	-21.95	-21.25	-3.13	-3.03
8	-4	-5	2.75	12.05	2.71	11.88	0.46	2.01
-0	-4	-5	5.50	6.50	0.02	0.03	-5.50	-6.50
-0	-4	5	8.09	7.29	-7.69	-6.94	2.49	2.24
1	-4	-6	33.45	35.44	33.34	35.31	2.80	2.96
1	-4	6	37.09	36.58	36.95	36.44	3.20	3.15
-1	-4	-6	40.30	42.51	-39.92	-42.11	-5.50	-5.80
-1	-4	6	17.70	15.99	-17.24	-15.57	-4.04	-3.65
3	-4	-6	17.22	16.56	-16.82	-16.18	-3.67	-3.53
3	-4	6	40.42	42.43	-40.04	-42.04	-5.49	-5.76
-3	-4	-6	15.43	15.86	15.28	15.70	2.17	2.23
-3	-4	6	12.48	11.17	-12.30	-11.02	-2.09	-1.87
4	-4	-6	34.50	36.19	-34.36	-36.04	-3.13	-3.28
4	-4	6	3.97	3.76	-3.78	-3.58	-1.22	-1.16
-4	-4	6	42.07	45.14	41.75	44.79	5.20	5.58
2	-4	-6	46.08	48.71	45.86	48.48	4.47	4.72
2	-4	6	6.75	6.85	6.73	6.83	0.53	0.53
-2	-4	-6	2.58	1.72	-2.20	-1.47	-1.34	-0.90
-2	-4	6	35.39	35.71	-35.24	-35.55	-3.29	-3.32
5	-4	-6	11.59	10.59	-11.35	-10.37	-2.31	-2.11
5	-4	6	15.69	16.70	15.55	16.56	2.09	2.22
7	-4	-6	2.25	8.79	2.21	8.63	0.43	1.66
6	-4	-6	39.88	44.73	39.57	44.39	4.96	5.56
-0	-4	-6	5.90	5.90	5.89	5.89	0.41	0.41
-0	-4	6	45.25	47.47	45.04	47.26	4.33	4.54
1	-4	-7	16.88	16.95	16.56	16.63	3.28	3.29
1	-4	7	16.74	15.95	16.42	15.65	3.24	3.09
-1	-4	-7	0.	1.41	-0.	-0.96	0.	1.03
-1	-4	7	2.84	3.82	-1.43	-1.92	-2.46	-3.30
3	-4	-7	3.36	3.86	-1.76	-2.02	-2.86	-3.28
3	-4	7	0.	1.16	0.	0.12	0.	1.15
-3	-4	7	6.58	6.89	4.08	4.27	5.17	5.41
4	-4	-7	0.98	0.85	-0.67	-0.59	-0.71	-0.61
2	-4	-7	33.50	35.27	-33.29	-35.05	-3.70	-3.89
2	-4	7	6.37	6.42	5.16	5.19	3.74	3.77
-2	-4	7	3.15	2.76	3.13	2.74	-0.42	-0.36
5	-4	-7	7.50	7.46	5.15	5.12	5.46	5.43
-0	-4	-7	6.11	5.65	4.70	4.35	3.90	3.61
-0	-4	7	34.67	36.54	-34.46	-36.32	-3.79	-3.99

-6	-5	-0	39.34	39.70	39.33	39.69	1.06	1.06
-5	-5	-0	6.58	2.81	6.53	2.79	0.78	0.33
-4	-5	-0	17.17	16.62	-17.17	-16.62	-0.06	-0.06
-3	-5	-0	29.49	30.23	-29.47	-30.22	-0.90	-0.93
-2	-5	-0	2.06	3.18	2.06	3.18	-0.00	-0.01
-1	-5	-0	41.87	48.67	41.87	48.66	0.39	0.45
-0	-5	-0	2.85	1.82	-2.77	-1.77	0.69	0.44
1	-5	-0	7.16	7.70	-7.16	-7.70	-0.15	-0.17
2	-5	-0	13.86	15.07	-13.85	-15.06	-0.47	-0.51
3	-5	-0	26.94	30.43	-26.94	-30.43	0.07	0.08
4	-5	-0	29.83	31.55	29.83	31.55	0.03	0.03
5	-5	-0	26.78	28.24	26.78	28.24	0.40	0.42
6	-5	-0	7.26	6.56	-7.25	-6.55	-0.40	-0.36
7	-5	-0	18.91	17.19	-18.91	-17.19	0.33	0.30
8	-5	-0	25.22	25.36	-25.22	-25.35	-0.43	-0.43
9	-5	-0	27.03	26.99	27.03	26.98	0.38	0.38
1	-5	-1	23.45	20.25	23.45	20.25	-0.10	-0.09
1	-5	1	12.67	10.70	-12.67	-10.70	-0.12	-0.10
-1	-5	-1	11.01	10.32	10.97	10.28	0.97	0.91
-1	-5	1	12.42	12.14	12.40	12.12	-0.63	-0.62
3	-5	-1	35.05	39.14	-35.04	-39.14	0.61	0.68
3	-5	1	10.35	8.86	10.30	8.81	-1.04	-0.89
-3	-5	-1	2.36	2.03	-2.24	-1.93	0.74	0.64
-3	-5	1	19.59	18.55	19.58	18.55	-0.38	-0.36
4	-5	-1	11.53	12.17	-11.53	-12.17	-0.05	-0.06
4	-5	1	30.01	31.66	30.01	31.65	0.52	0.55
-4	-5	-1	7.03	6.73	6.86	6.57	-1.51	-1.45
-4	-5	1	6.16	7.13	-6.12	-7.08	0.72	0.84
2	-5	-1	13.65	14.31	13.65	14.31	-0.33	-0.35
2	-5	1	14.79	12.63	14.78	12.62	0.56	0.48
-2	-5	-1	33.06	36.08	-33.06	-36.08	0.11	0.11
-2	-5	1	18.11	18.02	18.11	18.01	-0.32	-0.32
5	-5	-1	3.50	3.91	3.50	3.91	0.03	0.03
5	-5	1	22.79	24.43	-22.78	-24.42	-0.55	-0.59
-5	-5	-1	17.06	15.21	17.06	15.21	0.22	0.19
-5	-5	1	30.52	32.49	-30.51	-32.49	0.40	0.42
7	-5	-1	15.88	13.75	15.88	13.75	0.06	0.05
7	-5	1	7.90	6.91	-7.86	-6.87	-0.86	-0.75
6	-5	-1	26.00	26.71	26.00	26.71	-0.28	-0.29
6	-5	1	17.06	15.30	-17.03	-15.28	0.91	0.82
-6	-5	-1	9.00	8.15	9.00	8.15	-0.22	-0.20
-6	-5	1	12.96	14.86	12.96	14.86	-0.27	-0.31
8	-5	-1	33.71	33.24	-33.71	-33.24	0.03	0.03
8	-5	1	16.22	14.61	16.20	14.58	0.95	0.85
9	-5	-1	2.01	1.69	2.01	1.69	-0.04	-0.03
-0	-5	-1	4.46	3.87	4.35	3.77	-0.98	-0.85
-0	-5	1	34.30	36.49	-34.30	-36.48	0.74	0.79
1	-5	-2	4.83	4.54	-4.77	-4.49	-0.74	-0.70
1	-5	2	45.97	45.04	45.95	45.02	1.15	1.12
-1	-5	-2	22.47	20.58	-22.41	-20.52	-1.65	-1.51
-1	-5	2	18.39	18.06	-18.38	-18.05	0.33	0.32
3	-5	-2	8.52	8.07	-8.50	-8.05	-0.62	-0.58
3	-5	2	7.96	6.96	-7.87	-6.88	1.19	1.04
-3	-5	-2	22.64	23.96	22.64	23.96	-0.20	-0.21
-3	-5	2	28.85	29.01	28.82	28.98	1.28	1.29

4	-5	-2	12.04	12.54	-12.04	-12.54	0.37	0.39
4	-5	2	8.99	21.74	-8.97	-21.70	-0.50	-1.22
-4	-5	-2	11.77	12.76	11.71	12.70	1.17	1.26
-4	-5	2	15.75	16.72	15.75	16.72	-0.24	-0.25
2	-5	2	26.47	24.15	26.46	24.14	-0.73	-0.67
-2	-5	-2	5.24	4.23	4.99	4.03	1.58	1.27
-2	-5	2	13.83	13.55	-13.81	-13.53	-0.71	-0.70
5	-5	-2	29.58	31.99	-29.57	-31.98	-0.80	-0.86
5	-5	2	26.27	15.65	-26.21	-15.61	1.72	1.02
-5	-5	-2	12.89	14.17	-12.78	-14.05	-1.68	-1.84
-5	-5	2	12.39	11.96	-12.39	-11.96	0.06	0.06
7	-5	-2	22.29	21.26	22.29	21.25	-0.34	-0.33
7	-5	2	19.63	18.47	19.59	18.44	1.19	1.12
6	-5	-2	7.52	6.86	7.50	6.83	0.66	0.60
6	-5	2	6.83	5.86	6.70	5.75	-1.31	-1.12
-6	-5	-2	12.74	12.67	-12.73	-12.66	0.39	0.39
-6	-5	2	13.81	12.65	-13.75	-12.60	-1.28	-1.17
8	-5	-2	3.89	3.45	3.86	3.42	0.53	0.47
8	-5	2	3.00	4.80	2.91	4.66	-0.71	-1.14
9	-5	-2	0.	0.96	0.	0.89	-0.	-0.36
-0	-5	-2	35.27	32.62	-35.26	-32.61	0.39	0.36
-0	-5	2	42.63	44.44	-42.61	-44.43	-1.10	-1.15
1	-5	-3	33.22	32.57	-33.16	-32.52	1.90	1.87
1	-5	3	30.46	28.08	30.41	28.04	-1.71	-1.57
-1	-5	-3	34.63	34.44	34.62	34.43	0.82	0.82
-1	-5	3	17.08	15.84	-17.04	-15.81	-1.14	-1.06
3	-5	-3	32.38	32.15	32.37	32.14	0.71	0.70
3	-5	3	43.68	41.03	-43.67	-41.01	-1.29	-1.21
-3	-5	-3	23.05	21.61	22.99	21.56	1.61	1.51
-3	-5	3	15.50	15.02	-15.47	-15.00	-0.92	-0.89
4	-5	-3	6.13	5.84	5.96	5.67	-1.44	-1.37
4	-5	3	15.83	16.34	15.77	16.27	1.43	1.47
-4	-5	-3	23.97	24.69	-23.96	-24.69	-0.50	-0.52
-4	-5	3	16.94	15.70	16.94	15.69	0.53	0.49
2	-5	-3	4.15	3.08	3.86	2.87	-1.53	-1.13
2	-5	3	17.05	15.71	-16.98	-15.64	1.56	1.43
-2	-5	-3	3.17	3.77	-2.64	-3.14	-1.75	-2.09
-2	-5	3	13.04	11.85	-12.91	-11.74	1.82	1.65
5	-5	-3	2.92	2.56	-2.59	-2.27	1.35	1.18
5	-5	3	4.18	3.82	-3.85	-3.51	-1.63	-1.48
-5	-5	-3	2.64	2.08	-1.26	-0.99	2.32	1.83
-5	-5	3	4.11	3.77	-3.79	-3.47	-1.60	-1.46
7	-5	-3	6.52	6.22	6.45	6.15	0.96	0.92
7	-5	3	14.39	15.03	-14.32	-14.95	-1.46	-1.53
6	-5	-3	21.71	22.02	-21.70	-22.01	-0.67	-0.68
6	-5	3	33.12	34.21	33.09	34.18	1.42	1.47
-6	-5	3	18.14	16.41	18.10	16.37	1.20	1.09
8	-5	-3	6.91	5.88	-6.83	-5.81	-1.08	-0.92
8	-5	3	6.59	6.21	-6.43	-6.06	1.42	1.34
-0	-5	-3	21.40	18.57	-21.37	-18.55	-1.11	-0.96
-0	-5	3	27.76	27.41	27.74	27.39	0.95	0.94
1	-5	-4	32.44	31.60	-32.40	-31.56	-1.71	-1.67
1	-5	4	6.60	5.95	6.40	5.76	1.63	1.47
-1	-5	-4	16.81	16.89	16.77	16.85	-1.13	-1.13
-1	-5	4	21.27	32.34	21.23	32.28	1.27	1.93

3	-5	-4	23.72	22.17	-23.64	-22.10	-1.88	-1.76
3	-5	4	18.84	16.15	18.73	16.06	2.00	1.71
-3	-5	-4	25.43	28.81	-25.33	-28.70	-2.24	-2.54
-3	-5	4	17.53	17.37	-17.50	-17.34	0.95	0.94
4	-5	-4	19.27	18.86	19.18	18.78	1.78	1.75
4	-5	4	21.01	19.99	20.94	19.92	-1.76	-1.67
-4	-5	-4	6.28	7.00	-6.11	-6.82	1.44	1.60
-4	-5	4	9.93	9.32	-9.76	-9.16	-1.82	-1.71
2	-5	-4	8.59	8.25	-8.53	-8.19	1.00	0.96
2	-5	4	48.37	48.69	-48.33	-48.65	-1.86	-1.87
-2	-5	-4	5.74	6.33	-5.62	-6.20	1.14	1.25
-2	-5	4	5.91	5.68	5.72	5.49	-1.51	-1.45
5	-5	-4	20.06	19.47	20.03	19.45	-1.06	-1.02
5	-5	4	15.85	17.02	15.77	16.93	1.64	1.76
-5	-5	4	2.51	2.45	-1.89	-1.84	1.65	1.61
7	-5	-4	2.76	5.68	-2.66	-5.49	-0.71	-1.47
7	-5	4	15.88	16.23	-15.78	-16.12	1.80	1.84
6	-5	-4	8.12	2.10	-6.43	-1.66	4.96	1.28
6	-5	4	13.37	13.26	-13.27	-13.16	-1.70	-1.69
8	-5	-4	10.98	10.75	-10.93	-10.70	1.08	1.06
-0	-5	-4	46.37	45.65	46.32	45.59	2.32	2.29
-0	-5	4	5.87	3.68	-5.41	-3.39	-2.26	-1.42
1	-5	-5	7.81	6.30	7.67	6.19	1.45	1.17
1	-5	5	10.30	8.60	-10.09	-8.42	-2.09	-1.75
-1	-5	-5	2.60	2.61	-0.58	-0.58	2.53	2.54
-1	-5	5	19.13	19.86	-19.05	-19.77	-1.82	-1.88
3	-5	-5	2.40	2.67	1.30	1.44	2.03	2.25
3	-5	5	21.40	20.81	21.29	20.71	-2.10	-2.04
-3	-5	-5	14.12	15.54	14.04	15.45	1.49	1.64
-3	-5	5	8.49	7.77	-8.23	-7.53	-2.08	-1.90
4	-5	-5	28.83	29.62	-28.80	-29.59	-1.31	-1.34
4	-5	5	23.56	22.63	23.48	22.54	2.02	1.94
-4	-5	5	25.17	25.21	25.09	25.13	2.01	2.01
2	-5	-5	0.	2.12	0.	0.69	-0.	-2.00
2	-5	5	0.	1.96	-0.	-0.55	0.	1.88
-2	-5	-5	34.37	37.92	-34.35	-37.90	-1.10	-1.21
-2	-5	5	28.68	28.15	28.64	28.12	1.39	1.37
5	-5	-5	16.04	15.53	15.96	15.45	1.58	1.53
5	-5	5	34.13	38.54	-34.08	-38.49	-1.78	-2.01
7	-5	-5	33.22	34.53	33.19	34.50	1.39	1.45
6	-5	-5	12.45	12.19	-12.28	-12.03	-2.00	-1.96
6	-5	5	0.	2.07	-0.	-0.83	0.	1.90
-0	-5	-5	16.34	15.47	16.18	15.32	-2.26	-2.14
-0	-5	5	7.52	6.89	-7.16	-6.55	2.31	2.11
1	-5	-6	22.35	22.96	-22.25	-22.87	-2.03	-2.09
1	-5	6	31.05	33.08	30.98	33.00	2.07	2.20
-1	-5	-6	30.85	35.74	-30.77	-35.65	-2.18	-2.52
-1	-5	6	3.22	2.55	-2.35	-1.86	2.19	1.74
3	-5	-6	0.	1.63	0.	0.08	-0.	-1.63
3	-5	6	19.75	20.92	19.65	20.81	2.01	2.13
-3	-5	6	6.10	5.71	5.60	5.24	2.43	2.27
4	-5	-6	8.49	8.44	8.32	8.27	1.68	1.67
4	-5	6	30.33	32.72	-30.27	-32.65	-1.93	-2.09
2	-5	-6	32.67	34.14	32.57	34.03	2.53	2.64
2	-5	6	11.09	10.31	-10.88	-10.11	-2.17	-2.01

-2	-5	-6	15.15	17.01	14.97	16.81	2.34	2.62
-2	-5	6	21.11	21.38	-21.02	-21.29	-2.02	-2.04
5	-5	-6	21.14	22.02	-21.03	-21.90	-2.25	-2.34
6	-5	-6	11.14	13.04	-11.03	-12.91	1.55	1.81
-0	-5	-6	5.50	5.57	5.34	5.41	1.31	1.32
-0	-5	6	17.18	17.43	-17.05	-17.30	-2.13	-2.16
1	-5	-7	4.31	4.69	-3.40	-3.70	2.66	2.89
1	-5	7	4.24	5.35	-3.84	-4.84	-1.80	-2.27
-1	-5	7	7.95	7.04	-7.58	-6.72	-2.39	-2.12
3	-5	-7	17.11	18.15	17.04	18.07	1.58	1.68
2	-5	-7	16.02	18.58	-15.94	-18.49	-1.60	-1.86
2	-5	7	6.25	7.68	-5.98	-7.35	1.79	2.21
-0	-5	7	25.46	27.38	25.39	27.30	1.87	2.01
-5	-6	-0	25.01	24.74	-24.94	-24.67	-1.87	-1.85
-4	-6	-0	5.22	6.19	-2.67	-3.17	-4.49	-5.32
-3	-6	-0	26.79	24.73	26.22	24.20	5.47	5.05
-2	-6	-0	24.03	23.76	23.92	23.66	2.22	2.19
-1	-6	-0	19.37	19.84	19.18	19.65	2.68	2.74
-0	-6	-0	49.82	63.86	-49.50	-63.44	-5.66	-7.26
1	-6	-0	14.74	17.31	14.73	17.30	-0.45	-0.53
2	-6	-0	18.13	20.32	-18.12	-20.32	0.25	0.28
3	-6	-0	51.73	65.64	51.40	65.23	5.81	7.37
4	-6	-0	18.28	18.70	-18.13	-18.54	-2.38	-2.43
5	-6	-0	22.72	24.07	-22.63	-23.97	-2.04	-2.16
6	-6	-0	27.96	27.19	-27.42	-26.67	-5.47	-5.32
7	-6	-0	8.81	5.64	3.68	2.36	8.01	5.13
8	-6	-0	27.21	26.13	27.13	26.05	2.12	2.04
1	-6	-1	27.57	25.81	27.54	25.78	1.27	1.18
1	-6	1	8.46	8.27	-4.94	-4.83	-6.87	-6.72
-1	-6	-1	61.26	73.33	-60.95	-72.96	-6.15	-7.36
-1	-6	1	13.27	13.17	13.04	12.94	2.46	2.44
3	-6	-1	28.40	31.41	-28.22	-31.21	-3.25	-3.60
3	-6	1	8.81	8.08	8.78	8.05	-0.75	-0.68
-3	-6	-1	0.	2.03	-0.	-0.99	0.	1.78
-3	-6	1	34.72	32.48	-34.08	-31.88	-6.66	-6.23
4	-6	-1	12.52	12.50	-12.28	-12.27	-2.43	-2.43
4	-6	1	59.99	72.74	59.68	72.36	6.11	7.41
-4	-6	-1	29.40	29.43	28.86	28.88	5.63	5.63
-4	-6	1	11.28	9.76	11.16	9.66	-1.63	-1.41
2	-6	-1	8.56	8.02	4.37	4.09	7.36	6.89
2	-6	1	30.46	28.01	-30.42	-27.98	-1.55	-1.42
-2	-6	-1	20.39	20.40	20.33	20.34	1.51	1.51
-2	-6	1	29.95	29.53	29.66	29.24	4.18	4.13
5	-6	-1	29.91	32.32	-29.62	-32.01	-4.10	-4.43
5	-6	1	18.78	19.27	-18.74	-19.23	-1.15	-1.18
-5	-6	-1	44.23	44.92	-44.04	-44.73	-4.10	-4.17
-5	-6	1	6.57	5.75	-6.47	-5.66	-1.17	-1.03
7	-6	-1	9.31	7.75	-9.11	-7.58	1.94	1.62
7	-6	1	31.98	29.70	-31.35	-29.11	-6.31	-5.86
6	-6	-1	32.50	31.35	31.88	30.75	6.32	6.09
6	-6	1	0.	2.31	0.	1.55	-0.	-1.72
8	-6	-1	9.26	7.79	9.13	7.68	1.52	1.28
8	-6	1	43.04	42.96	42.86	42.78	3.93	3.92
-0	-6	-1	8.90	7.34	-8.89	-7.33	0.53	0.44
-0	-6	1	33.44	35.16	33.23	34.95	3.69	3.88

1	-6	-2	54.30	53.21	53.95	52.87	6.13	6.01
1	-6	2	22.59	19.33	21.88	18.73	5.62	4.81
-1	-6	-2	9.38	8.44	9.26	8.32	1.53	1.38
-1	-6	2	25.48	25.15	25.31	24.98	2.98	2.94
3	-6	-2	27.71	28.42	-27.60	-28.31	-2.43	-2.49
3	-6	2	4.60	4.08	-3.90	-3.45	-2.44	-2.16
-3	-6	-2	14.14	13.00	-14.14	-12.99	0.31	0.29
-3	-6	2	23.99	21.63	-23.97	-21.62	-0.90	-0.81
4	-6	-2	24.62	26.19	-24.42	-25.99	-3.08	-3.27
4	-6	2	15.02	11.20	-14.86	-11.09	-2.18	-1.62
-4	-6	-2	9.02	8.94	8.93	8.86	1.24	1.23
-4	-6	2	2.32	2.80	2.32	2.80	0.01	0.02
2	-6	-2	21.97	18.83	-21.31	-18.26	-5.33	-4.57
2	-6	2	52.66	49.98	-52.30	-49.64	-6.09	-5.78
-2	-6	-2	36.24	37.46	-35.60	-36.80	-6.79	-7.01
-2	-6	2	49.81	55.00	-49.42	-54.58	-6.16	-6.80
5	-6	-2	45.77	55.27	45.43	54.86	5.57	6.72
5	-6	2	34.76	38.27	34.18	37.62	6.36	7.00
-5	-6	2	38.44	37.72	37.84	37.13	6.77	6.65
7	-6	-2	0.	1.84	-0.	-1.83	0.	0.23
7	-6	2	8.56	8.35	-8.48	-8.27	-1.18	-1.15
6	-6	-2	23.50	22.60	23.48	22.58	1.06	1.02
6	-6	2	17.51	15.90	17.50	15.90	0.06	0.05
8	-6	-2	36.00	37.07	-35.39	-36.44	-6.59	-6.79
-0	-6	-2	3.55	3.74	3.03	3.19	1.85	1.94
-0	-6	2	29.65	28.65	29.53	28.55	2.56	2.48
1	-6	-3	19.66	16.76	-18.67	-15.92	-6.17	-5.26
1	-6	3	5.54	5.20	-4.97	-4.66	2.46	2.31
-1	-6	-3	22.95	22.10	22.80	21.96	2.60	2.50
-1	-6	3	57.89	63.37	-57.54	-62.98	-6.36	-6.97
3	-6	-3	16.51	15.24	-16.38	-15.12	-2.11	-1.94
3	-6	3	25.86	23.57	-25.38	-23.13	-4.97	-4.53
-3	-6	-3	18.54	18.95	-17.49	-17.88	-6.14	-6.27
-3	-6	3	3.26	2.59	-2.98	-2.37	1.33	1.06
4	-6	-3	54.69	63.50	54.36	63.11	5.99	6.96
4	-6	3	25.27	24.40	-25.11	-24.25	-2.79	-2.70
-4	-6	-3	2.11	1.65	-1.83	-1.44	-1.04	-0.82
-4	-6	3	24.77	21.99	23.74	21.08	7.07	6.27
2	-6	-3	3.48	3.46	2.55	2.54	-2.36	-2.35
2	-6	3	21.55	18.98	20.64	18.18	6.19	5.46
-2	-6	-3	16.28	15.74	16.12	15.58	2.29	2.21
-2	-6	3	13.43	13.11	13.42	13.11	-0.09	-0.09
5	-6	-3	11.46	12.42	-11.46	-12.41	0.28	0.30
5	-6	3	17.98	17.01	-17.79	-16.83	-2.59	-2.45
7	-6	-3	24.83	23.50	-23.87	-22.59	-6.84	-6.47
7	-6	3	3.46	3.75	3.29	3.57	1.07	1.16
6	-6	-3	4.35	3.90	4.25	3.81	-0.91	-0.82
6	-6	3	19.56	18.75	18.47	17.70	6.46	6.20
-0	-6	-3	27.39	25.85	26.92	25.39	5.10	4.81
-0	-6	3	14.77	13.38	14.66	13.28	1.76	1.59
1	-6	-4	20.93	13.78	-20.70	-13.63	-3.08	-2.02
1	-6	4	12.50	11.46	-12.49	-11.46	0.22	0.20
-1	-6	-4	41.59	45.27	41.47	45.14	3.13	3.40
-1	-6	4	7.56	6.51	-7.51	-6.47	0.79	0.68
3	-6	-4	23.67	23.83	22.69	22.84	6.72	6.77

3	-6	4	63.01	65.49	62.76	65.23	5.54	5.76
-3	-6	-4	14.71	14.77	14.43	14.49	2.86	2.87
-3	-6	4	33.78	31.77	33.27	31.29	5.86	5.51
4	-6	-4	8.34	7.83	8.32	7.82	-0.50	-0.47
4	-6	4	42.30	45.08	-42.20	-44.98	-2.89	-3.08
-4	-6	4	5.41	4.88	-3.66	-3.30	-3.98	-3.59
2	-6	-4	8.94	8.12	8.92	8.10	-0.62	-0.56
2	-6	4	16.93	15.14	16.78	15.01	2.19	1.96
-2	-6	-4	15.01	15.01	14.75	14.75	2.83	2.83
-2	-6	4	23.01	22.64	22.92	22.55	2.04	2.00
5	-6	-4	20.05	21.13	-19.98	-21.05	-1.69	-1.78
5	-6	4	15.40	15.14	-15.10	-14.84	-3.04	-2.99
7	-6	-4	2.58	3.70	1.01	1.45	2.37	3.40
6	-6	-4	33.34	33.99	-32.85	-33.50	-5.65	-5.76
6	-6	4	17.00	16.16	-16.69	-15.86	-3.25	-3.09
-0	-6	-4	58.88	65.53	-58.66	-65.29	-5.04	-5.61
-0	-6	4	24.92	24.40	-23.96	-23.46	-6.86	-6.72
1	-6	-5	3.68	2.94	3.56	2.84	0.95	0.76
1	-6	5	25.29	23.84	-24.45	-23.05	-6.44	-6.07
-1	-6	-5	18.30	18.98	-17.49	-18.14	-5.39	-5.59
-1	-6	5	10.52	9.97	10.10	9.57	2.93	2.78
3	-6	-5	19.16	19.36	-19.12	-19.32	-1.21	-1.22
3	-6	5	19.90	20.22	19.85	20.16	1.45	1.47
-3	-6	5	33.58	33.11	-33.31	-32.84	-4.28	-4.22
4	-6	-5	9.40	8.41	-8.94	-8.00	-2.89	-2.58
4	-6	5	18.83	19.32	17.99	18.46	5.55	5.69
2	-6	-5	24.29	24.28	23.49	23.49	6.18	6.18
2	-6	5	4.52	4.05	-4.34	-3.89	-1.24	-1.11
-2	-6	-5	7.26	6.96	-6.98	-6.69	2.00	1.91
-2	-6	5	35.32	36.33	35.06	36.06	4.29	4.41
5	-6	-5	35.94	37.75	-35.66	-37.45	-4.48	-4.70
5	-6	5	9.53	9.63	9.40	9.50	-1.55	-1.57
6	-6	-5	32.17	32.36	31.91	32.10	4.05	4.07
-0	-6	-5	20.69	21.33	-20.64	-21.28	-1.51	-1.56
-0	-6	5	20.40	20.78	20.35	20.74	1.40	1.43
1	-6	-6	30.76	36.74	30.44	36.36	4.39	5.24
1	-6	6	5.67	4.99	-5.16	-4.54	2.36	2.07
-1	-6	6	20.91	21.28	20.69	21.06	3.02	3.08
3	-6	-6	22.44	24.06	-22.25	-23.85	-2.94	-3.15
3	-6	6	4.65	5.66	-4.27	-5.19	-1.85	-2.24
4	-6	-6	21.84	22.27	-21.59	-22.01	-3.34	-3.40
2	-6	-6	6.33	6.11	6.02	5.81	-1.95	-1.88
2	-6	6	32.43	34.45	-32.08	-34.07	-4.79	-5.08
-0	-6	-6	2.55	3.06	1.99	2.40	1.58	1.90
-0	-6	6	23.34	23.82	23.12	23.59	3.25	3.32
-3	-7	-0	2.16	1.59	2.12	1.57	-0.37	-0.27
-2	-7	-0	31.04	30.89	31.03	30.89	0.40	0.40
-1	-7	-0	6.61	5.75	6.54	5.69	0.93	0.81
-0	-7	-0	4.61	0.25	-4.25	-0.23	-1.79	-0.10
1	-7	-0	20.45	25.66	-20.44	-25.65	-0.53	-0.67
2	-7	-0	10.44	10.50	-10.44	-10.50	-0.23	-0.23
3	-7	-0	17.21	18.15	17.21	18.15	0.21	0.22
4	-7	-0	13.12	13.12	13.10	13.10	0.62	0.62
5	-7	-0	16.81	16.42	16.80	16.42	-0.28	-0.27
6	-7	-0	21.67	20.10	-21.67	-20.10	-0.03	-0.02

7	-7	-0	24.32	24.33	-24.31	-24.33	-0.48	-0.48
1	-7	-1	5.61	4.38	-5.56	-4.33	-0.79	-0.62
1	-7	1	7.23	7.16	-7.21	-7.14	0.55	0.54
-1	-7	-1	0.	0.77	-0.	-0.05	-0.	-0.77
-1	-7	1	24.71	25.52	-24.71	-25.52	0.65	0.67
3	-7	-1	0.	0.97	-0.	-0.96	0.	0.17
3	-7	1	23.62	22.19	23.62	22.19	0.23	0.22
-3	-7	-1	19.78	17.81	-19.78	-17.81	0.16	0.14
-3	-7	1	19.78	19.34	19.77	19.34	-0.53	-0.52
4	-7	-1	13.92	15.03	-13.92	-15.03	0.07	0.07
4	-7	1	18.71	19.50	-18.70	-19.50	-0.40	-0.42
2	-7	-1	17.22	15.38	-17.19	-15.36	0.99	0.88
2	-7	1	14.71	13.02	14.67	12.98	-1.13	-1.00
-2	-7	-1	5.80	4.87	5.60	4.70	1.50	1.26
-2	-7	1	0.	1.01	-0.	-0.56	-0.	-0.83
5	-7	-1	23.09	23.84	23.08	23.83	-0.60	-0.62
5	-7	1	3.68	6.34	-3.64	-6.27	0.58	1.00
7	-7	-1	12.11	11.99	-12.10	-11.99	0.17	0.17
7	-7	1	14.22	13.15	14.21	13.14	0.59	0.55
6	-7	-1	16.35	15.66	16.35	15.66	0.01	0.01
6	-7	1	19.20	16.15	-19.19	-16.14	-0.76	-0.64
-0	-7	-1	28.41	27.85	28.41	27.85	-0.32	-0.31
-0	-7	1	0.	0.83	0.	0.79	0.	0.27
1	-7	-2	33.51	31.34	33.48	31.31	1.62	1.51
1	-7	2	9.81	9.43	9.80	9.43	-0.31	-0.30
-1	-7	-2	26.79	27.71	-26.79	-27.71	0.06	0.07
-1	-7	2	24.42	25.13	-24.38	-25.09	-1.29	-1.33
3	-7	-2	3.91	3.18	3.88	3.16	0.46	0.37
3	-7	2	28.83	27.13	-28.80	-27.10	-1.37	-1.29
-3	-7	-2	5.99	4.64	5.63	4.36	2.05	1.59
-3	-7	2	9.40	8.44	-9.39	-8.43	-0.34	-0.31
4	-7	-2	34.80	37.74	-34.78	-37.72	-1.10	-1.19
4	-7	2	20.54	19.18	-20.52	-19.17	0.74	0.69
2	-7	-2	5.23	4.60	5.22	4.59	-0.37	-0.33
2	-7	2	19.05	17.02	19.01	16.99	1.23	1.10
-2	-7	-2	9.49	9.49	-9.38	-9.38	-1.42	-1.42
-2	-7	2	13.58	13.57	-13.58	-13.56	0.13	0.13
5	-7	-2	0.	0.75	0.	0.50	0.	0.56
5	-7	2	9.00	9.08	8.94	9.03	-0.97	-0.98
7	-7	-2	18.64	18.30	18.63	18.28	0.71	0.70
6	-7	-2	6.88	7.89	6.88	7.89	-0.13	-0.15
6	-7	2	12.20	11.53	12.12	11.46	1.37	1.29
-0	-7	-2	3.99	2.14	-3.61	-1.94	-1.70	-0.92
-0	-7	2	26.63	26.48	26.62	26.46	0.95	0.95
1	-7	-3	15.34	15.25	-15.31	-15.23	-0.85	-0.84
1	-7	3	11.16	10.36	-11.09	-10.28	1.32	1.22
-1	-7	-3	17.36	16.67	-17.32	-16.63	-1.16	-1.11
-1	-7	3	22.10	21.76	22.08	21.74	0.77	0.76
3	-7	-3	20.26	21.36	20.20	21.30	-1.59	-1.67
3	-7	3	2.06	2.54	1.63	2.02	1.25	1.54
4	-7	-3	4.60	3.19	4.29	2.97	1.65	1.14
4	-7	3	0.	1.73	0.	0.82	-0.	-1.53
2	-7	-3	9.48	8.54	9.45	8.52	0.69	0.62
2	-7	3	21.06	20.08	-21.04	-20.06	-0.90	-0.85
-2	-7	-3	19.17	20.79	19.17	20.79	0.41	0.45

-2	-7	3	5.86	7.08	-5.84	-7.05	-0.54	-0.65
5	-7	-3	19.05	20.89	-19.05	-20.88	-0.42	-0.46
5	-7	3	26.92	28.81	26.90	28.78	1.06	1.14
6	-7	-3	4.30	3.47	-4.07	-3.28	1.38	1.12
-0	-7	-3	5.57	5.50	-5.16	-5.10	2.09	2.06
-0	-7	3	15.01	14.80	14.91	14.70	-1.74	-1.72
1	-7	-4	3.99	1.54	3.40	1.31	2.09	0.81
1	-7	4	35.92	35.98	-35.86	-35.92	-1.99	-2.00
-1	-7	-4	23.74	25.58	23.63	25.46	2.30	2.47
-1	-7	4	3.97	4.46	3.87	4.35	-0.89	-1.00
3	-7	-4	15.39	17.08	15.31	16.99	1.53	1.70
3	-7	4	2.28	1.85	1.56	1.26	-1.66	-1.35
4	-7	-4	17.59	18.66	17.58	18.65	-0.71	-0.75
4	-7	4	20.66	21.49	20.58	21.41	1.78	1.85
2	-7	-4	37.99	39.92	-37.94	-39.86	-1.94	-2.04
2	-7	4	25.46	24.02	25.41	23.97	1.57	1.48
-2	-7	4	22.31	22.16	22.22	22.08	1.92	1.91
5	-7	-4	15.88	14.54	15.80	14.46	1.57	1.44
-0	-7	-4	5.09	5.87	-4.96	-5.72	-1.17	-1.34
-0	-7	4	10.53	9.47	-10.43	-9.38	1.46	1.31
1	-7	5	11.48	12.26	11.37	12.13	1.64	1.75
3	-7	-5	15.27	16.15	-15.24	-16.12	-0.96	-1.01
2	-7	-5	3.78	4.51	-3.30	-3.94	1.84	2.20
2	-7	5	13.57	13.92	13.40	13.76	-2.10	-2.15
-1	-8	-0	21.13	21.52	-20.33	-20.70	-5.76	-5.86
-0	-8	-0	5.45	4.09	5.09	3.82	-1.95	-1.46
1	-8	-0	13.48	15.60	-13.45	-15.55	-1.01	-1.17
2	-8	-0	50.05	64.88	49.75	64.50	5.44	7.05
3	-8	-0	11.55	14.08	-11.53	-14.06	-0.65	-0.80
4	-8	-0	6.01	5.68	5.86	5.54	-1.35	-1.28
5	-8	-0	23.24	23.81	-22.46	-23.01	-5.97	-6.12
1	-8	-1	36.40	34.04	35.65	33.34	7.36	6.88
1	-8	1	22.10	22.28	-22.01	-22.19	-1.99	-2.00
-1	-8	-1	4.74	3.89	-4.64	-3.80	-0.97	-0.80
-1	-8	1	20.34	21.13	19.78	20.55	4.72	4.91
3	-8	-1	20.01	21.37	-19.94	-21.29	-1.73	-1.84
3	-8	1	35.66	34.43	34.95	33.75	7.04	6.80
4	-8	-1	18.29	19.37	-17.55	-18.58	-5.16	-5.47
4	-8	1	12.77	12.90	12.77	12.90	0.24	0.24
2	-8	-1	10.02	8.50	-9.79	-8.30	-2.16	-1.83
2	-8	1	12.61	10.30	-12.32	-10.07	-2.57	-2.18
5	-8	-1	17.31	17.68	16.70	17.06	4.54	4.63
5	-8	1	4.06	3.76	-4.01	-3.71	-0.65	-0.60
-0	-8	-1	10.19	10.03	10.19	10.03	-0.14	-0.14
-0	-8	1	17.67	17.52	-16.89	-16.75	-5.19	-5.15
1	-8	-2	23.33	20.11	-23.10	-19.92	-3.20	-2.76
1	-8	2	36.69	36.93	-36.46	-36.70	-4.09	-4.11
3	-8	-2	38.12	39.27	-37.87	-39.01	-4.36	-4.49
3	-8	2	24.50	21.91	-24.26	-21.69	-3.45	-3.09
4	-8	-2	24.35	26.91	23.85	26.36	4.90	5.42
4	-8	2	25.80	26.92	25.12	26.21	5.89	6.15
2	-8	-2	16.99	13.88	-16.77	-13.69	-2.74	-2.24
2	-8	2	17.60	14.67	-17.37	-14.47	-2.85	-2.37
-0	-8	-2	26.80	27.74	26.10	27.01	6.10	5.31
-0	-8	2	26.57	26.56	25.97	25.96	5.63	5.63

1	-8	3	37.38	39.78	36.95	39.32	5.65	6.01
3	-8	-3	35.20	38.98	34.79	38.54	5.30	5.87
2	-8	-3	22.97	22.60	-22.73	-22.36	-3.33	-3.28
2	-8	3	21.11	20.46	-20.90	-20.26	-2.95	-2.86

Pectolite structure factors

The FCAL's for pectolite were computed in the same way as for wollastonite except that the coordinates and temperature factors of Chapter IV were used together with a single overall scale factor.

H	K	L	FOBS	FCAL	AOBS	ACAL	BOBS	BCAL
1	0	0	12.43	11.46	11.90	10.98	3.58	3.31
0	0	1	16.49	16.44	16.11	16.06	3.50	3.49
1	0	-1	22.45	20.74	22.40	20.69	-1.57	-1.45
1	0	1	7.11	5.58	-0.47	-0.37	7.09	5.57
2	0	0	40.57	43.46	-40.54	-43.42	-1.56	-1.67
2	0	-1	5.21	5.27	-0.96	-0.97	-5.12	-5.18
0	0	2	44.90	49.64	-44.89	-49.63	-1.11	-1.22
1	0	-2	60.32	81.00	-60.20	-80.84	-3.79	-5.09
2	0	1	58.74	71.20	58.68	71.13	2.55	3.09
1	0	2	72.67	98.65	72.62	98.58	2.68	3.63
2	0	-2	55.67	69.32	-55.53	-69.15	-3.84	-4.78
3	0	0	62.72	76.68	-62.58	-76.51	-4.26	-5.21
3	0	-1	13.00	9.42	11.32	8.20	-6.40	-4.64
2	0	2	16.63	17.28	15.77	16.39	5.27	5.48
3	0	1	25.01	23.09	24.93	23.02	-2.02	-1.86
0	0	3	40.91	39.43	-40.59	-39.12	-5.13	-4.94
1	0	-3	71.65	95.14	-71.56	-95.01	-3.66	-4.86
3	0	-2	51.37	54.13	51.37	54.13	-0.55	-0.58
1	0	3	7.88	8.08	-7.82	-8.02	-0.96	-0.98
2	0	-3	34.35	33.67	-34.34	-33.66	-0.82	-0.81
3	0	2	42.69	41.66	-42.59	-41.57	2.91	2.84
4	0	0	31.79	28.67	-31.40	-28.32	-4.93	-4.45
2	0	3	23.41	20.39	-23.01	-20.04	4.29	3.73
4	0	-1	42.23	41.26	-42.22	-41.26	-0.36	-0.35
4	0	1	50.17	50.22	-49.90	-49.95	-5.18	-5.18
3	0	-3	4.66	4.50	2.39	2.30	4.01	3.86
4	0	-2	25.53	24.15	25.18	23.82	4.23	4.00
0	0	4	73.96	84.89	-73.84	-84.75	-4.26	-4.89
1	0	-4	27.05	24.82	27.02	24.80	-1.11	-1.02
1	0	4	51.21	51.76	-50.99	-51.55	-4.70	-4.75
3	0	3	52.93	55.08	52.68	54.82	5.12	5.33
2	0	-4	51.45	52.71	51.32	52.58	3.59	3.68
4	0	2	12.23	11.30	-12.03	-11.12	-2.19	-2.03
4	0	-3	60.12	65.31	59.93	65.10	4.89	5.31
5	0	-1	40.44	39.89	40.23	39.68	4.15	4.10
5	0	0	41.36	40.85	41.36	40.85	-0.12	-0.12
2	0	4	19.09	18.67	-19.07	-18.66	-0.75	-0.74
3	0	-4	19.11	19.22	18.36	18.46	5.30	5.33
5	0	1	87.12	104.71	-87.05	104.63	-3.51	-4.22
5	0	-2	49.69	49.28	49.41	49.01	5.27	5.22
4	0	3	41.18	40.51	41.10	40.43	2.61	2.57
1	0	-5	2.75	4.41	1.70	2.74	2.15	3.46
0	0	5	26.14	24.52	-26.11	-24.49	-1.30	-1.22
3	0	4	68.66	78.32	68.58	78.23	3.32	3.78
5	0	2	67.08	73.94	-66.92	-73.76	-4.62	-5.10
4	0	-4	44.42	44.61	-44.34	-44.53	2.61	2.63
2	0	-5	17.50	15.46	16.44	14.52	6.00	5.30
1	0	5	24.92	23.53	24.38	23.03	-5.15	-4.87
5	0	-3	60.44	65.43	60.40	65.39	2.24	2.42
6	0	-1	68.48	72.25	68.31	72.07	4.82	5.08
6	0	0	12.18	12.34	11.47	11.63	4.08	4.14
3	0	-5	52.30	55.50	52.24	55.43	2.64	2.80
2	0	5	5.58	5.76	3.48	3.58	-4.37	-4.50
6	0	-2	7.59	7.79	7.28	7.48	2.14	2.19

6	0	1	24.33	22.83	-24.33	-22.83	0.11	0.10
4	0	4	38.77	38.71	38.43	38.37	5.13	5.12
5	0	3	12.42	12.64	-12.23	-12.46	-2.12	-2.16
5	0	-4	30.23	29.83	-30.15	-29.75	-2.17	-2.14
4	0	-5	13.79	13.95	13.65	13.81	-1.91	-1.94
3	0	5	20.88	19.36	-20.88	-19.36	-0.54	-0.50
6	0	-3	43.69	44.42	-43.63	-44.36	-2.28	-2.32
6	0	2	38.78	38.82	38.58	38.62	-3.94	-3.95
1	0	-6	52.34	52.54	52.08	52.28	5.19	5.21
0	0	6	59.90	65.28	59.83	65.20	2.94	3.21
2	0	-6	42.45	44.61	42.36	44.51	2.80	2.94
1	0	6	18.93	18.90	-18.88	-18.85	-1.39	-1.39
7	0	-1	6.67	6.63	6.37	6.34	1.96	1.95
5	0	4	28.17	28.61	28.08	28.52	2.25	2.29
7	0	0	9.72	8.42	7.92	6.86	5.65	4.89
3	0	-6	56.66	61.25	-56.64	-61.22	-1.59	-1.71
5	0	-5	63.06	71.66	-62.91	-71.48	-4.39	-4.99
6	0	-4	11.64	13.55	10.81	12.58	-4.32	-5.02
2	0	6	54.70	58.02	-54.52	-57.82	-4.51	-4.79
6	0	3	33.59	30.74	-33.15	-30.34	-5.42	-4.96
7	0	-2	20.31	20.55	20.16	20.40	-2.44	-2.46
4	0	5	12.05	12.19	11.45	11.59	3.74	3.79
7	0	1	45.07	44.46	44.88	44.26	4.19	4.13
4	0	-6	4.97	5.42	-2.12	-2.31	-4.49	-4.90
7	0	-3	47.43	47.84	-47.17	-47.58	-4.96	-5.00
7	0	2	17.30	17.12	-17.30	-17.12	0.31	0.30
3	0	6	27.30	25.95	-26.94	-25.60	-4.45	-4.22
1	0	-7	8.69	6.37	7.64	5.60	4.15	3.04
0	0	7	28.71	28.76	28.26	28.31	5.05	5.06
6	0	-5	46.67	45.86	-46.49	-45.69	-3.99	-3.92
6	0	4	32.35	32.13	-32.27	-32.05	-2.27	-2.26
5	0	5	34.67	32.80	34.29	32.43	5.15	4.87
2	0	-7	27.93	28.95	27.90	28.91	-1.43	-1.48
7	0	-4	27.81	27.22	-27.55	-26.96	-3.84	-3.76
1	0	7	2.29	3.02	0.53	0.70	2.23	2.93
5	0	-6	18.92	17.27	-18.40	-16.79	-4.44	-4.05
8	0	-1	29.28	27.97	-29.16	-27.85	-2.70	-2.58
8	0	0	19.26	18.34	-19.18	-18.26	1.78	1.70
7	0	3	32.83	31.88	-32.61	-31.68	-3.76	-3.65
3	0	-7	26.83	25.31	-26.35	-24.86	-5.05	-4.76
4	0	6	17.92	16.31	17.91	16.31	-0.30	-0.27
8	0	-2	17.51	17.86	-16.83	-17.17	-4.82	-4.92
8	0	1	35.03	35.01	34.72	34.70	4.55	4.65
2	0	7	4.66	3.40	4.15	3.03	-2.11	-1.54
8	0	-3	14.28	12.44	-13.68	-11.92	-4.08	-3.55
4	0	-7	33.33	34.52	-33.09	-34.28	-3.98	-4.13
8	0	2	11.44	10.14	10.47	9.28	4.60	4.08
7	0	5	9.51	6.77	8.94	6.37	-3.25	-2.32
6	0	6	4.82	4.88	-1.66	-1.68	4.52	4.58
6	0	5	23.94	23.09	23.85	23.00	2.07	2.00
3	0	7	17.14	15.78	-16.38	-15.08	-5.05	-4.65
7	0	4	5.40	7.18	-4.04	-5.38	-3.58	-4.77
5	0	6	39.54	40.23	39.37	40.06	3.68	3.74
8	0	-4	10.04	7.86	10.03	7.85	0.58	0.46
5	0	-7	5.81	5.37	5.81	5.37	-0.17	-0.16

1	0	-8	26.66	26.79	-26.63	-26.76	-1.23	-1.24
0	0	8	16.45	17.57	16.20	17.30	2.90	3.10
2	0	-8	33.96	35.87	-33.68	-35.58	-4.33	-4.57
8	0	3	22.30	22.05	22.30	22.05	0.49	0.49
9	0	-1	34.96	32.11	-34.57	-31.75	-2.21	-4.79
9	0	0	8.54	7.59	8.00	7.11	-2.98	-2.65
1	0	8	17.43	17.15	16.71	16.44	4.94	4.86
9	0	-2	21.41	20.62	-21.13	-20.35	-3.44	-3.31
4	0	7	40.07	41.69	-39.89	-41.50	-3.76	-3.91
3	0	-8	10.88	11.12	10.09	10.31	-4.07	-4.16
9	0	1	16.73	16.00	16.66	15.94	1.50	1.44
7	0	-6	4.61	4.82	2.64	2.76	-3.78	3.95
2	0	8	29.58	30.80	29.48	30.69	2.54	2.65
8	0	-5	45.41	46.35	45.24	46.18	3.96	4.04
9	0	-3	30.63	30.92	30.62	30.92	0.64	0.64
7	0	5	6.64	6.77	6.24	6.37	-2.27	-2.32
6	0	-7	37.13	36.47	36.93	36.27	3.90	3.83
6	0	6	4.43	4.88	-1.53	-1.68	4.16	4.58
4	0	-8	6.32	8.18	-6.31	-8.17	-0.28	-0.36
0	1	0	3.52	2.96	-3.52	-2.95	0.11	0.10
-1	1	0	8.67	7.34	-8.67	-7.34	0.04	0.03
0	1	-1	3.46	2.97	-3.46	-2.97	-0.04	-0.03
0	1	1	3.12	1.63	3.08	1.60	0.49	0.26
1	1	0	15.03	13.69	15.03	13.69	-0.13	-0.12
-1	1	1	14.75	13.70	-14.75	-13.70	0.08	0.08
-1	1	-1	9.66	8.77	9.66	8.77	-0.03	-0.03
1	1	-1	28.10	26.99	28.10	26.99	-0.25	-0.24
1	1	1	11.32	9.97	-11.31	-9.97	0.23	0.20
-2	1	0	19.35	19.34	19.35	19.34	-0.08	-0.08
-2	1	1	36.29	36.26	36.29	36.26	0.01	0.01
-2	1	-1	12.89	12.12	-12.89	-12.12	-0.21	-0.19
0	1	-2	57.16	64.83	-57.16	-64.83	-0.02	-0.02
2	1	0	32.62	32.43	-32.62	-32.43	-0.46	-0.46
0	1	2	50.62	55.95	50.62	55.95	0.22	0.24
-1	1	2	52.73	57.30	-52.73	-57.30	-0.03	-0.03
-1	1	-2	31.20	31.29	31.20	31.29	0.04	0.04
2	1	-1	26.31	24.47	-26.31	-24.47	-0.34	-0.31
1	1	-2	27.31	25.66	27.31	25.66	-0.15	-0.14
2	1	1	2.28	1.43	2.25	1.42	-0.36	-0.22
1	1	2	10.86	10.46	-10.85	-10.45	0.49	0.47
-2	1	2	4.30	3.78	-4.30	-3.78	-0.04	-0.04
-3	1	0	39.53	41.55	-39.53	-41.55	0.06	0.06
-3	1	1	11.27	11.14	11.27	11.14	0.17	0.16
-2	1	-2	19.03	19.00	-19.03	-19.00	-0.16	-0.16
2	1	-2	12.88	11.58	12.88	11.58	-0.01	-0.01
-3	1	-1	2.39	1.27	2.36	1.26	-0.39	-0.21
3	1	0	44.52	43.12	44.52	43.12	-0.49	-0.47
0	1	-3	26.15	24.15	26.15	24.15	0.05	0.05
2	1	2	31.82	30.22	31.82	30.22	0.30	0.28
3	1	-1	30.12	28.30	-30.12	-28.30	0.01	0.00
-1	1	3	14.89	13.00	14.88	13.00	-0.26	-0.23
0	1	3	15.27	14.45	-15.27	-14.45	-0.05	-0.04
-3	1	2	5.17	4.35	5.17	4.35	0.11	0.09
1	1	-3	10.46	9.27	10.46	9.27	-0.01	-0.01
-1	1	-3	1.77	1.39	-1.76	-1.38	0.24	0.19

3	1	1	5.77	5.03	-5.72	-4.99	-0.77	-0.67
-2	1	3	28.93	27.47	28.93	27.47	-0.11	-0.11
1	1	3	8.39	6.12	-8.37	-6.11	0.56	0.41
-3	1	-2	30.47	30.12	30.47	30.11	-0.42	-0.41
3	1	-2	10.18	8.92	10.17	8.92	0.41	0.36
-4	1	0	45.08	45.64	45.08	45.64	0.36	0.37
-4	1	1	27.48	25.58	-27.48	-25.58	0.31	0.29
2	1	-3	35.87	34.10	-35.87	-34.10	0.19	0.18
-2	1	-3	1.53	0.48	-1.51	-0.47	0.28	0.09
-4	1	-1	7.16	6.94	7.16	6.94	0.13	0.13
3	1	2	40.47	41.05	-40.47	-41.05	-0.33	-0.34
-3	1	3	31.62	30.27	-31.62	-30.27	0.01	0.01
-4	1	2	13.97	12.30	13.97	12.30	0.05	0.05
2	1	3	2.78	2.06	-2.63	-1.95	0.91	0.68
4	1	0	35.40	33.30	-35.40	-33.30	0.04	0.04
4	1	-1	26.31	25.10	26.31	25.09	0.57	0.54
0	1	-4	9.26	8.89	9.26	8.89	0.01	0.01
3	1	-3	7.83	6.77	7.82	6.76	0.42	0.36
-1	1	4	2.65	1.54	-2.59	-1.51	-0.54	-0.31
0	1	4	32.68	31.61	-32.68	-31.60	-0.42	-0.40
1	1	-4	4.09	4.31	-4.09	-4.31	0.01	0.01
4	1	1	15.83	14.59	-15.82	-14.58	-0.67	-0.61
-3	1	-3	13.49	12.66	-13.49	-12.66	-0.32	-0.30
-4	1	-2	33.84	33.30	-33.83	-33.29	-0.33	-0.32
-1	1	-4	33.68	32.41	-33.68	-32.41	0.25	0.24
4	1	-2	5.36	4.96	5.33	4.93	0.62	0.57
-2	1	4	8.16	7.56	-8.16	-7.56	-0.05	-0.05
1	1	4	35.01	33.79	35.01	33.79	-0.04	-0.04
-5	1	0	15.04	13.29	-15.03	-13.28	0.53	0.46
2	1	-4	20.79	18.85	20.79	18.85	0.17	0.15
-5	1	1	3.68	3.44	-3.68	-3.44	0.07	0.07
-4	1	3	15.75	14.79	-15.75	-14.79	-0.12	-0.11
3	1	3	9.03	8.17	9.02	8.16	0.38	0.35
-2	1	-4	21.81	21.46	21.80	21.46	0.39	0.38
4	1	2	13.49	11.97	13.46	11.94	-0.99	-0.88
-5	1	-1	9.47	8.63	-9.44	-8.61	0.63	0.57
-3	1	4	26.37	24.84	26.37	24.84	0.03	0.03
-5	1	2	13.09	12.25	13.09	12.25	-0.28	-0.26
4	1	-3	16.50	15.71	16.50	15.71	0.21	0.20
2	1	4	12.86	11.30	12.84	11.29	0.66	0.58
3	1	-4	18.24	16.68	-18.24	-16.68	0.14	0.13
-4	1	-3	13.58	13.42	-13.56	-13.40	-0.63	-0.62
5	1	0	21.31	19.58	21.29	19.57	0.80	0.73
5	1	-1	19.83	18.80	19.82	18.78	0.80	0.76
-5	1	-2	14.29	13.66	14.29	13.66	0.22	0.21
-3	1	-4	18.66	16.81	18.66	16.81	0.13	0.12
5	1	1	18.78	17.39	18.78	17.39	0.09	0.09
5	1	-2	21.45	20.33	-21.45	-20.33	0.27	0.26
0	1	-5	15.85	14.47	15.85	14.47	-0.16	-0.15
-1	1	5	13.54	12.33	13.54	12.33	-0.13	-0.12
-4	1	4	29.27	27.72	-29.27	-27.72	-0.10	-0.09
-5	1	3	15.95	15.08	15.94	15.08	-0.32	-0.31
1	1	-5	10.22	9.50	-10.22	-9.50	-0.07	-0.06
0	1	5	8.64	7.71	-8.62	-7.69	-0.58	-0.52
4	1	3	17.68	17.24	17.68	17.23	-0.47	-0.46

-1	1	-5	1.53	0.55	-1.53	-0.55	0.14	0.05
-2	1	5	8.97	9.00	-8.97	-9.00	0.16	0.16
3	1	4	13.85	12.70	-13.81	-12.67	0.94	0.86
-6	1	0	23.93	22.58	23.93	22.58	0.07	0.07
-6	1	1	13.25	12.39	13.24	12.38	-0.45	-0.42
2	1	-5	1.76	0.37	-1.76	-0.37	0.18	0.04
1	1	5	3.18	3.15	-3.12	-3.10	-0.56	-0.56
4	1	-4	27.44	25.69	27.44	25.69	-0.22	-0.20
5	1	2	13.97	12.71	-13.95	-12.69	-0.80	-0.73
5	1	-3	8.26	8.05	-8.25	-8.04	-0.34	-0.33
-6	1	-1	10.52	10.81	10.51	10.79	0.61	0.62
-3	1	5	2.78	0.63	2.73	0.62	0.54	0.12
-2	1	-5	1.62	1.49	-1.55	-1.43	0.46	0.43
-6	1	2	28.02	27.20	-28.01	-27.20	-0.53	-0.51
-5	1	-3	16.03	15.53	16.03	15.53	-0.43	-0.41
-4	1	-4	20.29	20.19	-20.29	-20.19	-0.45	-0.45
3	1	-5	2.25	2.21	-2.24	-2.21	-0.09	-0.09
2	1	5	1.85	0.04	-1.57	-0.03	-0.97	-0.02
-5	1	4	19.00	17.99	19.00	17.99	-0.14	-0.13
6	1	-1	4.77	4.79	-4.76	-4.78	0.29	0.29
6	1	0	18.69	16.75	-18.66	-16.73	1.04	0.93
-6	1	-2	5.27	3.90	5.17	3.82	1.04	0.77
-6	1	3	1.30	1.89	-1.29	-1.87	-0.16	-0.23
-4	1	5	7.67	7.21	7.67	7.21	-0.01	-0.01
-3	1	-5	4.53	4.75	4.50	4.71	0.53	0.55
6	1	-2	9.59	6.63	9.56	6.62	-0.67	-0.46
4	1	4	13.02	11.89	13.01	11.88	0.43	0.39
6	1	1	0.	0.98	-0.	-0.36	0.	0.91
5	1	3	21.25	20.24	-21.23	-20.21	-1.12	-1.06
5	1	-4	33.96	34.17	-33.96	-34.17	-0.55	-0.56
0	1	-6	23.63	23.54	23.63	23.54	-0.27	-0.27
-1	1	6	31.60	31.35	31.60	31.34	0.27	0.26
1	1	-6	18.68	17.85	-18.68	-17.85	-0.07	-0.07
4	1	-5	4.41	3.00	4.38	2.98	-0.50	-0.34
3	1	5	2.32	3.04	-2.25	-2.95	0.57	0.75
0	1	6	26.16	26.50	-26.16	-26.50	-0.20	-0.20
-2	1	6	2.61	0.55	2.07	0.44	1.58	0.33
-7	1	1	2.69	2.34	-2.57	-2.23	-0.82	-0.71
-7	1	0	32.56	31.13	-32.56	-31.13	-0.61	-0.59
-1	1	-6	29.21	28.31	-29.21	-28.31	-0.29	-0.28
6	1	-3	3.32	1.64	-2.94	-1.45	-1.55	-0.76
-5	1	-4	9.09	8.02	9.04	7.98	-0.91	-0.81
2	1	-6	6.70	5.06	-6.70	-5.06	0.00	0.00
6	1	2	4.34	3.03	-4.33	-3.03	0.21	0.15
1	1	6	10.01	11.24	9.99	11.21	-0.63	-0.71
-7	1	2	4.84	2.90	4.81	2.88	-0.53	-0.32
-6	1	-3	5.96	5.38	-5.95	-5.37	0.33	0.30
-6	1	4	22.75	22.84	-22.75	-22.84	0.12	0.12
-7	1	-1	3.29	3.05	-3.29	-3.05	0.06	0.05
-5	1	5	12.40	12.60	12.40	12.60	0.04	0.04
-3	1	6	20.38	19.42	-20.38	-19.42	0.12	0.12
-4	1	-5	6.94	7.48	-6.94	-7.48	0.12	0.13
-2	1	-6	15.80	15.57	15.80	15.57	0.10	0.10
3	1	-6	19.49	18.23	19.49	18.23	-0.14	-0.13
5	1	4	22.12	21.17	-22.11	-21.16	-0.61	-0.58

7	1	-1	6.39	5.73	-6.36	-5.70	-0.67	-0.60
2	1	6	15.35	15.01	-15.34	-15.00	-0.71	-0.69
7	1	0	25.00	24.21	25.00	24.21	0.31	0.30
-7	1	3	3.12	0.35	-2.47	-0.28	1.89	0.21
5	1	-5	16.71	15.01	-16.71	-15.01	-0.39	-0.35
-7	1	-2	4.09	4.59	-4.03	-4.53	0.67	0.76
6	1	-4	15.29	14.12	15.28	14.11	-0.52	-0.48
4	1	5	17.29	17.52	17.26	17.49	1.01	1.02
-4	1	6	12.61	11.63	12.61	11.63	-0.02	-0.02
6	1	3	4.03	3.76	-3.93	-3.67	-0.88	-0.82
7	1	-2	9.98	7.35	-9.90	-7.28	-1.31	-0.96
7	1	1	7.06	6.60	6.97	6.51	1.16	1.08
-3	1	-6	4.03	0.97	3.14	0.76	2.52	0.61
4	1	-6	14.98	14.34	-14.98	-14.34	-0.22	-0.21
-6	1	-4	21.75	21.52	-21.75	-21.52	-0.49	-0.48
-6	1	5	23.89	22.63	-23.89	-22.63	0.28	0.27
-5	1	-5	3.12	2.98	3.06	2.92	-0.63	-0.60
7	1	-3	5.15	5.74	-5.13	-5.71	-0.53	-0.59
3	1	6	7.74	7.40	7.74	7.40	0.02	0.02
-8	1	1	0.81	0.51	0.54	0.34	-0.60	-0.38
-7	1	4	21.64	21.63	21.64	21.63	0.47	0.47
0	1	-7	8.13	8.40	8.13	8.39	-0.17	-0.18
1	1	-7	1.39	2.18	-1.38	-2.18	0.05	0.08
-1	1	7	4.86	5.10	4.84	5.07	0.50	0.53
-8	1	0	2.99	2.93	2.85	2.80	-0.90	-0.89
7	1	2	22.86	22.37	22.83	22.35	1.11	1.08
-7	1	-3	7.93	8.13	7.87	8.07	0.92	0.95
0	1	7	14.78	14.86	-14.78	-14.85	0.35	0.35
-2	1	7	5.29	4.08	5.28	4.07	0.33	0.26
-5	1	6	6.36	6.57	-6.36	-6.57	0.07	0.07
-8	1	2	1.66	0.47	1.24	0.35	1.10	0.31
-1	1	-7	10.67	10.49	-10.66	-10.48	-0.48	-0.47
2	1	-7	1.47	0.58	-1.46	-0.58	0.17	0.07
-8	1	-1	1.63	1.22	1.29	0.96	-1.01	-0.75
-4	1	-6	14.90	14.70	14.88	14.69	0.71	0.70
6	1	-5	17.29	16.42	17.29	16.42	0.08	0.07
1	1	7	2.86	2.59	2.84	2.57	-0.33	-0.30
5	1	5	5.23	4.61	5.21	4.59	0.46	0.41
6	1	4	14.28	13.76	14.22	13.71	-1.28	-1.23
-3	1	7	4.29	4.21	4.29	4.21	-0.06	-0.06
5	1	-6	15.86	15.40	15.86	15.40	0.03	0.03
-2	1	-7	2.76	0.59	-2.07	-0.44	-1.82	-0.39
3	1	-7	8.20	8.48	8.20	8.48	-0.05	-0.05
7	1	-4	8.03	7.59	-8.03	-7.59	0.14	0.13
-8	1	3	2.31	2.80	-2.24	-2.72	0.55	0.67
8	1	-1	10.56	11.00	-10.50	-10.94	-1.10	-1.14
4	1	6	8.93	8.67	-8.88	-8.62	0.93	0.90
8	1	0	5.24	4.48	-5.17	-4.42	-0.87	-0.74
7	1	3	3.28	3.27	-3.27	-3.26	0.22	0.22
-8	1	-2	13.62	13.26	13.62	13.26	0.02	0.02
2	1	7	2.25	2.51	-2.11	-2.35	-0.80	-0.89
-4	1	7	13.34	13.27	13.34	13.27	-0.12	-0.12
8	1	-2	9.59	8.15	9.56	8.12	-0.80	-0.68
-7	1	5	3.80	1.96	3.75	1.93	0.66	0.34
-6	1	-5	2.58	0.98	-0.26	-0.10	-2.57	-0.97

-6	1	6	24.28	25.12	24.28	25.12	0.17	0.18
-7	1	-4	18.40	18.23	18.39	18.22	0.40	0.40
8	1	1	4.45	4.63	-4.44	-4.63	0.29	0.30
-3	1	-7	3.57	3.48	-3.57	-3.48	0.17	0.17
4	1	-7	21.94	21.72	-21.94	-21.72	0.00	0.00
-5	1	-6	17.18	17.82	-17.18	-17.82	0.12	0.12
-8	1	4	3.64	3.41	3.60	3.37	0.52	0.49
8	1	-3	2.27	1.67	2.25	1.65	0.28	0.20
6	1	-6	16.91	17.07	-16.90	-17.07	0.44	0.45
7	1	-5	7.93	8.41	7.90	8.39	0.59	0.63
3	1	7	3.75	2.89	3.61	2.77	-1.04	-0.80
-8	1	-3	4.03	3.56	3.91	3.46	0.98	0.86
-9	1	1	2.70	2.40	-2.66	-2.36	0.48	0.42
-5	1	7	23.80	24.28	-23.80	-24.28	0.01	0.01
8	1	2	6.65	5.90	-6.51	-5.77	1.36	1.20
6	1	5	11.15	10.74	-11.13	-10.72	-0.73	-0.71
-9	1	0	2.31	1.09	-2.13	-1.00	-0.89	-0.42
-9	1	2	25.34	24.02	25.33	24.00	0.90	0.85
1	1	-8	6.49	8.49	6.49	8.49	0.20	0.26
0	1	-8	12.95	14.04	-12.95	-14.04	0.12	0.13
-1	1	8	8.60	9.75	-8.59	-9.74	0.35	0.40
7	1	4	16.87	16.34	-16.84	-16.32	-0.91	-0.88
5	1	6	21.50	22.09	21.47	22.06	1.12	1.15
-2	1	8	1.85	0.57	1.83	0.57	-0.28	-0.09
0	1	8	26.34	27.96	26.33	27.95	0.67	0.71
-9	1	-1	9.40	10.13	-9.35	-10.08	-0.97	-1.04
-4	1	-7	10.82	10.16	10.78	10.13	0.83	0.78
2	1	-8	14.32	15.56	-14.32	-15.56	0.10	0.11
5	1	-7	12.15	12.39	12.15	12.39	0.26	0.26
-1	1	-8	19.52	20.36	19.51	20.36	-0.28	-0.30
8	1	-4	2.07	2.13	1.91	1.97	0.79	0.82
-7	1	6	15.10	15.09	-15.10	-15.09	0.03	0.03
-3	1	8	19.97	20.70	-19.97	-20.70	-0.28	-0.29
-9	1	3	9.86	9.65	9.84	9.63	0.63	0.62
1	1	8	11.79	12.54	-11.78	-12.54	0.39	0.41
-8	1	5	12.25	13.05	12.25	13.05	0.02	0.02
-7	1	-5	6.37	6.65	-6.35	-6.63	-0.50	-0.52
3	1	-8	17.37	17.73	17.37	17.73	-0.01	-0.01
8	1	3	4.41	4.80	4.26	4.64	1.14	1.24
-6	1	-6	9.53	9.22	9.50	9.19	-0.76	-0.74
-2	1	-8	16.91	18.46	-16.90	-18.45	-0.60	-0.65
9	1	-1	4.60	4.28	-4.53	-4.21	-0.80	-0.75
4	1	7	9.82	9.38	-9.82	-9.38	0.07	0.06
-9	1	-2	18.55	17.77	-18.53	-17.75	-0.94	-0.90
-6	1	7	3.67	3.35	3.67	3.35	0.02	0.02
9	1	0	11.26	11.42	-11.18	-11.35	-1.28	-1.30
-8	1	-4	6.77	6.83	-6.68	-6.74	1.10	1.11
9	1	-2	16.52	14.88	-16.52	-14.87	0.32	0.28
-4	1	8	19.28	19.34	19.27	19.34	-0.17	-0.17
7	1	-6	15.09	14.99	15.08	14.98	0.60	0.60
2	1	8	4.51	5.01	4.50	4.99	-0.35	-0.39
0	2	0	14.25	10.84	13.89	10.56	3.20	2.44
-1	2	0	15.68	13.46	-15.39	-13.21	-3.00	-2.58
0	2	-1	28.90	23.82	-28.14	-23.20	6.56	5.41
-1	2	1	27.66	24.87	26.99	24.26	-6.05	-5.44

-1	2	-1	10.95	9.81	10.67	9.55	2.49	2.23
0	2	1	11.82	10.78	-11.54	-10.52	-2.59	-2.36
1	2	0	77.86	137.21	77.80	137.10	3.08	5.43
-2	2	0	72.86	137.14	-72.80	137.03	-2.91	-5.47
1	2	-1	42.14	42.85	41.94	42.65	4.08	4.15
-2	2	1	42.71	45.90	-42.54	-45.72	-3.78	-4.06
-2	2	-1	2.95	2.77	0.04	0.04	-2.95	-2.77
1	2	1	3.22	2.68	0.71	0.59	3.14	2.62
0	2	-2	20.97	22.79	20.59	22.38	3.95	4.30
-1	2	2	17.49	18.68	-17.05	-18.21	-3.92	-4.19
-1	2	-2	56.70	64.87	56.51	64.65	4.65	5.32
0	2	2	59.24	63.94	-59.03	-63.71	-4.94	-5.34
2	2	0	52.34	53.36	52.20	53.21	3.88	3.96
-3	2	0	48.58	52.98	-48.45	-52.84	-3.56	-3.88
1	2	-2	36.39	37.12	-36.39	-37.11	-0.24	-0.24
-2	2	2	34.06	35.35	34.06	35.35	0.38	0.39
2	2	-1	4.90	4.58	4.88	4.55	-0.50	-0.47
-3	2	1	5.35	3.63	5.27	3.57	0.92	0.62
-2	2	-2	10.57	10.03	10.36	9.83	2.10	1.99
1	2	2	15.88	15.02	-15.72	-14.87	-2.24	-2.12
-3	2	-1	59.19	76.11	-59.04	-75.91	-4.24	-5.45
2	2	1	66.20	74.01	66.02	73.81	4.82	5.39
2	2	-2	43.68	44.34	-43.45	-44.11	-4.46	-4.53
-3	2	2	41.36	41.37	41.11	41.11	4.63	4.63
0	2	-3	27.91	25.09	27.91	25.09	-0.01	-0.01
-1	2	3	27.07	24.93	-27.07	-24.93	0.18	0.16
-1	2	-3	30.51	29.50	30.17	29.17	4.54	4.39
0	2	3	32.72	30.70	-32.40	-30.40	-4.55	-4.27
-3	2	-2	45.74	48.97	-45.65	-48.88	-2.73	-2.92
3	2	0	20.04	18.89	-20.03	-18.88	-0.73	-0.69
1	2	-3	37.08	35.41	-36.79	-35.14	-4.60	-4.40
2	2	2	47.65	48.08	47.57	48.00	2.74	2.77
-4	2	0	22.02	21.13	22.00	21.11	0.88	0.84
-2	2	3	40.51	39.59	40.25	39.34	4.58	4.48
3	2	-1	23.58	23.54	-23.12	-23.09	-4.62	-4.61
-4	2	1	21.89	22.70	21.41	22.21	4.56	4.72
-2	2	-3	43.43	43.96	43.13	43.66	5.12	5.18
3	2	1	46.79	46.77	46.64	46.62	3.73	3.73
-4	2	-1	43.68	47.50	-43.55	-47.36	-3.37	-3.66
1	2	3	42.98	41.71	-42.65	-41.39	-5.34	-5.18
3	2	-2	78.04	98.11	-77.94	-97.98	-4.02	-5.06
2	2	-3	54.61	59.40	-54.40	-59.18	-4.74	-5.15
-4	2	2	75.56	98.60	75.46	98.47	3.86	5.04
-3	2	3	55.02	60.05	54.82	59.84	4.69	5.11
-4	2	-2	54.24	63.98	-54.05	-63.75	-4.55	-5.37
3	2	2	60.67	65.68	60.48	65.47	4.89	5.29
-3	2	-3	33.53	32.66	33.49	32.61	1.79	1.75
2	2	3	35.93	34.74	-35.87	-34.69	-1.93	-1.86
0	2	-4	26.18	25.23	-25.81	-24.88	-4.37	-4.22
-1	2	4	24.74	24.18	24.35	23.80	4.38	4.29
4	2	0	52.92	52.43	-52.71	-52.23	-4.68	-4.64
-1	2	-4	45.36	44.44	-45.36	-44.44	0.22	0.21
-5	2	0	52.27	55.15	52.07	54.95	4.52	4.77
4	2	-1	32.00	31.44	-31.61	-31.05	-5.00	-4.91
1	2	-4	37.57	38.10	-37.22	-37.74	-5.11	-5.19

0	2	4	47.74	47.70	47.74	47.70	-0.06	-0.06
-5	2	1	30.34	29.36	29.91	28.94	5.07	4.91
-2	2	4	36.03	34.90	35.64	34.52	5.30	5.13
3	2	-3	56.46	59.81	-56.44	-59.79	-1.61	-1.71
-4	2	3	54.04	58.79	54.02	58.77	1.45	1.58
4	2	1	27.62	26.26	27.61	26.24	-0.93	-0.89
-5	2	-1	27.42	26.09	-27.40	-26.06	1.10	1.04
-2	2	-4	87.12	110.97	87.05	110.88	3.48	4.43
4	2	-2	46.60	45.70	46.57	45.67	-1.51	-1.48
1	2	4	89.30	108.92	-89.23	108.84	-3.53	-4.31
-5	2	2	43.49	43.30	-43.47	-43.27	1.36	1.35
2	2	-4	11.53	11.54	11.37	11.38	-1.91	-1.92
-3	2	4	12.47	11.54	-12.32	-11.40	1.92	1.78
-4	2	-3	2.89	3.47	-1.40	-1.69	-2.53	-3.04
3	2	3	2.94	3.15	1.20	1.29	2.69	2.87
-5	2	-2	34.21	36.18	34.05	36.02	-3.23	-3.41
4	2	2	34.24	34.74	-34.07	-34.57	3.42	3.47
-3	2	-4	43.22	44.32	42.95	44.04	4.87	4.99
2	2	4	44.57	44.54	-44.30	-44.27	-4.98	-4.97
4	2	-3	16.19	14.91	15.86	14.59	3.29	3.03
-5	2	3	22.92	22.43	-22.69	-22.21	-3.24	-3.17
3	2	-4	45.27	46.84	45.19	46.75	2.76	2.86
-4	2	4	45.45	47.65	-45.36	-47.56	-2.85	-2.99
5	2	0	12.01	12.01	11.05	11.05	-4.72	-4.72
5	2	-1	28.92	27.87	-28.89	-27.85	-1.29	-1.25
0	2	-5	15.97	15.54	-15.06	-14.66	-5.31	-5.16
-6	2	0	11.95	11.51	-10.90	-10.49	4.90	4.72
-6	2	1	24.52	23.81	24.49	23.79	1.16	1.12
-1	2	5	15.14	14.37	14.15	13.44	5.36	5.09
1	2	-5	20.64	20.33	-20.53	-20.23	-2.13	-2.10
-1	2	-5	7.24	7.47	6.12	6.32	-3.87	-3.99
-2	2	5	19.46	19.12	19.36	19.02	1.99	1.96
0	2	5	4.49	4.65	-2.21	-2.29	3.91	4.05
5	2	1	21.84	19.82	-21.24	-19.28	-5.08	-4.61
-6	2	-1	21.34	20.18	20.74	19.61	5.03	4.75
5	2	-2	7.72	6.32	-6.68	-5.47	5.87	3.17
-6	2	2	8.91	8.90	8.27	8.26	-3.32	-3.32
-5	2	-3	9.89	9.21	-8.14	-7.58	-5.61	-5.23
2	2	-5	3.41	2.87	-1.30	-1.09	3.15	2.65
4	2	3	6.88	6.37	4.07	3.78	5.54	5.14
-2	2	-5	15.07	14.40	15.06	14.39	0.44	0.42
-3	2	5	1.83	2.79	0.17	0.26	-1.83	-2.77
-4	2	-4	17.77	18.42	17.71	18.36	1.44	1.49
1	2	5	16.51	15.77	-16.51	-15.77	-0.29	-0.28
3	2	4	17.80	17.84	-17.73	-17.76	-1.60	-1.60
4	2	-4	4.58	5.21	-0.22	-0.25	4.57	5.20
-5	2	4	4.43	5.57	1.51	1.90	-4.17	-5.24
5	2	2	14.76	12.64	-14.71	-12.60	-1.25	-1.07
-6	2	-2	14.56	12.95	14.49	12.89	1.38	1.23
5	2	-3	44.98	44.06	44.67	43.75	5.28	5.17
-6	2	3	42.88	43.50	-42.57	-43.19	-5.15	-5.22
3	2	-5	52.88	55.15	52.64	54.91	4.97	5.18
-3	2	-5	15.43	14.56	-14.70	-13.88	4.69	4.43
-4	2	5	52.21	54.36	-51.97	-54.11	-4.99	-5.20
2	2	5	15.85	14.90	15.18	14.27	-4.56	-4.29

6	2	-1	37.69	36.29	37.54	36.14	3.39	3.26
6	2	0	21.82	20.99	21.80	20.96	-1.05	-1.01
-7	2	1	36.43	35.67	-36.26	-35.50	-3.49	-3.42
-7	2	0	21.29	21.67	-21.27	-21.66	0.87	0.89
-5	2	-4	44.27	47.84	-44.18	-47.74	-2.88	-3.11
0	2	-6	25.99	26.36	-25.89	-26.27	-2.22	-2.25
4	2	4	45.72	46.54	45.63	46.45	2.89	2.94
6	2	-2	29.39	27.20	28.87	26.72	5.49	5.08
-1	2	6	25.95	25.95	25.87	25.86	2.11	2.11
1	2	-6	56.71	60.78	56.66	60.73	2.26	2.43
-7	2	2	32.12	31.01	-31.68	-30.58	-5.33	-5.15
-6	2	-3	42.18	43.71	-42.07	-43.60	-3.02	-3.13
6	2	1	72.17	76.87	-72.05	-76.74	-4.20	-4.47
5	2	3	46.46	45.86	46.55	45.75	3.22	3.18
-7	2	-1	69.28	80.51	69.17	80.39	3.87	4.49
-1	2	-6	43.36	42.81	-43.05	-42.51	-5.15	-5.08
-2	2	6	54.27	58.01	-54.22	-57.96	-2.37	-2.54
5	2	-4	8.51	7.25	7.59	6.47	3.85	3.28
0	2	6	41.79	40.34	41.46	40.03	5.18	5.00
-6	2	4	7.19	7.31	-6.46	-6.58	-3.14	-3.19
4	2	-5	48.09	49.29	47.98	49.17	3.37	3.45
-4	2	-5	19.64	18.60	18.99	17.99	5.01	4.75
-5	2	5	46.08	47.61	-45.97	-47.49	-3.25	-3.36
3	2	5	19.90	19.39	-19.31	-18.81	-4.84	-4.72
2	2	-6	25.39	23.82	24.80	23.27	5.43	5.10
-3	2	6	26.12	24.92	-25.56	-24.40	-5.34	-5.10
-2	2	-6	60.08	67.23	-59.99	-67.13	-3.34	-3.74
1	2	6	60.32	66.44	60.22	66.33	3.43	3.78
6	2	-3	26.78	24.57	26.57	24.38	3.35	3.07
-7	2	3	23.49	21.29	-23.26	-21.07	-3.31	-3.00
6	2	2	39.81	38.87	-39.54	-38.60	-4.64	-4.53
-7	2	-2	35.91	37.01	35.62	36.71	4.55	4.69
3	2	-6	22.74	22.78	22.46	22.49	3.58	3.58
-4	2	6	24.47	24.63	-24.23	-24.38	-3.46	-3.48
-3	2	-6	20.43	20.07	20.42	20.06	0.63	0.62
2	2	6	18.15	18.33	-18.14	-18.32	-0.47	-0.47
-6	2	-4	26.66	27.49	-26.21	-27.03	-4.88	-5.04
5	2	4	26.72	25.93	26.23	25.46	5.08	4.93
5	2	-5	2.66	3.55	2.55	3.40	-0.76	-1.01
-6	2	5	2.70	2.60	-2.42	-2.33	1.20	1.16
-5	2	-5	17.16	16.49	17.11	16.44	1.28	1.23
7	2	-1	54.19	54.65	53.97	54.42	4.89	4.93
4	2	5	17.24	16.25	-17.18	-16.19	-1.42	-1.34
-8	2	1	47.65	49.56	-47.40	-49.31	-4.82	-5.02
7	2	0	4.77	5.16	-3.66	-3.96	3.06	3.31
6	2	-4	28.59	27.84	-28.56	-27.81	-1.24	-1.21
-8	2	0	2.04	3.49	-0.15	-0.25	-2.03	-3.48
-7	2	4	27.92	27.87	27.89	27.84	1.36	1.36
-7	2	-3	4.09	3.42	3.74	3.13	1.65	1.38
6	2	3	1.98	1.39	-0.95	-0.67	-1.74	-1.22
7	2	-2	12.86	11.53	12.46	11.18	3.16	2.84
-8	2	2	15.90	15.74	-15.65	-15.49	-2.80	-2.77
4	2	-6	15.16	14.86	-15.14	-14.84	-0.82	-0.80
7	2	1	18.57	17.66	-18.55	-17.65	-0.81	-0.77
-8	2	-1	15.43	15.45	15.42	15.44	0.65	0.65

-5	2	6	14.46	13.40	14.42	13.37	1.02	0.94
0	2	-7	17.85	18.53	-17.72	-18.40	2.10	2.18
1	2	-7	21.93	22.98	21.41	22.44	4.73	4.96
-1	2	7	13.49	14.13	13.32	13.94	-2.18	-2.28
-2	2	7	23.99	24.35	-23.49	-23.84	-4.88	-4.95
-4	2	-6	43.50	47.22	43.31	47.01	4.02	4.37
-1	2	-7	19.85	19.72	-19.71	-19.58	-2.39	-2.38
3	2	6	42.78	44.10	-42.58	-43.90	-4.09	-4.22
0	2	7	19.48	19.17	19.35	19.04	2.26	2.23
7	2	-3	16.87	16.92	-16.81	-16.87	-1.38	-1.38
2	2	-7	30.81	29.86	30.57	29.63	3.79	3.67
-8	2	3	18.68	18.97	18.62	18.91	1.51	1.54
-3	2	7	26.60	25.80	-26.34	-25.56	-3.67	-3.56
7	2	2	3.42	5.01	1.87	2.74	-2.87	-4.20
-8	2	-2	2.76	5.17	-1.59	-2.98	2.26	4.23
-2	2	-7	18.27	17.47	-17.52	-16.76	-5.17	-4.94
1	2	7	19.95	19.53	19.32	18.92	4.95	4.85
6	2	-5	42.67	46.84	-42.48	-46.62	-4.09	-4.49
-7	2	5	39.51	43.21	39.28	42.97	4.20	4.59
-6	2	-5	1.74	4.68	1.29	3.47	-1.17	-3.14
5	2	5	3.58	4.23	-2.55	-3.01	2.51	2.97
3	2	-7	9.30	9.29	9.28	9.27	-0.59	-0.59
-7	2	-4	3.09	3.93	-2.13	-2.71	-2.23	-2.84
5	2	-6	3.22	4.55	0.78	1.11	-3.12	-4.42
6	2	4	3.31	3.80	2.16	2.48	2.51	2.88
-4	2	7	6.39	6.29	-6.35	-6.25	0.74	0.72
-6	2	6	6.30	6.13	4.28	4.17	4.62	4.50
7	2	-4	4.94	6.38	3.49	4.51	-3.50	-4.52
-8	2	4	3.60	5.44	-1.89	-2.86	3.06	4.63
-3	2	-7	10.66	11.39	-10.16	-10.86	-3.23	-3.45
-5	2	-6	4.53	6.28	3.18	4.41	3.23	4.47
4	2	6	5.32	6.27	-3.77	-4.45	-3.75	-4.43
2	2	7	10.94	11.50	10.42	10.96	3.31	3.48
8	2	-1	34.01	32.34	33.90	32.23	2.72	2.58
-9	2	1	33.03	32.53	-32.93	-32.43	-2.56	-2.52
-8	2	-3	49.56	51.71	49.36	51.51	4.38	4.57
7	2	3	50.40	49.24	-50.20	-49.04	-4.51	-4.41
8	2	0	28.46	26.69	28.00	26.26	5.05	4.74
-9	2	0	29.46	28.58	-29.03	-28.17	-4.98	-4.83
8	2	-2	12.18	12.01	12.08	11.91	-1.56	-1.54
4	2	-7	36.54	35.86	-36.27	-35.60	-4.37	-4.29
-9	2	2	9.15	9.31	-8.99	-9.15	1.67	1.70
-5	2	7	36.97	37.38	36.72	37.12	4.31	4.36
8	2	1	39.85	38.56	39.70	38.41	3.43	3.32
-9	2	-1	36.37	37.98	-36.22	-37.82	-3.35	-3.50
-4	2	-7	25.94	24.04	-25.93	-24.02	0.86	0.80
8	2	-3	51.14	51.09	-50.94	-50.89	-4.49	-4.49
0	2	-8	26.56	26.79	26.13	26.36	4.73	4.77
3	2	7	24.18	22.29	24.17	22.28	-0.70	-0.65
6	2	-6	12.18	12.68	-11.44	-11.91	-4.17	-4.34
-9	2	3	49.28	51.02	49.08	50.81	4.46	4.62
1	2	-8	3.00	4.78	1.88	3.00	2.34	3.72
-1	2	8	24.55	24.51	-24.09	-24.05	-4.76	-4.75
-7	2	6	14.92	15.96	14.37	15.36	4.03	4.31
7	2	-5	37.65	35.44	-37.38	-35.19	-4.48	-4.22

-2	2	8	2.97	4.68	-1.90	-2.99	-2.28	-3.60
-8	2	5	36.80	35.32	36.53	35.07	4.38	4.20
-1	2	-8	29.12	30.12	29.06	30.05	1.86	1.92
-7	2	-5	51.19	51.79	-50.97	-51.56	-4.74	-4.80
6	2	5	51.97	51.30	51.76	51.08	4.74	4.68
0	2	8	28.34	28.37	-28.27	-28.30	-2.01	-2.01
2	2	-8	23.00	21.98	-23.00	-21.97	-0.39	-0.37
8	2	2	20.02	18.67	-20.01	-18.67	-0.58	-0.54
-9	2	-2	20.24	19.80	20.23	19.80	0.44	0.43
-3	2	8	21.02	20.27	21.02	20.26	0.52	0.51
-6	2	-6	8.93	7.90	-8.86	-7.83	1.11	0.98
5	2	6	5.87	4.76	5.72	4.63	-1.33	-1.08
-1	3	0	4.73	4.51	-4.73	-4.51	0.20	0.19
0	3	0	9.14	6.27	-9.11	-6.24	0.77	0.53
-1	3	-1	14.13	13.27	14.13	13.27	0.32	0.30
-1	3	1	9.26	8.12	9.26	8.12	-0.19	-0.17
0	3	-1	17.64	14.90	17.64	14.89	0.38	0.32
-2	3	0	8.34	6.51	8.34	6.50	-0.12	-0.10
0	3	1	38.76	38.11	38.76	38.11	0.33	0.33
-2	3	1	5.67	5.76	5.66	5.75	-0.30	-0.31
1	3	0	6.24	5.78	6.22	5.76	0.49	0.45
-2	3	-1	35.43	34.78	-35.43	-34.78	0.08	0.07
1	3	-1	13.48	13.35	13.48	13.35	-0.09	-0.09
1	3	1	16.05	15.83	-16.03	-15.81	0.76	0.75
-1	3	-2	35.75	34.27	-35.75	-34.27	0.17	0.17
-1	3	2	12.06	10.17	12.05	10.16	-0.61	-0.51
0	3	-2	25.70	24.46	25.70	24.46	-0.05	-0.04
-3	3	0	8.65	8.78	8.65	8.78	-0.09	-0.09
0	3	2	48.58	50.83	-48.58	-50.83	-0.21	-0.22
-3	3	1	12.71	12.15	-12.71	-12.15	-0.14	-0.13
-2	3	2	43.79	45.52	-43.79	-45.52	-0.30	-0.32
-3	3	-1	3.36	2.69	-3.36	-2.69	-0.01	-0.01
-2	3	-2	43.71	43.95	43.71	43.95	0.08	0.08
1	3	-2	59.05	67.73	-59.05	-67.73	-0.39	-0.45
2	3	0	9.52	7.48	9.52	7.48	-0.21	-0.16
2	3	-1	1.74	0.71	0.69	0.28	-1.59	-0.65
1	3	2	27.31	27.65	27.31	27.64	0.46	0.47
-3	3	2	55.36	60.43	55.36	60.43	0.00	0.00
2	3	1	12.10	10.12	-12.08	-10.10	0.68	0.57
-4	3	0	7.59	6.60	-7.59	-6.60	0.04	0.04
-3	3	-2	6.63	5.82	6.63	5.82	-0.03	-0.03
0	3	-3	34.70	33.85	34.69	33.85	-0.25	-0.25
-1	3	-3	9.59	8.86	-9.59	-8.86	-0.01	-0.01
2	3	-2	23.14	22.08	23.13	22.08	-0.62	-0.60
-1	3	3	30.22	29.50	30.22	29.50	-0.52	-0.50
-4	3	1	25.30	25.34	-25.30	-25.34	0.00	0.00
-2	3	3	29.76	29.20	-29.76	-29.20	-0.02	-0.02
0	3	3	5.36	5.07	5.31	5.02	-0.74	-0.70
-4	3	-1	17.85	16.23	17.85	16.23	0.14	0.12
1	3	-3	4.35	4.34	-4.33	-4.32	-0.40	-0.40
-2	3	-3	14.16	13.66	-14.16	-13.66	0.01	0.01
2	3	2	29.08	28.09	29.06	28.07	0.98	0.95
3	3	0	19.88	18.01	-19.86	-17.99	-0.94	-0.86
-4	3	2	9.85	9.29	9.85	9.29	0.09	0.08
3	3	-1	30.21	28.91	-30.20	-28.90	-0.81	-0.77

-3	3	3	10.52	10.43	-10.51	-10.43	0.25	0.25
1	3	3	4.57	4.02	4.56	4.01	-0.28	-0.25
3	3	1	8.99	8.35	8.99	8.35	-0.26	-0.24
2	3	-3	12.60	11.99	-12.60	-11.99	-0.15	-0.14
-4	3	-2	13.12	11.52	-13.12	-11.52	0.11	0.09
3	3	-2	21.52	20.94	21.52	20.94	-0.17	-0.17
-3	3	-3	28.96	28.11	-28.96	-28.11	-0.14	-0.13
-5	3	0	24.46	23.17	24.46	23.17	-0.01	-0.01
-5	3	1	12.40	12.07	12.40	12.07	-0.10	-0.09
0	3	-4	38.45	39.53	-38.45	-39.53	-0.20	-0.20
-1	3	-4	22.40	22.33	22.40	22.33	-0.06	-0.06
-1	3	4	32.48	33.05	-32.48	-33.05	-0.06	-0.06
-4	3	3	4.35	3.87	4.34	3.87	0.19	0.17
-5	3	-1	6.25	5.69	-6.24	-5.68	0.21	0.20
2	3	3	32.54	32.73	-32.54	-32.72	0.61	0.62
-2	3	4	34.95	36.55	34.94	36.55	0.38	0.40
3	3	2	14.26	13.03	14.24	13.01	0.72	0.66
1	3	-4	20.14	19.98	20.14	19.98	-0.10	-0.10
0	3	4	2.07	1.20	-1.69	-0.98	-1.19	-0.69
-5	3	2	17.33	17.19	-17.33	-17.19	-0.04	-0.04
-2	3	-4	5.27	4.88	-5.27	-4.88	0.01	0.00
4	3	0	27.48	25.94	27.47	25.92	-0.99	-0.93
3	3	-3	6.11	5.49	6.09	5.47	0.50	0.45
4	3	-1	3.75	3.66	-3.75	-3.66	-0.17	-0.17
-3	3	4	18.42	17.92	-18.42	-17.92	0.39	0.38
-4	3	-3	17.06	15.71	17.06	15.71	-0.12	-0.11
1	3	4	17.33	16.87	-17.31	-16.84	-0.90	-0.87
2	3	-4	20.43	19.71	-20.43	-19.71	0.30	0.29
4	3	1	6.62	6.23	-6.52	-6.14	-1.12	-1.05
-5	3	-2	24.06	24.55	-24.06	-24.55	0.33	0.33
4	3	-2	0.	0.69	0.	0.32	0.	0.61
-3	3	-4	8.55	7.27	8.55	7.27	-0.19	-0.16
-5	3	3	4.97	5.66	-4.97	-5.66	0.01	0.01
3	3	3	3.47	2.91	-3.19	-2.68	1.36	1.14
-6	3	0	35.66	36.66	-35.66	-36.66	-0.27	-0.28
-6	3	1	3.70	3.62	3.69	3.62	-0.24	-0.24
-4	3	4	20.80	20.65	20.80	20.65	0.10	0.10
4	3	2	31.71	31.63	-31.71	-31.63	-0.34	-0.34
2	3	4	6.50	5.29	-6.49	-5.28	-0.32	-0.26
-6	3	-1	3.32	0.88	-3.32	-0.88	-0.17	-0.05
0	3	-5	19.03	17.73	-19.03	-17.73	-0.05	-0.05
3	3	-4	33.68	33.93	33.67	33.92	0.62	0.62
4	3	-3	21.79	22.51	-21.77	-22.49	0.81	0.83
-6	3	2	5.26	4.05	-5.26	-4.05	-0.08	-0.06
-1	3	-5	21.45	21.16	21.45	21.16	0.00	0.00
-1	3	5	22.74	22.62	-22.74	-22.61	0.54	0.53
-2	3	5	18.11	17.08	18.10	17.07	0.62	0.59
1	3	-5	4.32	4.28	4.32	4.27	0.15	0.15
-5	3	-3	24.03	24.93	24.02	24.93	0.20	0.20
0	3	5	17.46	17.48	17.46	17.48	-0.11	-0.11
-4	3	-4	25.45	25.96	25.44	25.95	-0.33	-0.33
5	3	-1	3.73	2.61	-3.57	-2.49	1.11	0.77
5	3	0	29.49	28.66	-29.49	-28.66	-0.16	-0.15
-2	3	-5	14.79	15.06	-14.79	-15.06	0.11	0.12
-3	3	5	13.42	13.82	13.42	13.82	0.19	0.20

-5	3	4	28.26	27.13	-28.26	-27.13	-0.06	-0.06
-6	3	-2	18.49	16.53	18.49	16.53	0.37	0.33
2	3	-5	22.47	22.41	22.46	22.41	0.41	0.41
5	3	-2	15.53	14.76	15.49	14.73	1.09	1.03
5	3	1	4.52	8.04	-4.48	-7.97	-0.60	-1.07
-6	3	3	32.11	33.49	32.11	33.49	0.05	0.05
1	3	5	8.81	8.05	-8.76	-8.00	-0.96	-0.87
4	3	3	24.38	24.69	24.37	24.68	0.71	0.72
3	3	4	49.14	51.82	49.14	51.82	0.72	0.76
4	3	-4	16.45	15.36	-16.45	-15.35	0.47	0.44
-3	3	-5	4.29	3.66	4.29	3.66	0.00	0.00
-4	3	5	14.95	15.20	-14.95	-15.20	-0.15	-0.15
-7	3	1	25.63	25.53	25.63	25.53	-0.11	-0.11
-7	3	0	10.88	11.22	10.87	11.22	-0.41	-0.43
5	3	-3	28.15	28.78	28.14	28.77	0.51	0.53
5	3	2	12.06	11.70	-12.00	-11.63	-1.27	-1.23
3	3	-5	7.76	8.97	-7.76	-8.96	0.29	0.34
-5	3	-4	43.40	47.20	-43.40	-47.20	-0.16	-0.17
2	3	5	4.11	4.67	-4.01	-4.56	-0.90	-1.02
-7	3	2	20.14	20.47	-20.14	-20.46	0.17	0.17
-7	3	-1	4.96	5.26	-4.94	-5.24	-0.43	-0.46
-6	3	-3	6.07	6.42	6.05	6.40	0.51	0.53
-6	3	4	19.73	17.91	19.73	17.91	0.03	0.03
0	3	-6	1.62	0.03	0.82	0.02	1.39	0.03
-1	3	-6	29.00	28.84	29.00	28.84	0.02	0.02
-1	3	6	8.67	7.27	-8.62	-7.23	0.93	0.78
-4	3	-5	4.95	3.10	-4.92	-3.09	-0.52	-0.33
-2	3	6	14.27	14.15	-14.26	-14.15	0.31	0.31
1	3	-6	14.13	14.31	-14.13	-14.31	0.19	0.19
-5	3	5	11.56	9.96	-11.55	-9.96	-0.21	-0.18
6	3	-1	34.01	34.56	33.99	34.54	1.19	1.21
6	3	0	26.00	24.07	25.98	24.05	1.01	0.94
0	3	6	37.91	38.08	37.91	38.07	0.64	0.64
4	3	4	21.77	21.55	-21.73	-21.52	1.32	1.31
-7	3	3	12.01	11.11	-12.01	-11.11	0.25	0.24
-7	3	-2	12.77	12.40	12.77	12.40	-0.10	-0.09
-3	3	6	2.52	1.33	2.48	1.31	-0.43	-0.23
-2	3	-6	17.00	16.74	-16.99	-16.74	0.21	0.20
6	3	-2	32.02	31.21	-32.01	-31.21	0.61	0.59
5	3	-4	8.78	7.62	8.77	7.61	-0.31	-0.27
5	3	3	13.86	13.31	13.86	13.30	-0.45	-0.44
4	3	-5	9.58	8.45	-9.58	-8.45	-0.20	-0.18
2	3	-6	3.55	4.39	3.55	4.39	0.17	0.22
6	3	1	4.21	2.71	-4.20	-2.71	-0.18	-0.12
3	3	5	2.99	2.37	-2.98	-2.36	-0.32	-0.25
1	3	6	8.74	9.74	-8.74	-9.73	-0.16	-0.17
-4	3	6	4.60	4.70	-4.58	-4.68	-0.37	-0.38
-6	3	-4	11.19	10.96	11.18	10.95	0.33	0.32
-3	3	-6	5.74	7.37	5.74	7.37	0.21	0.27
6	3	-3	5.35	4.92	5.34	4.91	-0.41	-0.37
-8	3	1	20.14	16.84	-20.14	-16.84	0.36	0.30
-8	3	0	27.36	26.18	-27.36	-26.18	-0.15	-0.15
-5	3	-5	6.19	6.42	-6.17	-6.40	-0.49	-0.51
3	3	-6	14.03	13.11	-14.03	-13.11	-0.11	-0.10
6	3	2	3.55	3.57	3.36	3.37	-1.17	-1.18

-6	3	5	2.11	0.46	2.10	0.46	-0.12	-0.03
-7	3	4	2.24	2.64	-2.24	-2.64	0.10	0.11
-7	3	-3	13.95	13.10	-13.94	-13.09	0.47	0.44
-8	3	2	38.36	38.16	38.36	38.16	0.44	0.44
-8	3	-1	2.77	0.62	0.77	0.17	-2.66	-0.59
2	3	6	1.76	1.07	-0.36	-0.22	-1.75	-1.04
5	3	-5	0.	1.08	-0.	-0.79	-0.	-0.74
-5	3	6	26.54	26.08	26.54	26.08	-0.18	-0.18
5	3	4	2.17	1.70	-1.94	-1.52	0.97	0.76
4	3	5	9.71	9.41	-9.66	-9.36	0.94	0.91
-4	3	-6	16.32	17.73	-16.32	-17.73	-0.02	-0.02
6	3	-4	8.27	8.49	-8.22	-8.44	-0.91	-0.94
0	3	-7	10.82	9.69	-10.82	-9.69	-0.01	-0.01
7	3	-1	11.55	10.66	11.53	10.64	0.69	0.63
-8	3	3	10.62	9.97	-10.62	-9.96	0.25	0.24
7	3	0	22.05	21.02	-22.00	-20.97	1.44	1.37
-1	3	-7	17.19	16.19	-17.19	-16.19	-0.08	-0.08
1	3	-7	21.25	20.96	21.25	20.96	0.09	0.08
4	3	-6	16.67	15.94	16.66	15.93	-0.56	-0.54
-1	3	7	11.44	10.49	11.44	10.48	0.47	0.43
-8	3	-2	7.98	6.56	-7.94	-6.53	-0.77	-0.63
-2	3	7	29.09	29.25	29.09	29.25	-0.28	-0.28
6	3	3	11.18	10.76	-11.08	-10.67	-1.45	-1.40
7	3	-2	17.24	15.77	17.24	15.77	-0.53	-0.48
0	3	7	10.30	10.13	-10.25	-10.09	0.98	0.96
-3	3	7	7.98	8.14	-7.96	-8.12	-0.55	-0.56
7	3	1	6.58	5.41	6.45	5.30	1.33	1.09
-2	3	-7	2.20	1.35	2.20	1.35	0.17	0.11
2	3	-7	10.23	8.25	10.23	8.25	-0.05	-0.04
3	3	6	29.47	30.13	-29.45	-30.11	-1.12	-1.14
-6	3	-5	16.20	16.12	16.20	16.12	-0.21	-0.21
-7	3	5	3.73	3.43	-3.73	-3.43	-0.01	-0.01
-7	3	-4	5.96	5.53	5.91	5.48	0.77	0.72
-6	3	6	9.18	9.02	-9.18	-9.02	0.02	0.02
7	3	-3	17.98	16.67	-17.93	-16.63	-1.22	-1.13
1	3	7	8.69	7.81	-8.65	-7.77	0.81	0.73
-8	3	4	5.64	4.70	-5.64	-4.70	-0.06	-0.05
-4	3	7	23.08	22.13	-23.08	-22.13	-0.35	-0.33
-5	3	-6	23.04	22.97	23.03	22.96	-0.49	-0.49
-9	3	1	20.62	20.72	-20.61	-20.71	0.62	0.63
7	3	2	3.61	4.02	3.61	4.02	-0.06	-0.07
-8	3	-3	11.04	12.25	-11.04	-12.25	-0.14	-0.15
-9	3	0	29.03	29.54	29.02	29.54	0.43	0.44
-3	3	-7	8.24	6.84	8.23	6.83	0.47	0.39
3	3	-7	12.87	12.29	-12.87	-12.28	-0.36	-0.34
6	3	-5	10.19	9.44	-10.16	-9.41	-0.82	-0.76
5	3	-6	0.93	1.23	-0.81	-1.07	-0.46	-0.61
-9	3	2	5.76	3.27	-5.72	-3.25	0.51	0.34
5	3	5	26.25	26.84	26.22	26.80	1.41	1.44
6	3	4	15.05	14.44	-15.04	-14.43	-0.56	-0.54
-9	3	-1	4.35	4.60	4.35	4.60	-0.15	-0.16
2	3	7	1.64	0.27	-0.71	-0.12	-1.48	-0.25
-5	3	7	1.45	0.39	-1.45	-0.39	0.10	0.03
7	3	-4	12.62	11.82	-12.59	-11.79	-0.95	-0.89
4	3	6	25.88	26.36	25.87	26.35	-0.22	-0.22

-9	3	3	8.09	6.18	8.09	6.18	-0.14	-0.11
-4	3	-7	12.52	12.46	12.51	12.45	0.40	0.40
0	4	0	13.34	11.46	-12.77	-10.97	-3.84	-3.30
-2	4	0	8.66	8.43	-8.06	-7.85	-3.16	-3.07
-1	4	-1	35.99	37.86	-35.83	-37.70	-3.31	-3.49
-1	4	1	35.57	39.55	-35.45	-39.41	-2.92	-3.24
0	4	-1	15.34	13.58	-15.28	-13.52	1.42	1.26
-2	4	1	7.79	5.51	-7.47	-5.28	2.19	1.55
-2	4	-1	17.43	18.69	-16.69	-17.90	-5.02	-5.39
0	4	1	15.14	17.31	-14.40	-16.46	-4.68	-5.35
1	4	0	14.93	11.53	14.81	11.43	1.89	1.46
-3	4	0	17.34	14.82	17.22	14.71	2.06	1.76
1	4	-1	4.32	4.99	0.74	0.86	4.26	4.92
-1	4	-2	33.78	32.53	33.76	32.52	1.08	1.04
-3	4	1	4.45	5.27	-1.22	-1.45	4.28	5.06
-1	4	2	35.66	34.95	35.63	34.92	1.34	1.32
0	4	-2	63.73	76.99	63.60	76.84	4.01	4.85
-3	4	-1	21.01	15.92	-20.67	-15.66	-3.79	-2.87
1	4	1	19.95	15.74	-19.56	-15.43	-3.90	-3.08
-2	4	2	60.82	74.81	60.69	74.65	4.03	4.96
-2	4	-2	48.89	49.64	-48.76	-49.51	-3.58	-3.64
0	4	2	48.04	47.23	-47.92	-47.11	-3.43	-3.37
1	4	-2	46.24	49.53	46.04	49.31	4.36	4.67
-3	4	2	44.33	47.28	44.13	47.07	4.26	4.54
2	4	0	47.29	44.47	47.00	44.20	5.25	4.94
-4	4	0	44.13	45.46	43.85	45.17	4.96	5.11
2	4	-1	31.61	33.19	31.31	32.88	4.31	4.52
-3	4	-2	42.21	46.71	-41.93	-46.41	-4.80	-5.31
-4	4	1	31.06	33.14	30.79	32.84	4.14	4.42
1	4	2	45.03	45.14	-44.73	-44.84	-5.23	-5.25
-1	4	-3	25.69	23.02	25.15	22.54	5.27	4.72
2	4	1	10.21	9.52	-10.06	-9.38	1.76	1.64
-4	4	-1	9.25	8.87	-9.02	-8.65	2.03	1.95
0	4	-3	33.80	30.52	33.39	30.14	5.28	4.77
-1	4	3	27.87	26.20	27.40	25.76	5.11	4.81
-2	4	3	36.46	32.91	36.10	32.59	5.11	4.61
2	4	-2	57.80	66.09	-57.80	-66.09	0.61	0.70
-2	4	-3	10.95	11.30	10.93	11.27	0.78	0.81
-4	4	2	53.74	61.86	-53.74	-61.85	0.36	0.42
0	4	3	13.07	13.59	13.03	13.55	1.04	1.08
1	4	-3	39.20	41.52	39.20	41.51	0.87	0.92
-3	4	3	34.51	34.99	34.50	34.99	0.62	0.63
-4	4	-2	17.85	16.41	17.61	16.19	-2.87	-2.64
2	4	2	14.39	12.38	14.01	12.05	-3.29	-2.83
3	4	0	11.41	8.55	9.84	7.38	5.77	4.32
-5	4	0	12.12	9.52	10.85	8.52	5.41	4.25
-3	4	-3	19.72	18.38	19.31	18.00	-4.01	-3.74
3	4	-1	34.62	32.19	34.61	32.18	0.51	0.48
1	4	3	18.08	15.70	17.63	15.31	-3.98	-3.46
-5	4	1	27.24	26.18	27.24	26.18	0.20	0.19
2	4	-3	3.17	3.80	0.99	1.19	-3.01	-3.61
3	4	1	41.72	41.46	41.43	41.17	4.92	4.89
-5	4	-1	40.99	43.26	40.71	42.96	4.83	5.10
-4	4	3	7.39	6.90	-6.14	-5.73	-4.11	-3.84
3	4	-2	15.66	12.87	-14.99	-12.31	-4.55	-3.73

-1	4	-4	72.83	85.55	72.71	85.42	4.09	4.81
0	4	-4	6.26	6.34	-6.16	-6.23	1.12	1.13
-5	4	2	14.75	12.55	-13.99	-11.90	-4.68	-3.99
-1	4	4	69.10	79.78	68.98	79.65	4.01	4.63
-2	4	4	8.91	6.79	-8.85	-6.74	1.10	0.84
-2	4	-4	21.70	16.55	20.87	15.91	5.97	4.55
1	4	-4	38.88	37.49	-38.71	-37.33	-3.57	-3.45
-4	4	-3	29.37	26.66	-28.81	-26.15	-5.71	-5.18
0	4	4	19.70	14.15	18.63	13.38	6.41	4.60
2	4	3	25.42	21.66	-24.71	-21.05	-5.97	-5.09
-3	4	4	37.28	36.10	-37.09	-35.91	-3.77	-3.65
-5	4	-2	20.01	19.57	19.89	19.46	2.16	2.12
3	4	2	19.51	17.52	19.40	17.42	2.00	1.80
3	4	-3	38.75	36.87	-38.37	-36.51	-5.37	-5.11
4	4	0	5.83	1.56	-5.76	-1.54	0.95	0.25
4	4	-1	45.24	45.66	-45.08	-45.50	-3.78	-3.81
-5	4	3	36.12	33.68	-35.70	-33.29	-5.49	-5.12
-3	4	-4	10.63	10.30	10.61	10.29	0.59	0.58
-6	4	0	8.97	5.98	-8.97	-5.98	-0.04	-0.03
-6	4	1	43.58	44.85	-43.39	-44.67	-3.97	-4.09
1	4	4	12.81	13.03	12.79	13.00	0.83	0.84
2	4	-4	21.46	19.73	-20.72	-19.05	-5.60	-5.15
-4	4	4	20.09	18.73	-19.32	-18.01	-5.51	-5.13
4	4	1	63.00	62.57	62.86	62.44	4.12	4.09
-6	4	-1	60.55	66.18	60.43	66.06	3.69	4.04
4	4	-2	44.70	45.23	-44.43	-44.95	-4.95	-5.01
-6	4	2	45.06	47.28	-44.81	-47.01	-4.82	-5.06
-5	4	-3	40.77	44.09	-40.71	-44.02	-2.21	-2.39
3	4	3	47.04	48.07	-46.97	-48.00	-2.50	-2.56
0	4	-5	5.32	5.02	-4.06	-3.83	-3.44	-3.24
-1	4	-5	7.91	5.45	7.67	5.29	1.92	1.32
-4	4	-4	59.46	67.87	-59.37	-67.76	-3.33	-3.80
-2	4	5	13.65	13.40	-13.19	-12.96	-3.49	-3.42
-1	4	5	10.81	8.50	10.73	8.43	1.31	1.03
2	4	4	58.89	62.05	-58.80	-61.96	-3.32	-3.50
3	4	-4	9.99	7.21	9.30	6.71	-3.66	-2.64
-6	4	-2	55.29	61.33	55.10	61.12	4.53	5.03
4	4	2	61.27	62.66	61.09	62.48	4.69	4.80
1	4	-5	31.86	31.96	-31.45	-31.55	-5.12	-5.13
-2	4	-5	4.98	5.40	-2.28	-2.48	4.43	4.80
4	4	-3	47.94	46.90	-47.87	-46.83	-2.49	-2.44
-5	4	4	11.00	7.71	10.44	7.32	-3.45	-2.42
-3	4	5	30.63	29.72	-30.18	-29.28	-5.24	-5.09
0	4	5	5.70	5.66	-3.34	-3.32	4.62	4.59
-6	4	3	44.86	45.95	-44.81	-45.90	-2.18	-2.23
5	4	-1	58.15	57.43	-57.94	-57.23	-4.92	-4.86
5	4	0	9.06	8.37	-8.05	-7.43	-4.16	-3.84
2	4	-5	31.98	30.24	-31.84	-30.11	-2.98	-2.82
-7	4	0	11.65	10.99	-10.79	-10.18	-4.39	-4.14
-7	4	1	52.47	55.80	-52.26	-55.58	-4.64	-4.94
-3	4	-5	16.91	18.13	16.42	17.61	4.04	4.33
-4	4	5	29.16	26.38	-29.02	-26.25	-2.85	-2.58
1	4	5	20.50	21.51	20.07	21.06	4.15	4.35
5	4	-2	11.26	11.51	11.05	11.30	-2.17	-2.21
5	4	1	6.15	2.94	6.15	2.94	0.09	0.04

-7	4	-1	2.93	0.78	-2.79	-0.74	-0.90	-0.24
-7	4	2	5.30	7.05	5.08	6.76	-1.51	-2.01
-5	4	-4	27.67	25.83	-27.14	-25.34	-5.35	-5.00
-6	4	-3	6.84	6.19	6.37	5.76	2.49	2.25
3	4	4	28.72	26.51	-28.23	-26.06	-5.28	-4.87
4	4	3	5.03	5.37	4.70	5.02	1.80	1.92
4	4	-4	31.69	32.91	31.64	32.85	1.85	1.92
-6	4	4	28.94	30.36	28.86	30.28	2.10	2.20
3	4	-5	2.71	2.64	2.04	1.99	1.78	1.73
-4	4	-5	6.55	4.78	6.53	4.77	0.48	0.35
5	4	-3	14.40	11.28	14.15	11.08	2.66	2.09
-5	4	5	4.78	4.62	4.31	4.16	2.07	2.00
2	4	5	5.29	3.02	5.18	2.96	1.06	0.61
5	4	2	14.58	12.11	-13.83	-11.50	4.59	3.82
-7	4	-2	15.38	14.31	-14.83	-13.80	4.07	3.79
0	4	-6	35.23	31.38	-34.77	-30.97	-5.68	-5.06
-7	4	3	23.47	20.40	23.31	20.26	2.74	2.38
-1	4	-6	53.45	58.00	-53.38	-57.92	-2.78	-3.01
-2	4	6	33.59	29.80	-33.11	-29.38	-5.61	-4.98
-1	4	6	49.46	52.28	-49.37	-52.18	-3.00	-3.17
1	4	-6	26.45	25.82	-26.28	-25.65	-3.03	-2.96
-2	4	-6	15.58	17.16	15.52	17.10	1.35	1.49
-3	4	6	27.79	28.38	-27.66	-28.26	-2.65	-2.71
0	4	6	11.43	12.74	11.38	12.68	1.07	1.19
6	4	-1	17.80	18.35	-17.69	-18.24	-1.91	-1.97
-6	4	-4	11.81	9.53	-11.51	-9.29	-2.63	-2.12
6	4	0	12.33	12.14	-11.39	-11.21	-4.74	-4.66
2	4	-6	38.08	36.54	38.04	36.51	1.59	1.52
-8	4	1	12.18	13.31	-12.07	-13.19	-1.63	-1.78
4	4	4	11.66	10.54	-11.38	-10.29	-2.52	-2.28
-8	4	0	14.05	13.33	-13.12	-12.45	-5.02	-4.76
4	4	-5	53.87	55.72	53.67	55.52	4.59	4.75
5	4	-4	3.97	4.78	0.23	0.27	3.96	4.77
-4	4	6	36.71	35.71	36.66	35.67	1.83	1.78
-3	4	-6	34.32	32.35	33.95	32.00	5.02	4.73
6	4	-2	11.10	10.91	-10.87	-10.68	2.26	2.22
-5	4	-5	14.93	13.82	-14.35	-13.29	-4.12	-3.81
-7	4	-3	27.64	27.40	27.19	26.96	4.95	4.91
5	4	3	24.96	22.54	24.43	22.05	5.15	4.65
-6	4	5	51.59	53.11	51.37	52.88	4.73	4.87
-7	4	4	7.28	6.31	4.56	3.95	5.68	4.92
3	4	5	14.82	14.00	-14.35	-13.55	-3.70	-3.50
1	4	6	30.71	27.10	30.29	26.72	5.10	4.50
-8	4	2	9.05	8.83	-8.67	-8.46	2.60	2.53
6	4	1	25.97	22.63	-25.60	-22.30	-4.39	-3.83
-8	4	-1	25.70	24.09	-25.32	-23.73	-4.42	-4.14
3	4	-6	3.86	4.93	1.21	1.55	3.66	4.68
6	4	-3	43.42	42.46	43.15	42.20	4.84	4.73
-5	4	6	4.83	6.19	3.08	3.95	3.72	4.77
-8	4	3	38.24	38.51	37.93	38.20	4.87	4.91
-4	4	-6	28.05	27.04	27.73	26.73	4.22	4.07
6	4	2	5.72	4.79	5.72	4.78	-0.19	-0.16
-8	4	-2	7.09	6.83	7.08	6.82	-0.45	-0.44
2	4	6	28.89	27.88	28.58	27.58	4.22	4.07
0	4	-7	22.36	21.66	-22.13	-21.45	-3.16	-3.06

-1	4	-7	20.07	18.92	-19.37	-18.27	-5.23	-4.93
5	4	-5	39.68	37.72	39.47	37.52	4.04	3.84
-2	4	7	17.45	16.34	-17.19	-16.10	-2.99	-2.80
-7	4	-4	19.92	18.44	19.76	18.29	2.53	2.35
-6	4	-5	40.94	41.50	-40.67	-41.23	-4.70	-4.77
1	4	-7	27.25	25.52	-27.22	-25.49	1.39	1.30
5	4	4	18.63	17.12	18.50	17.00	2.19	2.01
-1	4	7	23.34	23.26	-22.83	-22.75	-4.84	-4.83
-7	4	5	34.85	33.30	34.63	33.09	3.90	3.73
4	4	5	41.08	39.93	-40.80	-39.66	-4.75	-4.62
-3	4	7	21.68	19.98	-21.62	-19.92	1.68	1.55
6	4	-4	29.37	29.70	29.14	29.47	3.62	3.66
-2	4	-7	4.70	4.71	3.81	3.81	-2.75	-2.76
4	4	-6	11.28	9.09	10.15	8.18	4.92	3.97
7	4	-1	37.59	37.17	37.51	37.09	2.35	2.32
-8	4	4	30.04	30.03	29.83	29.81	3.58	3.58
0	4	7	2.63	2.99	0.65	0.73	-2.55	-2.90
7	4	0	10.82	8.84	10.61	8.67	-2.10	-1.72
-6	4	6	16.32	14.16	15.71	13.63	4.42	3.84
-9	4	1	33.65	34.87	33.56	34.77	2.56	2.65
-9	4	0	10.78	9.45	10.64	9.33	-1.76	-1.54
2	4	-7	23.07	21.10	22.52	20.60	4.99	4.56
-8	4	-3	25.88	25.08	25.62	24.83	3.62	3.51
6	4	3	28.68	26.88	28.43	26.64	3.76	3.52
-5	4	-6	5.46	2.78	-5.46	-2.78	0.26	0.13
7	4	-2	6.96	6.91	5.16	5.12	4.67	4.64
-4	4	7	26.01	24.36	25.54	23.92	4.94	4.62
3	4	6	0.68	2.26	0.67	2.22	0.12	0.39
-9	4	2	13.10	12.37	12.05	11.38	5.13	4.85
-1	5	0	6.85	7.85	-6.84	-7.84	-0.35	-0.40
-2	5	0	13.79	15.50	-13.78	-15.49	-0.51	-0.57
-1	5	-1	1.18	0.92	-1.15	-0.90	0.25	0.19
-1	5	1	7.45	9.00	7.42	8.96	-0.65	-0.78
0	5	0	2.78	1.80	2.74	1.78	0.45	0.29
-2	5	1	13.38	13.07	13.37	13.06	-0.44	-0.43
-2	5	-1	6.82	4.35	-6.80	-4.34	-0.46	-0.29
0	5	-1	33.20	33.21	-33.19	-33.20	0.74	0.74
0	5	1	13.18	10.27	13.17	10.26	-0.62	-0.48
-3	5	0	19.09	19.93	-19.09	-19.92	-0.26	-0.27
-3	5	1	39.79	39.74	-39.79	-39.74	0.11	0.11
-3	5	-1	22.82	21.55	22.82	21.55	-0.38	-0.36
-1	5	-2	53.31	58.61	53.31	58.61	0.48	0.52
1	5	0	41.57	42.41	41.56	42.40	0.93	0.95
-1	5	2	42.76	45.85	-42.76	-45.85	-0.55	-0.59
-2	5	2	42.80	44.71	42.80	44.71	0.12	0.13
-2	5	-2	16.14	16.14	-16.14	-16.14	0.11	0.11
1	5	-1	20.80	19.60	20.78	19.59	0.79	0.75
0	5	-2	6.08	8.10	-6.06	-8.07	0.44	0.59
1	5	1	14.34	14.38	-14.33	-14.38	0.40	0.40
0	5	2	7.93	6.00	-7.83	-5.92	-1.30	-0.98
-3	5	2	28.19	26.80	28.19	26.79	0.55	0.52
-4	5	0	42.52	47.35	42.52	47.35	0.07	0.08
-4	5	1	10.11	11.17	-10.11	-11.17	0.30	0.33
-3	5	-2	2.38	0.24	-1.64	-0.17	-1.73	-0.18
1	5	-2	26.73	24.26	-26.73	-24.26	0.06	0.05

-4	5	-1	9.08	9.32	-9.08	-9.32	-0.12	-0.13
2	5	0	35.41	33.48	-35.40	-33.47	0.93	0.88
-1	5	-3	25.73	23.51	-25.73	-23.50	0.46	0.42
2	5	-1	34.01	32.48	34.01	32.48	0.02	0.02
1	5	2	24.98	23.45	-24.97	-23.44	-0.58	-0.54
0	5	-3	10.45	10.29	10.45	10.29	0.07	0.06
-2	5	3	25.14	22.48	-25.12	-22.47	0.77	0.69
-1	5	3	6.01	5.82	6.01	5.82	0.13	0.12
-4	5	2	9.14	6.16	-9.12	-6.15	0.57	0.39
-2	5	-3	10.07	8.66	-10.06	-8.65	0.37	0.31
2	5	1	5.70	4.12	-5.47	-3.95	1.59	1.15
-3	5	3	14.79	15.29	-14.78	-15.28	0.56	0.58
-4	5	-2	37.61	39.01	-37.61	-39.01	-0.13	-0.14
0	5	3	18.67	16.59	18.65	16.57	-0.85	-0.76
2	5	-2	20.42	18.58	-20.40	-18.57	-0.81	-0.74
-5	5	0	30.04	29.29	-30.04	-29.29	0.14	0.14
1	5	-3	31.00	31.41	30.99	31.40	-0.55	-0.56
-5	5	1	29.92	29.18	29.92	29.18	0.20	0.19
-3	5	-3	4.90	3.78	4.90	3.78	0.06	0.04
-5	5	-1	18.66	18.92	-18.66	-18.92	0.02	0.03
2	5	2	47.14	49.70	47.14	49.70	0.50	0.52
-4	5	3	36.22	37.59	36.22	37.59	0.09	0.09
-5	5	2	25.64	24.87	-25.64	-24.87	0.04	0.04
1	5	3	7.09	5.87	6.95	5.76	-1.40	-1.16
3	5	0	10.52	9.72	10.52	9.72	-0.03	-0.03
3	5	-1	16.60	16.13	-16.57	-16.10	-0.95	-0.92
-1	5	-4	6.63	8.24	-6.63	-8.24	0.05	0.06
2	5	-3	13.51	13.77	-13.48	-13.74	-0.85	-0.86
0	5	-4	16.80	15.67	-16.79	-15.67	-0.41	-0.38
-2	5	4	15.38	13.26	15.35	13.24	0.90	0.78
3	5	1	31.76	30.43	31.74	30.42	1.04	1.00
-4	5	-3	25.23	25.21	25.23	25.21	-0.05	-0.05
-1	5	4	34.56	34.79	34.55	34.78	0.84	0.84
-5	5	-2	33.92	35.34	33.92	35.34	0.00	0.00
-2	5	-4	37.65	38.93	37.65	38.93	0.23	0.24
3	5	-2	2.49	2.17	2.17	1.89	-1.21	-1.05
-3	5	4	7.14	5.64	-7.14	-5.63	0.21	0.16
1	5	-4	15.78	14.89	-15.77	-14.87	-0.70	-0.66
0	5	4	24.56	24.34	-24.56	-24.34	0.11	0.10
-6	5	0	0.	0.72	-0.	-0.72	0.	0.01
-6	5	1	15.52	15.33	15.52	15.33	0.01	0.01
-5	5	3	14.59	14.53	14.59	14.52	-0.25	-0.25
2	5	3	13.40	13.11	-13.38	-13.10	-0.59	-0.58
-3	5	-4	3.20	1.63	-3.19	-1.63	0.22	0.11
3	5	2	3.67	3.85	-3.45	-3.61	1.27	1.33
-6	5	-1	13.67	12.59	13.67	12.59	-0.06	-0.06
-4	5	4	25.67	26.39	-25.67	-26.39	-0.36	-0.37
-6	5	2	13.99	13.84	-13.99	-13.84	-0.11	-0.11
3	5	-3	27.07	28.51	-27.07	-28.51	-0.40	-0.42
2	5	-4	25.56	26.95	25.55	26.95	-0.35	-0.37
1	5	4	24.13	23.18	-24.11	-23.16	-0.96	-0.92
-5	5	-3	16.01	15.61	16.01	15.61	0.07	0.07
4	5	0	16.10	15.98	-16.06	-15.94	-1.11	-1.10
4	5	-1	27.31	25.96	-27.28	-25.93	-1.29	-1.22
-4	5	-4	18.77	18.46	-18.77	-18.46	-0.01	-0.01

-6	5	-2	4.53	3.35	4.53	3.35	-0.05	-0.04
4	5	1	5.95	4.64	-5.95	-4.64	-0.11	-0.09
4	5	-2	23.53	22.83	23.53	22.83	-0.47	-0.46
-1	5	-5	0.83	1.86	0.82	1.85	-0.10	-0.22
0	5	-5	11.40	11.51	11.39	11.50	-0.45	-0.45
-2	5	5	2.33	2.81	-2.32	-2.80	0.20	0.24
-6	5	3	17.12	17.21	-17.12	-17.21	-0.22	-0.22
-5	5	4	21.25	21.14	21.25	21.13	-0.43	-0.43
6	5	1	31.11	22.35	-31.04	-22.30	-2.08	-1.49
-2	5	-5	1.41	0.06	1.05	0.04	0.94	0.04
-1	5	5	3.30	2.79	-3.10	-2.62	1.15	0.97
3	5	3	30.25	28.49	-30.24	-28.48	0.69	0.65
-3	5	5	17.24	17.62	17.23	17.61	-0.46	-0.47
1	5	-5	16.38	15.09	-16.37	-15.09	-0.32	-0.29
-7	5	0	21.01	21.57	-21.01	-21.57	-0.01	-0.01
2	5	4	4.49	3.96	-4.23	-3.73	-1.50	-1.32
-7	5	1	15.66	15.03	-15.66	-15.03	0.04	0.03
3	5	-4	12.33	11.89	-12.32	-11.88	0.43	0.41
0	5	5	3.91	3.56	-3.76	-3.42	1.07	0.97
4	5	2	4.02	3.00	-3.75	-2.80	1.45	1.09
4	5	-3	4.90	6.40	4.88	6.37	0.42	0.54
-3	5	-5	10.26	10.50	-10.26	-10.50	0.05	0.05
-7	5	-1	2.00	2.59	1.99	2.58	-0.12	-0.16
-7	5	2	26.53	27.23	26.53	27.23	-0.02	-0.02
-4	5	5	14.82	13.43	-14.80	-13.42	-0.70	-0.63
-6	5	-3	31.99	31.85	-31.99	-31.85	0.11	0.11
-5	5	-4	5.81	4.35	-5.81	-4.35	0.12	0.09
2	5	-5	3.29	4.20	-3.28	-4.19	0.23	0.29
5	5	-1	9.51	7.65	-9.49	-7.63	-0.59	-0.47
1	5	5	3.93	2.42	3.93	2.42	0.11	0.07
5	5	0	22.95	22.32	22.91	22.28	-1.41	-1.37
-6	5	4	6.61	5.90	-6.61	-5.89	-0.17	-0.15
-7	5	-2	2.16	2.13	-2.14	-2.11	-0.25	-0.25
-4	5	-5	5.34	5.75	-5.33	-5.75	-0.07	-0.07
5	5	-2	4.85	6.32	-4.82	-6.28	0.52	0.68
-7	5	3	12.27	11.10	-12.27	-11.10	-0.05	-0.04
-5	5	1	3.66	29.18	3.66	29.18	0.02	0.19
3	5	4	3.33	1.89	3.16	1.80	-1.05	-0.60
-5	5	5	11.19	11.83	-11.18	-11.83	-0.26	-0.28
4	5	3	24.25	22.82	24.20	22.77	1.59	1.50
4	5	-4	19.87	18.89	19.84	18.87	1.08	1.03
-1	5	-6	31.35	32.27	-31.35	-32.27	-0.24	-0.25
0	5	-6	23.38	21.29	23.38	21.29	-0.22	-0.20
3	5	-5	7.39	7.34	7.35	7.29	0.83	0.82
-2	5	6	40.92	41.02	-40.91	-41.02	-0.55	-0.56
2	5	5	10.30	11.19	10.25	11.14	-0.99	-1.08
-2	5	-6	8.05	8.84	8.05	8.84	-0.06	-0.07
-1	5	6	16.82	18.19	16.82	18.18	0.31	0.33
5	5	-3	16.39	15.43	16.34	15.38	1.30	1.22
-8	5	1	18.16	17.41	-18.16	-17.41	0.19	0.18
-8	5	0	27.19	27.79	27.19	27.79	0.18	0.19
1	5	-6	15.79	15.40	15.79	15.40	0.19	0.19
-3	5	6	2.20	0.98	-1.21	-0.54	-1.84	-0.82
-6	5	-4	2.39	4.01	-2.39	-4.00	0.16	0.27
5	5	2	3.34	3.90	-3.34	-3.89	-0.14	-0.16

-7	5	-3	1.68	0.20	1.34	0.16	-1.01	-0.12
0	5	6	5.32	4.56	5.15	4.42	1.33	1.14
-8	5	2	9.59	8.64	9.59	8.64	0.06	0.06
-8	5	-1	9.16	9.09	9.16	9.09	-0.01	-0.01
-5	5	-5	14.06	14.39	14.06	14.39	-0.03	-0.04
-7	5	4	21.39	21.44	21.39	21.44	0.06	0.06
-3	5	-6	8.96	8.99	-8.96	-8.99	0.00	0.00
-6	5	5	12.62	12.89	-12.61	-12.89	0.12	0.12
-4	5	6	21.49	21.08	21.48	21.07	-0.42	-0.41
2	5	-6	13.29	12.93	-13.27	-12.92	0.63	0.61
6	5	-1	14.83	13.84	14.80	13.81	0.88	0.82
4	5	4	25.28	24.90	25.27	24.88	0.78	0.77
4	5	-5	27.24	26.45	27.23	26.44	0.74	0.71
6	5	0	11.13	11.47	-11.12	-11.46	-0.45	-0.47
1	5	6	19.19	20.02	19.16	19.99	1.03	1.07
5	5	-4	21.70	21.31	-21.69	-21.29	0.84	0.83
-8	5	3	2.25	0.80	2.25	0.80	-0.03	-0.01
-8	5	-2	3.01	2.06	-2.98	-2.04	-0.46	-0.31
3	5	5	14.46	14.54	-14.38	-14.47	-1.44	-1.45
6	5	-2	6.05	4.99	-5.81	-4.79	1.70	1.40
5	5	3	13.59	13.85	13.54	13.80	1.12	1.15
-5	5	6	2.65	3.09	-2.65	-3.08	0.14	0.16
-4	5	-6	9.81	10.71	9.81	10.71	-0.12	-0.13
6	5	1	22.00	22.35	-21.95	-22.30	-1.47	-1.49
-1	6	0	19.77	25.09	19.70	25.00	-1.68	-2.14
-2	6	0	17.56	20.81	-17.43	-20.66	2.13	2.53
-1	6	-1	13.75	14.80	-12.94	-13.93	-4.64	-5.00
-2	6	-1	2.76	2.17	-1.22	-0.96	-2.48	-1.95
-2	6	1	9.52	10.16	8.24	8.79	4.76	5.08
-1	6	1	6.59	5.12	5.88	4.56	2.98	2.31
0	6	0	55.85	62.88	-55.67	-62.68	-4.44	-5.00
-3	6	0	52.43	63.03	52.26	62.82	4.27	5.13
0	6	-1	27.45	24.89	-27.10	-24.58	-4.35	-3.94
-3	6	1	31.94	31.44	31.72	31.22	3.74	3.69
-3	6	-1	31.43	34.38	31.33	34.27	2.48	2.71
0	6	1	32.58	34.02	-32.50	-33.94	-2.20	-2.30
-1	6	-2	29.10	29.69	-28.83	-29.41	-4.01	-4.09
-2	6	-2	35.65	32.53	-35.24	-32.16	-5.41	-4.93
-2	6	2	25.76	26.22	25.48	25.95	3.73	3.80
-1	6	2	34.81	32.01	34.39	31.62	5.41	4.97
1	6	0	26.86	24.90	-26.55	-24.62	-4.05	-3.75
0	6	-2	33.58	36.30	33.58	36.30	0.08	0.08
-4	6	0	21.50	19.94	21.16	19.62	3.81	3.53
1	6	-1	23.45	22.96	-23.45	-22.96	0.30	0.29
-3	6	2	34.18	36.69	-34.18	-36.69	-0.47	-0.51
-4	6	1	13.82	14.04	13.80	14.02	-0.71	-0.72
-3	6	-2	26.78	27.96	-26.73	-27.90	-1.66	-1.73
0	6	2	30.53	31.88	30.47	31.82	1.99	2.08
-4	6	-1	28.55	29.32	28.11	28.86	4.99	5.13
1	6	1	26.93	24.67	-26.38	-24.17	-5.40	-4.95
1	6	-2	35.26	34.61	35.01	34.36	4.20	4.12
-4	6	2	34.36	33.16	-34.06	-32.87	-4.55	-4.39
-1	6	-3	6.04	3.66	-6.04	-3.66	-0.21	-0.13
-2	6	-3	8.27	8.81	-7.28	-7.75	-3.93	-4.19
-2	6	3	3.53	0.89	3.33	0.84	-1.15	-0.29

0	6	-3	7.66	5.57	5.32	3.87	5.51	4.01
-1	6	3	9.47	8.80	8.50	7.91	4.16	3.86
2	6	0	4.88	2.93	4.81	2.89	0.83	0.50
-4	6	-2	31.20	29.48	31.05	29.34	3.03	2.86
1	6	2	27.82	26.79	-27.71	-26.68	-2.52	-2.43
-5	6	0	5.74	4.27	-5.60	-4.17	-1.25	-0.93
2	6	-1	35.09	36.32	34.86	36.08	4.04	4.18
-3	6	3	13.43	10.56	-12.30	-9.67	-5.39	-4.24
-5	6	1	34.96	37.46	-34.71	-37.19	-4.20	-4.50
-3	6	-3	31.17	31.81	-30.81	-31.44	-4.72	-4.82
2	6	1	30.23	28.54	-30.00	-28.32	-3.74	-3.53
-5	6	-1	29.87	28.79	29.67	28.59	3.46	3.34
0	6	3	31.92	31.55	31.55	31.18	4.87	4.81
1	6	-3	32.76	33.65	32.42	33.30	4.69	4.82
2	6	-2	44.84	47.33	44.62	47.09	4.47	4.72
-5	6	2	45.20	48.50	-44.99	-48.27	-4.34	-4.66
-4	6	3	31.74	32.99	-31.41	-32.65	-4.54	-4.72
-5	6	-2	51.52	57.99	51.32	57.76	4.50	5.06
-4	6	-3	11.93	9.15	-11.76	-9.02	-1.97	-1.51
2	6	2	55.94	59.42	-55.76	-59.23	-4.56	-4.84
-1	6	-4	16.26	14.77	15.69	14.26	4.24	3.85
1	6	3	15.98	13.96	15.84	13.84	2.10	1.84
-2	6	-4	3.61	1.62	3.54	1.59	-0.75	-0.34
3	6	0	15.33	12.26	14.41	11.52	5.25	4.20
-2	6	4	13.48	12.34	-12.74	-11.65	-4.42	-4.05
0	6	-4	37.06	37.24	36.74	36.92	4.85	4.87
3	6	-1	29.35	27.54	28.95	27.16	4.87	4.57
-6	6	0	16.62	12.84	-15.54	-12.01	-5.88	-4.55
2	6	-3	33.02	31.56	32.97	31.51	1.79	1.71
-6	6	1	27.54	26.90	-27.15	-26.51	-4.66	-4.55
-1	6	4	7.59	6.08	-7.59	-6.08	-0.10	-0.08
-3	6	4	32.85	31.19	-32.48	-30.83	-4.97	-4.72
-5	6	3	28.28	26.39	-28.24	-26.35	-1.43	-1.34
3	6	1	3.65	3.76	3.59	3.70	0.66	0.68
-6	6	-1	8.39	10.17	-8.34	-10.11	-0.92	-1.12
-3	6	-4	58.34	61.96	-58.21	-61.82	-4.00	-4.24
3	6	-2	25.14	23.10	-25.08	-23.05	1.63	1.50
1	6	-4	3.80	2.72	2.71	1.94	2.67	1.91
0	6	4	54.61	56.73	54.48	56.60	3.74	3.88
-6	6	2	23.42	21.63	23.39	21.60	-1.23	-1.14
-4	6	4	5.53	5.12	-5.28	-4.88	-1.65	-1.52
-5	6	-3	15.14	15.31	-14.85	-15.02	2.94	2.98
2	6	3	13.42	12.76	13.15	12.51	-2.55	-2.52
-6	6	-2	17.88	17.86	-17.61	-17.59	3.12	3.11
3	6	2	19.15	18.73	18.85	18.44	-3.34	-3.27
-4	6	-4	27.38	24.51	-26.88	-24.06	-5.20	-4.65
3	6	-3	6.47	4.64	-5.28	-3.79	-3.74	-2.69
2	6	-4	18.62	16.76	-18.41	-16.57	-2.82	-2.54
1	6	4	26.71	23.43	26.19	22.97	5.25	4.60
-6	6	3	14.20	13.79	13.84	13.44	3.17	3.08
-5	6	4	17.89	15.08	17.56	14.80	3.44	2.90
-1	6	-5	16.25	15.29	15.40	14.49	5.17	4.86
4	6	-1	15.95	14.18	15.89	14.12	1.43	1.27
4	6	0	13.00	13.28	12.28	12.54	4.28	4.37
-7	6	0	13.33	14.32	-12.69	-13.63	-4.09	-4.39

-7	6	1	10.73	9.14	-10.68	-9.09	-1.08	-0.92
0	6	-5	15.18	14.97	15.03	14.83	2.11	2.08
-2	6	-5	18.56	18.25	18.18	17.88	3.72	3.66
-2	6	5	15.70	14.13	-14.81	-13.33	-5.19	-4.67
-3	6	5	13.97	14.31	-13.88	-14.21	-1.65	-1.69
-1	6	5	25.86	25.56	-25.57	-25.27	-3.86	-3.81
4	6	-2	11.11	10.00	-10.66	-9.60	-3.12	-2.80
4	6	1	15.35	13.74	14.63	13.09	4.65	4.16
-7	6	-1	14.11	13.91	-13.34	-13.15	-4.61	-4.55
-7	6	2	11.22	11.25	10.75	10.78	3.22	3.22
1	6	-5	18.16	19.38	-18.02	-19.24	-2.21	-2.35
-6	6	-3	14.18	14.07	13.28	13.17	4.99	4.95
-3	6	-5	8.54	6.58	-8.51	-6.56	-0.69	-0.53
3	6	3	8.64	8.59	-7.24	-7.20	-4.71	-4.69
-5	6	-4	6.04	7.66	-5.96	-7.55	-1.01	-1.27
-4	6	5	24.91	26.38	24.78	26.24	2.54	2.69
0	6	5	9.53	8.90	9.52	8.90	0.13	0.12
2	6	4	9.21	9.91	9.09	9.78	1.47	1.59
3	6	-4	24.44	24.69	-23.97	-24.22	-4.75	-4.80
-6	6	4	27.57	27.32	27.12	26.87	4.95	4.90
4	6	-3	17.42	15.85	-16.61	-15.12	-5.23	-4.76
4	6	2	1.89	2.13	-1.74	-1.95	0.76	0.85
-7	6	-2	2.50	1.81	1.74	1.26	-1.79	-1.29
-7	6	3	12.31	10.21	10.80	8.96	5.91	4.90
2	6	-5	43.50	41.70	-43.21	-41.43	-5.00	-4.79
-4	6	-5	13.64	15.40	-13.11	-14.80	-3.76	-4.25
-2	7	0	11.44	12.37	-11.43	-12.36	-0.39	-0.42
-1	7	0	29.40	33.73	-29.38	-33.72	-0.87	-1.00
-2	7	-1	18.77	20.38	18.75	20.37	-0.73	-0.79
-2	7	1	12.78	12.70	-12.77	-12.69	0.37	0.37
-1	7	-1	3.65	2.81	-3.54	-2.73	-0.88	-0.68
-3	7	0	20.39	23.22	20.38	23.22	0.28	0.32
-1	7	1	6.94	8.64	6.93	8.62	-0.44	-0.55
-3	7	1	11.00	9.79	-10.96	-9.76	0.88	0.79
0	7	0	4.60	1.71	-4.08	-1.52	-2.11	-0.79
-3	7	-1	1.74	2.03	-1.72	-2.01	-0.25	-0.29
0	7	-1	7.44	5.68	-7.44	-5.68	0.18	0.14
0	7	1	12.61	11.85	12.54	11.79	-1.27	-1.19
-2	7	-2	6.60	7.11	6.58	7.09	-0.51	-0.55
-1	7	-2	10.21	10.95	-10.21	-10.95	0.07	0.07
-4	7	0	11.73	9.18	11.70	9.16	0.75	0.59
-2	7	2	5.33	3.40	5.11	3.25	1.52	0.97
-1	7	2	24.27	25.29	24.26	25.28	0.38	0.40
-4	7	1	3.15	4.00	-3.12	-3.97	0.40	0.51
-3	7	2	24.45	23.49	24.44	23.48	0.72	0.69
-4	7	-1	14.87	14.89	-14.87	-14.89	0.25	0.25
-3	7	-2	31.24	31.75	-31.23	-31.74	-0.57	-0.58
0	7	2	38.63	33.32	-38.62	-33.31	-0.80	-0.69
1	7	0	10.20	8.16	10.19	8.16	0.27	0.21
1	7	-1	15.14	14.21	-15.10	-14.17	1.10	1.04
0	7	2	30.01	33.32	-30.01	-33.31	-0.62	-0.69
1	7	1	11.54	12.48	-11.51	-12.45	-0.81	-0.87
-4	7	2	31.97	29.46	-31.97	-29.46	-0.02	-0.02
-1	7	-3	17.61	14.07	-17.59	-14.05	0.81	0.65
-5	7	0	6.54	9.05	6.54	9.05	0.25	0.34

-4	7	-2	13.24	16.53	13.24	16.53	-0.15	-0.18
-2	7	-3	3.86	5.68	-3.86	-5.68	0.02	0.03
1	7	-2	3.58	2.06	-3.11	-1.79	1.78	1.02
-5	7	1	22.80	20.94	22.80	20.94	-0.04	-0.04
-2	7	3	8.96	5.48	-8.85	-5.41	1.42	0.87
-3	7	3	25.17	24.30	25.17	24.30	0.01	0.01
0	7	-3	10.69	11.03	10.66	11.00	0.83	0.85
-5	7	-1	9.37	7.99	-9.36	-7.98	0.46	0.39
-1	7	3	5.75	6.01	-5.65	-5.90	1.08	1.13
-3	7	-3	11.42	11.71	11.41	11.71	-0.39	-0.40
1	7	2	12.21	7.08	-11.98	-6.95	-2.37	-1.37
2	7	0	31.96	32.97	31.94	32.95	1.19	1.22
2	7	-1	14.50	10.63	14.41	10.57	1.61	1.18
-5	7	2	11.03	10.78	-11.02	-10.77	-0.51	-0.50
-4	7	3	4.89	3.45	4.80	3.39	-0.91	-0.64
0	7	3	3.29	2.19	-3.23	-2.15	0.61	0.41
2	7	1	18.74	17.50	-18.74	-17.50	0.32	0.30
1	7	-3	19.15	17.70	19.15	17.70	0.31	0.29
-5	7	-2	13.84	9.95	13.84	9.95	0.25	0.18
2	7	-2	16.22	15.42	-16.22	-15.42	0.31	0.29
-4	7	-3	16.71	13.03	16.70	13.02	-0.47	-0.37
-6	7	0	31.34	32.95	-31.34	-32.95	-0.04	-0.04
-6	7	1	3.60	0.65	-3.08	-0.56	-1.86	-0.34
-1	7	-4	22.42	20.81	22.40	20.80	0.72	0.67
-2	7	-4	7.87	6.33	7.84	6.31	0.57	0.46
-2	7	4	2.82	2.42	2.82	2.42	0.07	0.06
-5	7	3	13.91	12.94	-13.90	-12.92	-0.68	-0.64
-6	7	-1	17.95	17.57	17.95	17.57	0.18	0.18
0	7	-4	21.31	22.91	-21.30	-22.91	0.25	0.26
2	7	2	2.34	1.65	-1.93	-1.36	-1.33	-0.94
1	7	3	22.65	20.98	22.63	20.96	-0.90	-0.83
-3	7	4	31.15	31.32	-31.14	-31.31	-0.76	-0.77
-1	7	4	11.32	9.11	11.25	9.05	1.29	1.04
-6	7	2	9.64	10.03	9.63	10.02	-0.42	-0.44
-3	7	-4	9.10	10.87	9.10	10.87	-0.00	-0.00
2	7	-3	5.09	3.59	-4.99	-3.52	-0.99	-0.70
3	7	0	23.14	22.32	-23.10	-22.28	1.36	1.31
3	7	-1	14.84	15.47	14.83	15.47	0.27	0.28

Biographical Note

Charles Thompson Prewitt was born on March 3, 1933, in Lexington, Kentucky. He is the son of John Burton and Margaret Thompson Prewitt. He attended the public schools in Mt. Sterling, Kentucky, and graduated from Mt. Sterling High School in June, 1951. All undergraduate and graduate schooling was taken at Massachusetts Institute of Technology, where he received an S. B. in Geology in June, 1955, an S. M. in Geology and Geophysics in June, 1960, and began work on a Ph. D. in Crystallography and Mineralogy in September, 1960. He received a National Science Foundation travel grant to attend the N. A. T. O. Advanced Study Institute on "Modern Methods of Crystal Structure Determination", held at the College of Science and Technology, Manchester, England, August 25-September 9, 1960.

He served on active duty as a second lieutenant with the U. S. Army from January to July, 1956, and is presently a member of the U. S. Army Reserve in the rank of captain. Professional experience includes a number of summer or part-time jobs in government, industry, and university positions, including a half-time Research Assistantship at M. I. T. during the graduate school years, 1956-57 to 1961-62. He is married to the former Gretchen Beatrice Hansen of Virginia, Minnesota.

Titles of publications:

The Crystal Structure of Cahnite, $\text{Ca}_2\text{BAsO}_4(\text{OH})_4$ (with M. J. Buerger)

X-ray Study of Pyrographite (with Otto J. Guentert)

The parameters χ and ϕ for equi-inclination, with application to the
single-crystal counter diffractometer

Professional societies:

Sigma Xi

American Crystallographic Association

The Geochemical Society

The Mineralogical Society of America